Antibacterial Properties Of The Diabetic Drug Metformin

Lina Mohamed ElSayed Aly Maarouf

For the degree of Doctor of Philosophy

University of East Anglia
Norwich Medical School, Faculty of Medicine and Health Sciences

Submitted May 2025

ABSTRACT

Antimicrobial resistance poses a serious global health threat, creating an urgent need for alternative therapeutic strategies. One promising approach is repurposing non-antibiotic drugs as antimicrobial agents or adjuncts to existing antimicrobial agents. Metformin, a widely used antidiabetic drug, has recently demonstrated antibacterial activity against various bacterial species. However, its mechanism of action and the bacterial response to metformin remain unclear and sometimes contradictory.

This thesis investigates the antibacterial effects of metformin, its underlying molecular mechanisms, and how bacteria may adapt to its presence, especially relevant for diabetic patients with long-term exposure. In this thesis, metformin's effects on bacterial growth, virulence factors, and efflux pump activity across multiple clinically relevant species were investigated. To gain mechanistic insight, transcriptomic profiling using RNA-seq was conducted, and TraDIS was used to identify essential genes under metformin stress. Additionally, combinations with mitochondrial inhibitors and different antibiotic classes were tested to assess synergistic or antagonistic interactions. In addition, an evolutionary experiment with continuous low-dose metformin exposure was performed to track phenotypic and genotypic changes.

Metformin was found to exert strain-specific antibacterial effects, disrupting bacterial metabolism, redox balance, and proton motive force. It may also mimic natural polyamines, interfering with enzymatic functions. These disruptions can enhance or reduce antibiotic efficacy depending on the strain and drug class.
Importantly, although prolonged exposure did not lead to resistant strains, it suggested that it might encourage the formation of persistent-like cells through energy depletion, which could contribute to chronic infections. These findings underscore the potential and limitations of metformin as an adjunct antimicrobial, highlighting the need for careful consideration in clinical applications involving diabetic patients.

ACKNOWLEDGEMENTS

Completing this PhD has been one of the most challenging, long and intense journeys of my life, and it would not have been possible without the support, encouragement, and love of many people to whom I am deeply grateful.

First and foremost, I would like to express my heartfelt thanks to my primary supervisor, Dr. Benjamin Evans, for your exceptional guidance, insightful feedback, and steady encouragement throughout every stage of my research. Your mentorship has shaped both my academic and personal growth, which I am sure will help me in my life. It would be impossible to finish without your guidance.

I am also sincerely thankful to my secondary supervisor, Dr. Mark Webber for your valuable insights and support along the way, and to his group members (Dr. Keith Turner and Dr. Muhammed Yasir) for their support and help in one of the biggest chapters of my thesis.

To my parents and my brother, thank you for your love and support. Your constant encouragement and belief in my abilities gave me the strength to keep moving forward, even in the most difficult moments. I am forever thankful.

To my dear husband, words are not enough to express my gratitude. You have been my pillar of strength. Your patience and support sustained me throughout this entire process. This work would not have been possible without you.

To my baby, Tala, your presence brought light into this journey. Though small, your impact was immense. You reminded me daily of what truly matters and gave me a new kind of motivation and strength I never knew I had. You are my greatest joy.

I would like to acknowledge the generous financial support provided by the Egyptian Ministry of Higher Education; the Egyptian Missions and the British Council, whose sponsorship made this research possible. Their investment in academic excellence and international collaboration has been crucial to the successful completion of this thesis.

This thesis is dedicated to all of you — with deep gratitude and love!

LIST OF CONTENTS

LIST OF ABBERVIATIONS

2-MCC	2-Methylcitrate Cycle
ABC Transporter	ATP-Binding Cassette Transporter
ADP	Adenosine Diphosphate
AGR	Accessory Gene Regulator
AMP	Adenosine Monophosphate
AMPK	AMP-Activated Protein Kinase
AMR	Antimicrobial Resistance
ANOVA	Analysis of Variance
ATCC	American Type Culture Collection
ATP	Adenosine Triphosphate
AUC	Area Under the Curve
CF	Cystic Fibrosis
CFU	Colony Forming Units
COPD	Chronic Obstructive Pulmonary Disease
COVID-19	Coronavirus Disease 2019
CRE	Carbapenem-Resistant Enterobacteriaceae
CSV	Comma-Separated Values
DGE	Differential Gene Expression
DNA	Deoxyribonucleic Acid
DS	Double Strength
ECDC	European Centre for Disease Prevention and Control
EDTA	Ethylenediaminetetraacetic Acid
ESBL	Extended-Spectrum Beta-Lactamase
ESKAPE	*Enterococcus, Staphylococcus, Pseudomonas, Klebsiella, Acinetobacter, E.coli*
ETC	Electron Transport Chain
FC	Fold Change
FDR	False Discovery Rate
FIC	Fractional Inhibitory Concentration
FICI	Fractional Inhibitory Concentration Index

GIT	Gastrointestinal Tract
GLP-1	Glucagon-Like Peptide-1
GLUT2	Glucose Transporter Type 2
GO analysis	Gene Ontology Analysis
GTP	Guanosine Triphosphate
HTH-type	Helix-Turn-Helix Type
INDELs	Insertions and Deletions
KEGG	Kyoto Encyclopedia of Genes and Genomes
LPS	Lipopolysaccharide
MATE	Multidrug And Toxin Extrusion
MBL-AB	Metallo-Beta-Lactamase-Producing Acinetobacter baumannii
MBL-PA	Metallo-Beta-Lactamase-Producing Pseudomonas aeruginosa
Mbp	Million base Pair
MDR	Multidrug-Resistant
MDR-ESKAPE	Multidrug-Resistant ESKAPE Pathogens
MFS	Major Facilitator Superfamily
mGPD	Mitochondrial Glycerol-3-Phosphate Dehydrogenase
MHB	Mueller-Hinton Broth
MRSA	Methicillin-Resistant Staphylococcus aureus
TOR	Target of Rapamycin
NAD	Nicotinamide Adenine Dinucleotide
NCTC	National Collection of Type Cultures
NSAIDs	Nonsteroidal Anti-Inflammatory Drugs
OD	Optical Density
ONT sequence	Oxford Nanopore Technologies Sequencing
PACE	Proteobacterial Antimicrobial Compound Efflux
PBS	Phosphate Buffered Saline
PCR	Polymerase Chain Reaction
PDH	Pyruvate Dehydrogenase
PDR	Pan Drug-Resistant
PMF	Proton Motive Force

RM-ANOVA	Repeated measured ANOVA
RNA	Ribonucleic Acid
RND	Resistance-Nodulation-Division
ROS	Reactive Oxygen Species
SGLT1	Sodium-Glucose Cotransporter 1
SMR	Small Multidrug Resistance
SNPs	Single Nucleotide Polymorphisms
SVIM-asm	Structural Variant Identification Method for Assemblies
SyRI	Synteny and Rearrangement Identifier
TCA	Tricarboxylic Acid (Cycle)
TraDIS	Transposon Directed Insertion-site Sequencing
TSB	Tryptic Soy Broth
Tukey's HSD	Tukey's Honestly Significant Difference
VRE	Vancomycin-Resistant Enterococci
WHO	World Health Organization
XDR	Extensively Drug-Resistant

LIST OF FIGURES

LIST OF TABLES

CHAPTER 1- Introduction

1. Introduction

1.1. Antimicrobial resistance

1.1.1. Definition of antimicrobial resistance and its history

Antimicrobial resistance (AMR) is defined as the ineffectiveness of an antimicrobial agent against the microorganism it is intended to inhibit and treat (World Health, 2024). The discovery of the first antibiotic, penicillin, by Sir Alexander Fleming, a Scottish physician and microbiologist, in 1928 marked a turning point in healthcare management. Subsequently, the 1940s to 1960s are regarded as the golden era of antibiotic discovery and treating bacterial infections; before that, many people were just dying because of minor, untreated infections. Because of that, they considered antibiotics as "magic bullets" for fighting against bacteria (Gaynes, 2017). During this time, antibiotic resistance began to emerge soon after the introduction of antibiotics, such as penicillin-resistant strains, followed by methicillin-resistant *Staphylococcus* strains in the 1960s. When vancomycin was introduced to combat methicillin-resistant *Staphylococci* (MRSA), vancomycin-resistant *Staphylococci* were reported shortly thereafter, along with the reporting of vancomycin-resistant *Enterococcus* (VRE) (Davies & Davies, 2010; Leclercq & Courvalin, 1997). Additionally, cephalosporins began to be used for treating penicillin-resistant cases, leading to the development of multiple generations of this antibiotic, up to the fifth generation, which demonstrated high efficacy against extended beta-lactamases (ESBLs) producing gram-negative bacteria. However, various bacterial species have started to develop resistance against all these generations (Paterson & Bonomo, 2005). One significant antibiotic discovered was tetracycline, to which the first strain of tetracycline-resistant gram-negative bacteria was reported within less than ten years (Chopra & Roberts, 2001). When fluoroquinolones such as Levofloxacin were introduced into antimicrobial therapeutics, levofloxacin-resistant *Pneumococcus* was reported in the same year. Another class introduced was carbapenems, which were reserved for enterobacterales, particularly in cephalosporin-resistant cases. However, due to their high level of use, carbapenem-resistant enterobacterales (CRE) have been reported since 2006. Despite aminoglycosides and polymyxins being powerful bactericidal agents, reports of resistant strains towards them have also emerged (Hooper, 2001; Nordmann et al., 2011; Poirel et al., 2017).

The chronology of antibiotic discovery and resistance emergence illustrated by Salam et al. (2023) in (Figure 1-1), provides a framework for understanding the current global landscape of antimicrobial resistance discussed in the previous section.

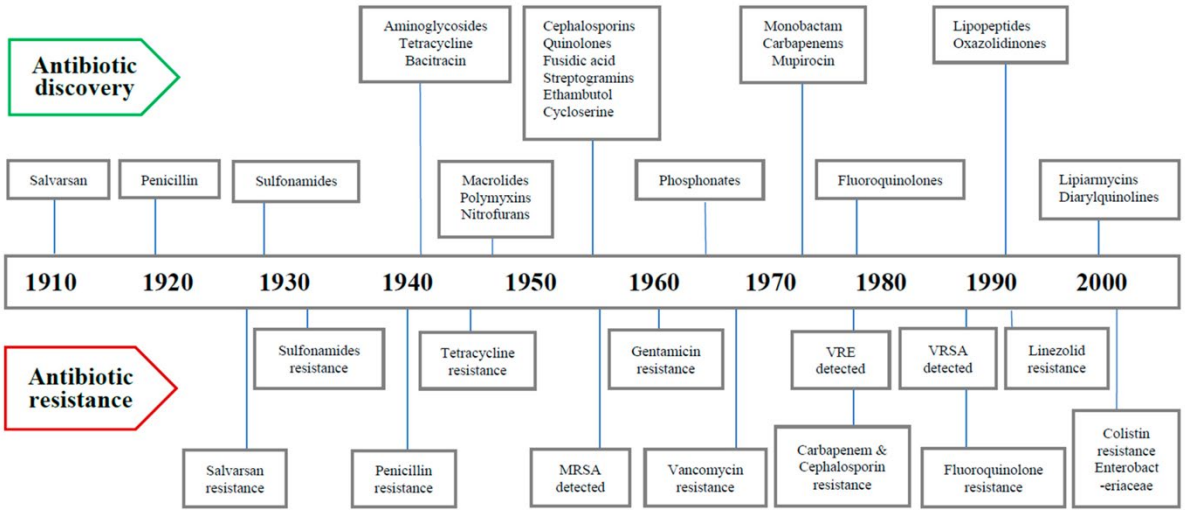

Figure 1-1: The timeline for the discovery of different antibiotic classes and the emergence of antibiotic resistance (Salam et al., 2023).

1.1.2. Various mechanisms of antibiotic resistance

In general, antimicrobial resistance can occur through different mechanisms by reducing the entering of the agent, taking it out the cells, drug inactivation or modification in the structure of the drug target (Figure 1-2).

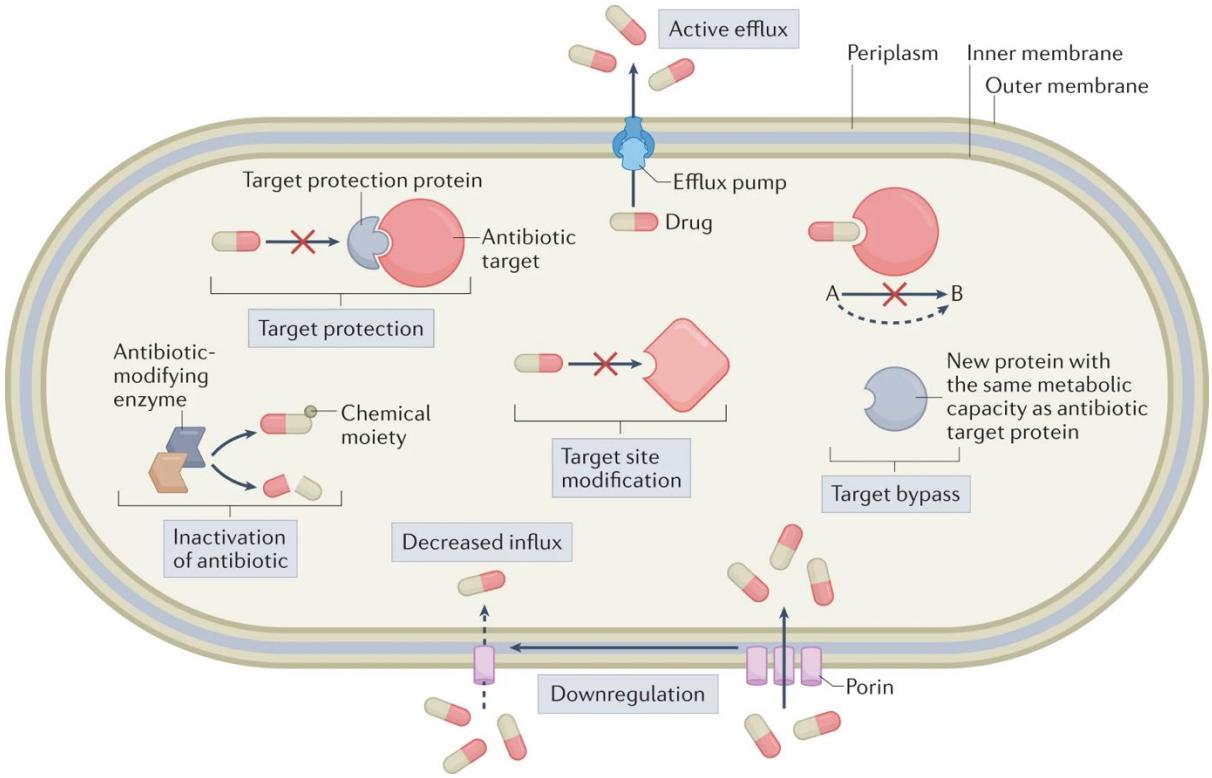

Figure 1-2**:** The general mechanisms of antibiotic resistance.
It is showing four main mechanisms which are efflux pump, change in the membrane permeability, modification of the target site and inactivation of the drug (Darby et al., 2023).

The Gram-negative bacterial cells can develop resistance by reducing the entry of antimicrobial agents through a decrease in the number of porins in the lipopolysaccharide layer or by altering its selectivity. One of these porins, OmpC, is found to have its alteration in *E. coli* strains potentially causing a reduction in susceptibility to various antibiotics, such as cefotaxime, gentamicin, or imipenem (Darby et al., 2023; Reygaert, 2018). Moreover, in *P. aeruginosa,* the loss of OprD porins results in the diminished efficacy of carbapenems. This mechanism is less prevalent in Gram-positive bacteria due to the lack of an outer membrane layer; however, some *S. aureus* have been found to thicken their cell walls, making it more difficult for vancomycin to penetrate, thereby increasing vancomycin resistance. Furthermore, enterococci are intrinsically not susceptible to aminoglycoside antibiotics, as these are polar compounds that struggle to cross the cell wall (Darby et al., 2023; Reygaert, 2018).

Normally, bacterial cells can eliminate any toxic substances, including antimicrobial agents, through efflux pumps that are either intrinsically expressed or induced and overexpressed after environmental stimuli. These pumps are found in both Gram-positive and Gram-negative bacteria. They are typically classified into six families: ATP-binding cassette (ABC), Multidrug and Toxic compound Extrusion (MATE), Major Facilitator Superfamily (MFS), resistance–nodulation–division (RND), Small Multidrug Resistance (SMR), and Proteobacterial Antimicrobial Compound Efflux (PACE) superfamilies (L. Huang et al., 2022). For example, PatA/B from the ABC family reduces the activity of almost all classes of fluoroquinolones in *Streptococcus*. NorM efflux, from the MATE family, has been reported to expel quaternary ammonium compounds and fluoroquinolones in Gram-negative bacteria. Mef efflux pumps from the MFS family show increased resistance to macrolides in *E. coli*. From the RND family, AcrAB-TolC and MexAB-OprM expel many substrates in Gram-negative bacteria, such as *E. coli* and *P. aeruginosa.* Members of the SMR family have been shown to efflux a broad spectrum of drugs, including polyamine compounds like spermidine, such as EmrE in *P. aeruginosa* (L. Huang et al., 2022).

The antimicrobial agents could be inactivated either by degradation through hydrolysing enzymes like β-lactamases, which hydrolyse the β-lactam antibiotics. Carbapenems can be hydrolysed by carbapenemases. Tetracycline hydroxylases degrade tetracyclines. Tetracyclines may be inactivated by Tet enzymes that catalyse their oxidation. The antimicrobial agent could be inactivated by certain chemical groups that stop its action, such as acetylation, phosphorylation, and adenylation. One of the well-known examples is the inactivation of aminoglycosides by ApmA acetyltransferase, which causes aminoglycoside resistance (Darby et al., 2023; Reygaert, 2018).

Bacterial cells can develop antimicrobial resistance by overexpressing or altering the target of the antimicrobial agent, either by changing the target itself or by adding an extra component that acts as

protection against the antibiotic. *Pneumocystis carinii* is found to develop resistance against trimethoprim–sulfamethoxazole by overproduction of dihydrofolate reductase and dihydropteroate synthase, which are the targets of this combination (Darby et al., 2023; Reygaert, 2018). The structure of the target can be modified through the acquisition of specific resistance genes or chromosomal mutations. For instance, one of the primary resistance mechanisms of β-lactams is the modification of penicillin-binding proteins (PBPs), as seen in *S. aureus,* which acquires the *mec*A gene that expresses PBP2a with low drug affinity. Additionally, vancomycin resistance can occur through the acquisition of the *van* gene, leading to modified peptidoglycan precursors; consequently, this reduces vancomycin's affinity for them. Moreover, fluoroquinolone resistance can arise from mutations in the genes encoding DNA gyrase and topoisomerase IV, resulting in modifications that diminish the drug's ability to bind to them. In some instances, two mechanisms may occur simultaneously to enhance resistance, such as mutations in DNA gyrase coupled with the acquisition of *qnr,* which protects topoisomerase from fluoroquinolone inhibition (Darby et al., 2023; Reygaert, 2018).

1.1.3. Reasons and consequences of antimicrobial resistance

Nowadays, antimicrobial resistance is a serious problem described by the World Health Organisation (WHO) as a “silent pandemic” due to its widespread dissemination. One of the main reasons for antibiotic resistance is the misuse of antibiotics, especially in developing countries, through overuse in unnecessary situations, such as viral infections, including the common cold, which is one of the primary instances in which people tend to use antibiotics (Maarouf et al., 2023). Therefore, some studies have investigated the effect of COVID-19, which is a viral infection, on antimicrobial resistance. Despite an increase in hygiene and reduced travel during the pandemic, which may reflect a reduction in infections, one of the measures that some people adopted during the pandemic is taking antibiotics, which could affect AMR. Additionally, the incorrect duration of treatment, which is often shorter than the intended course, is another significant cause of antibiotic resistance. Moreover, the use of antibiotics in livestock and agriculture, along with the improper treatment of wastewater, is another reason for the emergence of AMR (Maarouf et al., 2023; Palmer & Buckley, 2021; Tsalidou et al., 2023).

When antibiotics become ineffective in combating microorganisms, this could lead to the persistence of life-threatening microbial diseases. It is found that the consequences of infection with a resistant strain of bacterial species are twofold higher than those from an infection with a susceptible strain of the same species (Chandra et al., 2020), leading to health complications that may result in death. According to the WHO report of 2022, around 1.27 million deaths are directly attributed to bacterial AMR, while around 5 million people died due to the contribution of resistant bacterial infections (Murray et al., 2022). Furthermore, AMR increases the cost burden on healthcare systems due to prolonged infections and the use of various second-line treatments, which could also lead to a greater emergence of resistance to last-

resort antibiotics, creating a vicious cycle. According to the report by Jim O'Neill, the global cost resulting from antibiotic resistance will become unmanageable and could reach around 100 trillion dollars by 2050, with death rates of 10 million people annually if the world does not take any protective measures against this problem (O'Neill, 2016).

Due to the emergence of antimicrobial resistance to various antibiotic classes, several terms have been established by the European Centre for Disease Prevention and Control (ECDC). The first term is multi-drug-resistant bacteria (MDR), defined as antibiotic resistance to more than one antimicrobial agent; however, it is noted that some bacteria, like MRSA, inherently possess significant cross-resistance, thus they are considered MDR. Another term is extensive drug resistance (XDR), which refers to bacteria resistant to more than one antibiotic in two or more different classes. Finally, pan-drug resistant bacteria (PDR) exhibit resistance to nearly all antimicrobial agents across different classes (Magiorakos et al., 2012).

As a result of antimicrobial resistance, some of the most significant MDR bacteria reported include vancomycin-resistant enterococci, methicillin-resistant *S. aureus* (MRSA), carbapenemase-producing *K. pneumoniae*, metallo-beta-lactamase-producing *A. baumannii* (MBL-AB), metallo-beta-lactamase-producing *P. aeruginosa (MBL-PA*), and extended-spectrum beta-lactamase (ESBL)-producing *Enterobacter spp.* These six bacterial species are collectively known by the acronym MDR-ESKAPE and are garnering global attention due to their high mortality rates worldwide (Founou et al., 2017). In 2024, the WHO updated the priority list of MDR bacteria, categorising them as critical, high, and medium priority according to their mortality rates and resistance to last-resort antibiotics. The ESKAPE organisms are classified as critical and high concern at the top of this list (WHO, 2024).

In 2011, the WHO said that "combat drug resistance: no action today, no cure tomorrow" (Sharma, 2011). As such, it is important to investigate other drugs either by having novel agents, which is a long process, costly and time-consuming till reaching the final stage of clinical trials. Therefore, the repurposing of existing drugs to act as new antimicrobial agents or to be used as adjunct therapy with the actual antimicrobial agents would be one of the best things to overcome the emergence of antibiotic resistance (Alexia Barbarossa et al., 2022).

1.2. Repurposing of non-antibiotic drugs as new antimicrobial targets

Many pharmaceutical drugs have begun to be investigated for their antimicrobial effects and whether they can help increase the susceptibility of bacteria and overcome antimicrobial resistance.

From these drugs, the non-steroidal anti-inflammatory drugs (NSAIDs) such as diclofenac, acetylsalicylic acid, and ibuprofen have been investigated. Some studies conducted on diclofenac showed antibiofilm activity against various bacterial species, including *E. coli, S. aureus,* and *Bacillus*

and *Enterococci spp.*. Ibuprofen demonstrated bacterial growth inhibition for *E. coli and S. aureus* at therapeutic concentrations. In addition, it was showed that diclofenac could downregulate the expression of some genes related to some efflux pumps (e.g., *mepRAB* and *emrAB/qacA*), and some of the adherence genes like *asa1* and *efeA* and interferes with DNA synthesis, suggesting a multi-target antibacterial effect (Dastidar et al., 2011; Mazumdar et al., 2021). Acetylsalicylic acid has been studied for its antibacterial effect, showing impacts on certain virulence factors of bacteria, such as reduced flagellar production in *E. coli* and *Proteus spp.,* and diminished fibronectin binding in *S. aureus* (A. Barbarossa et al., 2022). Also, ibuprofen has shown growth inhibitory effects and antibiofilm activity against *E. coli, S. aureus* and *P. aeruginosa* at therapeutic concentrations. It was found that this could be a result of disruption of some of the genes responsible for quorum sensing like *lasI, lasR, pqsR,* and *pqsA*) in *P. aeruginosa* and *icaA* in *S. aureus* (Alzahrani & Alzahrani, 2025). Generally, it has been found that the NSAIDs' effects on bacterial cells may be due to alterations in gene expression or a reduction in the production of virulence factors such as hemolysin, elastase, protease, pyocyanin, teichoic acid, and urease in various bacterial species (Lagadinou et al., 2020).

In addition to NSAIDs, local anaesthetics such as lidocaine, bupivacaine, and ropivacaine have shown some antibacterial effects against different Gram-positive and negative bacteria like *E. coli, S. aureus*, *P. aeruginosa, Enterococci spp., Listeria monocytogenes, Bacillus spp.* and *Mycobacterium smegmatis*. The exact mechanism of action is still under investigation; however, there are some proposed mechanisms including their effects on the electrical potential of the cytoplasmic membrane (Begeç et al., 2007; Mutlu, 2018).

Phenothiazine,antipsychotics, like chlorpromazine and trifluoperazine have been investigated for their antibacterial effects, demonstrating promising results against Gram-positive cocci like *S. aureus* and *Streptococcus spp.* and some Gram-negative rods like *E. coli Salmonella* and *Vibrio spp.*. This activity was observed at concentrations exceeding the highest physiological levels in plasma; thus, they cannot be utilised as antibacterials on their own. However, they may enhance the efficacy of antimicrobial agents when used in combination. Their synergistic effect may result from the inhibition of certain efflux pumps. Phenothiazines could inhibit efflux systems belonging to the MFS and ABC transporters. In addition, it is found that they could disrupt the membrane potential, causing the collapse of the proton motive force, which depletes energy in bacterial cells (Grimsey & Piddock, 2019; Mohiuddin et al., 2022).

Antidepressants, including the main groups of Serotonin Reuptake Inhibitors (SSRIs) such as sertraline and fluoxetine, as well as tricyclic antidepressants like amitriptyline, have been studied for their antimicrobial properties. It has been found that they affect a wide range of bacteria, including *S. aureus,*

Enterococcus, P. aeruginosa, and *E. coli.* The suggested mechanism involves the inhibition of efflux pumps particularly those belonging to the major facilitator superfamily MFS and RND efflux systems, leading to a synergistic effect with certain antibiotics such as tetracyclines and fluoroquinolones against various antibiotic-resistant strains. In addition to efflux inhibition, some antidepressants have been shown to alter membrane integrity further contributing to their antibiotic-adjuvant activity (Bohnert et al., 2011).

Cetirizine, an antihistaminic drug, has been the subject of several studies regarding its antibacterial effect. In one study, it exhibited inhibitory effects when tested against different bacterial strains from both Gram-positive and Gram-negative groups including *S. aureus*, a few *Bacillus spp*., one *Enterococcus*, several *E. coli*, several *V. cholerae*, several *Shigella spp.*, and many *Salmonella spp* (Maji et al., 2017). Additionally, it is reported that loratadine, another antihistaminic, can significantly potentiate the activity of β-lactam antibiotics and vancomycin against *S. aureus*, including MRSA and VRSA strains. Loratidine also showed notable antibiofilm activity against those species. It was suggested that loratidine targets resistance mechanisms specific to *S. aureus* like the regulatory serine/threonine kinases involved in biofilm formation and antibiotic resistance (Cutrona et al., 2019).

Interestingly, statins, including atorvastatin and simvastatin, long-term treatments for hypercholesterolemia, displayed antibacterial activity against a broad range of microorganisms. Reported susceptible organisms include several Gram-positive pathogens such as *S. aureus* (including MRSA), *S. epidermidis*, *E. faecalis*, and *S. pneumoniae*, as well as certain Gram-negative species including *E. coli, K. pneumoniae, P. mirabilis,* and *A. baumannii* (Masadeh et al., 2012). Some studies also reported their effect on the reductions of biofilm formation (Graziano et al., 2015). The proposed mechanisms underlying these observations include interference with bacterial cell surface structures such as cell wall teichoic acids and lipoteichoic acids and lipopolysaccharides (Ko et al., 2017).

In brief, there are many classes of pharmaceutical drugs that have been studied for their antimicrobial effects. They exhibit different mechanisms and synergistic effects with existing antibiotics. In addition to these classes, there is the antidiabetic drug metformin, which has demonstrated some antimicrobial activity in recent years. Due to the heightened vulnerability of diabetic patients to bacterial infections, they are treated with antibiotics at a higher rate than non-diabetic individuals; consequently, this increases the prevalence of MDR bacteria among diabetics (Toniolo et al., 2019). Therefore, the antibacterial effect of metformin was the focus of this study. So, before digging into the information about metformin, it would be important to highlight the vulnerability of diabetic patients to bacterial infections.

1.3. Bacterial infection and diabetic patients

Diabetic patients are more vulnerable to bacterial infection due to the dysfunction of the immune system. Hyperglycemia decreases the production of interferon-I and interleukin-II which impacts immunity by decreasing the antimicrobial effect and affecting the mucosal barrier of the Gastrointestinal tract (GIT). This could be explained by that interferon-I and interleukin-II have antimicrobial activity, in addition to the preservation effect of interleukin-II to the intestinal barrier which acts as a defence barrier to harmful things like microorganisms. Moreover, the uncontrolled glycemic level causes the downregulation of the macrophages and impairment of their function (Toniolo et al., 2019). Also, it was found that the degranulation of polymorphonuclear cells could occur in diabetic patients and this led to their dysfunction, the absence of the C4 component of the complement system and decreased the level of cytokines (Casqueiro et al., 2012).

Other than the effects of poor glycemic control, diabetic patients may be predisposed to get infectious diseases because of the complications of diabetes itself. For instance, one of the main complications of diabetes is neuropathy, which may cause impairment in the bladder emptying resulting in an increase in urinary tract infections. Besides, the presence of complications in peripheral vascular systems with neuropathy may result in increasing the probability of skin ulcers and infections (Simonsen et al., 2015).

One of the most crucial skin infections resulting from diabetes is the diabetic foot infection, which is typically caused by *S. aureus* or *S. epidermidis*. Another bacterial infection caused by *E. coli* can lead to necrosis of the renal tissue, with this pathogen being the most prevalent, followed closely by *Klebsiella spp. P. aeruginosa* can result in severe otitis externa in diabetic patients, potentially reaching the skull base and affecting nearby regions, with around 50% of patients experiencing facial paralysis (Casqueiro et al., 2012). Therefore, investigating the antidiabetic drug metformin may provide significant assistance to these patients in controlling the bacterial infections, which could be multi-drug resistant and lead to more complicated conditions.

1.4. Metformin

1.4.1. History and Discovery

Metformin is a synthetic compound derived from the herbal compound galegine, which is extracted from the plant *Galega officinalis*. It was discovered in the 1920s that galegine, an isoprenyl derivative of guanidine, can reduce blood glucose levels; however, this compound was found to be highly toxic and cannot be used as a drug. During the same period, metformin was synthesised as a biguanide derivative of galegine (Figure 1-3), and its hypoglycaemic effect has been studied (Nasri & Rafieian-Kopaei, 2014; Rena et al., 2017). Metformin was not used for a significant time until 1957, when its efficacy was confirmed (Nasri & Rafieian-Kopaei, 2014). In 1958, it was approved for use as an antidiabetic drug in

the United Kingdom and in 1995 in the United States. The ADA association has classified metformin as the first-line treatment for type 2 diabetes mellitus (Wang et al., 2017).

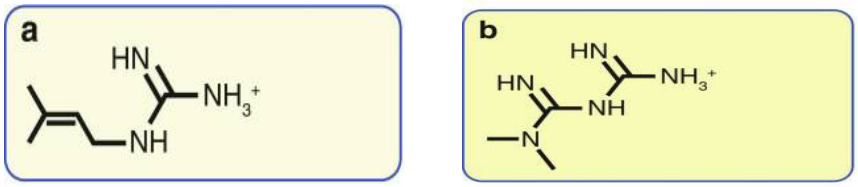

Figure 1-3: Chemical structures of galegine and metformin.
Where (a)galegine, (b)metformin (Rena et al., 2017).

1.4.2. Dose and pharmacokinetics

Metformin is typically administered as oral tablets with a dosage of 500 to 2500 mg per day, based on the patient's glycemic control and therapeutic response (Wang et al., 2017). Approximately 70% of the oral dose is fully absorbed from the intestine (Rena et al., 2017). Furthermore, most of the absorbed metformin is excreted unchanged through renal excretion, as it is not subject to hepatic metabolism (Gong et al., 2012). The metformin concentration in plasma ranges reported to be from 1-113 mg/L, with an average therapeutic concentration of 1-2 mg/L; however, it has been noted that the concentration of the drug is over 30-300 times higher in tissues such as the liver, intestine, and kidneys (J.-D. Lalau et al., 2011; Lee et al., 2021).

1.4.3. The mechanism of action of metformin in the human body

1.4.3.1. Hepatic mechanism of action

The blood glucose-reducing effect of metformin arises from multiple mechanisms of action. The most significant is the reduction of hepatic gluconeogenesis. This occurs through metformin's action on the mitochondria by inhibiting complex 1 in the respiratory chain reaction; thus, it suppresses ATP production, which is essential for glucose production (Rena et al., 2017). Additionally, it has been found that metformin can inhibit the glycerophosphate shuttle in the mitochondria by suppressing glycerophosphate dehydrogenase (mGPD), affecting the oxidation of NADH, and consequently reducing gluconeogenesis while increasing lactate production instead (Madiraju et al., 2014). Furthermore, it was discovered that metformin can activate AMP-activated protein kinase (AMPK) in the cell, a cellular energy sensor. When cellular energy decreases, indicated by rising AMP: ATP and ADP: ATP ratios, AMPK is activated to restore depleting metformin (Agius et al., 2020). A schematic representation of these mechanisms is provided in (Figure 1-4).

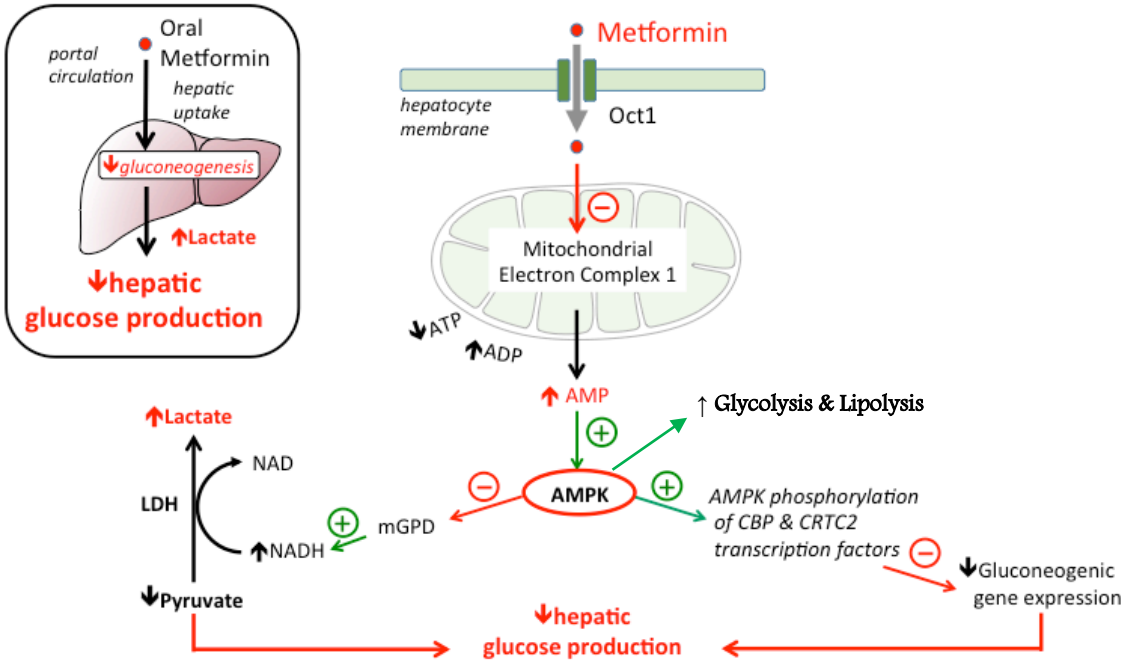

Figure 1-4: The effect of metformin on hepatocytes.
Where (+) indicates the stimulatory effect of metformin, and (-) indicates its inhibitory effect (Pearson et al., 2007b as cited in (Sarah et al., 2020)).

1.4.3.2. Intestinal mechanism of action

It has been found that the acute effect of metformin upon oral administration results from its impact on enterocytes, enhancing their anaerobic metabolism and preventing glucose uptake from the intestine into the bloodstream by influencing certain transporters on the surface of the cells. Normally, glucose enters the enterocytes from the lumen through Na(+)/glucose co-transporter, also known as Sodium-glucose transport proteins (SGLT1), which are located on the apical surface of the enterocytes, and is transported into the bloodstream through uniporter glucose transporters 2 (GLUT2), found on the basolateral membrane (Figure 1-5) (Lee & Cha, 2018). It has been discovered that metformin increases the expression of SGLT1, thereby enhancing glucose uptake into enterocytes, while it translocates some GLUT2 to the apical surface instead of the basolateral membrane, which reduces glucose transport into the blood (Horakova et al., 2019). Additionally, metformin has been found to increase the secretion of GLP-1, which regulates the blood sugar level by stimulating of the insulin secretion (Rena et al., 2017).

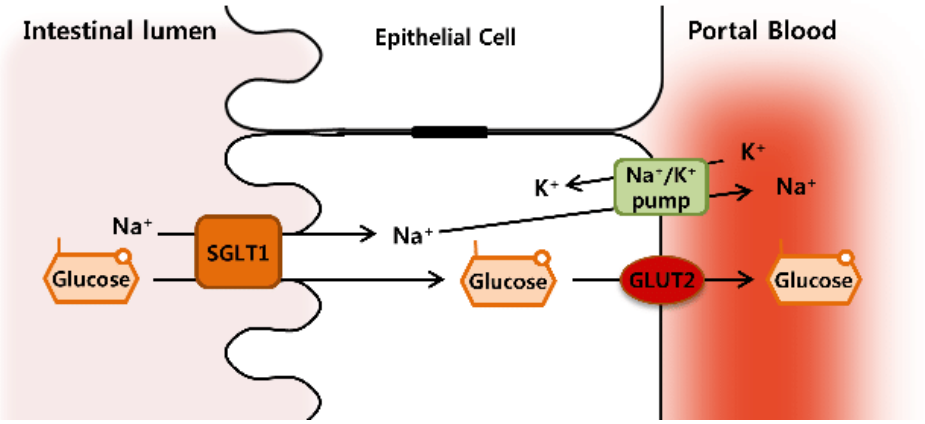

Figure 1-5: The transportation of glucose through the enterocytes.
Where it depends on SGLT1 and GLUT2 transporters to move from intestinal lumen to blood (Lee & Cha, 2018).

1.4.4. Side effects and Safety

While metformin is beneficial for the treatment of diabetes, it can cause adverse effects; some of them are common and mild like gastric upset, nausea, vomiting, and diarrhoea, while the most serious and rare one is lactic acidosis, which is estimated to be 1 in 30,000 patients taking metformin (Nasri & Rafieian-Kopaei, 2014; Wang et al., 2017). The symptoms of lactic acidosis include GIT symptoms, muscle ache, difficulty in breathing, drowsiness and paleness of skin. However, it was found that metformin is safe in pregnancy; despite the effect of pregnancy on its pharmacokinetics, it is the safer choice for gestational diabetes (Nasri & Rafieian-Kopaei, 2014; Wang et al., 2017).

1.5. Non-glycemic Applications of Metformin

Some researchers are beginning to regard metformin as a 'wonder drug', which means it has been discovered for a specific condition; glycemic control in diabetic patients (Clyne, 2014). However, many studies have shown that it possesses other clinical properties with proposed mechanisms of action. One of these effects is its anti-ageing effect, which relates to its activation of AMPK, which then inhibits the mammalian target of rapamycin (mTOR) pathway, a key regulator that is responsible for cell growth and ageing processes (Cheng et al., 2022). Through AMPK activation at around 5 μM, metformin enhances mitochondrial function, reduces oxidative stress, and promotes autophagy, all of which contribute to improved cellular health and longevity. Additionally, it has been found that metformin could protect telomeres, the chromosome-end structures that shorten with age, which helps increase lifespan (Foretz et al., 2023; Soukas et al., 2019).

Metformin could have also some anticancer effects, indicating its potential use in combination with other anticancer drugs to enhance their efficacy. This was observed in epidemiological studies that showed reduced cancer incidence and improved survival in diabetic patients treated with metformin (Decensi et al., 2010). Mechanistically, this could be explained by its activation of AMPK and the subsequent inhibition of mTOR signalling, which relates to tumour progression. The activation of AMPK may inhibit fatty acid synthesis, and it is known that cancer cell proliferation depends on the presence of fatty acids. Moreover, metformin can also induce the production of reactive oxygen species (ROS) as a result

of inhibiting the mitochondrial respiratory-chain complex I, potentially leading to DNA damage in tumour cells (Zhu et al., 2024). It is notable to mention that the *in vitro* concentrations having the anticancer effects are in millimolar concentrations, which are quite higher than the physiological concentrations (Aljofan & Riethmacher, 2019). This could be explained by the presence of some growth factors that suppress the metformin metabolic stress (Menendez et al., 2012). Also, as mentioned before, metformin needs OCT transporters to enter the cells, and these are not present in the *in vitro* cell lines, so it needs high extracellular concentrations to achieve its effect (Chowdhury et al., 2016).

Metformin has shown some anti-inflammatory effects which could be efficient as a therapeutic relevance in chronic inflammatory, autoimmune, metabolic, and fibrotic diseases. There are some studies showing that metformin could modulate multiple pro-inflammatory cytokines, including TNFα (Tumour necrosis Factor), IL-6 (Interleukin), and TGFβ (Transforming Growth Factor) by suppressing their expression and downstream signalling (Sakata, 2024). In addition, metformin has been reported to target NF-κB (Nuclear factor-κB), which is an important transcriptional factor that plays role in many chronic inflammatory diseases, and by the binding of metformin to this factor causing the inhibition of its inflammatory effect (Sakata, 2024).

Metformin has demonstrated significant cardioprotective effects independent of its glucose-lowering action, through activation of AMPK, which improves endothelial nitric oxide production, reduces oxidative stress, and limits inflammatory signalling (Rena et al., 2017). Some studies showed that metformin could reduce myocardial infarct size and improves the heart recovery following ischemia–reperfusion injury through AMPK-dependent pathways and this could happen even at normal glucose levels (Calvert et al., 2008; Lexis et al., 2012).

Due to metformin's effect on fatty acid synthesis and the regulation of lipogenesis, it has been found that metformin could lower body weight in both diabetic and non-diabetic patients. It has also been shown that metformin could affect the gut microbiome (which will be discussed in the next section), increasing insulin sensitivity, aiding in its effect for obesity, and this is the same proposed mechanism behind its off-label use in the treatment of polycystic ovaries (Ziqubu et al., 2023). Due to these effects as well, metformin was found to have potential benefits in non-alcoholic fatty liver disease and metabolic dysfunction–associated fatty liver disease. And there are some clinical studies showed improvements in ALT/AST (liver enzymes) levels, insulin resistance, and metabolic parameters in fatty liver patients treated with metformin (Y. Huang et al., 2022).

1.6. Metformin and bacteria

1.6.1. Metformin and the gut microbiome

Some studies have indicated that the microbiome may play a role in the therapeutic effect of metformin. They have found that metformin can increase the number of *Akkermansia muciniphila* both *in vivo* and *in vitro* and can be considered a growth factor for *Akkermansia*; it was found to be increased by around 18-fold after using metformin (Lee & Ko, 2014). It has been established that *Akkermansia* spp. enhance the production of short-chain fatty acids, which may help improve the integrity of the mucin layer in the intestine, thereby strengthening the mucosal barrier. Furthermore, it can decrease insulin resistance by reducing the transport of lipopolysaccharides that inhibit insulin signalling; moreover, it can improve glucose homeostasis and control lipid metabolism, thus playing a role in the treatment of type 2 diabetes (de la Cuesta-Zuluaga et al., 2017). Furthermore, metformin stimulates the gut microbiome to increase the production of butyrate and propionate, which reduce hepatic glucose production and assist in energy homeostasis; besides, it contributes to a reduction in appetite and weight (Forslund et al., 2015). Conversely, it has been noted that metformin decreases the diversity of the microbiome by diminishing the prevalence of certain species in the family *Peptostreptococcaceae*, one of which is *Intestinibacter spp.* A high level of bacteria belonging to this family is correlated with health issues such as ulcerative colitis and colorectal cancer. These changes in microbiome diversity may suggest that metformin could positively influence the potentially unfavourable composition of the human gut microbiome (Elbere et al., 2018).

Other impacts on microbial bacterial diversity have also been identified. Many studies have found that *E. coli* and *Shigella* species are increased, where they are considered pathogenic organisms and are responsible for the gastrointestinal side effects of metformin. As these species could produce hydrogen sulphide during their proliferation, it may cause bloating as a result of metformin. It is thought that the effect of metformin is indirect in altering the prevalence of these pathogens by improving their growth competitiveness through a decrease in the abundance of other competitor species, resulting in an increase in those species (Elbere et al., 2018; Ezzamouri et al., 2023). Kim *et al.* (2024) suggested that one of the other side effects of using metformin and the rise in this bacterium could be an increase in antibiotic resistance genes, particularly the multidrug-resistant efflux pumps such as the *acr, emr, tolC,* and *mdt* (Kim et al., 2024). Furthermore, there is a study that showed metformin could enhance vitamin B12 accumulation in intestinal *E. coli* as a result of the overexpression of their transporters in the bacteria. This may explain the side effect of metformin in causing vitamin B12 deficiency in diabetic individuals (Yao et al., 2023).

The effect of metformin on the liver and GIT is summarised in (Figure 1-6).

.

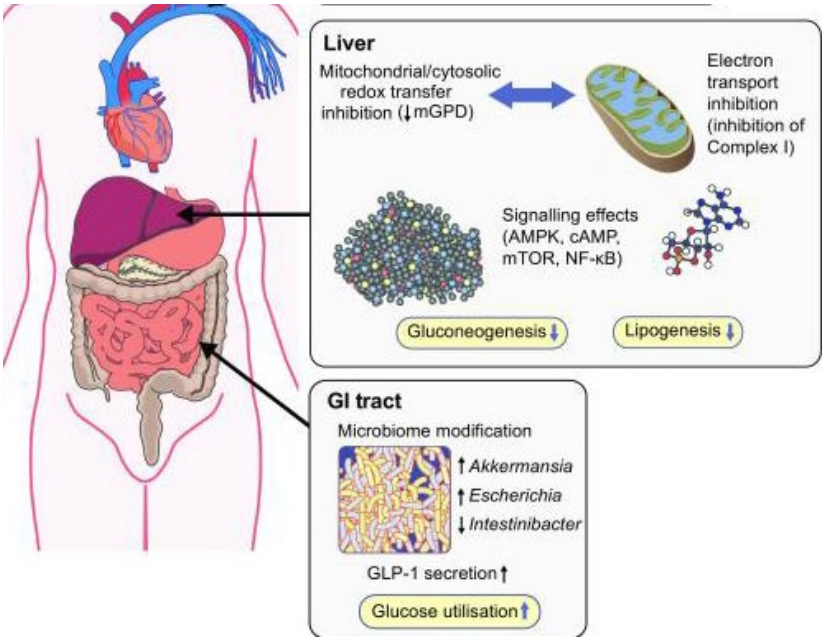

Figure 1-6: Summarizing the action of metformin on liver and GIT.
Where it decreases the hepatic gluconeogenesis and lipogenesis, and increases glucose utilisation (Rena et al., 2017).

1.6.2. Antibacterial effect of metformin

In the last few years, there has been a growing interest in the antimicrobial effects of metformin and how bacteria respond to it. This interest is mainly driven by the global antibiotic resistance crisis and the growing focus on drug repurposing as a strategy to identify non-antibiotic compounds with antimicrobial or resistance-modifying activity. Metformin is of particular interest due to its long-standing clinical use, favourable safety profile, and its effects on cellular metabolism, which suggests that it may influence bacterial physiology either directly or indirectly through host-mediated mechanisms (Table 1-1).

Meherunisa *et al* (2018) studied the antibacterial effect of metformin on various multidrug-resistant bacteria, including Gram-positive organisms like *S. aureus* and Gram-negative bacteria such as *P. aeruginosa, E. coli, Salmonella paratyphi,* and *Vibrio parahaemolyticus*. Using standard susceptibility testing methods, they found that metformin had a significant inhibitory effect against these genera at a concentration of 50 mg/mL (Meherunisa et al., 2018). While these findings suggest that metformin can directly inhibit bacterial growth *in vitro*, the concentration required to achieve this effect is rather higher than the physiological concentrations as mentioned in Section 1.4.2. Therapeutic plasma levels of metformin are generally in the micromolar range, highlighting a major limitation in translating these findings directly to *in vivo* antimicrobial efficacy.

The nature of metformin's antibacterial activity has been further explored by Cabriero *et al.* (2013), who suggested that metformin is a bacteriostatic agent rather than bactericidal, based on their investigation of its effect on inhibiting *E. coli* growth by coculturing it with the nematode worm, *Caenorhabditis*

elegans. Generally, the worm's elementary canal can become blocked through the proliferation of *E. coli* within it. Therefore, it was found that metformin could help increase the worm's lifespan by disrupting the folate metabolism cycle of the bacteria. It is estimated that metformin acts similarly to the antibiotic trimethoprim by inhibiting dihydrofolate reductase (DHFR), leading to an increase in dihydrofolate and 5-methyl tetrahydrofolate. Consequently, this will decrease the synthesis of important compounds such as purines and pyrimidines (in DNA synthesis) and methionine (Cabreiro et al., 2013). However, it is important to note that direct inhibition of bacterial DHFR by metformin has not been universally demonstrated, and the exact proposed mechanism remains subject to debate.

Vashisht & Brahmachari (2015) claimed that metformin can be used in combination with the first-line antibiotics for *Mycobacterium tuberculosis* (*Mtb)* treatment because metformin typically inhibits mitochondrial complex I, resembling the structure and function of the bacterial respiratory chain complex – I (NDH-I). This provides solid evidence that metformin could inhibit NDH-I and aids in the eradication of *Mtb* (Vashisht & Brahmachari, 2015). However, it remains challenging to confirm the effect of direct inhibition of bacterial respiratory components from indirect effects. Therefore, more studies on the effect of metformin on the membrane potential and proton motive force quantitatively were performed on *E. coli* and *K. pneumoniae* strains, where the effective concentrations were in the range of 2.5 - 20 mg/mL (Jiang et al., 2023; Y. Xiao et al., 2022; Ye et al., 2021).

The host-mediated antimicrobial effects of metformin have been more directly investigated by Singhal *et al.* (2014), who examined whether metformin-induced activation of AMPK could inhibit the growth of intracellular *Mtb* within macrophages. AMPK plays a crucial role in various metabolic processes within human cells. One of these cells are the macrophages, where AMPK enhances the production of mitochondrial reactive oxygen species (mROS) and stimulates the autophagy process, thereby increasing their antimicrobial effect. Singhal *et al.* showed that metformin treatment caused a signifcant inhibtion of the intracellular *Mtb* growth in macrophages, improved the lung inflammation and increase the efficacy of the conventional antituberculosis drugs (Singhal et al., 2014). This finding is particularly significant as intracellular pathogens are often escaped from conventional antibiotics, and host-directed strategies may offer an alternative means of controlling infection.

Metformin has been shown to potentiate the activity of conventional antibiotics and reverse bacterial resistance. Liu *et al.* (2020) discovered that metformin could re-sensitise doxycycline-resistant *E. coli* strains carrying the tetracycline resistance gene *tet*A. This can be explained by metformin displacing Mg^{2+}, which stabilises the outer membrane that is highly impermeable to many antibacterials, especially in the presence of efflux pumps such as that encoded by *tet*A. Therefore, metformin disrupts the outer membrane, allowing greater access to the antibiotic. In addition, metformin inhibits some efflux pumps

by decreasing their expression, particularly the genes responsible for ABC transporters. Both effects result in the accumulation of doxycycline inside the bacterial cells and potentiate its effect (Liu et al., 2020a). Notably, similar mechanisms have been reported across multiple Gram-negative pathogens, suggesting that membrane disruption and efflux inhibition represent recurring themes rather than isolated observations. Abbas *et al.* (2021) showed that metformin could inhibit the efflux pump of AcrAB and TolC in *K. pneumoniae,* which exhibited increased susceptibility to different antibiotics (Abbas et al., 2021a). Moreover, Xiao *et al.* (2022) suggested that metformin could restore the resistance of *K. pneumoniae* to tigecycline through its combination with metformin, due to the disruption of the membrane potential and inhibition of the efflux pumps, which consequently increases the accumulation of the drug within the cells and enhances bacterial susceptibility (X. Xiao et al., 2022). The same finding was observed by Guo *et al.* (2022) in *A. baumannii* regarding the restoration of susceptibility to minocycline through its combination with metformin, attributed to its effect on membrane potential and outer membrane integrity (Guo et al., 2022). Across these findings, it is notable to mention that the metformin concentrations used were gnerally in millimolar range and mostly at the MIC level or higher. Therefore, it is crucial for more investigation as to whether metformin causes the efflux inhibition directly or it is a more generalized effect due to the effect on the proton motive force. Further support for metformin's potential as an adjunct therapy was revealed through a study conducted by Valadbeigi *et al.* who showed that metformin could have a synergistic effect with amoxicillin against *H. pylori* (Valadbeigi et al., 2023).

Beyond growth inhibition and antibiotic potentiation, metformin has also been shown to impact bacterial virulence. In contrast to conventional antibacterial agents that primarily target bacterial growth or viability, antivirulence drugs aim to attenuate pathogenicity by disrupting the expression of virulence factors without necessarily inhibiting bacterial proliferation (Rasko & Sperandio, 2010). In this context, metformin has been reported to interfere with some quorum-sensing systems that regulate the bacterial virulence factors. Abbas *et al.* (2017) discussed that metformin has a quorum-sensing inhibitory effect, which blocks many virulence factors of *P. aeruginosa,* such as motility and biofilm formation, along with the inhibition of certain excreted substances like elastase, protease, haemolysin, and pyocyanin. Generally, one of the primary mechanisms by which bacteria regulate the production of virulence factors is quorum sensing, which serves as a signal between bacterial cells based on their numbers and environmental conditions. It has been found that metformin competitively binds to the LasR and RhlR receptors through hydrogen bonds. Consequently, quorum sensing is inhibited, resulting in reduced production of virulence factors (Abbas et al., 2017). The same research group has investigated the effect of metformin on the virulence factors of *K. pneumoniae,* which showed an inhibitory effect on several of these factors, including biofilm, protease, urease, and haemolysin, as well as downregulation of their corresponding genes (M. Shafik et al., 2023). Chadha *et al.* (2023) confirmed these findings through the

downregulation of various quorum-sensing *genes (*like *pqsA/pqsR, rhlI/rhlR, and lasI/lasR*) and virulence genes (like *lasA, lasB, toxA, aprA, & plcH),* resulting in the inhibition of virulence factors in *P. aeruginosa* (J. Chadha et al., 2023). In the study by Zuo *et al.* (2023), it was found that metformin could inhibit the biofilm formation of *Streptococcus spp.* and downregulate some of the quorum-sensing genes (Jing Zuo et al., 2023). A study by Ye *et al.* (2022) has shown that metformin could inhibit the flagellar motility of *E. coli*, which is one of the important virulence factors for the bacteria (Ye et al., 2022). However, while antivirulence effects may reduce infection severity, the long-term consequences on the bacterial regulatory networks need to be more investigated.

Garnett *et al.* (2013) were the first to discuss the effect of metformin on the growth of a MRSA strain causing respiratory infection in a diabetic patient. This was achieved by investigating the effect of metformin through tissue culture of human airway epithelial cells inoculated with *S. aureus*, as well as employing an animal model. The results revealed that metformin reduces staphylococcal respiratory infections, which can be explained by its ability to decrease the permeability of glucose into the airway system through the activation of AMPK. It is known that *S. aureus* proliferates and its growth increases in the presence of glucose. Therefore, this could be beneficial in reducing the vulnerability of diabetic patients to serious diseases such as chronic obstructive pulmonary disease (COPD) and cystic fibrosis (CF) caused by *S. aureus* (Garnett et al., 2013). It is important here to mention that the observed reduction in staphylococcal burden was not attributed to direct bactericidal activity at supraphysiological concentrations like many previously mentioned *in vitro* studies, but it was due to host-mediated effects of metformin at normal physiological concentrations.

Table 1-1: The proposed antibacterial mechanisms of metformin as a result of metformin on different bacterial genera as found in the literature, arranged in ascending order according to the year of publication.

Name of the bacteria	The Mechanism of the antibacterial effect of metformin	Year	Reference
E. coli	By inhibition of the bacterial DHFR and blocking the MTHFR.	2013	(Cabreiro et al., 2013)
S. aureus	By activation of AMPK, which decreases the permeability of glucose into the airway system, so reduces the staphylococcal respiratory infection.	2013	(Garnett et al., 2013)
M. tuberculosis	By activation of AMPK of the macrophages, which leads to increase of mROS inside and promotes the autophagy that inhibit the growth of the intracellular *Mtb,* so metformin can be used as adjunct therapy.	2014	(Singhal et al., 2014)
M. tuberculosis	By inhibition the bacterial NDH-1 which resembles the mitochondrial complex 1	2015	(Vashisht & Brahmachari, 2015)
S. aureus, P. aeruginosa, E. coli, S. paratyphi* and *V. parahaemolyticus	Inhibition of the bacterial growth in disc diffusion experiment	2018	(Meherunisa et al., 2018)
E. coli	By disruption to the outer membrane and inhibition of efflux pumps so increase the susceptibility to doxycycline	2020	(Liu et al., 2020)
K. pneumoniae	By inhibition of the efflux pump of AcrAB and TolC so has synergestic effect with different antibiotics	2021	(Abbas et al., 2021)
K. pneumoniae	By the disruption of the membrane potential and inhibition of the efflux pumps, so could restore the resistance to tigecycline	2022	(Xiao et al., 2022)
A. baumannii	By the disruption of the membrane potential and outer membrane integrity, so could restore the resistance of towards minocycline.	2022	(Guo et al., 2022)
E. coli	By inhibition of the flagellar motility and swimming	2022	(Ye et al., 2022)
H. pylori	Synergistic effect with amoxicillin	2023	(Valadbeigi et al., 2023)
Streptococcus spp.	By inhibition of the biofilm formation and downregulate some of the quorum-sensing genes	2023	(Zuo et al., 2023)
P. aeruginosa	By inhibition of the quorum sensing through inhibition of some virulence factors of like motility and biofilm formation and some excreted substances.	2017 & 2023	(Abbas et al., 2017; Chadha et al., 2023)

In conclusion, the antibiotic resistance crisis is a pivotal issue today, particularly for more vulnerable individuals such as diabetic patients, due to the impact of diabetes on their immunity. Therefore, it is essential to explore solutions to this crisis, including non-antibiotic antimicrobial agents like metformin. Previous studies suggest that metformin can affect bacterial growth, physiology, virulence, and other antibiotic susceptibilities through both direct and host-mediated mechanisms. While these findings demonstrate the potential of metformin as an adjunct antimicrobial agent, they also raise important concerns about the consequences of long-term exposure of bacteria to this drug, particularly at sub-inhibitory, physiological concentrations. Such exposure may exert selective pressures that promote bacterial adaptation, stress responses, and potentially the emergence of reduced susceptibility or cross-resistance to conventional antibiotics. However, the extent to which these effects occur, the molecular mechanisms behind bacterial responses to metformin, and their clinical relevance remain insufficiently understood. These knowledge gaps form the basis of this thesis, which aims to further investigate and clarify the mechanism of metformin as an antibacterial agent and whether its use may eliminate or contribute to the development of antimicrobial resistance.

1.7. Aims and Objectives

Aim

The overall aim of this project is to investigate the crucial impacts of metformin on clinically relevant bacteria like *S. aurues, E. coli, P. aeuroginosa* and *K. pneumoniae* to determine whether it should be used as a new repurposed antimicrobial agent or adjunct therapy or whether its prolonged use may lead to selection for reduced susceptibilty multidrug-resistant bacteria and the potential for this bacteria to develop cross-resistance. Therefore, this study seeks to clarify the molecular and phenotypic bacterial responses to metformin exposure and determine the potential clinical significance of these responses.

Objectives

1. To characterise the inhibitory effects of metformin on the growth, and virulence factors metabolic activity of clinically relevant bacterial species. (addressed in Chapter 3)
2. To evaluate the antibacterial activity of metformin in combination with antibiotics and identify any synergistic interactions. (addressed in Chapter 3)
3. To assess whether physiological concentrations of metformin can select for reduced bacterial susceptibility and identify associated phenotypic and genotypic changes. (addressed in Chapter 4 and 5)
4. To determine whether metformin-induced evolved strains exhibit altered susceptibility to different classes of antibiotics or changes in virulence, indicating potential shared resistance mechanisms. (addressed in Chapter 4)
5. To elucidate the molecular mechanisms underlying metformin's antibacterial activity using transcriptomic and genetic approaches. (addressed in Chapter 5)

CHAPTER 2- Methods

2. Methods

2.1. Bacterial isolates collection

Eight isolates were involved in this study, divided into four genera (*Staphylococcus aureus, Pseudomonas aeruginosa, Escherichia coli,* and *Klebsiella pneumoniae)*, each containing two isolates, all of which were previously identified control strains. They are summarised with their codes in the following table (Table 2-1).

These species were selected due to their clinical significance in diabetic patients. As they are one of the common causes of infection for diabetic people (Maity et al., 2024), it is relevant here for investigating the antidiabetic drug, metformin, against them. In addition, they are from the WHO high-risk group due to their development into multidrug-resistant bacteria (WHO, 2024). Moreover, there is limited information in the literature about the effect of metformin on these genera.

For the strains, these were selected based upon being well characterised and defined control strains that were considered unlikely to have had exposure to metformin, rather than a pool of uncharacterised clinical strains, as the area of studying metformin still has many knowledge gaps regarding its molecular mechanisms and bacterial adaptation. Therefore, using well characterised naive control strains would provide a clear preliminary picture, and in future work, clinical strains could be tested accordingly

Table 2-1 The bacterial strains that were used in this study showing their codes in the culture collection, reference number and their genera

Code	Reference number	Genera
C17	NCTC 10662	*Pseudomonas aeruginosa*
C45	ATCC 27853	*Pseudomonas aeruginosa*
C4	NCTC 10418	*Escherichia coli*
C36	ATCC 25922	*Escherichia coli*
C42	NCTC 6571	*Staphylococcus aureus*
C48	ATCC 25923	*Staphylococcus aureus*
K89	ATCC 700721	*Klebsiella pneumoniae*
K90	ATCC 700603	*Klebsiella pneumoniae*

2.2. Phenotypic assays for bacteria exposed to metformin

2.2.1. Bacterial growth curve analysis

The inhibitory effect of metformin was first investigated by performing growth curves in different concentrations of metformin against the eight different strains in Table 2-1.

A stock solution of metformin was prepared by dissolving 200 mg in 10 mL of sterile distilled water, which was then sterilised by filtration. This solution was diluted in sterile distilled water to produce fourteen different concentrations, resulting in final concentrations for the experiment of 10, 5, 2.5, 1.25,

0.5, 0.25, 0.125, 0.05, 0.025, 0.0125, 0.004, 0.002, 0.0005, and 0.00025 mg/mL. Then, 90 µL of each concentration was distributed into a sterile 96-well microtiter plate.

Overnight cultures of the eight isolates, grown at 37°C for 24 h with shaking at 200 rpm, were normalised in Müller-Hinton broth (MHB) to OD_{600} = 0.1. They were then diluted in double strength MHB in a 1:100 ratio to achieve approximately 10^6 CFU/mL, and then 90 µL of the diluted culture was added to each concentration in the 96-well microtiter plate to reach a final count of 5×10^5 CFU/mL.

Negative controls without the drug and blank without bacteria were included along with the experiment. This experiment was done in three biological replicates (where, for only the controls, there were 4 technical replicates due to the setup of the microtiter plate).

The optical density (OD) was measured every 10 minutes at 600 nm for 16 hours using the FLUOstar® Omega spectrophotometer, with shaking before each reading.

Statistical analysis was performed on the growth curve data for each strain using a repeated-measures ANOVA, followed by Tukey's HSD post hoc test for pairwise comparisons with the control; significance was defined as $p \leq 0.05$ (IBM SPSS Statistics Version 28.0). In addition, the area under the curve (AUC) at each concentration was calculated using the Python v3.9.0 package (numpy.trapezoid). Statistical analysis started with the assessment of data normality using the Shapiro-Wilk test (stats.shapiro), where the data was considered normal with $p > 0.05$. Using the statsmodels library in Python, one-way ANOVA (sm.stats.anova_lm) was performed for each strain, followed by Tukey's HSD post hoc test (pairwise_tukeyhsd) for pairwise comparisons with the control; significance was defined as $p \leq 0.05$. The data was visualised mainly as AUC against the various concentrations tested for all bacterial species, allowing comparison of overall growth across different drug concentrations. Also, it is a presentable way of showing the differences in the drug concentrations, compared to the visualisation using the growth curves themselves. However, selected representative growth curves are plotted as optical density against time to illustrate crucial kinetic features such as lag phase, growth rate, and maximal density.

2.2.2. Minimum inhibitory concentrations (MIC)

The measurement of the minimum inhibitory concentration (MIC) of metformin against various bacterial species was conducted using the broth microdilution method in a 96-well plate according to the Clinical & Laboratory Standards Institute (CLSI, 2015), using the same inoculum preparation as described in the growth curve method explained above in section 2.2.1. The final concentrations were 2-fold dilution from 80 mg/mL to 5 mg/mL. All the plates were incubated at 37°C for 20 hr and the results were

visualised for the least drug concentration that showed an absence of growth. The experiment was performed in three biological replicates.

2.2.3. Virulence factors assays

2.2.3.1. Skimmed milk agar assay for protease activity

To assess the effect of metformin on protease secretion (Abbas et al., 2017) overnight cultures of the eight bacterial strains listed in Table 3-1 were conducted in five universal tubes per isolate. Each tube contained 4 mL of MHB and five different concentrations of metformin (10, 1.25, 0.5, 0.1, and 0.002 mg/mL), along with a negative control for each isolate included in the experiment in drug-free broth.

After incubating for 24 h at 37°C, the cultures were centrifuged at 10,000 rpm for 15 min to separate the supernatants. Subsequently, 100 µL of these supernatants was added to wells created in sterilised 5% skimmed milk agar (composed of 1.5% agar-agar with 5% skimmed milk) using the backside of 1000 µL micropipette tip. The plates were incubated for 24 h at 37°C, and the clear zones indicating the lysis of milk proteins around the wells were measured. The data were plotted as the diameter in mm against the concentrations and analysed using the Kruskal-Wallis test (IBM SPSS Statistics Version 28.0) with Dunn's post hoc test, where significance is defined as $p \leq 0.05$. The experiment was conducted in three biological replicates (n=3).

2.2.3.2. Crystal violet assay for biofilm formation

To investigate the effect on biofilm formation, the optimised method from Stepanovic *et al* (2007) was used. Overnight cultures of the various tested strains were diluted to $OD_{600} = 0.1$ in double-strength (DS) tryptone soy broth (TSB) to achieve 10^6 CFU/mL, which was distributed as 90 µL per well of a sterile 96-well microtiter plate containing 90 µL of different concentrations of metformin, resulting in final concentrations of 10, 1.25, 0.5, 0.1 and 0.002 mg/mL , along with negative control and blank. The plates were then incubated for 24 h at 37°C (Stepanović et al., 2007).

After incubation, the plates were washed using 300 µL of sterile phosphate-buffered saline (PBS). This was followed by drying at 60°C for 1 h for *S. aureus* strains, and using 180 µL methanol added to the microtiter plates for 10 min followed by washing with PBS and air drying until complete dryness in the case of the other tested species.

For biofilm staining, 180 µL of crystal violet was added to each well and left for 15-20 min. Following the removal of the excess of the stain by flipping the plates gently upside down towards the waste and washing with distilled water till clear water from washing, 180 µL 33% glacial acetic acid was added

and left for 30 min. The absorbance was measured using a spectrophotometer at 595 nm. The data were plotted as the absorbance value against the concentration of metformin and analysed using the Kruskal-Wallis test (IBM SPSS Statistics Version 28.0) integrated with Dunn's post-hoc test, where the significance is $p \leq 0.05$. The experiment was conducted in three biological replicates (n=3).

2.2.3.3. Swimming and twitching motility assays

The influence of metformin on the swimming motility for *P. aeruginosa* and *E. coli* isolates was investigated by stabbing without reaching the bottom of the agar of dried swimming plates (1% tryptone, 0.5% NaCl and 0.2% agar) containing different concentrations of metformin (10, 1.25, 0.5, 0.1, and 0.002 mg/mL) with 2 µL of diluted overnight culture in tryptone broth (OD_{600}=0.1), then the plates were incubated at 37°C in upright position for 16-18 h (Abbas et al., 2017; Calvio et al., 2005). After that, the diameters of the swimming zones were measured and plotted against the concentration of metformin.

The effect of metformin on the twitching motility of *P. aeruginosa* and *E. coli* isolates was assessed using the method of Xu & Wozniak (2015) with some modifications. Agar plates made with 10 mL of 1% LB agar containing different concentrations of metformin (10, 1.25, 0.5, 0.1, and 0.002 mg/mL) were inoculated by stabbing to reach the bottom of the plate with 2 µL of diluted overnight culture in LB broth (OD_{600} = 0.1), then the plates were incubated in an upright position for 48 h at 37°C. After incubation, the agar layer was removed carefully, the plates were left for drying, and then the twitching zones attached to the plate were measured (Xu & Wozniak, 2015). The data was plotted as twitching diameters against the concentration of metformin,

Both tests statistically analysed using Kruskal-Wallis test (IBM SPSS Statistics Version 28.0) integrated with Dunn's post-hoc test, where the significance is $p \leq 0.05$. Each set of the experiments was conducted in three biological replicates (n=3).

2.2.4. Ethidium bromide efflux assay

The effect of metformin on efflux was investigated using the optimised ethidium bromide method to achieve the most appropriate fluorometer saturation, either by cell density or ethidium bromide concentration.

Firstly, a boiled overnight culture of *S. aureus* NCTC 6571 was utilised at various concentrations (0-10^5 fold dilution) against different concentrations of ethidium bromide (0.25-50 µg/mL), alongside bacteria-free and dye-free controls. Following this, fluorescence was measured using the FLUOstar® Omega spectrophotometer at excitation and emission wavelengths of 544 and 590 nm, respectively.

Accordingly, the ethidium bromide efflux experiment was conducted using the same isolate alongside the other seven bacterial strains listed in Table 3-1. The process began with inoculating 5 mL of MHB with 100 µL of overnight culture, which was then incubated at 37°C with shaking until it reached the mid-log phase (OD_{600} = 0.6). This was followed by centrifugation at 7,000 rpm, after which the sample was resuspended in PBS to achieve OD_{600} = 0.2. Ethidium bromide was subsequently added to reach a final concentration of 1.5 µg/ml. The mixture was then incubated in the dark at 37°C for 45 minutes, after which it was centrifuged and resuspended in PBS (OD_{600} = 0.2).

Finally, the mixture was distributed as 42.5 µL in a 96-well black sided/clear-bottomed microtiter plate. In the plate contained four different sets. The first set consisted of 7.5 µL of PBS added to the mixture as a control. The second set included 2.5 µL of PBS with 5 µL of a 5% glucose solution to energise the bacterial cells and activate their efflux pumps. The third set comprised 5 µL of the glucose solution combined with 2.5 µL of a 100 mm sodium salicylate solution, serving as a control for the efflux inducer. The final set contained 5 µL of the glucose solution along with 2.5 µL of varying concentrations of metformin (10, 1.25, 0.5, 0.1, and 0.002 mg/mL). The blank in this experiment was represented by wells containing 50 µL of PBS.

The fluorescence was measured using the FLUOstar® Omega spectrophotometer for 1 h with fluorescence (excitation 540 nm, emission 590 nm) recorded at 2 min intervals. The results were plotted as fluorescence against time. The statistical analysis was performed using repeated measures ANOVA, with Tukey's HSD as a post-hoc test, where a significant difference compared to the drug-free medium efflux activity is identified by $p \leq 0.05$. The experiment was done in three biological replicates.

2.3. Checkerboard assay for antibiotic-metformin combinations

To investigate the effect of combining different antibiotics with metformin, the checkerboard assay was employed (Masadeh et al., 2021). This was conducted on eight different bacterial strains Table 2-1 with three antibiotics selected for each strain. For *the P. aeruginosa* and *K. pneumoniae* strains, doxycycline, gentamicin, and imipenem were tested in combination with metformin. For the *S. aureus* strains, doxycycline, linezolid, and ciprofloxacin were chosen for the experiment. For *E. coli,* doxycycline, ciprofloxacin, and gentamicin were tested in the combinations.

The bacterial cultures for the different strains were prepared as previously mentioned in section 2.2.1to achieve a prepared culture with a concentration of 10^6 CFU/mL in DS MHB, reaching a final concentration of 5×10^5 CFU/mL after mixing with the antibiotic solutions.
The concentrations of the antibiotics and metformin were prepared 4x the desired final concentration. In a 96-well plate, metformin was serially diluted two-fold vertically (with the highest concentration in row

A and the lowest in row G), while in another 96-well plate, the antibiotic being tested was diluted two-fold serially horizontally (with the highest concentration in column 1 and the lowest in column 10). Consequently, column 11 contained the metformin-only solution, while row H contained the antibiotic-only solution. The two drugs were then mixed in one plate in a 1:1 ratio, with 25 µL of each well. Subsequently, 25 µL of the prepared culture was added to each well, except for column 12, which represented the blank of a free bacteria medium. For the drug-free negative control, it was the well H11.

Subsequently, the plates were incubated for 24 hours at 37°C, after which the optical density was measured at 600 nm using the Agilent® BioTek Cytation 7 plate reader. The MIC for each antibiotic/metformin alone and in combination was determined by identifying the well that contained the lowest concentration with no growth (its optical density was close to the blank). The fractional inhibitory concentration (FIC) for each antibiotic and metformin for each plate was calculated by this equation:

$$FIC = \frac{MIC\ of\ the\ drug\ in\ combination}{MIC\ of\ the\ drug\ alone}$$

Then the fractional inhibitory concentration index (FICI) was calculated according to the following equation:

$$FICI = FIC_{Antibiotic} + FIC_{metformin}$$

If the FICI average is ≤ 0.5, it is considered synergistic; if 0.5 < FICI ≤ 1, it is additive; if 1 < FICI < 2, it is indifferent; if FICI ≥ 2, it is antagonistic. The experiment was done in two biological replicates.

2.4. Experimental evolution under continuous metformin exposure

2.4.1. Estimation of the minimum evolutionary timeframe

To determine the optimal number of passages for the evolutionary study, this experiment measured the expected generation time for different bacterial strains. Two bacterial strains from the bacterial collection used in this project (Table 2-1) were selected, where one was a representative Gram-negative bacterium, *P. aeruginosa* ATCC 27853, and one representative Gram-positive bacterium, *S. aureus* NCTC 6571.

Overnight cultures in MHB, done in four biological replicates, were prepared for each of the tested bacterial strains. These cultures were subsequently diluted to an OD_{600} of 0.1 in MHB.

Surface viable count was conducted by taking a sample from these diluted cultures, doing serial dilution in PBS and inoculating MHA plates, which were divided into six sectors, with 10 µL for each sector. The plates were then incubated at 37 °C for 24 h, the colonies were counted, and the following equation was applied for calculating the total viable count (time point 1):

CFU/mL = (Average number of colonies per sector × dilution factor) / volume of culture per sector

After incubating the tested cultures at 37 °C for 24 h, another sample from each replicate was serially diluted and a surface viable count was performed as described above (time point 2).

To determine the expected number of mutants generated in one day of incubation, the equation below was used (Pope et al., 2008):

$$r_2 = \frac{\mu}{\ln\left(\frac{N2}{N1}\right)} \times N2$$

Where:

- (μ) is the mutation rate. *S. aureus*, it is 2.8×10^{-4} mutations per genome per generation (Pray, 2008), and for *P. aeruginosa*, it is approximately 5×10^{-4} mutations per genome per generation (Dettman et al., 2016), with considering the genomic sizes of these species are approximately 2.8 Mbp (Pray, 2008) and 6.8 Mbp (Fang et al., 2012), respectively.
- (r_1) is the number of mutants present at time point 1, which is assumed to be 0.
- (r_2) is the number of mutants seen at time point 2, which is the one needed.
- (N1) and (N2) are the number of cells present at time points 1 and 2, respectively, which are counted from the surface viable counts.

The total number of mutations expected per day (from r_2) was then used to calculate the minimum number of days required to accumulate mutations at every base pair:

$$Minimum\ time\ for\ mutation\ per\ genome\ in\ days = \frac{Genomic\ size\ (bp)}{r_2}$$

And this time was used as a minimum time to perform the evolutionary experiment.

2.4.2. Evolution experiment in a therapeutic concentration of metformin

To study the effect of continuous exposure to metformin on different bacterial species, this experiment was conducted on the two selected bacterial strains that were continuously exposed to a selected physiological concentration of metformin.

Overnight cultures in MHB were prepared for two bacterial strains: one *P. aeruginosa* and one *S. aureus,* in six biological replicates represented as parallel cultures originating from the same ancestral population. Each culture was normalised in MHB to an OD_{600} of 0.1, which was used to inoculate the experimental evolution lines.

For each biological replicate, two experimental conditions were established: a drug-free control and a metformin-exposed condition. Each condition consisted of a tube containing 10 mL of MHB only, representing the control (C), and the other contained 10 mL of MHB with 1.25 mg/mL of metformin (D). From each normalised replicate, 100 µL was inoculated in each of control and drug tubes in the

corresponding experimental set yielding paired control-evolved and drug-evolved lines originating from the same ancestor.

Each independently evolved population was assigned an identifier: metformin-exposed lines were assigned as Met-R1 to Met-R6, and drug-free control lineages were assigned as Ctrl-R1 to Ctrl-R6, where R indicates independent biological replicates.
All the tubes were then incubated at 37 °C for 24 h while shaking at 180 rpm. This passage was repeated 18 times, and after each passage, 1 mL of each culture was stored in a cryotube containing a final concentration of 20% glycerol at -80 °C (Figure 2-1).

For downstream analyses, frozen stocks from the final passage were recovered by streaking onto MHA plates and incubated at 37 °C for 24 h. Colonies from these plates were then used to inoculate fresh liquid cultures, which served as the starting material for all subsequent experiments.

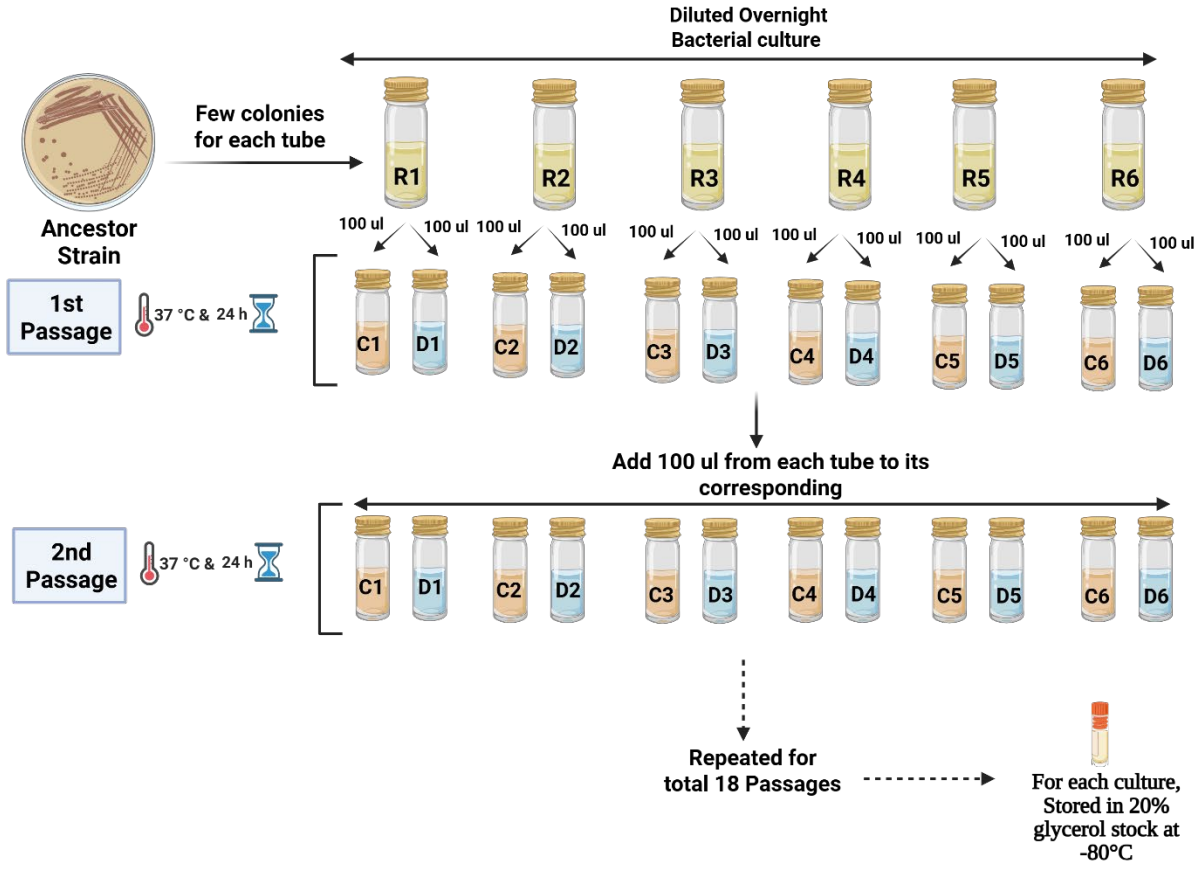

Figure 2-1 : Illustration of the laboratory evolutionary experiment using continuous exposure to metformin. Where R represents the biological replicates from the ancestor strain, C represents the control without the drug, and D represents the presence of 1.25 mg/mL metformin. Created in https://BioRender.com.

2.4.3. Phenotypic characterisation of metformin-evolved populations

2.4.3.1. Bacterial Growth curves and MICs

2.4.3.1.1. Growth curves and MIC determination for metformin

The alterations in the inhibitory effect of metformin on the drug-exposed evolved lines, following continuous exposure compared to the ancestors and controls, were initially examined using the growth curve method.

The experiment was conducted as previously mentioned (in section 2.2.1), where the final concentrations of metformin were 10, 5, 2.5, and 1.25 mg/mL, along with the negative control and blank as those were mainly the concentrations that showed significance in most of the whole set of the previously tested strains, so they were selected to assess for any changes after the evolutionary experiment.

This experiment was conducted in three biological replicates. The statistical analysis of the growth curves was done as in section 2.2.1**.**, in addition to the calculation of the AUC for each sample. The statistical analysis for the AUC data began with an assessment of the normality of the data using the Shapiro-Wilk test (stats.shapiro), where it was considered normal with $p > 0.05$. This was followed by pairwise comparisons at each concentration between the drug and control evolved lineages using an unpaired t-test (stats.ttest_ind), with significance indicated by $p \leq 0.05$. All statistical analyses were performed using Python v3.9.0 along with its SciPy package. The data was visualised using both growth curves as OD_{600} against time and as AUC against the various concentrations tested for all different the drug-evolved populations paired with their corresponding controls.

The MICs of metformin for all the drug and control evolved lines were tested as mentioned in section **2.2.2.**

2.4.3.1.2. Growth curves and MIC determination for other antibiotics

Using the growth curve method, the changes between the drug- and control-evolved populations, and the ancestor strain growth were investigated in the presence of different concentrations of some selected antibiotics. The experiment was done as mentioned before in section **2.2.1** where for each antibiotic, ten concentrations were tested, starting with the highest concentration in the first column and then 2-fold serially diluted concentrations. For the *P. aeruginosa* strains, the experiment was performed using colistin, ceftazidime, gentamicin and ciprofloxacin. For *S. aureus* strains, the experiment was done using erythromycin, doxycycline, linezolid, ciprofloxacin, gentamicin and vancomycin.

The AUC for each sample at each concentration was calculated and plotted as mentioned in **2.4.3.1.1.** This experiment was done in one biological replicate due to time constraints; therefore, the results should be interpreted cautiously, as statistical analysis was limited. Therefore, to understand the change pattern

in the different antibiotics tested across the different drug-evolved populations, the proportional AUC for each antibiotic was calculated as following:

$$proportional\ AUC = \frac{AUC_{drug-evolved}}{AUC_{control-evolved}}$$

Therefore, if:

proportional AUC >1, the AUC drug-evolved is larger than the control-evolved.

proportional AUC< 1, the AUC drug-evolved is smaller than the control-evolved.

proportional AUC=1, the AUC drug-evolved is equal to control-evolved.

Then, the proportional AUC for all six drug-evolved lineages for each antibiotic was plotted together as a box plot, where the x-axis was the different concentrations tested, and the y-axis was the proportional AUC. The statistical analysis was done using Python v3.9.0 with its package of SciPy starting with checking the normality of the data checked using the Shapiro-Wilk test (stats.shapiro), where it was considered normal with $p > 0.05$. Then, it was tested to find if it was significantly different than 1 (AUC drug-evolved is different than control in either way; more or less) using one-Sample t-test (stats.ttest_1samp) if the data at the tested concentration was normal, or Wilcoxon Signed-Rank test (stats.wilcoxon) if the data was not normal. The significance was considered at $p \leq 0.05$.

The MICs of the tested antibiotics for all the drug and control evolved lines were tested as mentioned in section **2.2.2.**

2.4.3.2. Skimmed milk agar assay for protease activity

For investigating the change in the inhibitory effect of metformin on the protease activity of the drug and control evolved populations, skimmed milk agar was used. The experiment was done in the same way as mentioned before in the section **2.2.3.1** in two biological and two technical replicates, where the final concentrations of metformin were 10, 5, 1.25, 0.5 mg/mL along with the negative control of free-drug broth. Those concentrations were selected here as the lower concentration did not give any significant inhibitory effect for the protease in the inhibitory studies. The data were plotted as in section **2.2.3.1** as a pairwise comparison of the drug- and control-evolved lines.

The statistical analysis was performed using Python v3.9.0 with its package of SciPy; however, due to the lack of biological replicates ≥ 3, the statistical tests were done using both unpaired t-test (stats.ttest_ind), and Mann-Whitney U test (stats.mannwhitneyu, two-sided) for comparison, where the significance was considered at $p \leq 0.05$. And this is because the non-parametric tests are usually more conservative, which gives higher p-values, especially in small sample sizes (de Winter, 2013).

2.4.3.3. Crystal violet assay for biofilm formation

To investigate the effect of metformin on the biofilm formation of the drug- and control-evolved populations of *P. aeruginosa* and *S. aureus,* alongside the controls and the ancestors, overnight cultures of the bacteria were normalised to OD_{600} = 0.1 in DS LB low salt broth. The normalised cultures were then distributed at 90 µL per well of a sterile 96-well microtiter plate, starting from the second row and second column, and leaving the first and last rows and columns without media. To these surrounded wells, 200 µl of sterile water was added to reduce evaporation in the plate. A volume of 90 µL of different concentrations of metformin was introduced to achieve final concentrations of 10, 5, and 1.25 and 0.5 mg/mL, alongside negative controls and blank. The plates were incubated for 24 h at 37°C. After incubation, all the steps were performed as mentioned in section **2.2.3.2**. The data were plotted as in section **2.2.3.2** as a pairwise comparison of the drug- and control-evolved lines. Statistical analysis was performed as in section **2.4.3.2**.

2.4.4. Genotypic characterisation of metformin-evolved populations

2.4.4.1. Identifying mutations using short-read sequencing

2.4.4.1.1. Extracting and purifying the genomic DNA

For whole genome sequencing, overnight cultures for the drug- and control-evolved populations, and the ancestors were done in 5 mL LB broth. Then 1 mL from each sample was used to extract the genomic DNA using the Promega Wizard® Genomic DNA Purification Kit according to the manufacturer's instructions, with some optimisation described in the subsequent sections.

For the *P. aeruginosa* strains, the Gram-negative protocol was used, with some conditions optimised as follows: the initial centrifugation was for 5 min. Then, after adding the nuclei lysis solution and RNase, the incubation was for 60 min, followed by cooling at room temperature for 5 min. For the protein precipitate solution, it was ice cold, and after adding it, the incubation was for 10 min. Also, after the centrifugation step and transferring the supernatants to clean tubes, the samples were kept on ice. In the final step of rehydrating the DNA precipitate, 100 µL of ultra-purified sterile water was used instead of the rehydrating solution.

In the case of the *S. aureus* strains, the Gram-positive protocol was used with the same above optimisation conditions, but with some additional steps in the lysis stage. After adding the nuclei lysis solution to each cell pellet and mixing gently, the suspension was transferred to a BeadBug™ prefilled tube and was put inside the beadbeater homogeniser using the maximum speed for 3 runs, each for 2 min.

After that, the quality of the purified DNA was assessed using a Nanodrop Spectrophotometer 2000 with 2 µL of each sample with purified water as the blank for the device, targeting the A260/A280 and A260/A230 ratios and the absorbance curve to check the purity of the samples.

Then, for quantification, Qubit™ dsDNA BR Assay Kit (Invitrogen) with the Qubit™ fluorometer (Invitrogen) was used for analysing 1 µL of each sample according to the manufacturer instructions. All samples were then normalised to 5 ng/mL.

2.4.4.1.2. Sequencing the DNA samples

All the purified and normalised genomic DNA samples were sent to the core sequencing service at the Quadram Institute for Biosciences (Norwich, UK) to have them sequenced in forward and reverse directions using the Illumina short read sequencing technique.

2.4.4.1.3. Bioinformatic analysis

The raw sequence data were first trimmed using Trimmomatic v0.39 (Bolger et al., 2014) to remove the adapters, where the headcrop, leading, and trailing parameters were set to 20; a sliding window to 4:20, and the minimum length of sequence to 36 with Illumina-clip to remove the Nextra adapters. The quality of trimmed sequencing reads was then assessed with FastQC v0.11.9 (Andrews, 2010) to check the removal of the adapters, and mostly the per-base sequence quality would be in the green area (with a score > 28).

The trimmed paired-end forward and reverse reads for each sample were used for de novo genome assembly using SPAdes v3.14.0 (Prjibelski et al., 2020), where the k-mer sizes were 21, 33, 55, 77, 99 and 127. The assembled genomes were then annotated using Prokka v1.14.6 (Seemann, 2014) using minimum contig length 200. Some efflux pump genes were further manually annotated by sequence similarity searches against reference databases using Basic Local Alignment Search Tool (BLAST) and by examining gene organization within operons. RND efflux systems were classified based on gene similarities and the presence of associated outer membrane proteins (e.g., OprM, OprJ).

The drug- and control-evolved populations trimmed forward and reverse reads were first investigated for any insertions and deletions (INDELS) or single-nucleotide polymorphisms (SNPs) using Snippy v4.6.0 (Seemann, 2015). The ancestor's annotated assemblies were used as the reference genomic files. For identifying the intergenic modifications and larger deletions, Breseq v0.37.1(Deatherage & Barrick, 2014) was used, where the reference genomes were the annotated assembled ancestors.

2.4.4.2. Identifying the mutations using long-read sequencing

2.4.4.2.1. Extracting and purifying the genomic DNA

Overnight cultures for the drug- and control-evolved populations and ancestors were done in 5 mL LB broth. Then 1 mL from each sample was used to extract the genomic DNA using the Fire Monkey® High Molecular Weight DNA extraction kit according to the manufacturer's instructions, with some optimisation described below.

For the *P. aeruginosa* strains, the Gram-negative protocol was used. In the case of the *S. aureus* strains, the Gram-positive protocol was used where a mixture of lysozyme (20 mg/mL) and lysostaphin (0.1 mg/mL) added after optimising different conditions till reaching the best one for the extraction of *S. aureus*.

After that, the quality of the purified DNA was assessed using Nanodrop and quantity by Qubit as described for short-read sequencing above.

2.4.4.2.2. Sequencing the DNA samples

All the purified and normalised genomic DNA samples were sent to the core sequencing service at the Quadram Institute for Biosciences (Norwich, UK) for sequencing in forward and reverse directions using the Oxford Nanopore long-read sequencing technique.

2.4.4.2.3. Bioinformatic analysis

For the *Pseudomonas* samples:

Hybracter v0.7.3 (Bouras et al., 2024), an automated pipeline, was run on the raw data of the *P. aeruginosa* samples with the hybrid command to make hybrid assembly using both long and short reads. This tool starts with trimming the sequences and removing the adapters, followed by quality check, then long reads and plasmid assembly, followed by long reads and short reads polishing to result in a fully assembled genome.

On the assembled genome, the Synteny and Rearrangement Identifier (SyRI) v1.7.0 (Goel et al., 2019) was utilised to identify structural variations using the ancestor assembled genome as the reference. To run this programme, the assembled genomes were aligned to the reference genome using Minimap2 v2.28 (Li, 2018), then converted to BAM files, sorted, and indexed by SAMtools v1.20 (Li et al., 2009). Subsequently, these files served as input for SyRI to generate an output file, which was then input for Plotsr v1.1.0 (Goel & Schneeberger, 2022) to visualise any rearrangements. Socru v2.2.4 (A. J. Page et al., 2020) was employed to identify any changes in the order and orientation of complete genomes around ribosomal operons.

For the *Staphylococcus* samples:

Canu v 2.2 (Koren et al., 2017), an assembly pipeline for high noise raw sequence data, was employed for trimming and then assembling the raw ONT sequence data for the *S. aureus* samples. Subsequently, unicycler v0.5.1(Wick et al., 2017) was utilised for hybrid assembly, using the paired-end fasta files from the short-read sequencing with the --existing_long_read_assembly option to incorporate the output file from the Canu assembler as input for Unicycler, followed by a quality check using Quast v5.0.2. The assembled genomes were polished with the short-read sequences through three rounds of polishing, beginning with Pilon v1.24 (Walker et al., 2014), which requires the assembled genomes to be aligned with the short reads using Burrow-Wheeler Aligner (BWA) v0.7.17, starting with the index tool, followed by the mem one, then converting to bam files, sorting, and indexing using Samtools v1.16.1. The output from Pilon was then used to prepare the input for Polypolish v0.6.0 (Wick & Holt, 2022), beginning with indexing using the BWA index tool, followed by aligning with the short reads using BWA mem with the option '-a' to align all possible locations, not just the best location, and finally running the Polypolish tool. The third polishing round involved POLCA (Zimin & Salzberg, 2020), which is part of the MASURCA v3.4.1 tools.

For detection of the structural variations, the Structural variant identification method – assembly edition (SVIM-asm v1.0.3) (Heller & Vingron, 2020) was used, where the assemblies were aligned first to the annotated ancestor genome as a reference genome using Minimap2 v2.28, then converted to BAM files, sorted, and indexed by Samtools v1.20. Then, the sorted BAM files were used as input for SVIM-asm 'haploid' version. For the detection of the INDELs and SNPs, Snippy v4.6.0 was used.

2.5. Transcriptomic and functional genomic analyses

2.5.1. RNA sequencing

2.5.1.1. Preparation of the samples for RNA extraction and sequencing

For studying the transcriptome in the presence of metformin in different conditions, RNA sequencing was performed. Overnight subculture for the ancestor, one drug-evolved line and its corresponding control-evolved line of *P. aeruginosa* and *S. aureus* was done in MHB broth. Then the cultures were diluted to OD_{600} of 0.1 in MHB containing metformin at specific final concentrations, depending on the strain and experimental group.

For the ancestor of *P. aeruginosa,* the final concentrations of metformin tested were 1.25 and 10 mg/mL, and its drug-evolved line and the control were exposed only to 10 mg/mL. For the ancestor of *S. aureus*, the metformin final concentrations were 1.25 and 5 mg/mL, and for its drug-evolved line and the corresponding control, the concentration of 5 mg/mL was only tested. Negative control cultures for all strains were prepared in drug-free MHB. The samples were prepared in three biological replicates.

All diluted cultures were incubated at 37°C with shaking at 180 rpm until reaching the mid-log phase of OD_{600} around 0.5. Immediately after the incubation, 300 µL of each culture was added to 1,200 µL of RNAprotect® reagent (QIAGEN) in sterile microcentrifuge tubes. Then, the suspensions were centrifuged at 5,000 rpm for 10 minutes, the supernatants were discarded, and the cell pellets were frozen at -80 °C.

All the cell pellets were sent to GENEWIZ, part of Azenta Life Sciences (Frankfurt, Germany), for RNA extraction, library preparation, and high-throughput RNA sequencing using the Illumina NovaSeq platform.

2.5.1.2. Bioinformatic analysis

The raw sequence data was first checked for its quality and adapter content using FastQC v0.12.1, which revealed the presence of Illumina universal adapter. Then Trimmomatic v0.39 (Bolger et al., 2014) was used to remove the adapters using the Illuminaclip of the TruSeq adapter, where the leading and trailing parameters were set to 30, a sliding window of 4:20 was used, and the minimum length of the sequence was set to 36. The quality of the trimmed sequencing reads was then double-checked again with FastQC.

For RNA-seq read quantification, Salmon v1.10.3 (Patro et al., 2017) was used with the trimmed reads, but it required first indexing the references using the command 'salmon index', which needs the annotated genome in .fna format. The reference genomes for *P. aeruginosa* and *S. aureus* generated from the annotation of the long-read sequenced genomes using Prokka (in section **2.4.4.1.3**) were used for indexing. Following that, the command 'salmon quant' was used for the transcript-level quantification of the RNA-seq data, producing a CSV file for the differential gene expression (DGE) analysis. However, the resulting file contained locus tags, so it was necessary to retrieve the gene names from the annotated .tsv files generated by the Prokka output.

Degust v4.1.1 (Powell, 2019), the online web tool, was utilised for the differential gene expression (DGE) analysis of the transcriptome, employing the CSV count output files from Salmon, with three replicates for each condition in comparison. Within the program, edgeR's quasi-likelihood method estimates the differential gene expression, represented as $\log_2$ fold change ($\log_2$FC), indicating the extent of expression change when comparing two conditions. Additionally, the false discovery rate (FDR) serves as the statistical measurement for false positive expression. The data were visualised using a volcano plot with the matplotlib.pyplot and seaborn packages in Python v3.9.0. The cutoff values for significance used in the comparisons were (FDR) ≤ 0.05 ($-\log(\text{FDR}) \leq 1.3$) and $\log_2\text{FC} \geq |1|$; if $\log_2\text{FC} \geq 1$, it is considered upregulated gene expression, and if $\log_2\text{FC} \leq -1$, it is considered downregulated. The comparisons were made between the different concentrations of metformin used with the parent strains.

Moreover, the unique changes in DGE between the parent and evolved strains, with and without treatment, were investigated.

Furthermore, the enrichment gene analysis using ShinyGO v0.82 (Ge et al., 2019) was conducted with criteria of (FDR) ≤ 0.05 depending on the number of genes for each pathway, and the 20 most enriched pathways were presented. The input consisted of gene names from the significant upregulated and downregulated genes derived from gene expression. The data was visualised using lollipop plots that represented the fold enrichment according to the number of genes for each pathway, as well as a tree plot illustrating the relationships among the pathways. Then, to provide detailed information about the pathways of the involved genes, pathway analysis using the Kyoto Encyclopedia of Genes and Genomes (KEGG) was performed. However, it required annotation with K numbers (KO), so BlastKOALA (KEGG Orthology And Links Annotation) (Kanehisa et al., 2016) was used, followed by the KEGG Mapper – Reconstruct tool (Kanehisa & Sato, 2020) for assigning KEGG pathways to the selected genes. The data was visualised using a heatmap created with matplotlib.pyplot and seaborn packages of Python v3.9.0.

2.5.2. Transposon mutagenesis in P. aeruginosa strain using the TraDIS-Xpress technique

This experiment was performed in collaboration with and under the supervision of Prof. Webber's group members (Dr. Keith Turner and Dr. Muhammed Yasir).

2.5.2.1. Preparation of transposons

This section was done by Dr. Turner. Bacterial strains of *E. coli* DH5α harbouring constructed plasmids carrying the chosen transposons with outward-facing promoters were streaked onto L-agar plates (Lennox formulation, containing 5 g/L NaCl) supplemented with gentamicin (15 µg/mL) and ampicillin (200 µg/mL) and then incubated overnight at 37°C.

For preparation of the overnight subculture, L-broth supplemented with gentamicin (15 µg/mL) and ampicillin (200 µg/mL) was inoculated with single colonies from the streaked plates. The cultures were incubated overnight at 37°C with 180 rpm shaking.

The cells were harvested from 1.4 mL of each overnight culture by centrifugation, and plasmid DNA was extracted using the QIAprep Spin Miniprep Kit (QIAGEN) following the manufacturer's instructions. Plasmid DNA was eluted from the spin column using 50 µL of the elution buffer.

Plasmid DNA (0.5 µL) was digested in a 20 µL reaction containing 1× rCutSmart buffer and 0.3 µL BsaI-HF (New England Biolabs). For most plasmids, digestion targeted the two BsaI sites located within or near the AmpR gene. However, for plasmid "B" (pBR-Tn5Gm-PsPlpx02), digestion was performed

with SalI and SphI in 1× rCutSmart buffer due to the presence of a BsaI site within the promoter sequence. Reactions were incubated at 37°C for 1 hour.

Following digestion, the samples were diluted 1:10 in 10 mM Tris (pH 8.0) containing 1 mM EDTA. Diluted samples were stored at -20°C for further analysis.

To prepare three different transposons (A, B and C) (Table 2-2) each was in pairs, 1,110 µL of 1x Q5 DNA polymerase master mix (New England Biolabs) was mixed with 2.6 µL each of the primers Tn5Cm-03P: /CTGTCTCTTATACACATCTGACGC and Tn510P /CTGTCTCTTATACACATCTTTGTG To each tube in an eight-tube PCR strip, 165 µL of the master mix and oligos was added to 1.5 µL diluted prepared DNA templates, mixed thoroughly by gentle pipitting, and split into 8 × 20 µL reactions per template using a multichannel micropipette.

The tubes were sealed with lids and subjected to thermal cycling using the following program: an initial denaturation step at 98°C for 25 seconds; 30 cycles of 98°C for 5 seconds, 55°C for 50 seconds, and 72°C for 30 seconds; a final extension at 72°C for 2 minutes; and a hold at 20°C to reach the room temperature for 2 seconds before taking out. Upon completion, the 20 µL reactions for each transposon for the both pairs were pooled, yielding approximately 300 µL per transposon with a DNA concentration of up to 40 ng/µL.

The pooled reactions for each template were quantified using 2 µL of the pool using a Qubit dsDNA BR kit. The pooled amplified reactions for each transposon (A, B and C) were cleaned and concentrated using the DNA Clean and Concentrator-25 kit (Zymo Research), eluting the DNA with 2 × 25 µL of elution buffer. The DNA yield was optimised by passing the PCR reaction and DNA binding buffer mix down the column twice and microwaving for approximately 20 seconds, reaching an estimated temperature of around 65°C, before eluting with the elution buffer. The final elution volume was approximately 45–50 µL. EDTA (pH 8) was added to a final concentration of 1 mM, which was 5 µl of 10 mM EDTA. The DNA concentration was measured again using the Qubit dsDNA BR kit (Invitrogen), yielding a concentration of around 200 ng/µL.

An equal volume (around 50 µL) of glycerol was added to each transposon preparation to achieve a final glycerol concentration of 50%. The glycerol-transposon preparations were stored at -20°C.

The same steps were repeated for transposons D and G (Table 2-2).

Table 2-2 The structure of the different plasmids used in the 5 transposons preparation

Transposon codes	Plasmid structure
A	pBR-Tn5Gm-PsPdnaA
B	pBR-Tn5Gm-PsPlpx02
C	pBR-Tn5Gm-PsPrplJ
D	pBR-Tn5Gm-PsPrplK
G	pBR-Tn5Gm-PsPfabI

2.5.2.2. Preparation of transposomes

For Viva Biotech Tn5 transposase, 1 µL of the enzyme was diluted in 50 µL of transposase storage buffer prior to mixing. Then an equal volume of the transposon and the diluted enzyme was mixed (45 µL for each of them). Control reactions were prepared by substituting the transposase with an equivalent volume of transposase storage buffer. The transposon DNA and transposase enzyme mixtures were then incubated at 37°C for around 90 minutes.

2.5.2.3. Preparation of the electrocompetent cells

P. aeruginosa strain ATCC 27853 was streaked on LB-low salt agar plates and incubated overnight at 37°C. The plates were then stored at 4°C for 2 weeks before use. Several colonies from the agar plate were inoculated into 400 mL of L-broth and incubated overnight at 37°C with 180 rpm shaking.

Cells were harvested by centrifugation at 10,000 × g for 10 minutes, and the supernatant was discarded. The cell pellet was washed three times in 300 mM sucrose, each time the volume of sucrose was half the previous step. Then the cell pellets were resuspended in 2 mL 300 mM sucrose.

2.5.2.4. Electrotransformation of the prepared electrocompetent cells

To perform electrotransformation, 1,000 µL of prepared cell suspension was mixed with 50 µL of transposons. For the control mixture, 100 µL of the cell suspension was mixed with 5 µL of the control transposon solution. The mixture was gently pipetted to ensure homogeneity.

Electroporation was carried out using an electroporator set to 2.5 kV, 25 µF capacitance, and 200 Ω resistance. A 100 µL aliquot of the cell suspension/transposome mixture was transferred to a 2-mm electrode gap electroporation cuvette. Immediately following electroporation, 1 mL of Super Optimal broth with Catabolite repression (S.O.C.) medium was added to the cuvette, and cells were resuspended by gentle pipetting. The suspension was transferred to a 30 mL universal tube. Suspensions from two

identical transformations were pooled into a single tube. The cell suspensions were incubated at 37°C for 2 hours.

After incubation, the cell suspensions were spread on L- agar plates supplemented with different concentrations of gentamicin at 2, 4, 6, 10, 15 and 20 µg/mL using a spreader. Initially, 10 and 50 µL of the cells/transposome mixture and 50 µL of control mixture were plated onto 9 cm Petri dishes and incubated 18-20 hr to confirm the transformation efficiency and yield of transposon mutants. The remaining suspension was stored at 4°C.

The remaining cell suspensions from the transformations were spread onto 23 cm² bioassay dishes containing 20 µg/mL gentamicin. Each bioassay dish was inoculated with 1 mL of the cell suspensions. The plates were incubated for 18-20 hr at 37°C. Colonies were harvested using L-broth in the bioassay dish and suspending the cells by gently rubbing with a glass spreader. Cell suspensions were kept as concentrated as possible by resuspension of the transformants by with the same L-broth from each plate following the other. The pooled suspensions were transferred into 50 mL Falcon tubes, and glycerol was added to a final concentration of 15%. The mixtures were thoroughly mixed, aliquoted as around 1.5 mL per cryovial, and stored at -80°C.

2.5.2.5. The exposure of the mutant library to metformin

For testing the mutant library with metformin, five different concentrations of metformin were prepared in MHB, where the final concentrations in each 10 mL volume were 40, 20, 10 and 1.25 mg/mL in addition to the drug-free control. From the pooled library of the 5 different transposons, 5 µL was added to each tube. Each condition was repeated in duplicate. All the cultures were incubated overnight at 37°C with 180 rpm shaking. After incubation, the DNA was extracted using the Quick-DNA Miniprep Plus Kit (Zymo Research) according to the manufacturer's instructions. The concentrations of the extracted DNA were measured using the Qubit dsDNA BR kit. Purified genomic DNA was then sent for Illumina sequencing, which was done by Dr. Yasir.

2.5.2.6. Bioinformatic analysis

In the analysis of the TraDIS data, the reference genome of *P. aeruginosa* strain ATCC 27853 was used, which was long-read sequenced and then analysed as discussed previously in section **2.3.4.2.3**. The reads from the FASTQ files generated from TraDIS sequencing were mapped to the reference genome and analysed using Bio-TraDIS v1.4.5 (Barquist et al., 2016) to create the insertion plots of the transposons at each concentration tested. These insertion plots were then used for comparison analysis between each condition and the control using AlbaTraDIS v1.1.2 (Andrew J. Page et al., 2020), which calculates the number of insertions within each gene and performs statistical analysis to identify the significant

knockouts. The generated output file contains values for the $\log_2$ fold change between control and condition ($\log_2$FC), where positive values indicate an increase in the insertions in the treated samples and negative values represent the opposite. Counts of reads located at each locus per million total reads for the sample were converted to $\log_2$ ($\log_2$CPM), a p-value of statistical significance, and a q-value (the adjusted p-value by the multiple testing correction using the Benjamini–Hochberg Method) were calculated. Subsequently, the data was further filtered according to its significance using the cut-off of $q \leq 0.001$ to ensure higher significance. Additionally, the insertion plots were visualised manually using Artemis v18.2.0 (Carver et al., 2012) for the selected genes to assess the reproducibility between the replicates and capture images for the insertions.

2.6. Metabolic phenotyping using Biolog Mitoplates

Metabolic activity was assessed in the presence and absence of metformin for eight strains of four different bacterial species, *S. aureus, P. aeruginosa, E. coli,* and *K. pneumoniae,* that were mentioned in (section **2.1.**). This experiment used the MitoPlate I-1 (Appendix Figure 7-1), following the manufacturer's instructions alongside the protocols for PM9+ plates, for Gram-positive and Gram-negative bacteria, with some modifications to suit the experimental requirements.

For *S. aureus*, the Gram-positive protocol was used. This process began with the preparation of four different PM additive solutions containing MgCl2, 6H2O (2mM), CaCl2, 2H2O (1mM), yeast extract (0.005%), tween 80 (0.005%), D-glucose (2.5mM), which was substituted with sterile distilled water for the wells without glucose, metformin (10 mg/mL), which was substituted with sterile water for the plates without metformin, and sterile water. All the concentrations in brackets were calculated as final concentrations after adding the rest of the inoculating solutions components. All the solutions were filter sterilized and stored at 4°C.

To prepare the bacterial cell suspensions, *S. aureus* was streaked onto BUG+B agar plates and incubated overnight at 37°C. A second streaking was performed using the same medium. Cells were gently harvested using a sterile swab and suspended in a capped tube containing IF-0a buffer, ensuring even distribution by gentle stirring. The turbidity of the suspension was adjusted to 81% transmittance using a Biolog turbidimeter.

The final inoculating fluid was then prepared by combining IF-10b, Dye Mix H, the PM additive solution, the bacterial suspension, and sterile water, where the concentrations of all components were appropriately diluted to the desired levels according to the manufacturer's protocol.

For *P. aeruginosa, E. coli,* and *K. pneumoniae*, the Gram-negative protocol was applied. The inoculating solutions for these bacteria were prepared using IF-10a buffer, Dye Mix A, and the bacterial cell suspension, where the concentrations of all components were appropriately diluted to the desired levels according to the manufacturer's protocol. Four different inoculating solutions were prepared to ensure testing presence and absence of 10 mg/mL metformin as final concentration with and without glucose as a substrate. For the bacterial suspension, it was prepared similarly to *S. aureus* by streaking the bacteria twice on BUG+B agar plates. After transferring the cells into IF-0a buffer, the initial turbidity was adjusted to 42% transmittance, followed by a 1:5 dilution in IF-0a+dye solution to achieve the desired final density.

Once the inoculating solutions were prepared, the MitoPlates, were inoculated with 100 µL of solution in each well, where for each condition there are four technical replicates. Each strain was tested in biological duplicates (i.e. two independent mitoplates), with one plate treated with metformin and another as a control without metformin. The plates were incubated at 37°C for 20 hours, and the absorbance of the solutions was measured at 590 nm with 15 minutes readings interval.

The data was extracted using Data Analysis® 1.7 software (Biolog Hayward, CA). From the extracted data, the average of the readings from each of the 4 replicates was calculated, and the AUC was calculated using the Python v3.9.0 package (numpy.trapezoid). Then, the percentage reduction of the AUC for metformin alone, inhibitors alone, and the different combinations compared to the control was calculated using the following equation:

$$\%\text{Reduction of AUC} = \frac{AUC_{control} - AUC_{Drug}}{AUC_{control}} \times 100$$

The percentage reduction in AUC was used as a normalised measure to quantify the extent to which each treatment decreased the overall response relative to the control. By showing the changes in AUC as a percentage of the control AUC, differences between treatment groups could be compared more directly than with absolute AUC values.

Then the average percentage reduction of the two biological replicates under each condition was calculated and plotted as a bar chart, with standard deviations represented as error bars.
As a limitation here, there were only two independent biological replicates for each condition, so the assessment of the normality test was not reliable. However, the normality of the data was assumed, and accordingly, the statistical analysis of the effects of metformin alone, the inhibitor alone, and the

combination was performed using one-way ANOVA followed by Tukey's HSD post hoc test; the significance was defined as $p \leq 0.05$.

For the combinations with significant difference compared to metformin alone, the expected percentage reduction was calculated using the Bliss independence model (Zhao et al., 2014) according to the following equation:

$$Expected\ \%\ reduction\ of\ AUC_{A+B} = \%\ Reduction\ of\ AUC_A + \%\ Reduction\ of\ AUC_B - (\%\ Reduction\ of\ AUC_A \times \%\ Reduction\ of\ AUC_B)/100$$

This model calculates the expected percentage reduction in AUC for the combination (A + B) based on the individual reductions caused by drug A (metformin) and drug B (the other mitochondrial inhibitors) alone. The interaction is indicated for the overlap between their independent effects, preventing overestimation of the combined inhibition. The resulting percentage reduction reflects the level of inhibition expected if there are no synergistic or antagonistic interactions.

Then, by comparing to the observed percentage reduction, which is the calculated percentage reduction from the actual experiment,

The combination had a synergistic effect if:

$$Observed\ \%\ reduction\ of\ AUC_{A+B} > Expected\ \%\ reduction\ of\ AUC_{A+B}$$

The combination had an additive effect if:

$$Observed\ \%\ reduction\ of\ AUC_{A+B} = Expected\ \%\ reduction\ of\ AUC_{A+B}$$

The combination had an antagonistic effect if:

$$Observed\ \%\ reduction\ of\ AUC_{A+B} < Expected\ \%\ reduction\ of\ AUC_{A+B}$$

CHAPTER 3-

Metformin's Inhibitory Effects On Bacterial Phenotypes And Antibiotic Interactions

3. Metformin's Inhibitory Effects On Bacterial Phenotypes And Antibiotic Interactions

3.1. INTRODUCTION

Metformin is an old antidiabetic drug widely used and classified as a first-line treatment for type 2 diabetes mellitus (Wang et al., 2017). In addition to its glucose-lowering effects, several studies have reported that metformin inhibits bacterial growth across different species and alters bacterial metabolism and virulence following exposure to the drug (Abbas et al., 2017; J. Zuo et al., 2023). Therefore, it was crucial to investigate the repurposing of non-antibiotic drug, its effects on bacterial behaviour, and whether it could act alone or as adjunct therapy with other antibiotics, which may help reduce the emergence of antibiotic resistance.

In this chapter, multiple bacterial species and strains were selected to represent both Gram-positive and Gram-negative organisms with differing physiological characteristics and clinical relevance, including important members of the MDR bacteria and the most common causes of infection among people with diabetes. Thus, the assessment could cover a range of antibiotic susceptibilities, indicating whether metformin's effects are conserved across bacterial taxa or vary in a strain-dependent manner. Furthermore, it indicates whether a difference in bacterial susceptibility would be reflected in responsiveness to metformin, which may indicate potential cross-resistance.

Initial analysis of bacterial growth was undertaken to determine whether metformin exerts a growth-inhibitory effect over time across a wide range of concentrations, from high concentrations commonly used in the literature to low physiological and therapeutic concentrations, thereby providing an essential baseline for interpreting downstream phenotypic changes.

The effect of metformin on several bacterial virulence factors was investigated. Metformin's effect on protease production was assessed because bacterial proteases are key enzymes involved in nutrient acquisition, protein metabolism, and host-pathogen interactions, and their activity has been directly linked to bacterial virulence and infection prognosis (Lindsay et al., 2017).

Metformin's effect on biofilm formation was investigated to assess bacterial survival strategies and persistence. The ability to form biofilms is closely linked to chronic infection, surface colonisation and antimicrobial resistance, making it a critical phenotype to characterize (Hall-Stoodley et al., 2004).

Another bacterial virulence factor investigated was motility, which reflects the ability of the studied strains to move and initiate surface interactions, both vital for bacterial fitness and pathogenic behaviour. Swimming motility, driven by flagellar rotation, enables cells to move and facilitates colonisation. Twitching motility, mediated by the extension and retraction of type IV pili, is a surface-associated form

of locomotion that promotes surface translocation and early stages of biofilm development (Kearns, 2010).

Metformin was also tested to determine whether it could inhibit efflux pump activity at high or low concentrations. This is because efflux pumps play a key role in antibiotic resistance by reducing intracellular accumulation of antimicrobial compounds in both Gram-positive and Gram-negative bacteria. Bacterial efflux pumps are membrane-integrated transport systems that actively pump out toxic compounds, thereby lowering intracellular drug concentrations and contributing significantly to antibiotic resistance in many pathogenic species (Kabra et al., 2019). Assessing metformin's effect on efflux pump activity is therefore highly important for determining whether it can act as a general efflux pump inhibitor to restore antibiotic efficacy, or whether its effect is concentration-dependent and strain-specific.

Finally, the interaction between metformin and selected antibiotics was evaluated using checkerboard assays to determine whether metformin affects antibiotic activity in a synergistic, additive, or antagonistic manner. Such interactions could provide evidence for the feasibility of adjunctive therapeutic strategies.

3.2. RESULTS

3.2.1. The effect of metformin on bacterial growth

The activity of metformin against the tested isolates followed a similar pattern with minor differences between the various isolates, with the most inhibitory effect observed at higher concentrations in a more or less dose-dependent manner.

For *S. aureus* NCTC 6571, the growth of the bacteria was reduced significantly by metformin at all concentrations tested ($p = < 0.00001$ - 0.0066) except (1.25 and 2.5 mg/mL) (Figure 3-1). However, it was crucial to analyse the growth curves themselves for a deeper look at the differences in the growth pattern between some of the concentrations used and the negative control. Therefore, at the concentration of 2.5 mg/mL, it was revealed that there was significant inhibition ($p = 0.015$) compared to the control especially in the prolongation of lag phase (Figure 3-2). While the growth curve in presence of 1.25 mg/mL did not show any significant difference compared to the control (Figure 3-3). As a representative example of the growth curve that showed significant difference as in the AUC data of the same the same concentration, the growth curve of the bacterial growth at the concentration of 0.5 mg/mL of metformin was plotted in (Figure 3-4), which showed that both drug treated and the negative control had the same lag phase then the drug started to slow down the exponential phase of the bacterial growth. At the concentrations 5 and 10 mg/mL, the AUC became almost zero, which indicates no growth.

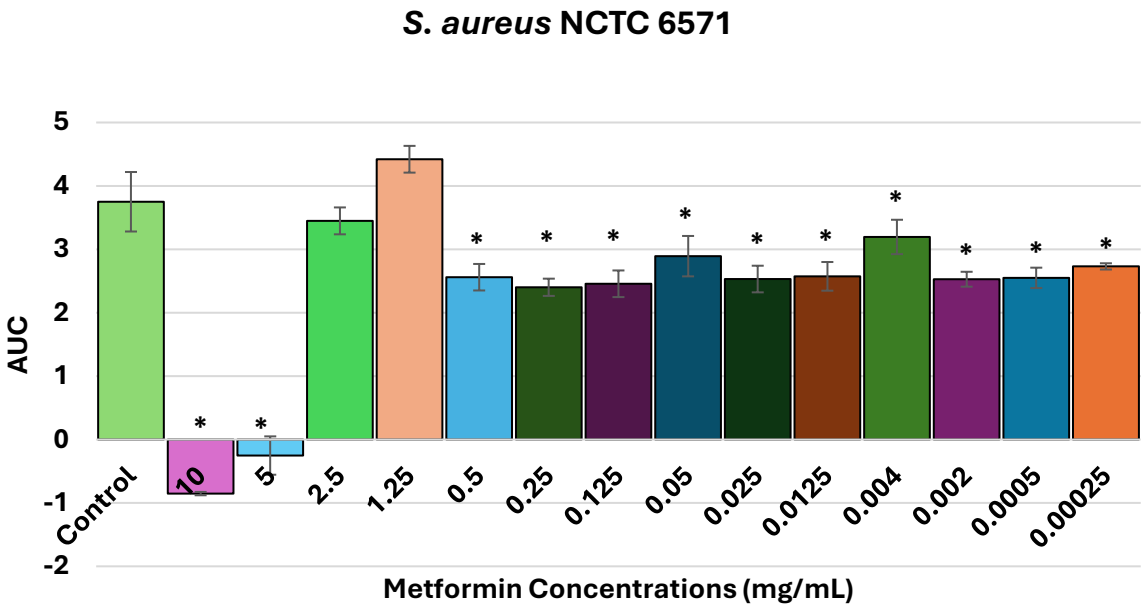

Figure 3-1: Area under the curve (AUC) analysis of *S. aureus* NCTC 6571 growth in the presence of metformin. AUCs derived from the growth curves of *S. aureus* NCTC 6571 in the presence of different concentrations of metformin (10, 5, 2.5, 1.25, 0.5, 0.25, 0.125, 0.05, 0.025, 0.0125, 0.004, 0.002, 0.0005, and 0.00025 mg/mL) along with the drug-free negative control; where the bars represent mean AUC values ± standard deviation (error bars) and the asterisks '*' represents statistical significance with $p \leq 0.05$ analysed by one-way ANOVA with Tukey's post-hoc test. Each set of the experiment was done in three biological replicates (n=3).

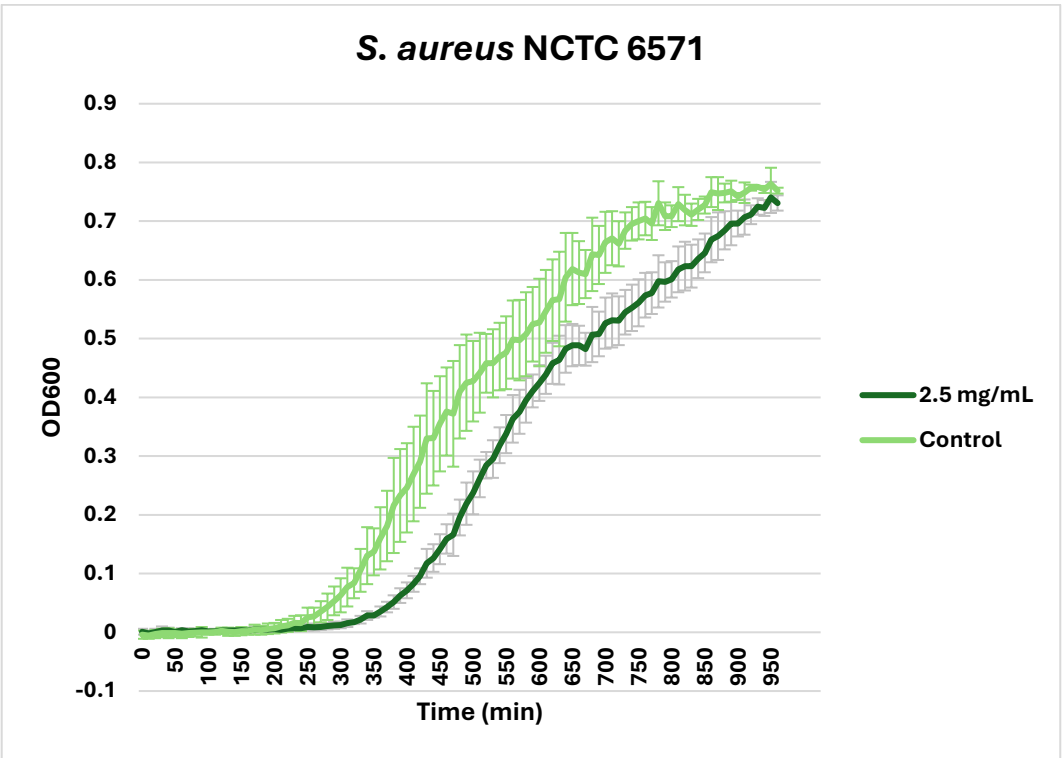

Figure 3-2: Growth profiles of *S. aureus* NCTC 6571 in the presence of metformin (2.5 mg/mL.) The drug-free broth was used as negative control; where the curves represent mean of OD_{600} ± standard deviation (error bars). Each set of the experiment was done in three biological replicates (n=3).

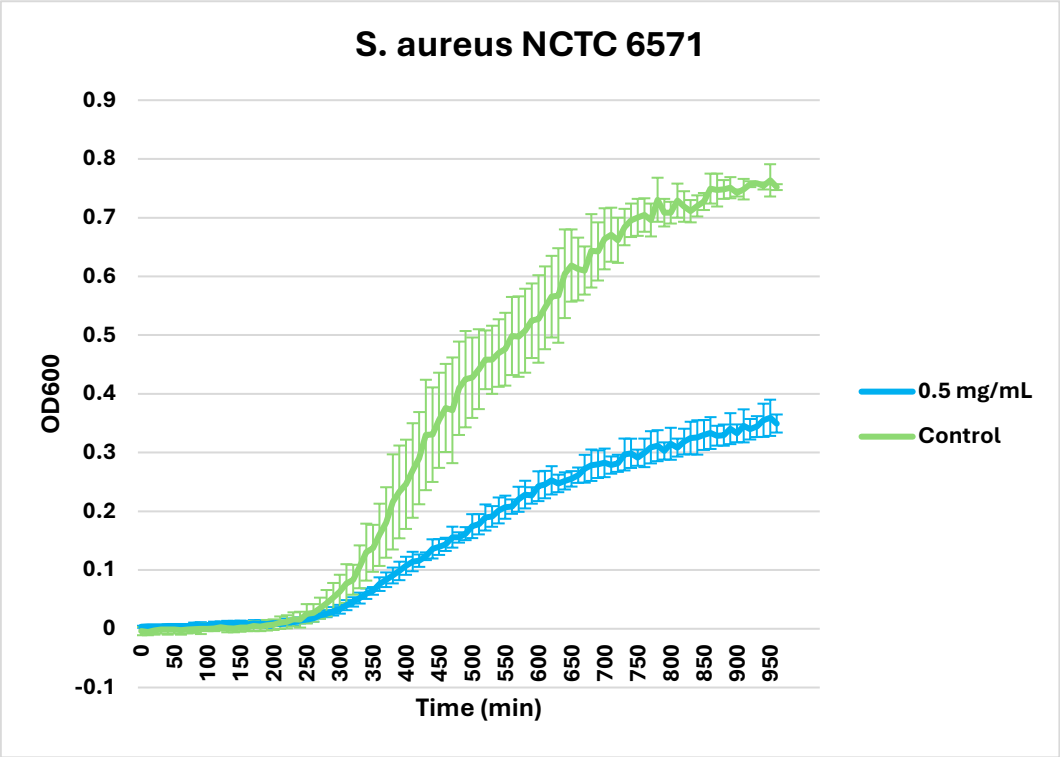

Figure 3-3: Growth profiles of S. aureus NCTC 6571 in the presence of metformin (1.25 mg/mL)
The drug-free broth was used as negative control; where the curves represent mean of OD_{600} ± standard deviation (error bars). Each set of the experiment was done in three biological replicates (n=3).

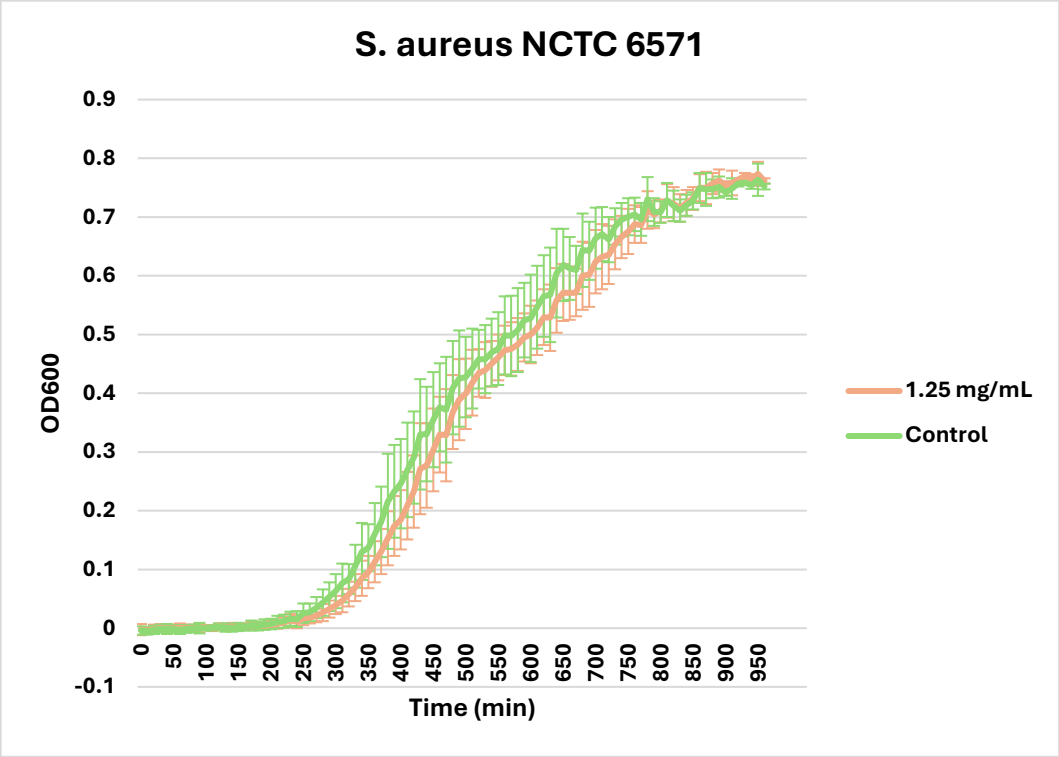

Figure 3-4: Growth profiles of S. aureus NCTC 6571 in the presence of metformin (0.5 mg/mL)
The drug-free broth was used as negative control; where the curves represent mean of OD_{600} ± standard deviation (error bars). Each set of the experiment was done in three biological replicates (n=3).

In contrast, *S. aureus* ATCC 25923 had significantly reduced growth at (1.25 -10 mg/mL) with $p < 0.00001$, but none of the concentrations tested inhibited growth completely. There was no significant inhibition at the lower concentrations (Figure 3-5). The growth curves themselves did not show difference in the results between them and the interpretation of the AUC data. Therefore, representative curve was plotted here of the effect of metformin at the concentration of 1.25 mg/mL (presence of significance difference $p = 0.014$), which showed that metformin caused inhibition of the bacterial growth starting from the active growing phase comparing to the control (Figure 3-6). Another representative example of the growth curve was its effect at the concentration of 0.5 mg/mL, which showed absence of the significance difference (Figure 3-7).

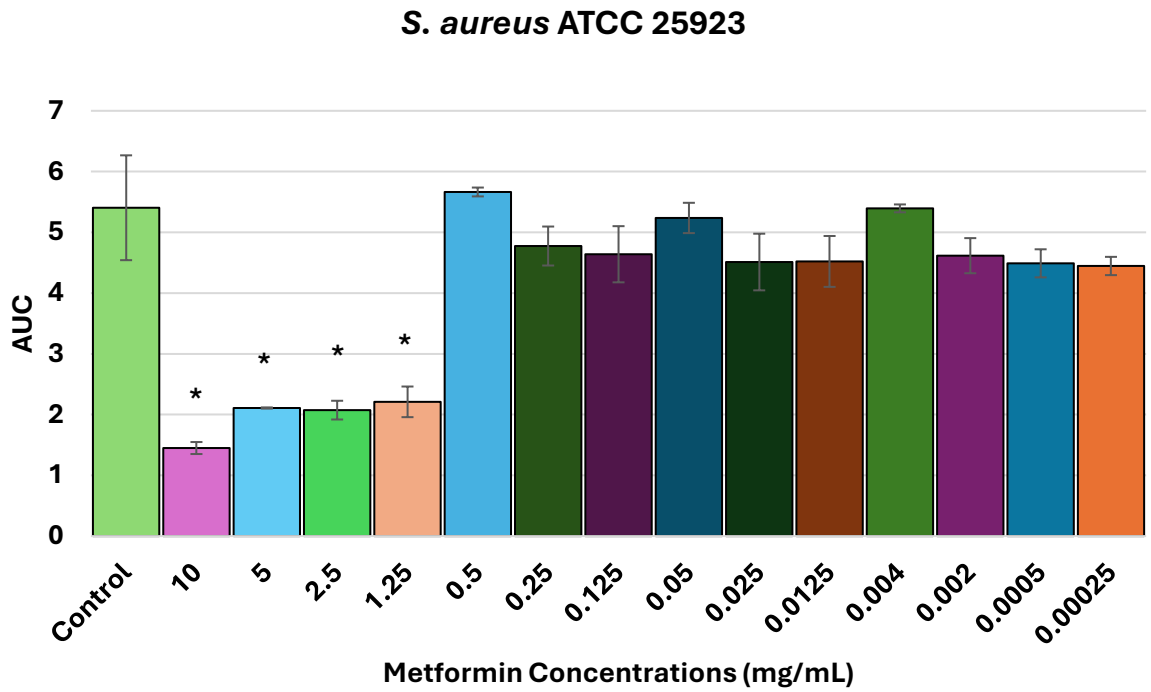

Figure 3-5: Area under the curve (AUC) analysis of *S. aureus* ATCC 25923 growth in the presence of metformin. AUCs derived from the growth curves of *S. aureus* ATCC 25923 in the presence of different concentrations of metformin (10, 5, 2.5, 1.25, 0.5, 0.25, 0.125, 0.05, 0.025, 0.0125, 0.004, 0.002, 0.0005, and 0.00025 mg/mL) along with the drug-free negative control; where the bars represent mean AUC values ± standard deviation (error bars) and the asterisks '*' represents statistical significance with $p \leq 0.05$ analysed by one-way ANOVA with Tukey's post-hoc test. Each set of the experiment was done in three biological replicates (n=3).

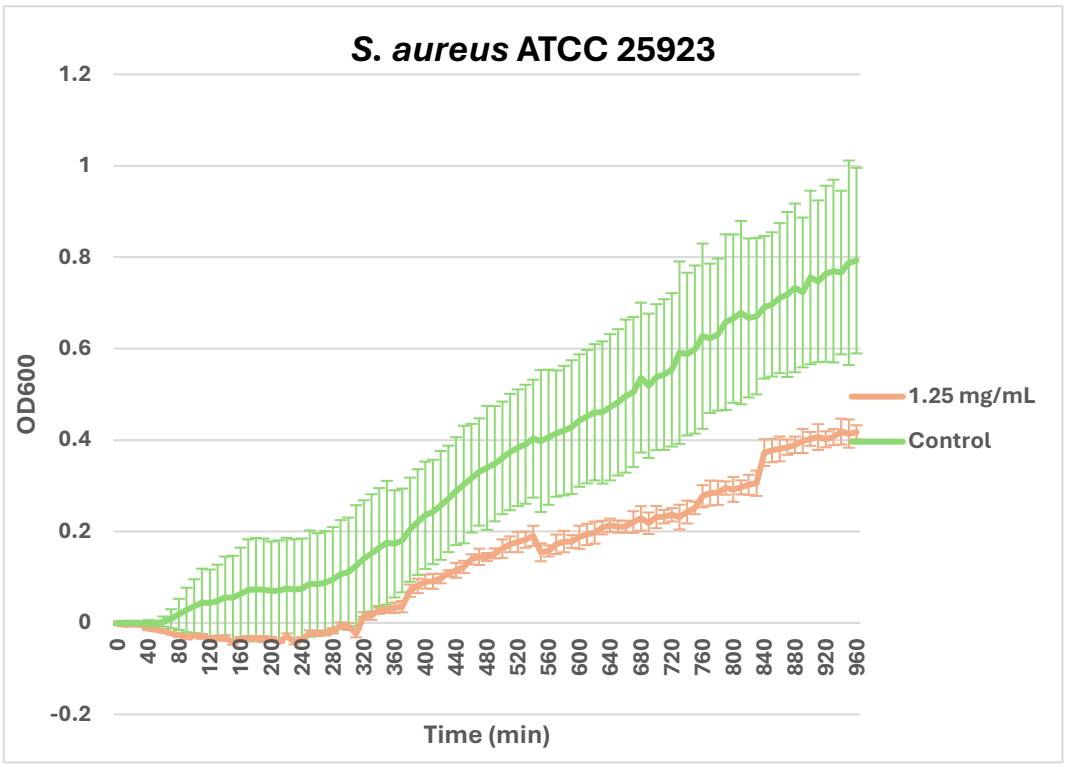

Figure 3-6: Growth profiles of *S. aureus* ATCC 25923 in the presence of metformin (1.25 mg/mL)
The drug-free broth was used as negative control; where the curves represent mean of OD_{600} ± standard deviation (error bars). Each set of the experiment was done in three biological replicates (n=3).

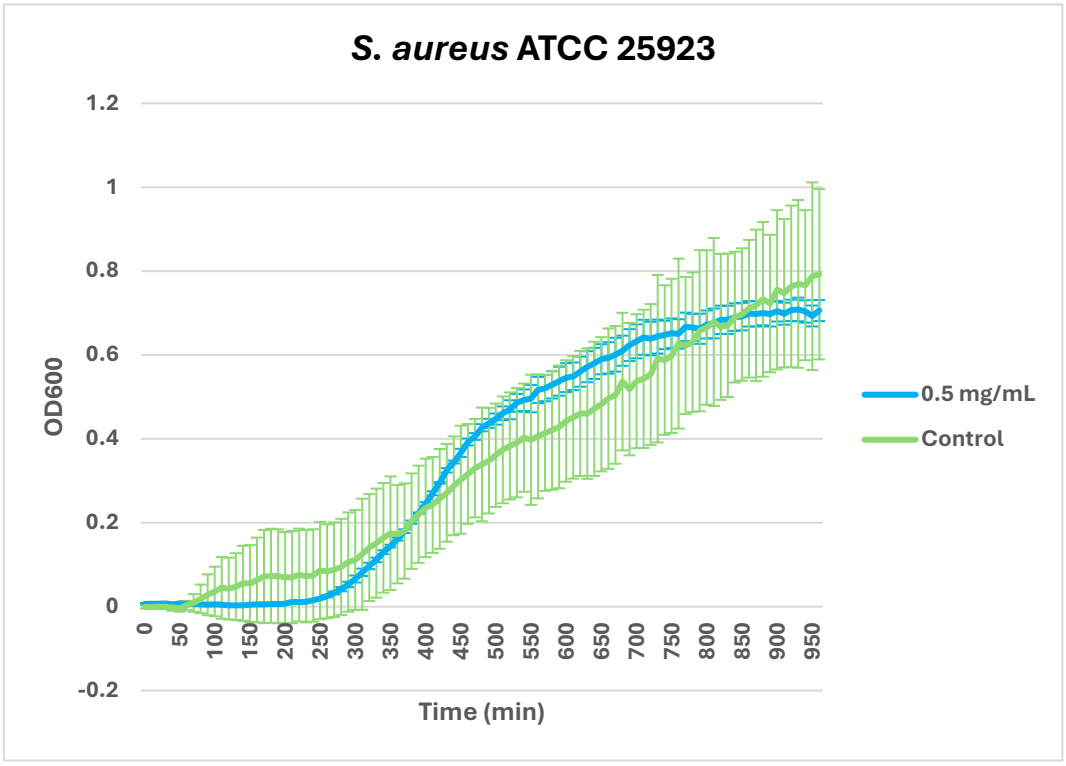

Figure 3-7: Growth profiles of *S. aureus* ATCC 25923 in the presence of metformin (0.5 mg/mL)
The drug-free broth was used as negative control; where the curves represent mean of OD_{600} ± standard deviation (error bars). Each set of the experiment was done in three biological replicates (n=3).

For both *P. aeruginosa* strains, metformin exhibited a significant inhibitory effect at the highest concentrations of 2.5 to 10 mg/mL, with p values ranging from < 0.00001 to 0.0006. However, *P. aeruginosa* NCTC 10662 demonstrated a significant reduction in growth at 0.25 mg/mL (p=0.0092) (Figure 3-8), whereas metformin significantly reduced the growth of *P. aeruginosa* ATCC 27853 at the concentration of 1.25mg/mL as well (p = 0.02) (Figure 3-9).

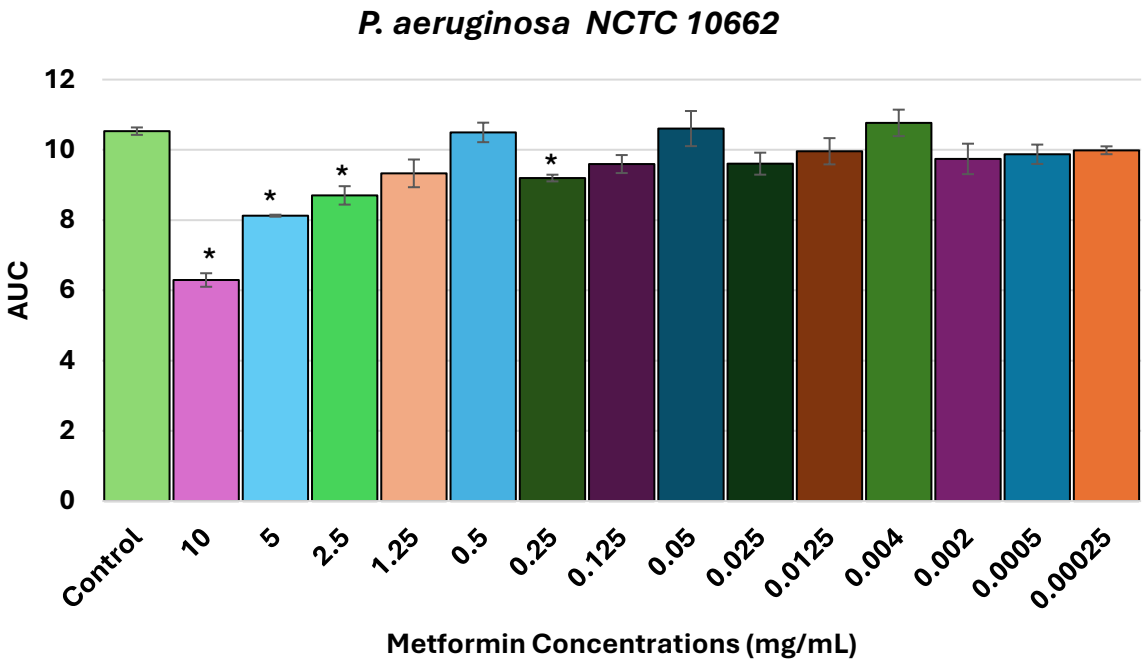

Figure 3-8: Area under the curve (AUC) analysis of *P. aeruginosa* NCTC 10662 growth in the presence of metformin.
AUCs derived from the growth curves of *P. aeruginosa* NCTC 10662 in the presence of different concentrations of metformin (10, 5, 2.5, 1.25, 0.5, 0.25, 0.125, 0.05, 0.025, 0.0125, 0.004, 0.002, 0.0005, and 0.00025 mg/mL) along with the drug-free negative control; where the bars represent mean AUC values ± standard deviation (error bars) and the asterisks '*' represents statistical significance with $p \leq 0.05$ analysed by one-way ANOVA with Tukey's post-hoc test. Each set of the experiment was done in three biological replicates (n=3).

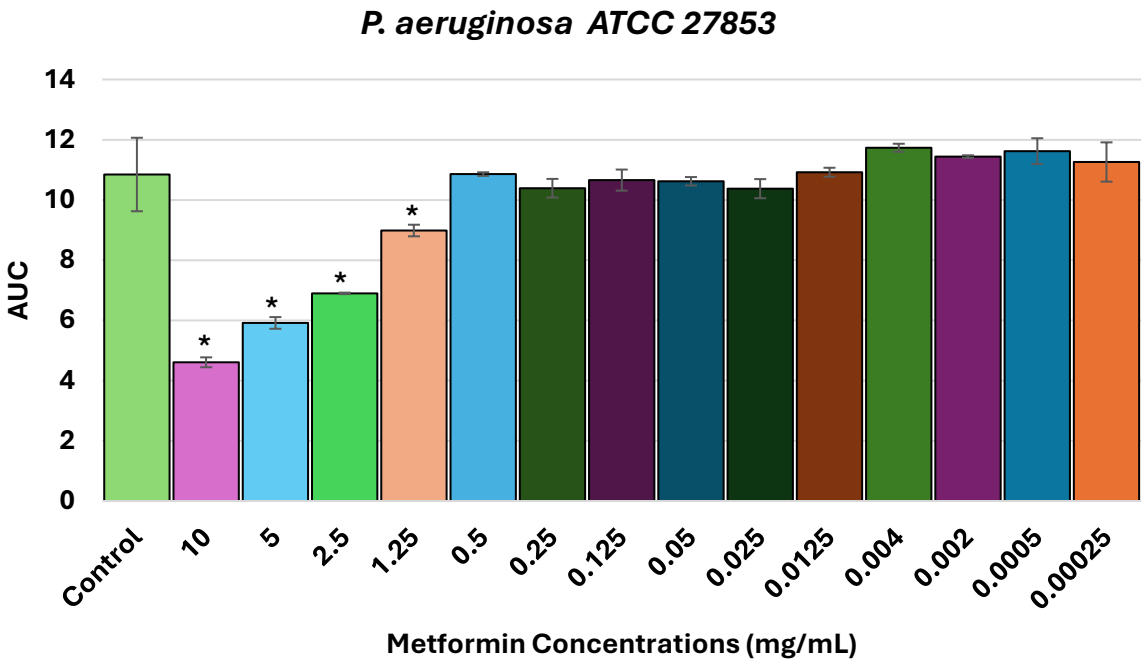

Figure 3-9: Area under the curve (AUC) analysis of *P. aeruginosa* ATCC 27853 growth in the presence of metformin.
AUCs derived from the growth curves of *P. aeruginosa* ATCC 27853 in the presence of different concentrations of metformin (10, 5, 2.5, 1.25, 0.5, 0.25, 0.125, 0.05, 0.025, 0.0125, 0.004, 0.002, 0.0005, and 0.00025 mg/mL) along with the drug-free negative control; where the bars represent mean AUC values ± standard deviation (error bars) and the asterisks '*' represents statistical significance with $p \leq 0.05$ analysed by one-way ANOVA with Tukey's post-hoc test. Each set of the experiment was done in three biological replicates (n=3).

For deeper investigation, the growth curves were plotted. Notably, the growth curve of *P. aeruginosa* NCTC 10662 at 1.25 mg/mL showed a significant difference from the control ($p = 0.009$), whereas the AUC analysis did not show a significant change. The difference in the growth curve was characterised by a prolonged exponential phase, with the stationary phase reached after a longer time. However, it reached a steady state at a higher growth level than the negative control, which could explain the lack of significance in the AUC (Figure 3-10). The same slowing effect was also observed at the concentration of 2.5 mg/mL of metformin ($p = 0.004$); however, it reached the same OD value in the steady state, making it a representative example in which both AUC and the growth curve were significant (Figure 3-11). The growth curve of the concentration 0.5 mg/mL against the control was plotted as a representative example for both AUC and the growth curve, with no significant effect (Figure 3-12).

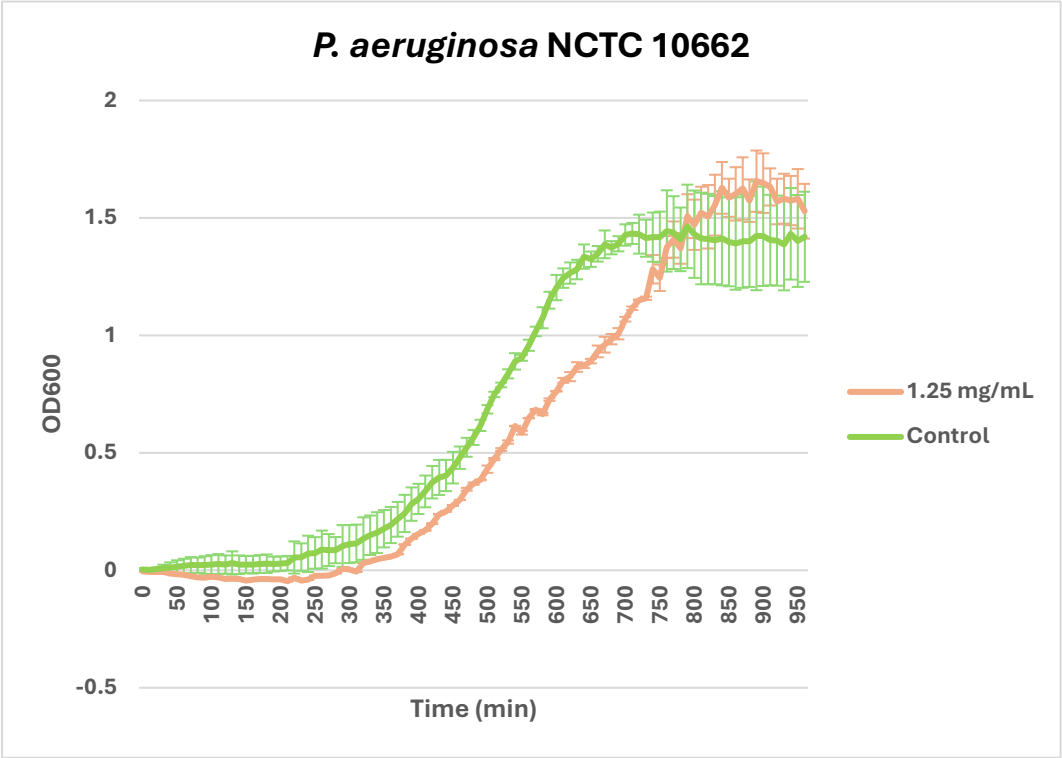

Figure 3-10: Growth profiles of *P. aeruginosa* NCTC 10662 in the presence of metformin (1.25 mg/mL) The drug-free broth was used as negative control; where the curves represent mean of OD_{600} ± standard deviation (error bars). Each set of the experiment was done in three biological replicates (n=3).

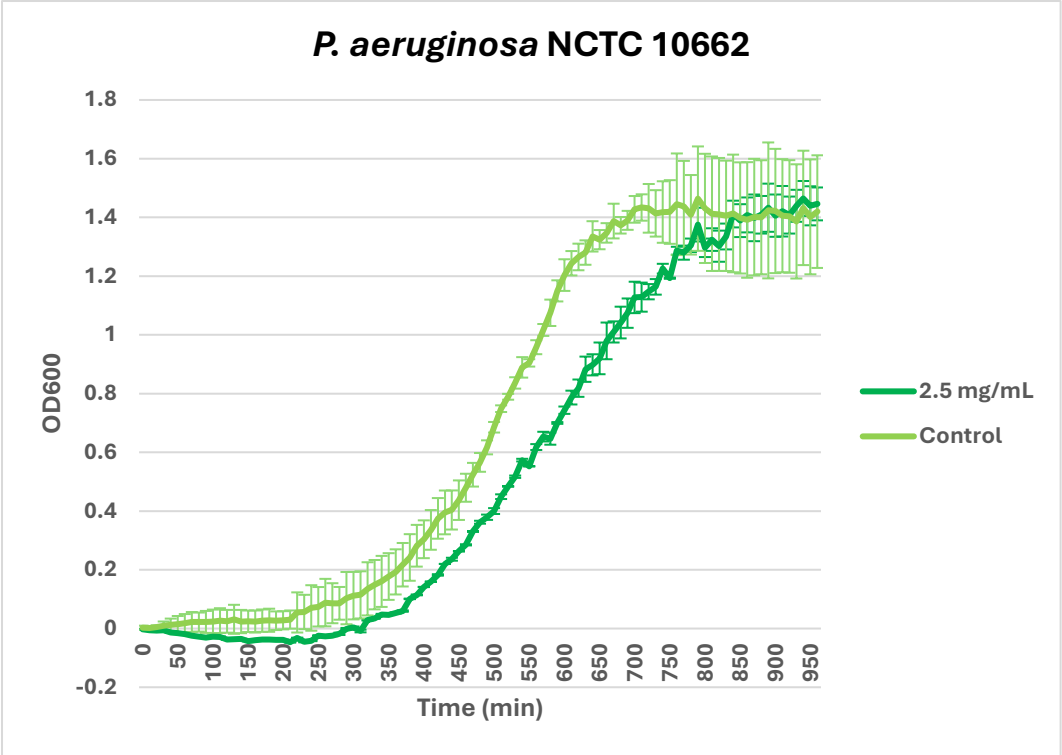

Figure 3-11: Growth profiles of *P. aeruginosa* NCTC 10662 in the presence of metformin (2.5 mg/mL) The drug-free broth was used as negative control; where the curves represent mean of OD_{600} ± standard deviation (error bars). Each set of the experiment was done in three biological replicates (n=3).

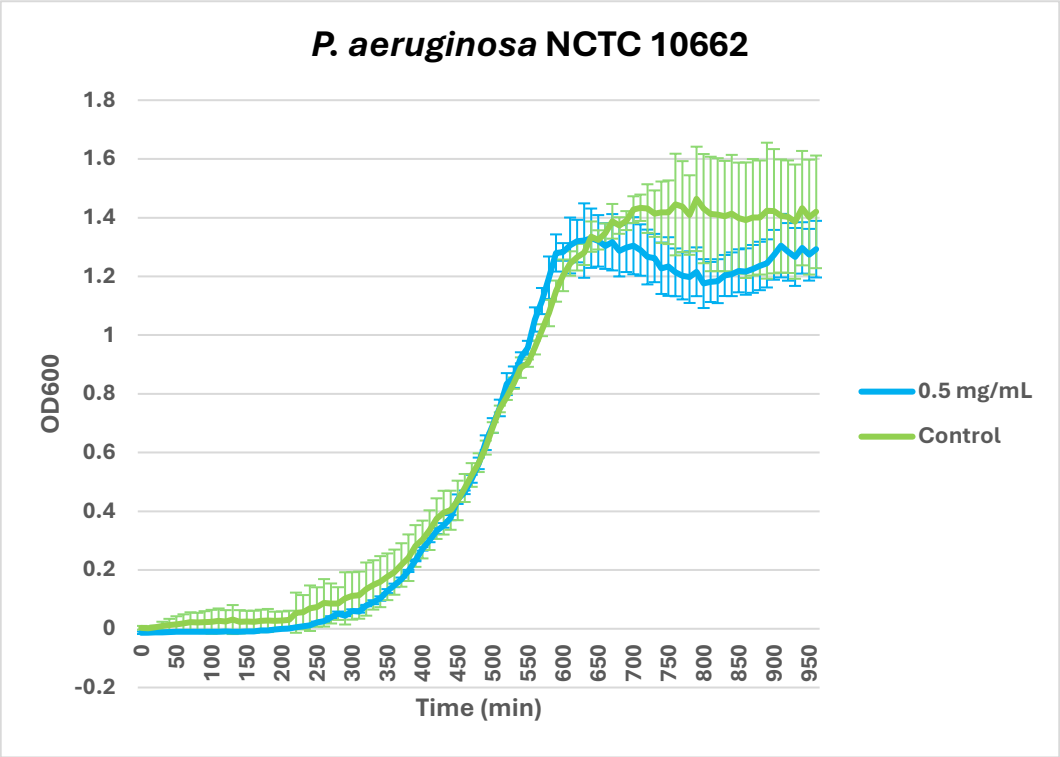

Figure 3-12: Growth profiles of *P. aeruginosa* NCTC 10662 in the presence of metformin (0.5 mg/mL) The drug-free broth was used as negative control; where the curves represent mean of OD_{600} ± standard deviation (error bars). Each set of the experiment was done in three biological replicates (n=3).

For *the P. aeruginosa* ATCC 27853 strain, the effect of metformin on the bacterial growth curve was markedly different from that of the other strain. This was evident in the growth curve for 1.25 mg/mL of metformin compared with the control, which showed no significant difference in the overall curve, despite a clear difference in the time to reach steady state. The presence of the drug caused the bacteria to reach the stationary phase faster and at lower OD values, which explains the significant difference in AUC (Figure 3-13). The same effect was observed at 2.5 mg/mL, although it was slightly more prominent, as it slowed the exponential phase as well, which led to a statistically significant difference ($p = 0.012$), and this is a representative example of both the growth curve and AUC being significant (Figure 3-14). As a representative example of both AUC and growth curve analysis showing no significant difference, the effect of 0.5 mg/mL of metformin on the bacterial growth was plotted in comparison with the negative control (Figure 3-15).

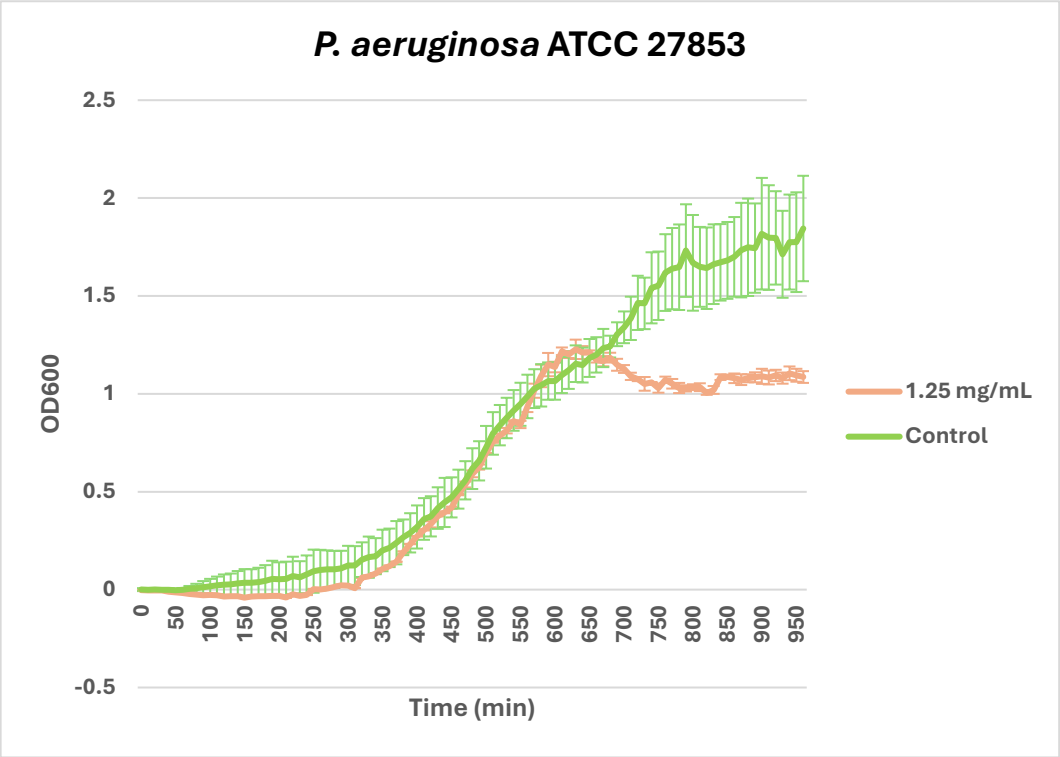

Figure 3-13: Growth profiles of *P. aeruginosa* ATCC 27853 in the presence of metformin (1.25 mg/mL) The drug-free broth was used as negative control; where the curves represent mean of OD_{600} ± standard deviation (error bars). Each set of the experiment was done in three biological replicates (n=3).

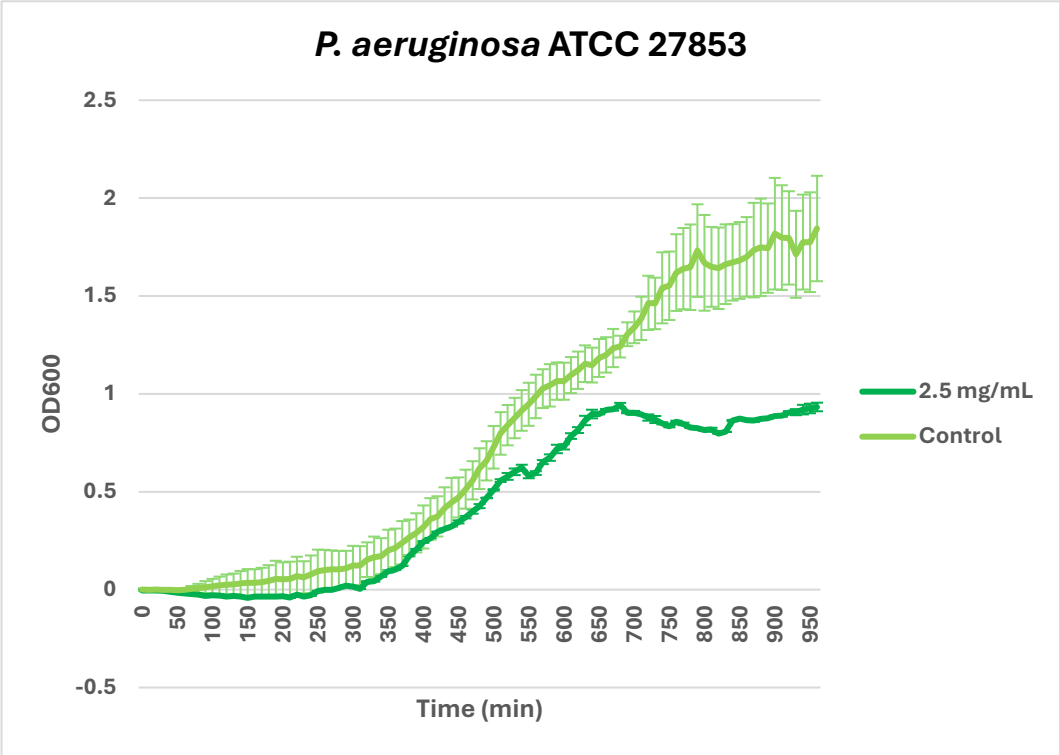

Figure 3-14: Growth profiles of *P. aeruginosa* ATCC 27853 in the presence of metformin (2.5 mg/mL) The drug-free broth was used as negative control; where the curves represent mean of OD_{600} ± standard deviation (error bars). Each set of the experiment was done in three biological replicates (n=3).

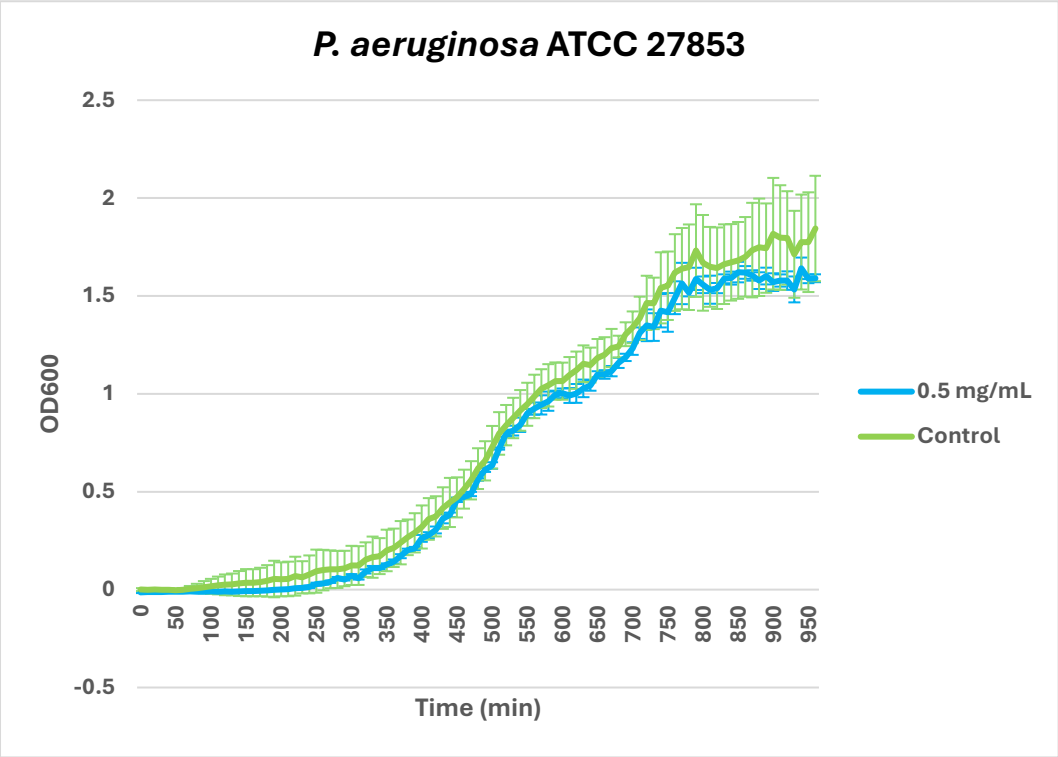

Figure 3-15: Growth profiles of *P. aeruginosa* ATCC 27853 in the presence of metformin (0.5 mg/mL) The drug-free broth was used as negative control; where the curves represent mean of OD_{600} ± standard deviation (error bars). Each set of the experiment was done in three biological replicates (n=3).

For *E. coli* NCTC 10418, metformin caused significant inhibition of growth at concentrations of 2.5-10 mg/mL (p = <0.00001 - 0.0033), with no significance in the other concentrations tested (Figure 3-16).

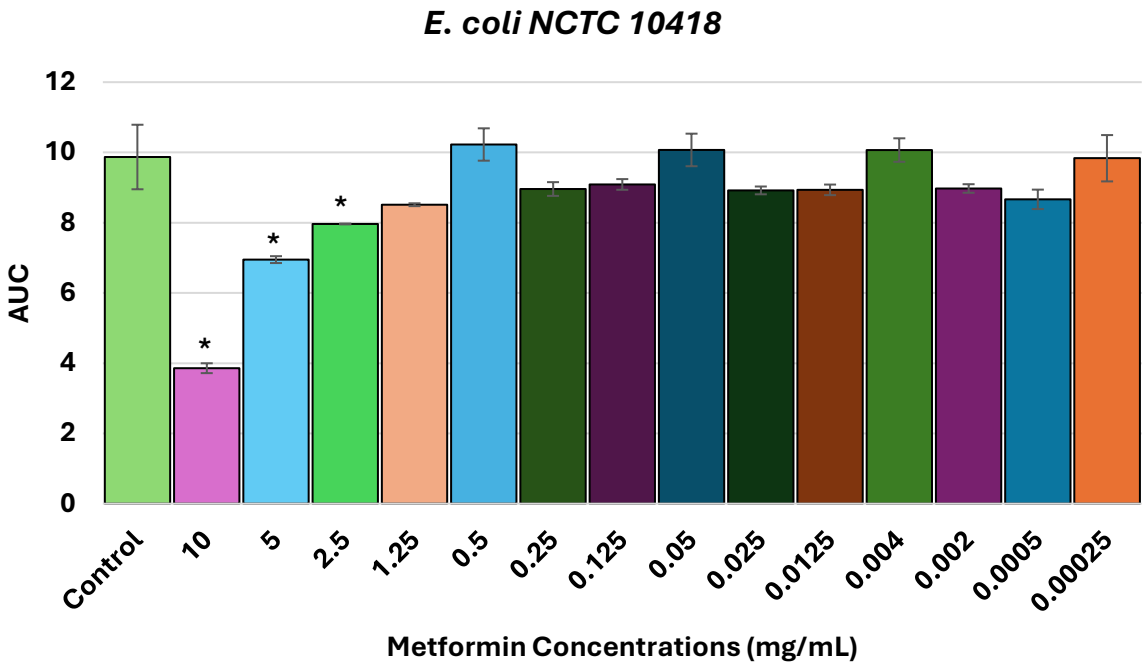

Figure 3-16: Area under the curve (AUC) analysis of *E. coli* NCTC 10418 growth in the presence of metformin. AUCs derived from the growth curves of *E. coli* NCTC 10418 in the presence of different concentrations of metformin (10, 5, 2.5, 1.25, 0.5, 0.25, 0.125, 0.05, 0.025, 0.0125, 0.004, 0.002, 0.0005, and 0.00025 mg/mL) along with the drug-free negative control; where the bars represent mean AUC values ± standard deviation (error bars) and the asterisks '*' represents statistical significance with $p \leq 0.05$ analysed by one-way ANOVA with Tukey's post-hoc test. Each set of the experiment was done in three biological replicates (n=3).

The analysis of the growth curves at different concentrations of metformin on *E. coli* NCTC 10418 did not differ from the AUC analysis. As a representative example of a non-significant difference between the treated and untreated samples, the growth curve at the concentration of 1.25 mg/mL was plotted in comparison with the negative control (Figure 3-17). While the concentration of 2.5 mg/mL showed significant inhibition ($p = 0.027$) of growth, as appeared in the AUC analysis, it also showed a slowing effect on bacterial growth during the stationary phase, reaching the same plateau OD at a longer time than the negative control (Figure 3-18).

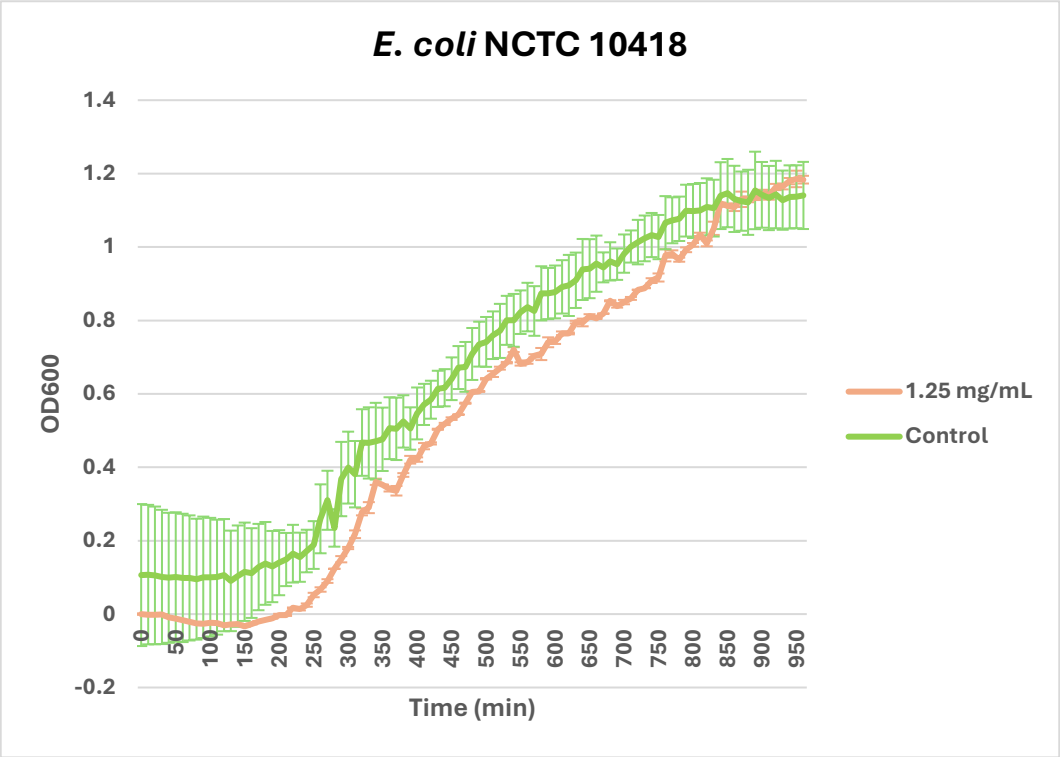

Figure 3-17: Growth profiles of *E. coli* NCTC 10418 in the presence of metformin (1.25 mg/mL) The drug-free broth was used as negative control; where the curves represent mean of OD_{600} ± standard deviation (error bars). Each set of the experiment was done in three biological replicates (n=3).

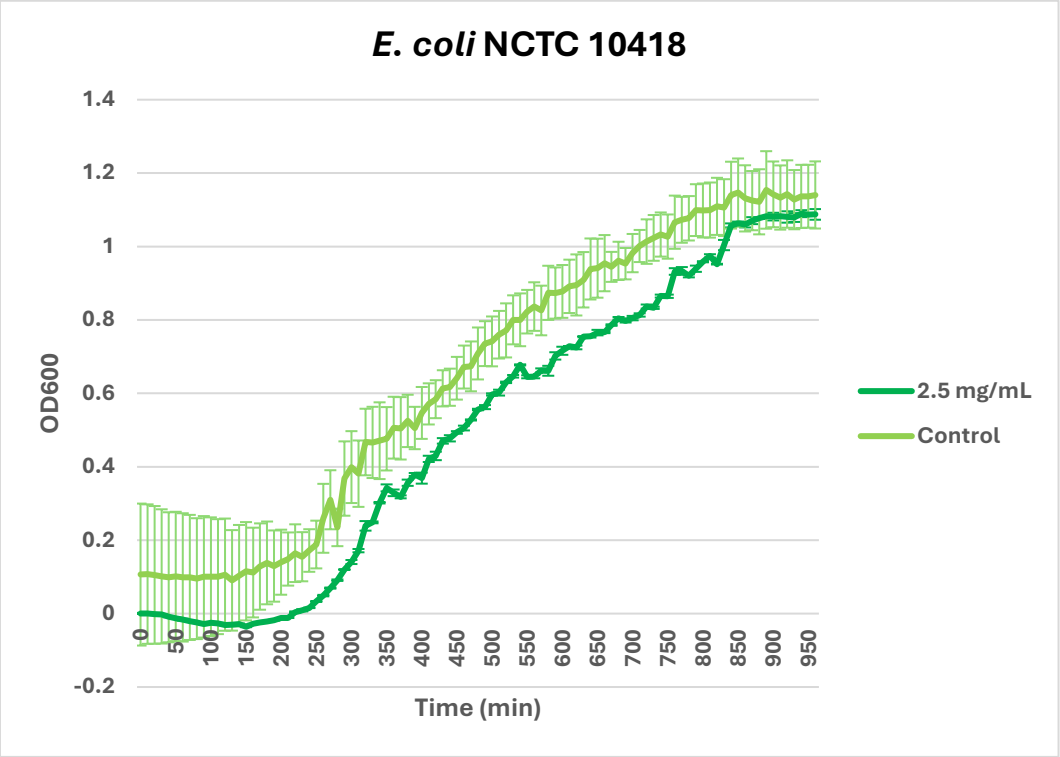

Figure 3-18: Growth profiles of *E. coli* NCTC 10418 in the presence of metformin (2.5 mg/mL) The drug-free broth was used as negative control; where the curves represent mean of OD_{600} ± standard deviation (error bars). Each set of the experiment was done in three biological replicates (n=3).

Conversely, the other *E. coli* strain (ATCC 25922) did not show any significant difference in the AUC of the treated cultures compared to the control (Figure 3-19); however, after plotting the growth curve itself, it indicated a significant difference at the concentrations of 5 and 10 mg/mL compared to the control ($p = 0.048$ and 0.007, respectively). The difference was more apparent in the prolongation of the lag phase before the start of the exponential phase, which was also slower at both concentrations (Figure 3-20 and Figure 3-21). While the other concentrations did not show any significant difference upon analysis their growth curves in comparison with the negative control. And as a representative example, the growth curve at the concentration 2.5 mg/mL was plotted as shown in (Figure 3-22).

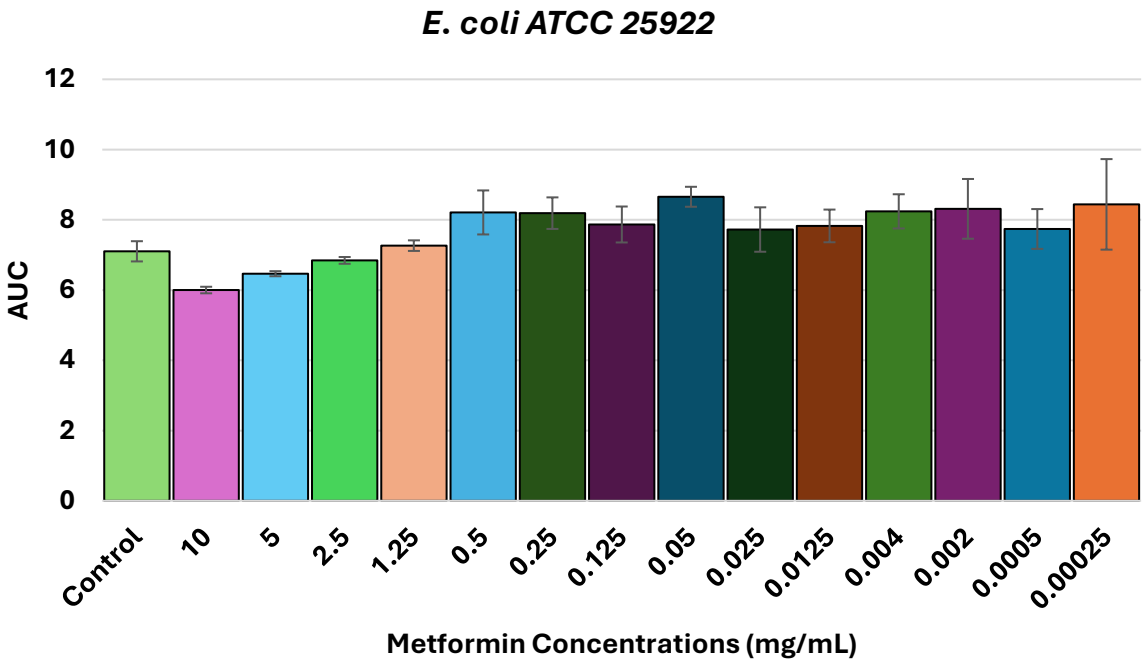

Figure 3-19: Area under the curve (AUC) analysis of *E. coli* ATCC 25922 growth in the presence of metformin. AUCs derived from the growth curves of *E. coli* ATCC 25922 in the presence of different concentrations of metformin (10, 5, 2.5, 1.25, 0.5, 0.25, 0.125, 0.05, 0.025, 0.0125, 0.004, 0.002, 0.0005, and 0.00025 mg/mL) along with the drug-free negative control; where the bars represent mean AUC values ± standard deviation (error bars) and the asterisks '*' represents statistical significance with $p \leq 0.05$ analysed by one-way ANOVA with Tukey's post-hoc test. Each set of the experiment was done in three biological replicates (n=3).

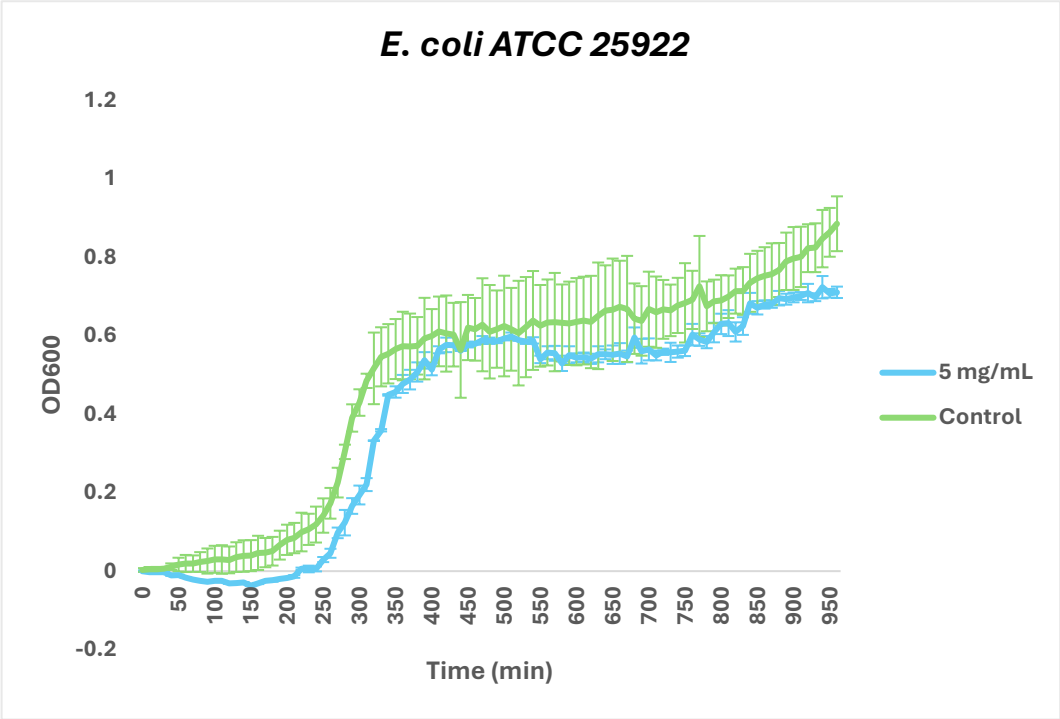

Figure 3-20: Growth profiles of *E. coli* ATCC 25922 in the presence of metformin (5 mg/mL)
The drug-free broth was used as negative control; where the curves represent mean of OD_{600} ± standard deviation (error bars). Each set of the experiment was done in three biological replicates (n=3).

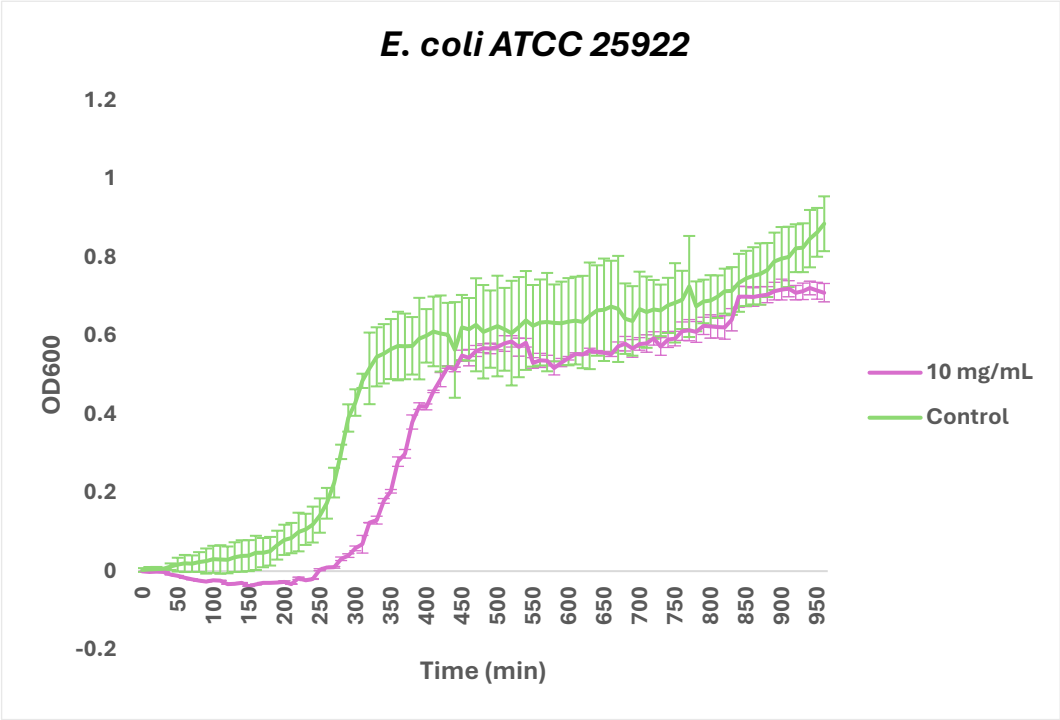

Figure 3-21: Growth profiles of *E. coli* ATCC 25922 in the presence of metformin (10 mg/mL)
The drug-free broth was used as negative control; where the curves represent mean of OD_{600} ± standard deviation (error bars). Each set of the experiment was done in three biological replicates (n=3).

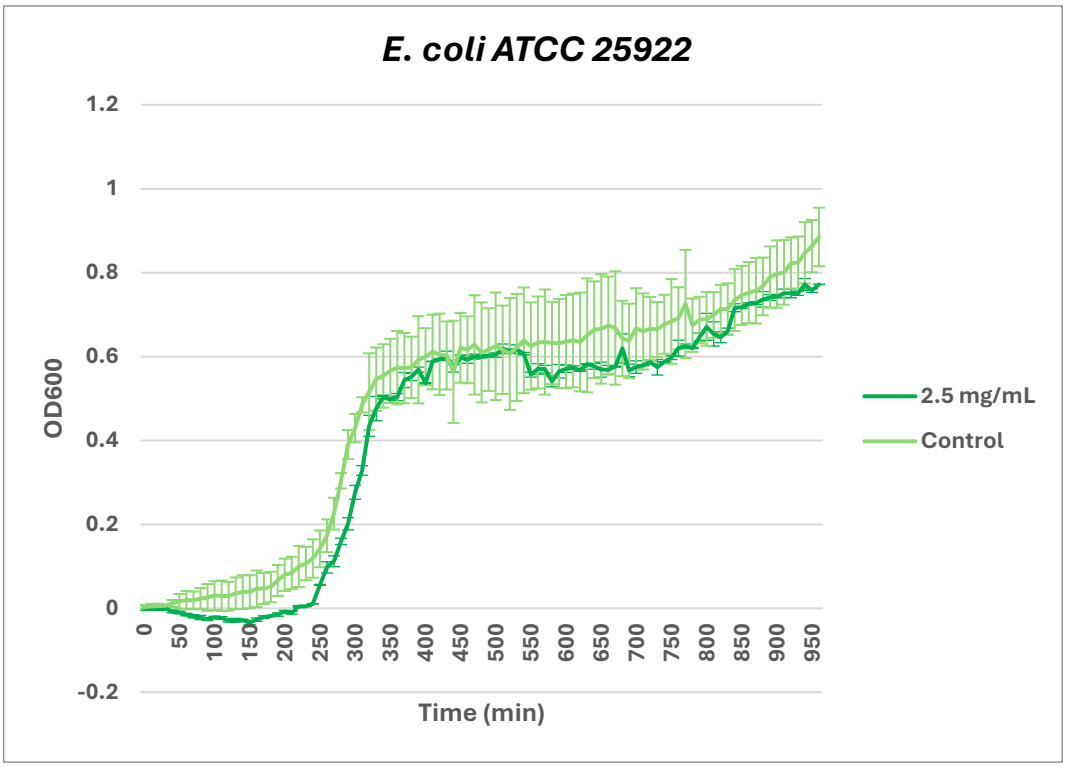

Figure 3-22: Growth profiles of *E. coli* ATCC 25922 in the presence of metformin (2.5 mg/mL)
The drug-free broth was used as negative control; where the curves represent mean of OD_{600} ± standard deviation (error bars). Each set of the experiment was done in three biological replicates (n=3).

For *K. pneumoniae* strains, both of them showed significant reduction in their growth at the concentration 10 mg/mL (p = 0.0003 and 0.0002); however, *K. pneumoniae* ATCC 700603 showed a significant inhibition of growth at lower concentrations of metformin (0.004, 0.05 and 0.5 mg/mL) ($p <$ 0.00001– 0.0006) (Figure 3-23 and Figure 3-24).

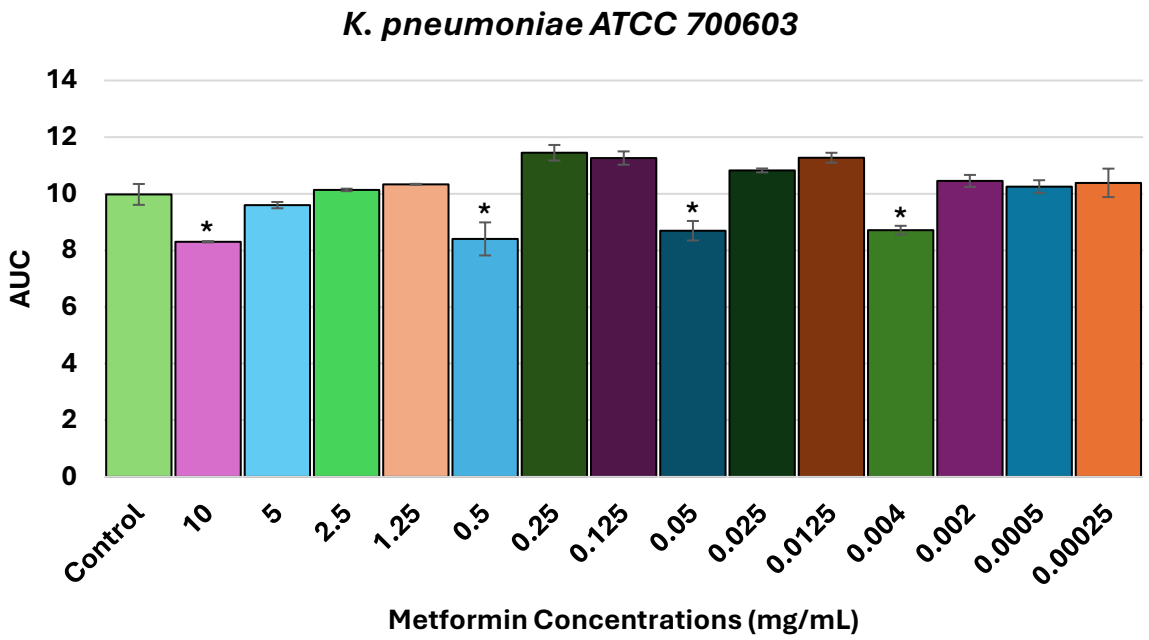

Figure 3-23: Area under the curve (AUC) analysis of *K. pneumoniae* ATCC 700603 growth in the presence of metformin.
AUCs derived from the growth curves of *K. pneumoniae* ATCC 700603 in the presence of different concentrations of metformin (10, 5, 2.5, 1.25, 0.5, 0.25, 0.125, 0.05, 0.025, 0.0125, 0.004, 0.002, 0.0005, and 0.00025 mg/mL) along with the drug-free negative control; where the bars represent mean AUC values ± standard deviation (error bars) and the asterisks '*' represents statistical significance with $p \leq 0.05$ analysed by one-way ANOVA with Tukey's post-hoc test. Each set of the experiment was done in three biological replicates (n=3).

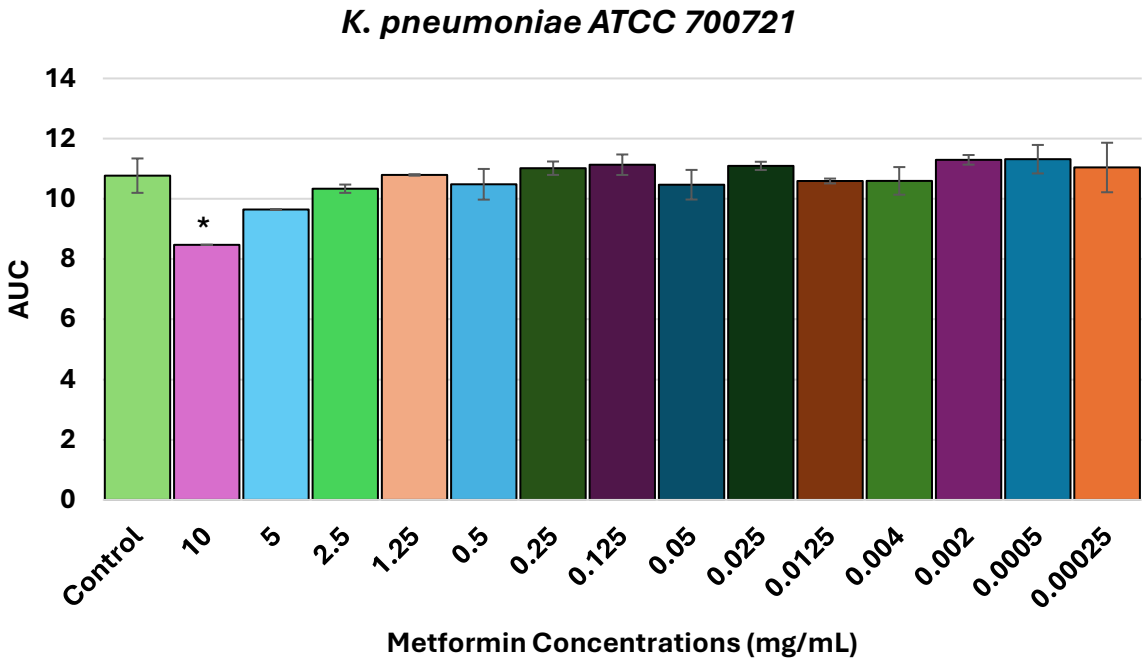

Figure 3-24: Area under the curve (AUC) analysis of *K. pneumoniae* ATCC 700721 growth in the presence of metformin.
AUCs derived from the growth curves of *K. pneumoniae* ATCC 700721 in the presence of different concentrations of metformin (10, 5, 2.5, 1.25, 0.5, 0.25, 0.125, 0.05, 0.025, 0.0125, 0.004, 0.002, 0.0005, and 0.00025 mg/mL) along with the drug-free negative control; where the bars represent mean AUC values ± standard deviation (error bars) and the asterisks '*' represents statistical significance with $p \leq 0.05$ analysed by one-way ANOVA with Tukey's post-hoc test. Each set of the experiment was done in three biological replicates (n=3).

Analysis of the growth curves for both *K. pneumoniae* strains showed no difference between them, as confirmed by the AUC analysis. Therefore, the effect of metformin at a concentration of 10 mg/mL on *K. pneumoniae* ATCC 700603 was plotted, showing that metformin prolonged the lag phase and slowed the exponential phase ($p = 0.003$), which altered the curve shape and resulted in the stationary phase being reached at a lower OD (Figure 3-25). The slowing effect was also evident at the concentration of 0.5 mg/mL ($p = 0.003$) (Figure 3-26). In contrast, as a representative example of a non-significant change, the growth curve at the concentration of 1.25 mg/mL was plotted. However, there was a slight increase in the OD in the treated sample compared to the negative control (Figure 3-27).

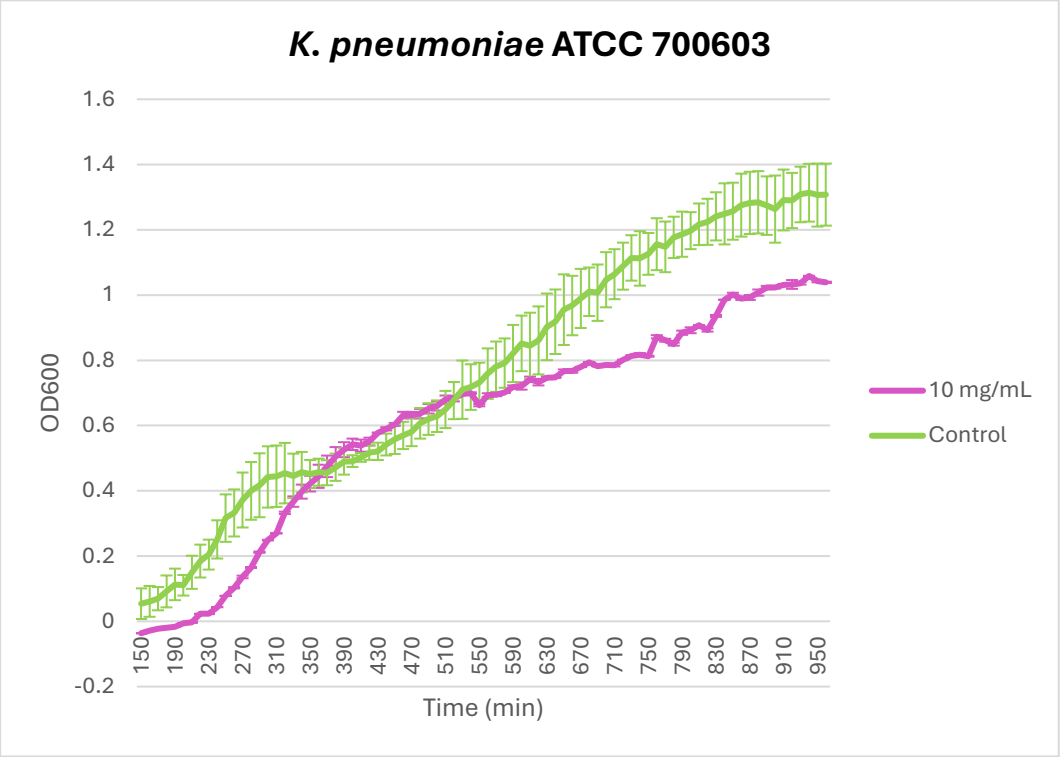

Figure 3-25: Growth profiles of *K. pneumoniae* ATCC 700603 in the presence of metformin (10 mg/mL) The drug-free broth was used as negative control; where the curves represent mean of OD_{600} ± standard deviation (error bars). Each set of the experiment was done in three biological replicates (n=3).

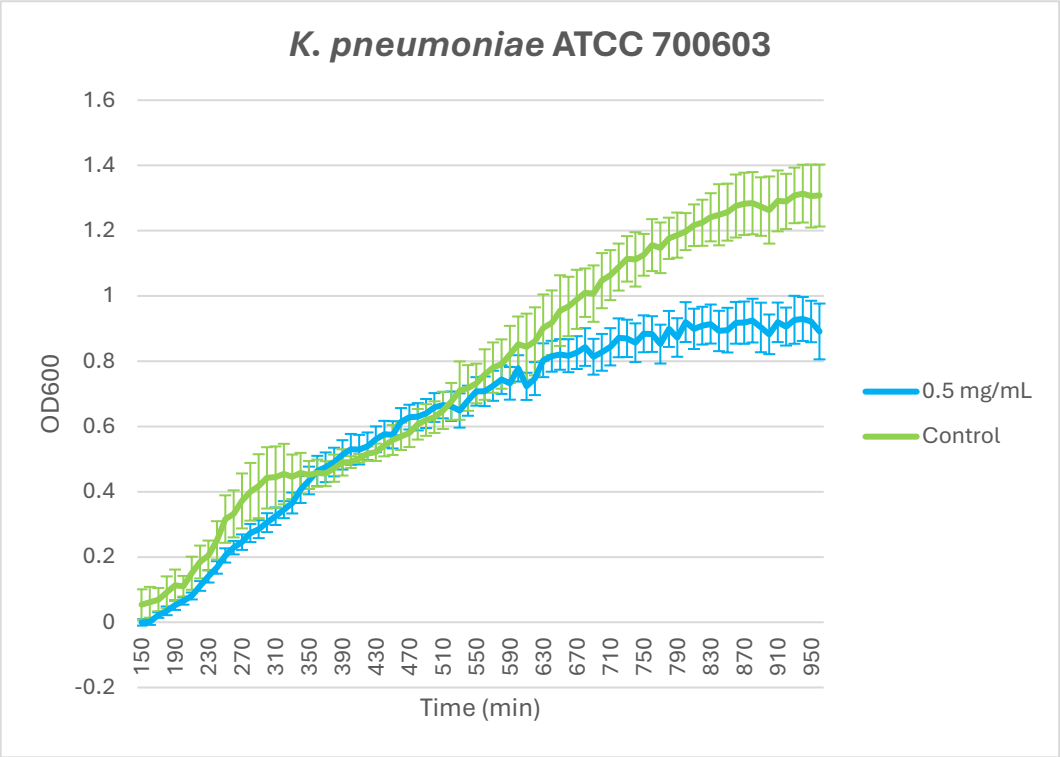

Figure 3-26: Growth profiles of *K. pneumoniae* ATCC 700603 in the presence of metformin (0.5 mg/mL) The drug-free broth was used as negative control; where the curves represent mean of OD_{600} ± standard deviation (error bars). Each set of the experiment was done in three biological replicates (n=3).

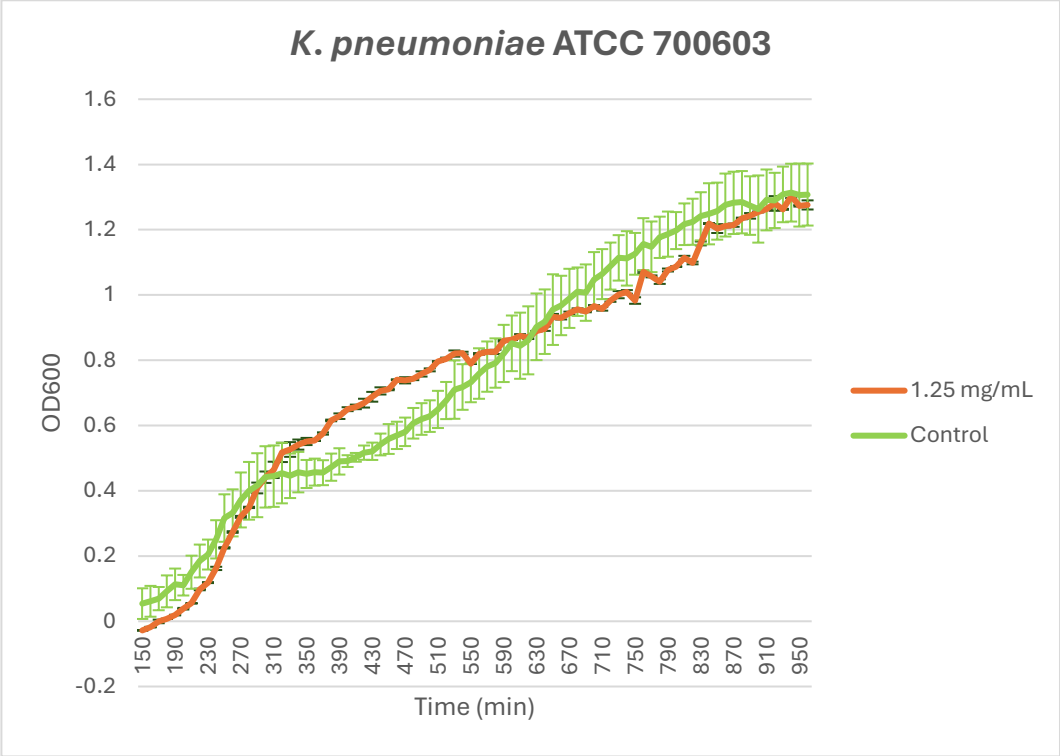

Figure 3-27: Growth profiles of *K. pneumoniae* ATCC 700603 in the presence of metformin (1.25 mg/mL) The drug-free broth was used as negative control; where the curves represent mean of OD_{600} ± standard deviation (error bars). Each set of the experiment was done in three biological replicates (n=3).

The analysis of the growth curves and the AUC for the effect of metformin on *K. pneumoniae* ATCC 700721 did not show a difference in the results. Therefore, as a representative example of both growth curves and the AUC were significant, the effect of metformin at the concentration 10 mg/mL was plotted, where metformin showed elongation of the lag phase and a slowing effect on the exponential phase ($p = 0.005$) (Figure 3-28). By contrast, the growth curve at the concentration 5 mg/mL was the representative example for the non-significant difference for both growth curve analysis and AUC (Figure 3-29).

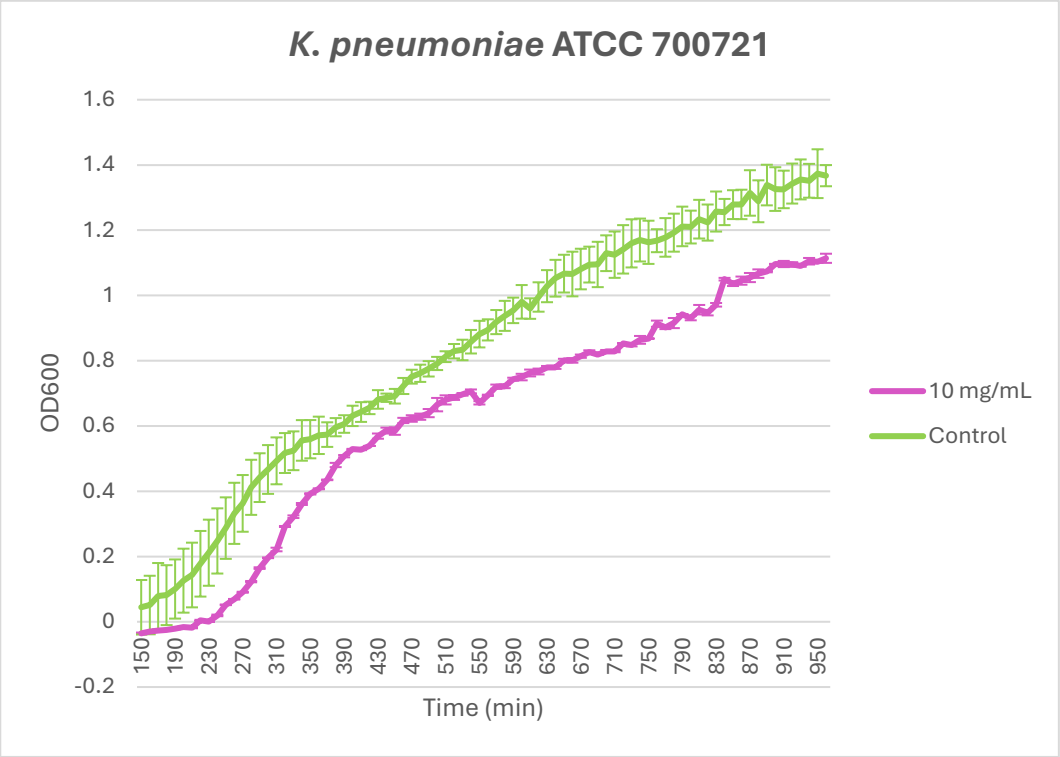

Figure 3-28: Growth profiles of *K. pneumoniae* ATCC 700721 in the presence of metformin (10 mg/mL) The drug-free broth was used as negative control; where the curves represent mean of OD_{600} ± standard deviation (error bars). Each set of the experiment was done in three biological replicates (n=3).

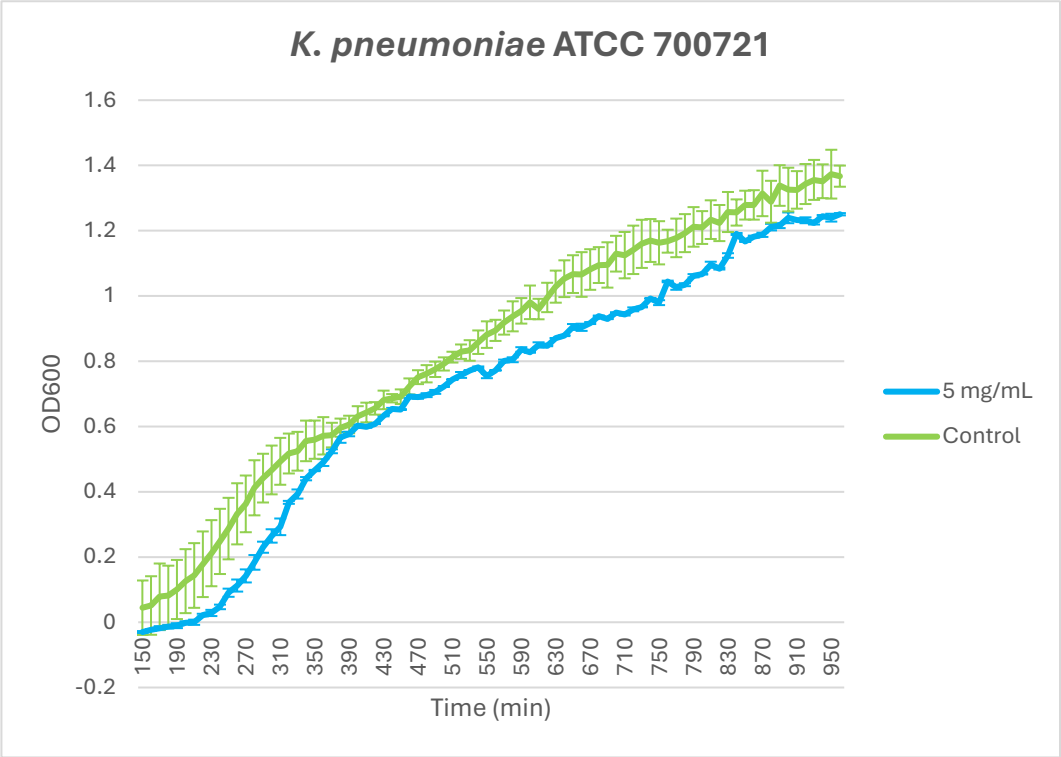

Figure 3-29: Growth profiles of *K. pneumoniae* ATCC 700721 in the presence of metformin (5 mg/mL) The drug-free broth was used as negative control; where the curves represent mean of OD_{600} ± standard deviation (error bars). Each set of the experiment was done in three biological replicates (n=3).

It is notable to mention that from the growth curves it was observed that the error bars of the control samples are larger in comparison to the drug treated ones.

Following the growth curves, the MIC of metformin against the different bacterial species was investigated. It was found that all the bacterial strains had an MIC of 40 mg/mL except *S. aureus* NCTC 6571 had the lower MIC value, which was 10 mg/mL, and *K. pneumoniae* strains had the higher MIC values which were 80 mg/mL (Table 3-1).

Table 3-1: Minimum inhibitory concentration values of metformin in mg/mL against eight different bacterial species measured by broth microdilution method

Bacterial Strain	MIC (mg/mL)
P. aeruginosa NCTC 10662	40
P. aeruginosa ATCC 27853	40
E. coli NCTC 10418	40
E. coli ATCC 25922	40
S. aureus NCTC 6571	10
S. aureus ATCC 25923	40
K. pneumoniae ATCC 700721	80
K. pneumoniae ATCC 700603	80

3.2.2. The effect of metformin on different virulence factors:

3.2.2.1. Effect of metformin on protease activity:

The effect of various concentrations of metformin on the proteolytic activity of the bacterial species towards milk protein was investigated. The results are plotted as a relationship between the diameter of the hydrolysed zone in mm and the different concentrations of metformin used (Figure 3-30).

It was primarily found that the concentrations of 1.25 and 10 mg/mL significantly reduced the protease activity for the *P. aeruginosa* and *S. aureus* strains compared to the drug-free control, with p values as follows (NCTC 10662: 10 mg/mL, $p = 0.009$; 1.25 mg/mL, $p = 0.022$; ATCC 27853: 10 mg/mL, $p = 0.008$; 1.25 mg/mL, $p = 0.05$; NCTC 6571: 10 mg/mL, $p = 0.011$; 1.25 mg/mL, $p = 0.011$; ATCC 25923: 10 mg/mL, $p = 0.021$; 1.25 mg/mL, $p = 0.021$). Furthermore, the concentration of 0.5 mg/mL significantly decreased the hydrolysed zone by approximately 62% ($p = 0.03$) in the case of *S. aureus* ATCC 25923. However, there was no significant effect of the tested concentrations of metformin on the protease activity of *K. pneumoniae* isolates, and the *E. coli* isolates did not exhibit any proteolytic activity in this assay (data not shown).

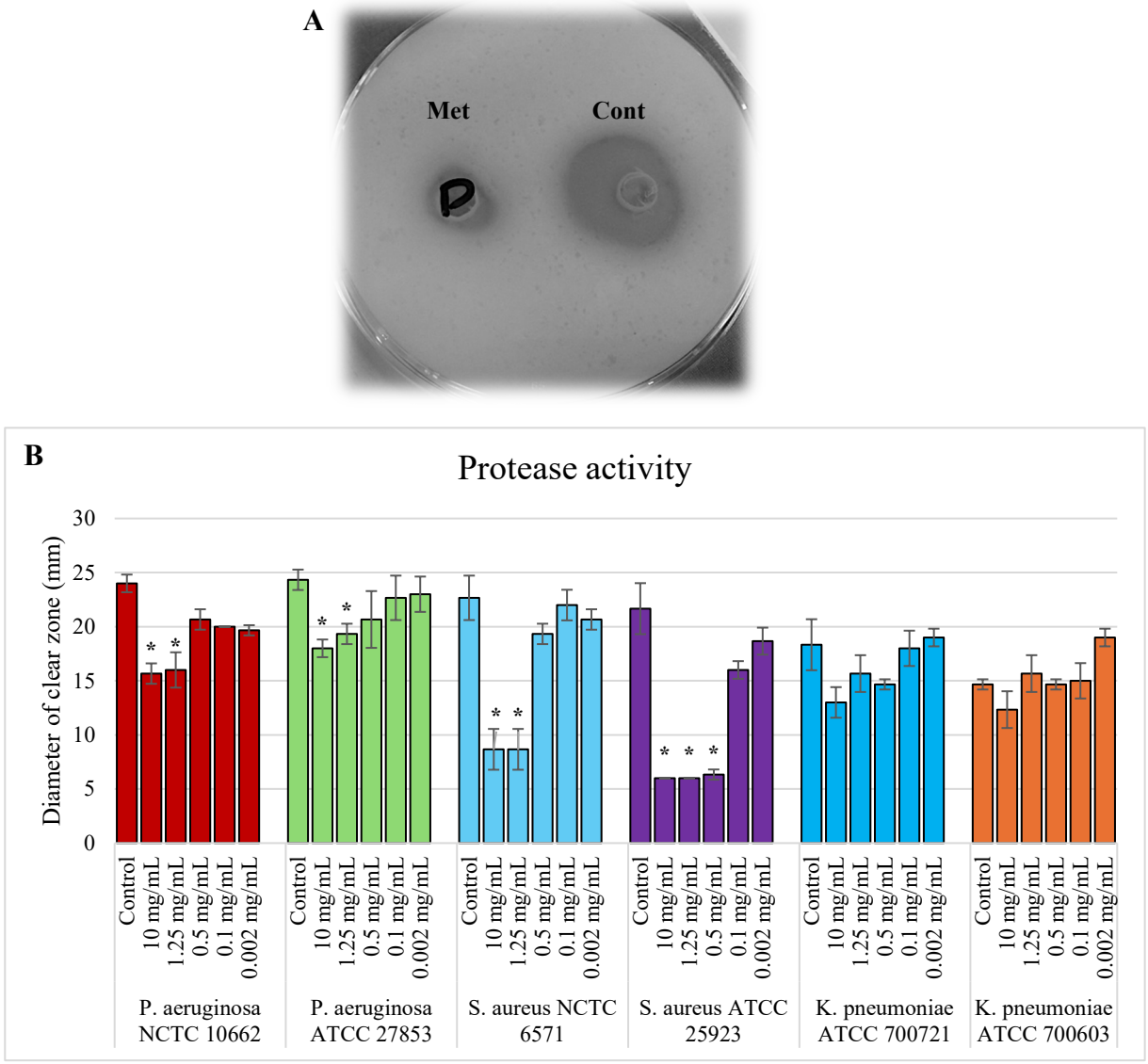

Figure 3-30: Effect of metformin on protease activity of the different bacterial species.
A) Skimmed milk agar plate assay for determination of the protease activity, showing the proteolytic zones around the wells in the agar plate with a comparison of Met (metformin treated samples) and Cont. (Control; untreated samples). B) Bar chart showing the inhibitory effect of different concentrations of metformin (10, 1.25, 0.5, 0.1 and 0.002 mg/mL) on protease activity of *P. aeruginosa, S. aureus* and *K. pneumoniae* strains, along with the drug-free negative control; where the bars represent mean diameter values (mm) ± standard deviation (error bars) and the asterisks '*' represents statistical significance with $p \leq 0.05$ analysed by Kruskal-Wallis test with Dunn's post-hoc test. Each set of the experiment was done in three biological replicates (n=3).

3.2.2.2.Effect of metformin on biofilm formation:

The ability of metformin to inhibit the biofilm formation was studied using the crystal violet assay on the eight different bacterial strains using different concentrations of the drug (Figure 3-31).

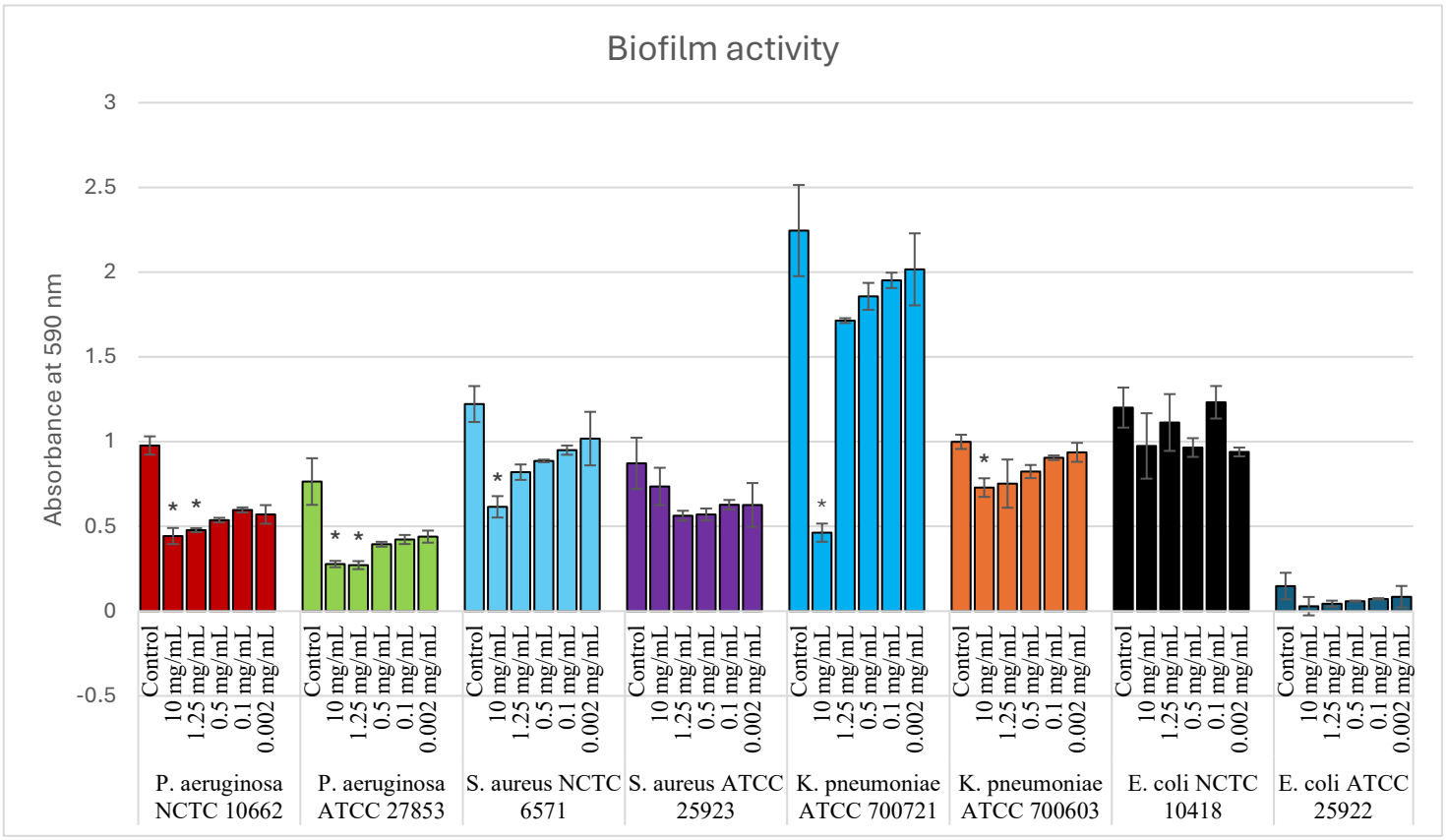

Figure 3-31: Effect of metformin on biofilm formation of the different bacterial species.
The inhibitory effect of different concentrations of metformin (10, 1.25, 0.5, 0.1 and 0.002 mg/mL) on biofilm formation of *P. aeruginosa, E. coli, S. aureus and K.pneumoniae* isolates, , along with the drug-free negative control; where the bars represent mean absorbance reading ± standard deviation (error bars) and the asterisks '*' represents statistical significance with $p \leq 0.05$ analysed by Kruskal-Wallis test with Dunn's post-hoc test. Each set of the experiment was done in three biological replicates (n=3).

It is revealed that in case of *P. aeruginosa* isolates, metformin could inhibit the biofilm formation significantly at the concentrations 1.25 and 10 mg/mL to be less than half of the control; (NCTC 10662: 10 mg/mL, $p < 0.00001$; 1.25 mg/mL, $p = 0.002$; ATCC 27853: 10 mg/mL, $p = 0.001$; 1.25 mg/mL, $p = 0.001$). The concentration of 10 mg/mL showed a significant inhibition of the biofilm formation in *S. aureus* NCTC 6571 by around 48% ($p = 0.009$) and the *K. pneumoniae* isolates, where it was around 80% inhibition in case of ATCC 700721 ($p = 0.007$) and one third of the biofilm in ATCC 700603 ($p = 0.017$). However, there was no effect of any concentration of metformin on the biofilm of *S. aureus* ATCC 25923 and the *E. coli* isolates.

3.2.2.3.The effect of metformin on swimming and twitching motilities:

By inoculating the swimming plates containing different concentrations of metformin with *P. aeruginosa* and *E. coli* isolates, it is shown that the concentration of 10 mg/mL metformin significantly reduced the swimming zone of *E. coli* NCTC 10418 by 34% (p = 0.01). There was no effect on the other tested isolates with different concentrations of the drug (Figure 3-32).

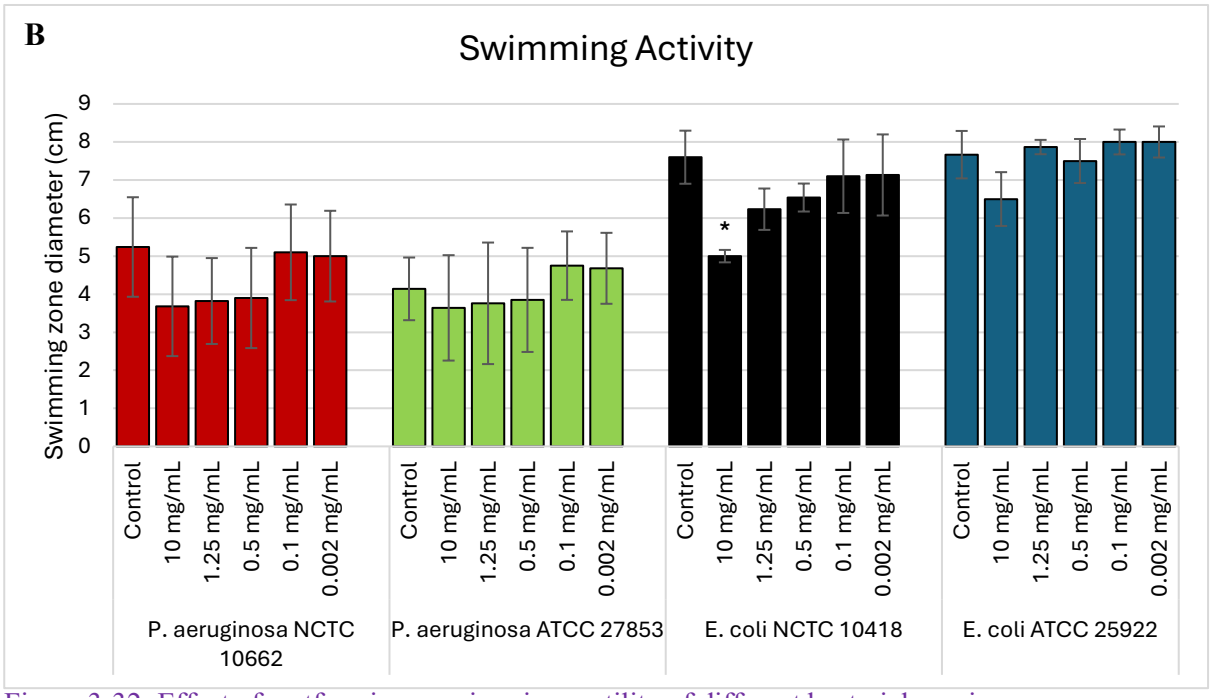

Figure 3-32: Effect of metformin on swimming motility of different bacterial species.
A) Swimming motility assay after inoculation with the bacteria, showing the large swimming zone in the middle of 0.2% tryptone agar plate. B) Bar chart showing the inhibitory effect of different concentrations of metformin (10, 1.25, 0.5, 0.1 and 0.002 mg/mL) on swimming motility of *P. aeruginosa* and *E. coli*, along with the drug-free negative control; where the bars represent mean swimming diameter (cm) ± standard deviation (SD) (error bars), and the asterisks '*' represents statistical significance with $p \leq 0.05$ analysed by Kruskal-Wallis test with Dunn's post-hoc test. Each set of the experiment was done in three biological replicates (n=3).

By testing the effect of metformin on the twitching activity, the results revealed that there was no significant effect of any concentration used on reducing the twitching activity of either *P. aeruginosa* or *E. coli* isolates comparing to the control (Figure 3-33).

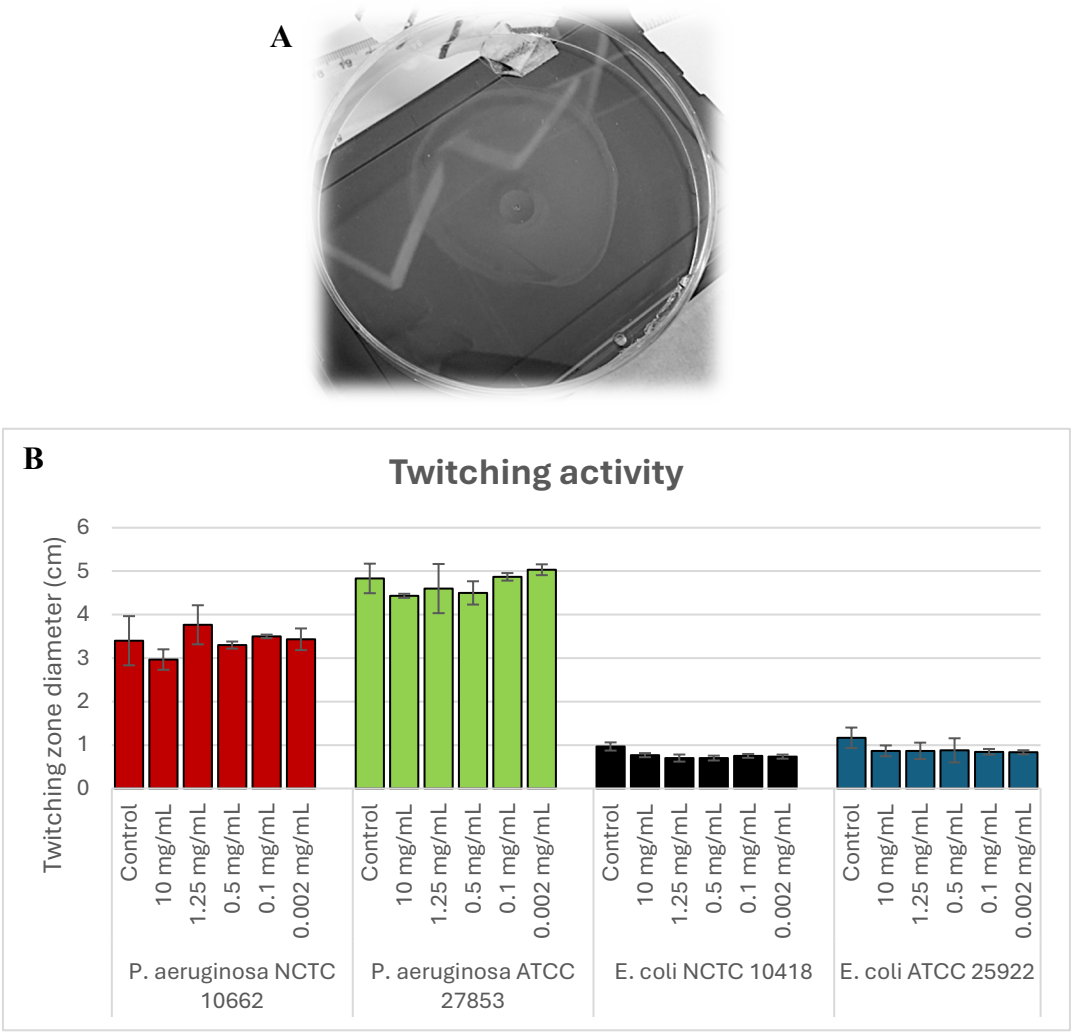

Figure 3-33: Effect of metformin on twitching motility of different bacterial species.
A) Twitching motility assay after inoculation with the bacteria, showing the large twitching zone on the petri dish itself after removing the agar. B) Bar chart showing the inhibitory effect of different concentrations of metformin (10, 1.25, 0.5, 0.1 and 0.002 mg/mL) on twitching motility of *P. aeruginosa* and *E. coli*, along with the drug-free negative control; where the bars represent mean twitching diameter values (cm) ± standard deviation (error bars). Each set of the experiment was done in three biological replicates (n=3).

Table 3-2: Summarising table for all the inhibitory effects of metformin (mg/mL) against the eight strains of the different bacterial species *S. aureus, P. aeruginosa, E. coli,* and *K. pneumoniae,* showing the significantly effective concentration in mg/mL for each phenotypic property.

	***P. aeruginosa* NCTC 10662**	***P. aeruginosa* ATCC 27853**	***S. aureus* NCTC 6571**	***S. aureus* ATCC 25923**	***E. coli* NCTC 10418**	***E. coli* ATCC 25922**	***K. pneumoniae* ATCC 700721**	***K. pneumoniae* ATCC 700603**
MIC	40	40	10	40	40	40	80	80
Growth (AUC)	10,5,2.5	10,5,2.5,1.25	10,5, all sub MIC except 1.25 and 2.5	10,5,2.5,1.25	None (10,5 on curve)	10,5,2.5	10	10,0.5,0.05,0.004
Protease Activity	10,1.25	10,1.25	10,1.25	10,1.25,0.5	NA	NA	NS	NS
Biofilm	10,1.25	10,1.25	10	NS	NS	NS	10	10
Swimming	NS	NS	NA	NA	10	NS	NA	NA
Twitching	NS	NS	NA	NA	NS	NS	NA	NA

Notes: NS means that it did not reach the statistical significance level; NA means it was not applicable to investigate the effect.

3.2.3. Effect of metformin on efflux pumps:

The efflux assay using ethidium bromide showed that the concentration of 10 mg/mL metformin could inhibit the efflux of ethidium bromide of *S. aureus* NCTC 6571 significantly compared to the control ($p < 0.00001$; Figure 3-34).

Without adding the glucose (i.e. the no-efflux control), the fluorescence was almost stable during the experimental time. In all other treatments, which had glucose in the mixture except the sodium salicylate one, the same pattern was seen with an initial slow decrease in the fluorescence until 10 minutes of the experiment, where the treatment with 10 mg/mL metformin slowed its rate of decrease until reaching the steady state concentration after 4 further minutes. However, the control and other treatments reached almost the same steady state concentration at 32 minutes. By referring to the sodium salicylate curve, which was used as efflux inducer control, it was obvious that the sodium salicylates worked quicker and caused a steep decrease in the fluorescence at the start and reached a steady state concentration after around 15 min that indicated efflux activity was unaffected by all metformin concentrations except for 10 mg/mL, which inhibited efflux activity.

For the *S. aureus* ATCC 25923, the analysis did not reveal any significant difference among the various concentrations of metformin compared to the control, with all others displaying a similar pattern to the control, which closely resembled the pattern of the previous *S. aureus* strain (Figure 3-16). For the remaining species, this protocol for evaluating the efflux activity could not be optimised efficiently (for *Pseudomonas,* the readings were so small to be detected by the plate reader; for *E. coli* and *Klebsiella* the control did not work as expected (data not shown), so it was not applicable for further statistical analysis.

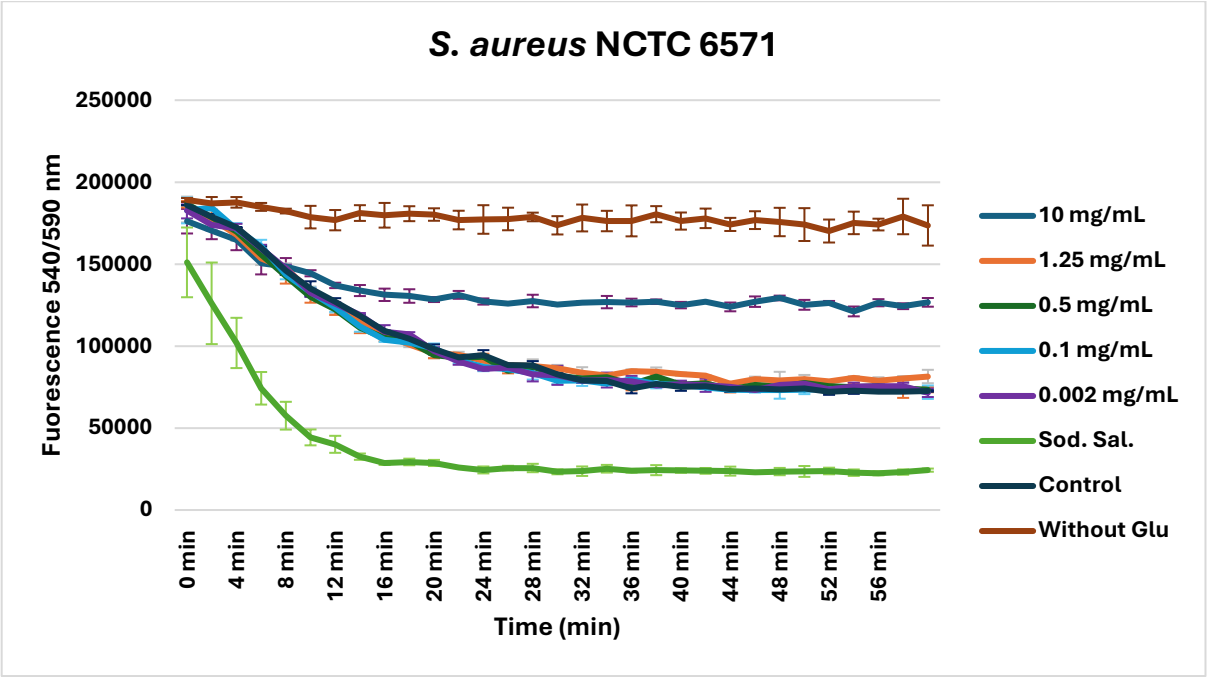

Figure 3-34: Effect of metformin on efflux pumps of *S. aureus* NCTC 6571 using the ethidium bromide assay. Ethidium bromide efflux assay to study the effect of different concentrations of metformin (10, 1.25, 0.5, 0.1 and 0.002 mg/mL) along with a negative control without glucose (Without Glu), a control with glucose (Control), and sodium salicylate (Sod. Sal.) as an efflux pump inducer on *S. aureus* NCTC 6571; presented as relation between the fluorescence at 540/590 nm excitation/emission, where each line represents the mean of fluorescence ± standard deviation (error bars). Each set of the experiment was done in three biological replicates (n=3).

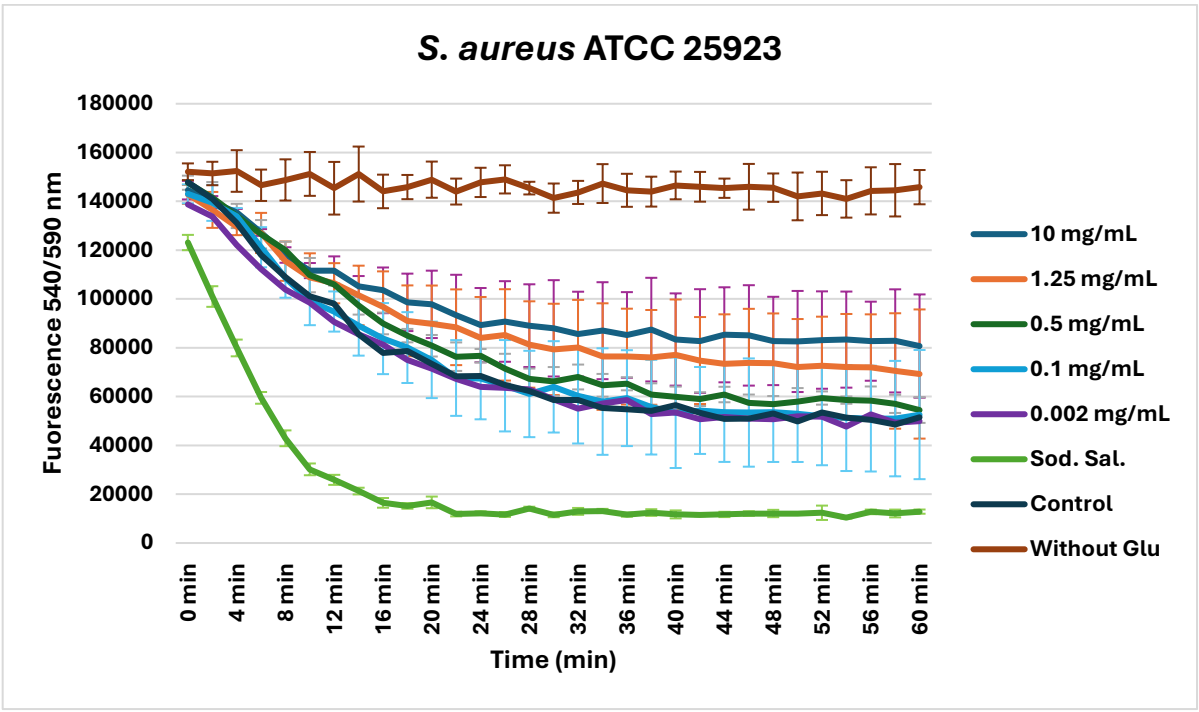

Figure 3-35: Effect of metformin on efflux pumps of *S. aureus* ATCC 25923 using the ethidium bromide assay. Ethidium bromide efflux assay to study the effect of different concentrations of metformin (10, 1.25, 0.5, 0.1 and 0.002 mg/mL) along with a negative control without glucose (Without Glu), a control with glucose (Control), and sodium salicylate (Sod. Sal.) as an efflux pump inducer on *S. aureus* ATCC 25923; presented as relation between the fluorescence at 540/590 nm excitation/emission, where each line represents the mean of fluorescence ± standard deviation (error bars). Each set of the experiment was done in three biological replicates (n=3).

3.2.4. The effect of the combination of different antibiotics with metformin

Different antibiotics were tested in combination with metformin using a checkerboard assay, and the average FICI for the two replicates of each combination was calculated (Table 3-3).

It was noticed that the combinations of doxycycline, gentamicin and imipenem gave the same effect in both *P. aeruginosa* strains, where the combination of doxycycline showed a synergistic effect (FICI = 0.375) with metformin compared to both drugs alone, and gentamicin and imipenem combinations with metformin showed an additive effect. For *S. aureus* strains, the ciprofloxacin combination showed an additive effect in both of them. While doxycycline and linezolid showed indifference with *S. aureus* NCTC 6571 and additive effect with *S. aureus* ATCC 25923, the FICIs values were so close, 1.1 and 1, respectively. For the *E. coli* strain, all the combinations showed an additive effect compared to both drugs alone. In *K. pneumoniae* strains, the combination with doxycycline showed a synergistic effect with FICI around 0.3. Imipenem with metformin combination showed an additive effect with *K. pneumoniae* ATCC 700721, but with no difference in the other strain. On the other hand, the combination of gentamicin showed an antagonistic effect (FICI= 2.02) for the *K. pneumoniae* ATCC 700603 and an indifferent effect against *K. pneumoniae* ATCC 700721; however, it was noticeable in the experiment against this strain that there was bacterial growth at high concentrations of metformin (> 0.3125 mg/mL) despite the presence of gentamicin at high concentrations reaching the MIC values (Figure 3-36).

Table 3-3: The effect of the combination of different antibiotics against the eight bacterial strains, showing the values of their FICs and FICIs

Bacterial Strain	Antibiotic	FIC (AB)	FIC(MET)	FICI (AB+MET)	Interpretation
***P. aeruginosa* NCTC 10662**	Doxycycline	0.125	0.25	0.375	Synergistic
	Gentamicin	0.5	0.008	0.508	Additive
	Imipenem	0.5	0.012	0.512	Additive
***P. aeruginosa* ATCC 27853**	Doxycycline	0.25	0.125	0.375	Synergistic
	Gentamicin	0.5	0.008	0.508	Additive
	Imipenem	0.5	0.008	0.508	Additive
***S. aureus* NCTC 6571**	Doxycycline	0.375	0.75	1.125	Indifference
	Linezolid	0.016	1	1.016	Indifference
	Ciprofloxacin	0.023	0.75	0.773	Additive
***S. aureus* ATCC 25923**	Doxycycline	0.5	0.5	1	Additive
	Linezolid	0.5	0.5	1	Additive
	Ciprofloxacin	0.5	0.012	0.512	Additive
***E. coli* NCTC 10418**	Doxycycline	0.063	0.5	0.563	Additive
	Gentamicin	0.5	0.008	0.508	Additive
	Ciprofloxacin	0.375	0.25	0.625	Additive
***E. coli* ATCC 25922**	Doxycycline	0.5	0.125	0.625	Additive

	Gentamicin	0.5	0.5	1	Additive
	Ciprofloxacin	0.5	0.25	0.75	Additive
***K. pneumoniae* ATCC 700721**	Doxycycline	0.375	0.004	0.379	Synergistic
	Gentamicin	1	0.004	1.004	Indifference
	Imipenem	0.5	0.07	0.57	Additive
***K. pneumoniae* ATCC 700603**	Doxycycline	0.25	0.004	0.254	Synergistic
	Gentamicin	2	0.018	2.018	Antagonistic
	Imipenem	1	0.016	1.016	Indifference

Notes: FIC refers to the fractional inhibitory concentration; FICI denotes the fractional inhibitory concentration index for the combination; AB represents the antibiotic used in the combination; MET signifies metformin; AB+MET indicates the combination tested.

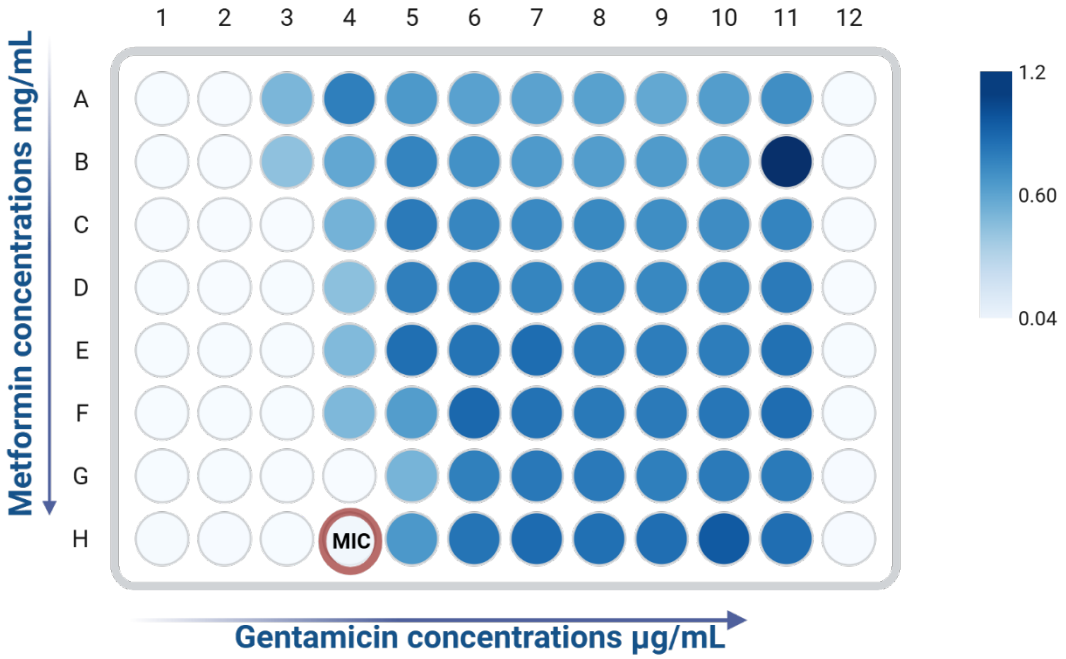

Figure 3-36: Heat map showing the combination of gentamicin with metformin against *K. pneumoniae* ATCC 700721 using a checkerboard assay.
The vertical arrow indicates the direction of the 2-fold serial dilution of metformin and the horizontal arrow indicates the direction of the 2-fold serial dilution of gentamicin. The column 11 contains the metformin-only solution (starting concentration is 20 mg/mL), while the last row at the bottom (row H) contains the gentamicin-only concentration (starting concentration is 512 µg/mL). Alongside the last column on the right (column 12) as blank. The varying shades of blue represent the OD600 values; the darker the colour, the more growth is observed in that well. The MIC of gentamicin is indicated with the red ring. Created in https://BioRender.com.

3.3. DISCUSSION

Antibiotic resistance is an urgent and challenging problem today. The effective antimicrobial agents are decreasing, and many known bacterial species have developed multidrug resistance, leading to incurable infections, increased mortality and morbidity rates, and a negative impact on the economic situation of the countries by affecting healthcare costs and reducing productivity (Friedman et al., 2016; Frieri et al., 2017). Therefore, it was crucial to investigate new agents to work as antibacterial or adjunct therapy with existing antibiotics to reduce the emergence of antibiotic resistance (Gajic et al., 2025). One of these agents is metformin, which is the focus of this study.

3.3.1. The inhibitory effect of metformin on bacterial growth

The effect of metformin on the bacterial phenotype was first investigated with respect to growth inhibition of different bacterial species. The results revealed that the MICs for all tested strains were 40 mg/mL, except for *S. aureus* NCTC 6571, where it showed the lower MIC value of 10 mg/mL indicating greater susceptibility to metformin, while the MIC for *K. pneumoniae* strains were 80 mg/mL, which were the higher MIC values among all the tested strains suggesting reduced susceptibility to growth inhibition. This observation was consistent with the established use of *S. aureus* NCTC 6571 as a susceptible reference organism in antimicrobial susceptibility testing, where it is routinely used as a quality-control strain to validate the assay (British Society for Antimicrobial, 2013). In contrast, *K. pneumoniae* ATCC 700603 strain is commonly used reference strain which is famous for its resistance-associated phenotypes and is widely used as control strains for extended-spectrum β-lactamase detection in susceptibility testing.

In the literature, the MIC values determined here were supported as well, with similar ranges of MICs between 8-100 mg/mL, differing by strain. For *P. aeruginosa*, the MIC for PAO1 and P14 was 100 mg/mL (J. Chadha et al., 2023; Khayat et al., 2023) and for ATCC 27853 (the same strain as this study) and some clinical isolates was 50 mg/mL (Gomaa et al., 2022). For *S. aureus,* the MIC was 10 mg/mL against MRSA T144 and *S. aureus* 215 (Liu et al., 2020a), ATCC 6538 was 50 mg/mL and for other clinical isolates was 12.5-50 mg/mL. For *E. coli,* the MIC values were 20 mg/mL for *E. coli* B2 (Abbas et al., 2022). For *K. pneumoniae*, the MICs ranged between 8 mg/mL (M. Shafik et al., 2023) to 50 mg/mL (Abbas et al., 2021a; X. Xiao et al., 2022) in different clinical isolates. The MICs of metformin against other bacterial species were in the same range like in *Acinetobacter baumannii* (Guo et al., 2022) and in vancomycin-resistant *Enterococcus* (Liu et al., 2020a). This indicates that metformin could inhibit the bacteria completely at high concentrations under *in vitro* conditions with a strain-species specific effect, which is still much higher than the physiological concentrations of metformin found in the human body. It also shows that the reduced susceptibility to metformin could be a sharable mechanism with other antibiotics.

Although the measuring of MIC as an endpoint experiment determines the effect of the antibacterial agent against the bacteria, it is not enough to show the characteristics of the bacteria towards the antibiotics, which makes it crucial to investigate the growth kinetics through growth curves (Bing Li et al., 2016). A range of concentrations were tested, including therapeutic concentrations of metformin, concentrations that could be found in the human body (1-113 µg/L), and some *in vitro* experimental concentrations (J. D. Lalau et al., 2011). Both growth curve analysis and the AUC were employed to provide a comprehensive insight into the effect of metformin on bacterial growth. AUC provides an integrated measure of total growth over time, capturing cumulative differences that may not be evident from single time-point or endpoint measurements alone. In addition, it is a presentable way to display growth curves, especially under different conditions (Sprouffske & Wagner, 2016). In contrast, growth curve analysis enables the evaluation of growth kinetics, including lag-phase duration, exponential growth rate, and maximum population density, which are key descriptors of microbial behaviour under different conditions (Zwietering et al., 1990).

Given that AUC integrates growth across all phases, it was used as the primary method to evaluate the overall impact of sub-inhibitory concentrations on bacterial growth. Mainly, all the tested concentrations were sub-inhibitory for all bacterial strains, except one *S. aureus* strain. The higher concentrations (1.25, 2.5, 5, and 10 mg/mL, which are 1/4, 1/8, and 1/16 of MIC, respectively, for most strains) showed significant inhibition of growth, exceeding physiological concentrations. For the other concentrations, there was no significant inhibition, except in the *S. aureus* strain, which interestingly showed significance at all sub-inhibitory concentrations below 1.25 mg/mL, including the physiological one. This could be explained by the fact that this strain is known to be susceptible to many antibiotics, making it more vulnerable to metformin. On the other hand, the *K. pneumoniae* strains demonstrated significant growth reduction only at 10 mg/mL (1/8 MIC), which supports the notion that the more susceptible a strain is to other antibiotics, the more pronounced the effect of metformin, and vice versa, as seen with *K. pneumoniae* strains that are recognised as specific clinical strains with a high level of multidrug resistance. This may suggest that metformin could share cross-resistance mechanisms with other antibiotics. Furthermore, it provides additional confirmation that the effect of metformin is species-strain specific. In the literature, the effect of ½ and ¼ MIC showed significant inhibition against PAO1 and P14 (J. Chadha et al., 2023). While other studies indicated that the sub-inhibitory concentrations of metformin do not show significant inhibition of growth curves for PAO1 at 1/10 MIC (Abbas et al., 2017), *Streptococcus suis* at ½ MIC (Jing Zuo et al., 2023) and *K. pneumoniae* at 1/8 MIC (M. Shafik et al., 2023). Therefore, this may confirm that metformin could have inhibitory effects on various bacterial species, demonstrating strain-specificity across a wide range of concentrations, including some physiological ones.

The growth curve analysis showed that metformin followed a general pattern across most of the affected samples, particularly at high concentrations, where it caused elongation of the lag phase and a slowing of the exponential phase. This could indicate a stress effect of metformin on the bacterial cells rather than complete killing. Although the literature does not have sufficient knowledge of this type of analysis for the effect of metformin on the growth curve, some studies have shown the effect of different antibiotics, such as beta-lactams, aminoglycosides and fluoroquinolones, on the extension of the lag phase (B. Li et al., 2016; Theophel et al., 2014).

Generally, the results from the growth curve analysis and the AUC analysis were comparable and led to the same observation. However, there were exceptions showing significant differences between the two analyses. The data showed that although metformin did not show a significant effect on overall bacterial inhibition, it affected the bacterial growth kinetics in *S. aureus* NCTC 6571 at 2.5 mg/mL, *P. aeruginosa* NCTC 10662 at 1.25 mg/mL, and *E. coli* ATCC 25922 at 5 and 10 mg/mL, indicating a strain- and dose-dependent effect. For those strains, the effect could be observed in specific phases, such as an extended lag phase and a slower exponential phase. The analysis of the growth curves here was beneficial in revealing these effects, which were masked by the overall AUC analysis. This observation was supported in the literature, where Angaroni et al. (2025) showed that single-point metrics like AUC cannot show the growth-phase-specific effect of the drug (Angaroni et al., 2025). In contrast, the effect of metformin was captured by the AUC rather than the growth curve analysis in *P. aeruginosa* ATCC 27853 at 1.25 mg/mL, where it appeared to enter the stationary phase earlier in the latter part of the curve. Due to its small number of time points, the growth curve analysis missed this statistically, whereas the AUC captured it, providing a superior point here for this type of analysis. Ram et al. (2019) showed that AUC is useful for combining both the growth rate and the maximal bacterial density, in addition to the ease of integration of the growth curve data using AUC (Ram et al., 2019). Therefore, combining both analysis methods is recommended for a more comprehensive view of the effect of the drug on the bacterial growth curve.

It should also be noted that the error bars for the control growth curves were generally much higher than those for the treated samples. Since the error bars in the growth curves represented standard deviation, they reflected greater variability among biological replicates rather than uncertainty in the mean (Altman & Bland, 2005). Therefore, the limitation occurred in the experimental setup due to an unequal number of technical replicates, which should not have enlarged the error bars here. However, this could be explained by the fact that the drug normally induces stress in bacterial cells, which constrains population growth, especially in the exponential phase, thereby reducing variability between biological replicates. In the absence of this stress, as in control samples, unrestricted exponential growth occurs, and small differences in the initial physiological state are amplified over time (Balaban et al., 2019).

3.3.2. The inhibitory effect of metformin on bacterial virulence factors

The effect of metformin on various virulence factors was investigated. These factors included protease activity, biofilm formation, and bacterial motility. Generally, with some exceptions, the concentrations of 1.25 and 10 mg/mL metformin demonstrated an inhibitory effect on the different virulence factors tested. This may indicate that the impact of metformin as an antivirulence agent might require high concentrations, although it could be lower than what is needed for growth inhibition. This was evident with *S. aureus* NCTC 6571, where the concentration of 1.25 mg/mL did not show significant inhibition of growth; however, it significantly inhibited protease activity. The same concentration did not exhibit significant inhibition in *P. aeruginosa* NCTC 10662, although it caused significant inhibition of protease activity and biofilm formation. Additionally, the concentration of 0.5 mg/mL did not show significant inhibition against *S. aureus* ATCC 25923, but it did demonstrate a significant decrease in proteolytic activity. These findings align with some studies in the literature. One study indicated a significant reduction in protease and biofilm formation in *K. pneumoniae* isolates at a concentration of 1 mg/mL, which was explained by the down-regulation of some virulence-encoding genes as a result of metformin exposure (M. Shafik et al., 2023). Another study also reported significant inhibition of certain virulence factors in PAO1 following exposure to 10 mg/mL (Khayat et al., 2023), 6.25 mg/mL and 12.5 mg/mL (J. Chadha et al., 2023) , which was attributed to the down-regulation of key quorum sensing genes. One study examined the effect of metformin on various virulence factors at 1/10 of the MIC against different bacterial strains of *S. aureus*, revealing that despite some strains having the same MIC, there was a notable difference in the significant reduction of biofilm formation (Abbas et al., 2022). This may support that metformin could have antivirulent activity against various bacterial species even at non-growth-inhibitory concentrations.

3.3.3. The effect of metformin on bacterial efflux

Upon the investigation of the effect of metformin on efflux systems in the bacteria using the ethidium bromide assay, it was revealed that only for *S. aureus* NCTC 6571 at the concentration of 10 mg/mL there was significant inhibition to ethidium bromide efflux. This may indicate that metformin causes inhibition of efflux pump activity; however, it is worth noting that for this strain, the MIC of metformin was 10 mg/mL. Therefore, this inhibition of ethidium bromide efflux could be due to the effect of metformin on the cell itself, not a direct effect on the efflux pump, especially because of the absence of the inhibitory effect at lower concentrations. This is aligned with the literature as there is a study that investigated the effect of metformin on the efflux of Rhodamine B in *K. pneumoniae*, which showed an inhibitory effect at 50 mg/mL (MIC) and no effect at sub-inhibitory concentrations (X. Xiao et al., 2022). In the literature, there is a study that suggests metformin as a direct efflux pump inhibitor using ethidium bromide cartwheel, which is a qualitative method, on *S. aureus* and *K. pneumoniae* strains (Abbas et al.,

2021a). Also, another study using an ethidium bromide accumulation assay showed the inhibitory effect of metformin on the accumulation of ethidium bromide of the cells in *S. aureus* and *E. coli* (Liu et al., 2020a). In the same study, it showed that metformin could disrupt the proton motive force, which is known to affect the cell membrane permeability and affects efflux pumps as they need energy to work (Yamaguchi et al., 2015). So, collectively, it may support the hypothesis that metformin could inhibit the efflux of the agents, but indirectly, which could not be detected using the qualitative method or the accumulation assay.

3.3.4. The effect of metformin in combination of other antibiotics on bacterial growth

Different antibiotics were tested in combination with metformin against different bacterial genera to investigate whether this combination could affect the activity of the antibiotic alone. The combinations of the different antibiotics with metformin showed an additive effect against the different bacterial species, except for two antibiotics that behaved in a different pattern.

It was found that the combination of metformin with doxycycline showed a synergistic effect only in both strains of *P. aeruginosa* and *K. pneumoniae*. It is worth noting that those strains were resistant to doxycycline, with MIC > 16 for all of them, while the combinations had an additive effect in the *S. aureus* and *E. coli* strains, which were susceptible to doxycycline. This synergy is aligned with several studies in the literature that showed synergistic combinations between different tetracyclines and metformin. One study was on resistant *S. aureus* and *P. aeruginosa* strains using the combination of doxycycline (Masadeh et al., 2021). The other one was on colistin-resistant *E. coli B2*, carbapenem-resistant *S. enteritidis* H8, vancomycin-resistant *enterococci* (VRE) A4 and MRSA that show a synergistic effect using doxycycline with metformin as well. In that study, they found that the impact of this combination was less on the susceptible strains (Liu et al., 2020a). The same finding was seen with the combination of tetracycline (Abbas et al., 2021a) and tigecycline (X. Xiao et al., 2022) with metformin against MDR *K. pneumoniae* strains. This could be explained by the previously discussed hypothesis that metformin may indirectly inhibit the efflux pump by disruption of energy production; however, it may exert an inhibitory effect on a specific function or protein associated with tetracyclines reistance (including doxycycline), which could be specific efflux pumps found in the resistant strains, not the susceptible ones.

The other interesting combination was that of gentamicin with metformin. Generally, this combination demonstrated an additive effect with metformin against all the tested bacterial strains; however, it exhibited an antagonistic effect in *K. pneumoniae* strains. Although only in *K. pneumoniae* ATCC 700603, the FICI exceed 2, there was also growth in the other strain with combinations containing MIC of gentamicin and high concentrations of metformin greater than 0.3125 mg/mL. This aligned with one

study in the literature that revealed an antagonistic interaction between metformin and gentamicin against *K. pneumoniae* strains (X. Xiao et al., 2022). Gentamicin, an aminoglycoside antibiotic, depends on the bacterial respiration to enter the cell as it needs the proton motive force (PMF) which is formed during the oxidative phosphorylation step in the aerobic respiration (Webster & Shepherd, 2022), and from the hypothesis of this study that metformin could inhibit the bacterial respiration, therefore this could be the explanation of the antagonism at high concentration of metformin.

In conclusion, metformin demonstrated an inhibitory effect against various bacterial species at different concentrations, including some physiological ones, with its effect being strain-species specific. Additionally, it exhibited some antivirulent activity against bacterial proteases and biofilm formation. When testing its effect on efflux, it showed an inhibitory effect only in one strain at the MIC concentration. Finally, the combination of doxycycline and metformin produced a synergistic effect against the resistant strains tested, whereas the combination with gentamicin resulted in an antagonistic effect in *K. pneumoniae* strains.

CHAPTER 4-

Adaptive Evolution of Bacteria Under Continuous Metformin Exposure

4. Adaptive Evolution of Bacteria Under Continuous Metformin Exposure

4.1. INTRODUCTION

The exceptional genetic capability of the microbes has benefited from the extensive overuse of antibiotics, which has led to the acquisition of various resistance genes and the evolution of numerous resistance mechanisms against nearly all antibiotics used (Davies & Davies, 2010). Although antibiotics are mainly responsible for the emergence of antimicrobial resistance, the role of non-antibiotic pharmaceuticals with antimicrobial effects in AMR has become increasingly important due to their prolonged use. It has been found that these drugs can also influence bacterial adaptation by exerting selective pressure at clinically relevant sub-inhibitory concentrations, similar to the effects of antibiotics, which is relevant to their long-term use as in some lipid-lowering, anti-inflammatory and antipsychotic drugs (Maier et al., 2018; Wang, Lu, et al., 2020).

Metformin is the first-line pharmacological treatment for type 2 diabetes mellitus and is typically administered continuously over extended periods. It is also found to affect bacterial growth, metabolism, and community structure, particularly within the gut microbiome (Wu et al., 2017). In the previous chapter, metformin was shown to exhibit direct antibacterial activity against a range of bacterial species. Together, these observations raise the hypothesis that the prolonged exposure to metformin may exert selective pressures that drive bacterial adaptation, with potential consequences for bacterial growth, virulence-associated properties, and susceptibility to clinically relevant antibiotics. Therefore, this chapter aims to investigate the effect of continuous exposure of bacteria to one of the physiological concentrations of metformin using the experimental evolution experiment.

Experimental evolution is a powerful and well-known approach for investigating microbial adaptation under laboratory conditions, exposing them to continuous stress, providing a predictive model of what happens in the environment and in humans. It is carried out by continuously exposing serial bacterial generations to the tested stress. This is followed by phenotypic analysis and investigation of the emergence of resistance-associated traits. Nowadays, with high-quality sequencing, the resulting mutations can be easily investigated and compared with the ancestors (Barrick & Lenski, 2013). Specifically, this approach has been widely used to study antibiotic resistance, revealing crucial principles such as the adaptive pathways underlying resistance and the emergence of cross-resistance to other antimicrobial agents under long-term exposure rather than short-term treatment (Lázár et al., 2013).

In this chapter, the experimental evolution was employed using a physiologically relevant concentration of metformin on two selected bacterial strains, depending on the results of Chapter 3. The two selected

strains were one gram-negative species, *P. aeruginosa*, and one gram-positive species, *S. aureus*. The selection depends on the fact that *S. aureus* was the only gram-positive tested, and this strain was the most susceptible one to metformin. While the *P. aeruginosa* was selected as representative of the gram-negative bacteria, where it had comparable effects, especially at the used physiological concentration in the evolutionary experiment.

Following the prolonged exposure to metformin, the evolved populations were characterised using a range of phenotypic assays previously investigated in Chapter 3. Therefore, these assays were used to compare the evolved lines with their ancestors. Bacterial growth was assessed through growth curve analyses in the presence and absence of metformin. In addition, biofilm formation and protease activity were investigated under metformin exposure to assess the potential effects of the experimental evolution on virulence-associated traits. Furthermore, cross-resistance between metformin and other antibiotics was tested using the growth curve assay, with a panel of clinically relevant antibiotics applied to the evolved populations in comparison with their controls, to evaluate potential changes in antibiotic susceptibility.

Finally, genomic changes that occurred during experimental evolution were investigated using WGS of the evolved lines and their ancestors, with a combination of short- and long-read sequencing approaches. Short-read sequencing is important for detecting SNPs and small insertions or deletions that frequently occur as adaptive responses during experimental evolution (Didelot et al., 2012; Nielsen et al., 2011) and for linking them to phenotypic changes. However, adaptive evolution can also result in more complex genomic changes, like gene amplifications, deletions, inversions, and other structural variants, which may be difficult to detect using the short-read data alone (Barrick & Lenski, 2013). Therefore, long-read sequencing could be used to reveal complex genomic structural variations, enabling the accurate identification of structural variants as a result of adaptation under selective pressure (De Coster & Van Broeckhoven, 2019; Peng et al., 2025). However, this sequencing method is found to have a higher nucleotide-level error rate than short-read sequencing. Therefore, the combined use of short- and long-read sequencing has been increasingly recommended in antimicrobial resistance studies to generate high-quality genome assemblies (Berbers et al., 2023). In this study, the combination of these sequencing approaches enabled the identification of point mutations, structural variants, and larger genomic rearrangements associated with prolonged metformin exposure.

4.2. RESULTS

4.2.1. Estimation of minimum evolutionary timeframe

To estimate the minimum duration required for sufficient mutational diversity in the experimental evolution, an approach based on established methods for calculating mutation accumulation during

bacterial growth was used. Using the equation described by Pope *et al.* (2008), the number of mutant cells (r_2) generated over a 24-hour incubation period was calculated. Assuming a uniform mutation distribution and no selection pressure, a minimum of one mutation per base pair across the genome would be required to ensure full mutational coverage. In *P. aeruginosa* (genome size 6.8 Mbp), an estimated mutant yield of approximately 5.78×10^5 per day suggests a minimum duration of around 12 days to achieve genome-wide mutation saturation. In *S. aureus* (genome size 2.8 Mbp), an estimated mutant yield of approximately 2.35×10^5 per day suggests a minimum duration of around 12 days to achieve genome-wide mutation saturation. This estimate provides a conservative lower bound for the timeframe needed to allow sufficient genetic variation for selection to act during subsequent experimental evolution. (Table 4-1)

Table 4-1: The calculation of the estimated minimum timeframe for the evolutionary experiment in *P. aeruginosa* and *S. aureus*

Bacterial strain	N1	N2	r_2	Time (days)
P. aeruginosa	1.8×10^8	3.4×10^9	5.78×10^5	12
S. aureus	7.1×10^7	3.2×10^9	2.35×10^5	12

N1 and N2 are the number of cells/mL present at time 1 (0 time) and 2 (1 day) of the experiment; r_2 is the number of mutants that occurred per day of incubation; time is the minimum days of the evolutionary experiment for full genome coverage.

4.2.2. Phenotypes of metformin-exposed evolved populations

4.2.2.1. The effect of metformin on bacterial growth

Firstly, measuring the MIC using the broth microdilution method revealed that the MICs of the evolved populations and controls were similar and did not change after the evolutionary experiment, remaining at 10 and 40 mg/mL for *S. aureus* and *P. aeruginosa*, respectively.

Since the MIC method cannot identify changes in growth patterns, the growth curves method was used to investigate the effects of different concentrations of metformin on the six evolved lines of *P. aeruginosa* and *S. aureus* in parallel with their controls. (Table 4-2 and Table 4-3)

For *P. aeruginosa*, the evolved populations of Met-R1 and Met-R4 exhibited remarkably similar behaviour, demonstrating a pattern in which their growth was significantly enhanced at all concentrations of metformin tested when compared to the controls (Figure 4-1). And for deeper view, the growth curve analysis showed the same result as the AUC, with the evolved lines Met-R1 and Met-R4 growing significantly better, almost identically, compared with their controls at all concentrations of metformin (Figure 4-2 and Figure 4-4). Generally, the effect was an acceleration of the exponential phase, especially from the mid-log phase, leading to a higher OD than the control at 10 mg/mL, particularly for Met-R1, and to reach the same OD as the control more quickly

at the other concentrations. In contrast, the evolved line of Met-R2, growth was significantly worse compared to its control in the absence of the drug, whilst no significant changes were observed in the other evolved populations (Figure 4-1). This was also confirmed with the growth curve analysis where the growth of this evolved line was slowing down of the growth in general, starting with the elongation of the lag phase and slowing of the exponential phase to reach lower OD compared to its control in the absence of metformin (Figure 4-3).

The metformin-exposed population of the lineage Met-R5 showed some significant differences in the growth curve analysis compared with its control, which were not evident in the AUC analysis. The evolved line grew slightly worse than the control, especially at 5 and 1.25 mg/mL, particularly towards the end of the exponential phase; however, it recovered and reached the same OD at the final endpoint (Figure 4-5). In contrast, the evolved line of Met-R6 showed better growth in the absence of metformin than its control, a difference that was not revealed by the AUC analysis (Figure 4-6).

Table 4-2: The significant *p*-values resulted for the unpaired t-test of the pairwise comparisons of changes in the area under the curve (AUC) and the RM-ANOVA of the growth curve analysis of the evolved lines and its corresponding control against different concentrations of metformin in *P. aeruginosa*

P. aeruginosa			
Concentration (mg/mL)	**Pairwise comparison**	***p*-value (t-test)**	***p*-value (RM-ANOVA)**
0	Met-R2 vs Ctrl-R2	0.018	0.02
0	Met-R6 vs Ctrl-R6	-	0.005
1.25	Met-R1 vs Ctrl-R1	0.0388	0.0001
1.25	Met-R4 vs Ctrl-R4	0.0347	0.005
1.25	Met-R5 vs Ctrl-R5	-	0.011
2.5	Met-R1 vs Ctrl-R1	0.0118	0.011
2.5	Met-R4 vs Ctrl-R4	0.0413	0.009
5	Met-R1 vs Ctrl-R1	0.0327	0.035
5	Met-R4 vs Ctrl-R4	0.0059	0.009
5	Met-R5 vs Ctrl-R5	-	0.024
10	Met-R1 vs Ctrl-R1	0.0013	0.018
10	Met-R4 vs Ctrl-R4	0.0027	0.002
10	Met-R5 vs Ctrl-R5	-	0.023

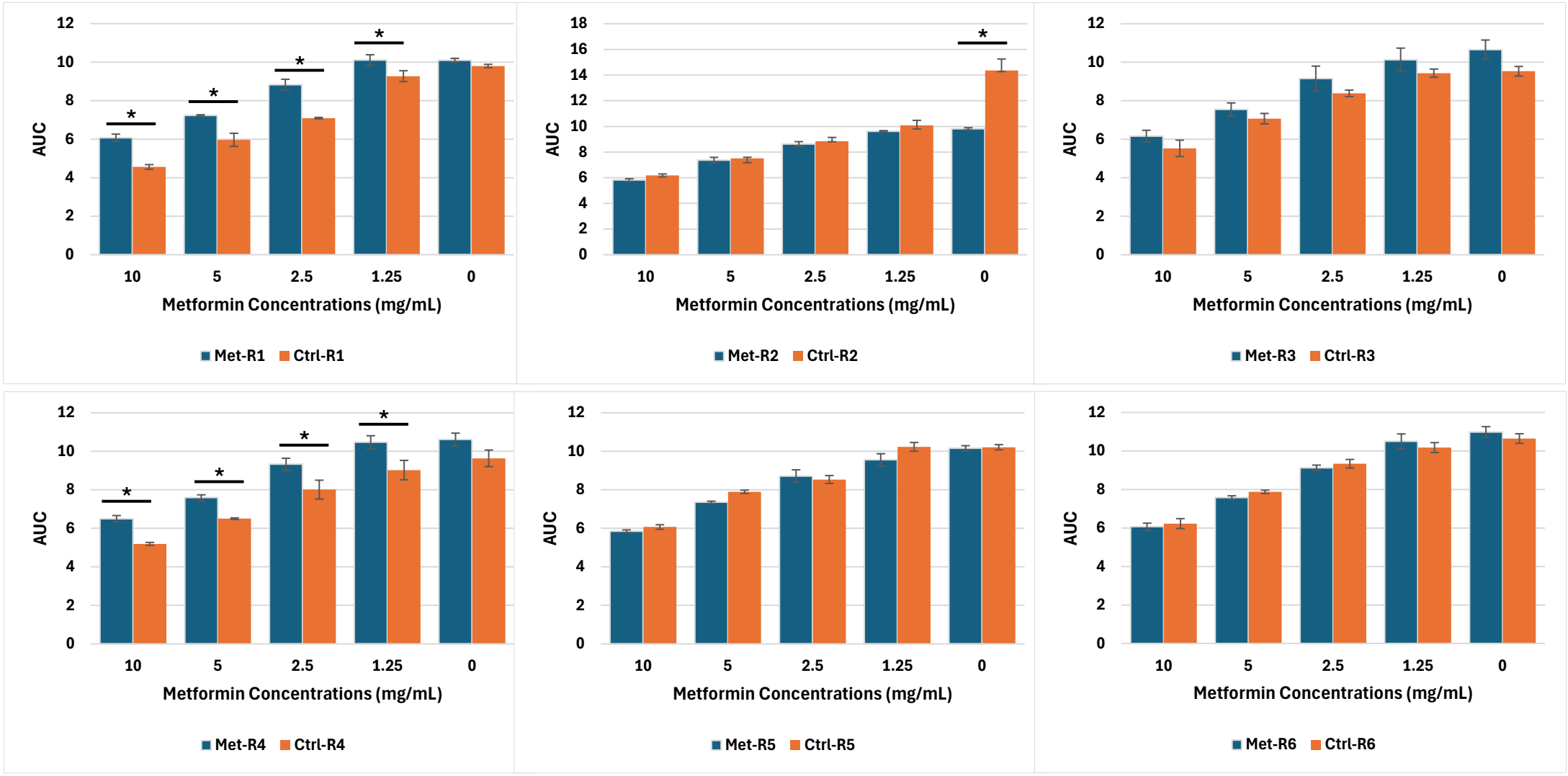

Figure 4-1: Area under the curve (AUC) analysis of the evolved lines and their controls of *P. aeruginosa* ATCC 27853 in the presence of metformin.
AUCs derived from the growth curves of the evolved lines (Met-R1- Met-R6) and their controls (Ctrl-R1-Ctrl-R6) of *P. aeruginosa* ATCC 27853 in the presence of different concentrations of metformin (10, 5, 2.5, and 1.25 mg/mL) along with the negative control; where the error bars represent mean AUC values ± standard deviation and the asterisks '*' represents statistical significance with $p \leq 0.05$ analysed by the unpaired t-test. Each set of the experiment was done in three biological replicates (n=3).

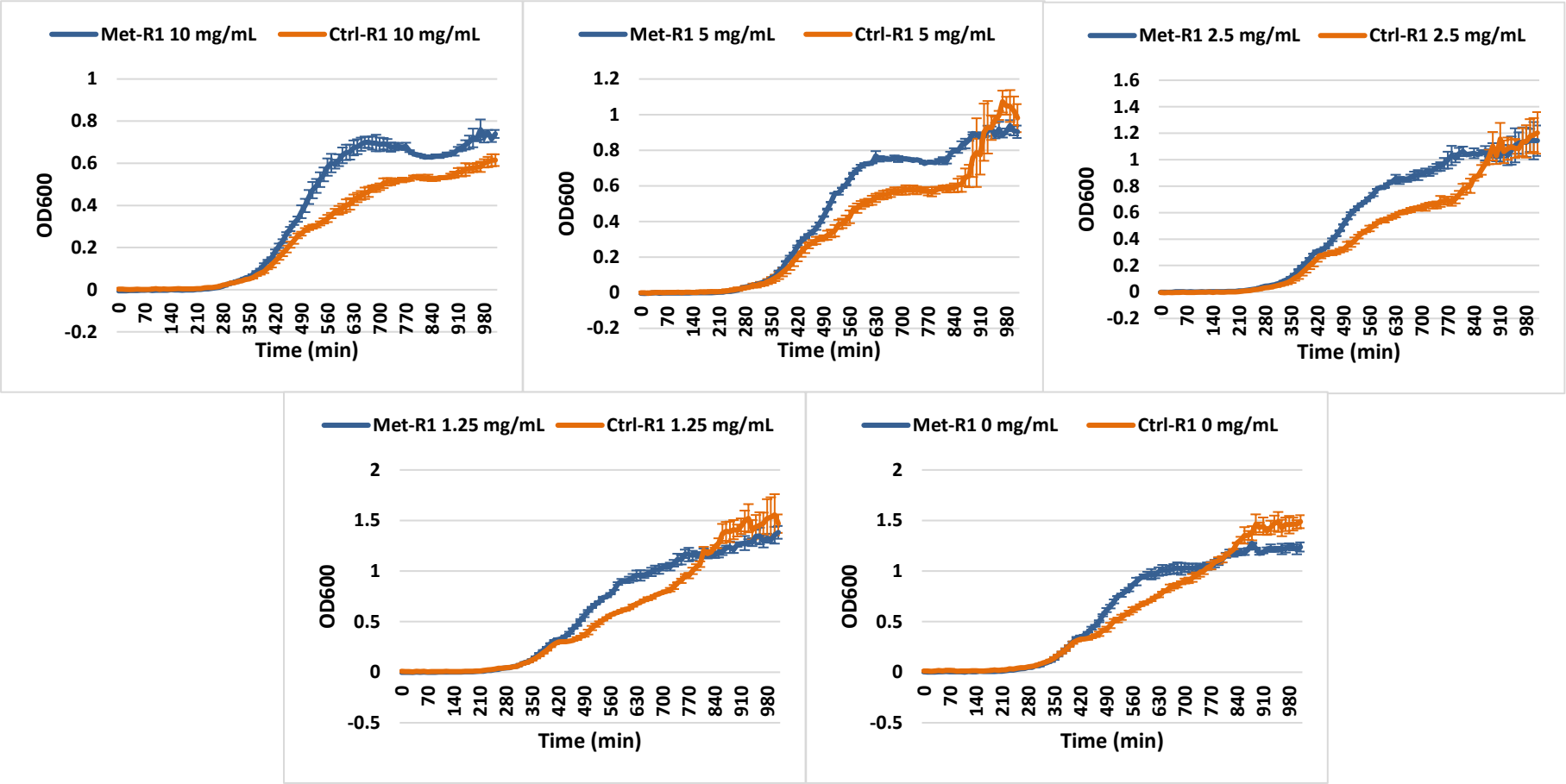

Figure 4-2: Growth profiles of the evolved population Met-R1 and its control Ctrl-R1 of *P. aeruginosa* ATCC 700603 in the presence metformin (0, 1.25, 2.5, 5, 10 mg/mL)
The drug-free was used as negative control; where the curves represent mean of OD_{600} ± standard deviation (error bars). Each set of the experiment was done in three biological replicates (n=3).

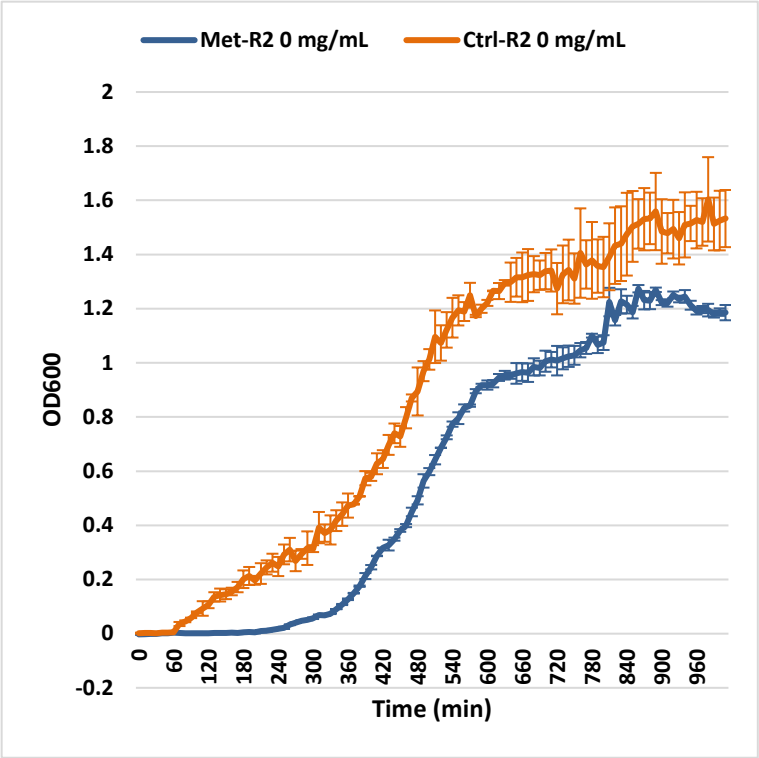

Figure 4-3: Growth profiles of the evolved population Met-R2 and its control Ctrl-R2 of *P. aeruginosa* ATCC 700603 in the absence metformin
The drug-free broth was used as negative control; where the curves represent mean of OD_{600} ± standard deviation (error bars). Each set of the experiment was done in three biological replicates (n=3).

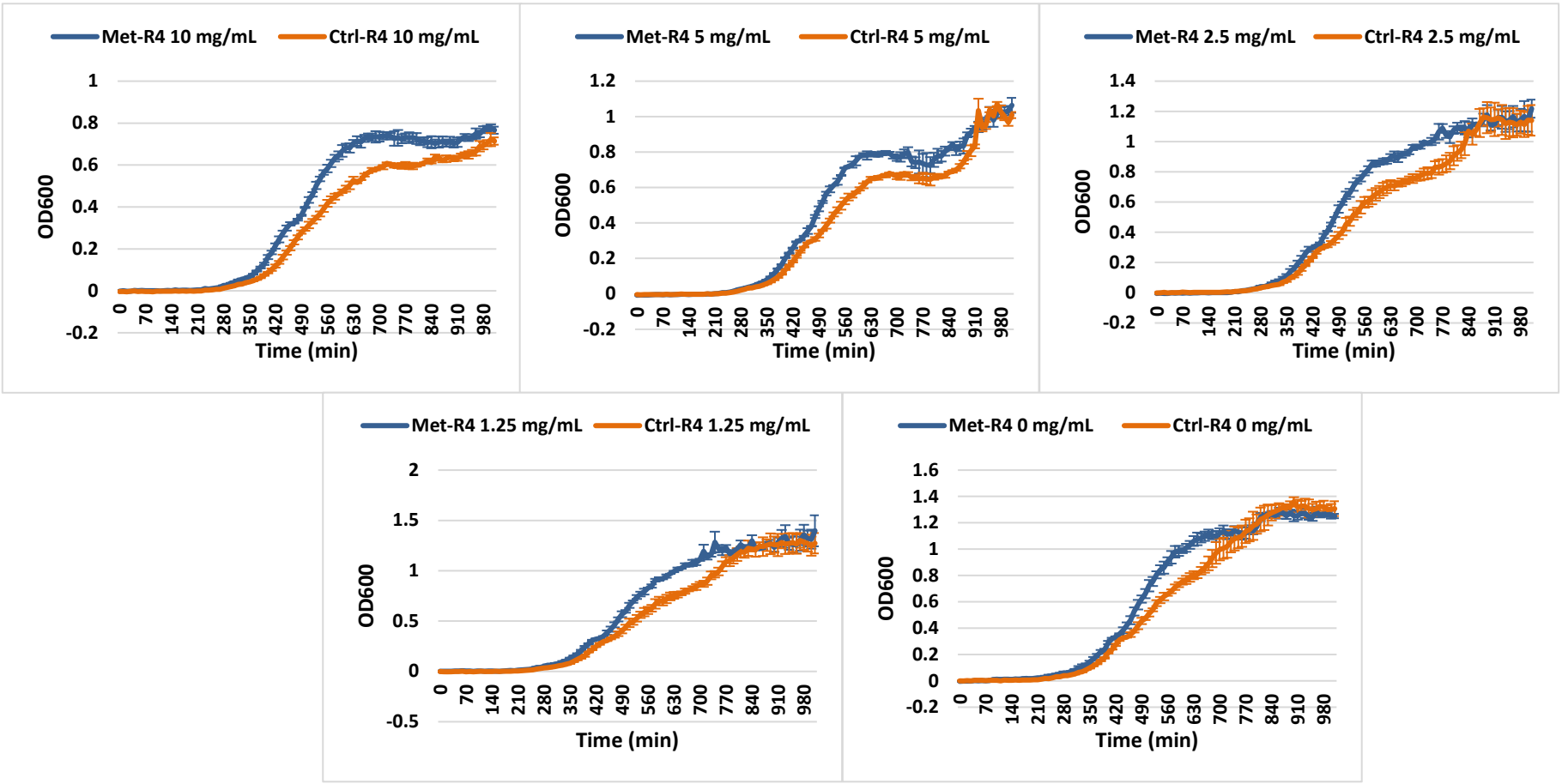

Figure 4-4: Growth profiles of the evolved population Met-R4 and its control Ctrl-R4 of *P. aeruginosa* ATCC 700603 in the presence metformin (0, 1.25, 2.5, 5, 10 mg/mL)

The drug-free broth was used as negative control; where the curves represent mean of OD_{600} ± standard deviation (error bars). Each set of the experiment was done in three biological replicates (n=3).

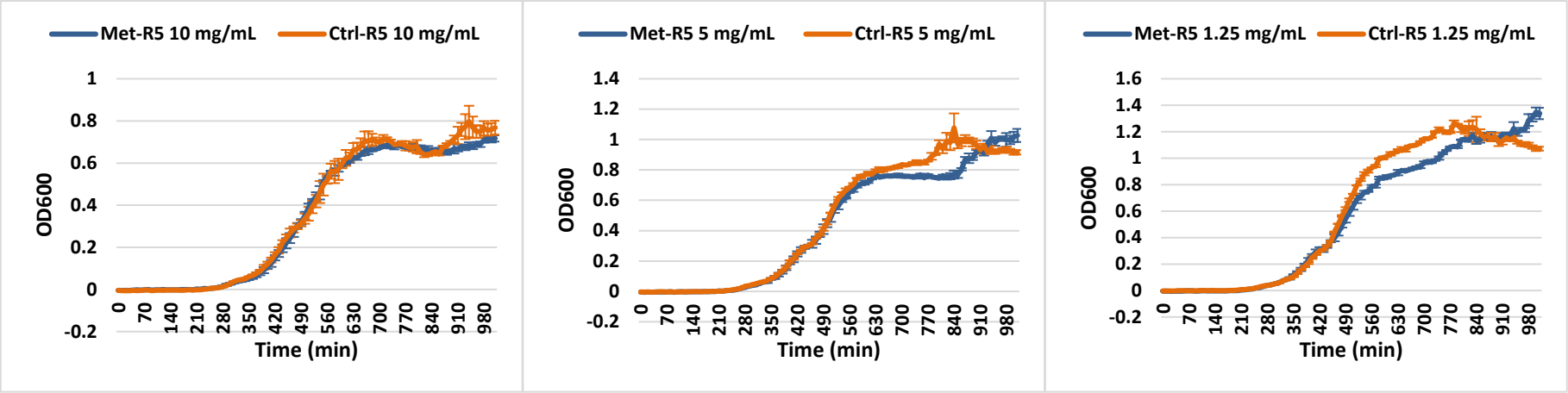

Figure 4-5: Growth profiles of the evolved population Met-R5 and its control Ctrl-R5 of *P. aeruginosa* ATCC 700603 in the presence metformin (1.25, 5, 10 mg/mL) The drug-free broth was used as negative control; where the curves represent mean of OD_{600} ± standard deviation (error bars). Each set of the experiment was done in three biological replicates (n=3).

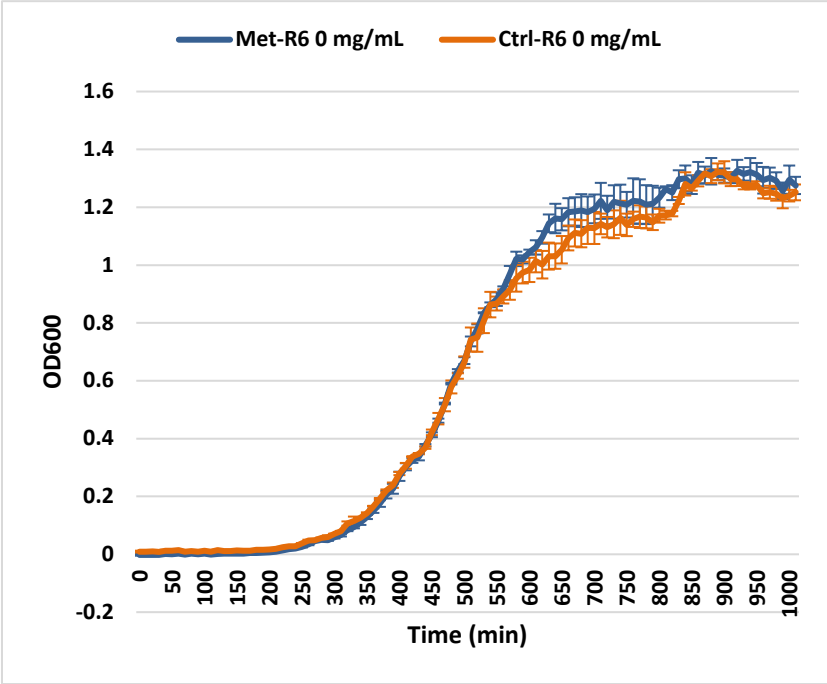

Figure 4-6: Growth profiles of the evolved population Met-R6 and its control Ctrl-R6 of *P. aeruginosa* ATCC 700603 in the absence of metformin
The drug-free broth was used as negative control; where the curves represent mean of OD_{600} ± standard deviation (error bars). Each set of the experiment was done in three biological replicates (n=3).

For *S. aureus*, the evolved line Met-R4 exhibited significantly better growth at a concentration of 2.5 mg/mL, as well as in drug-free media, compared to its corresponding control. In the growth curve analysis of the *S. aureus* samples, Met-R4 showed results similar to those of the AUC, with the evolved population generally growing better than the control at 2.5 mg/mL and in the absence of the drug at the start of the exponential phase. The same effect was observed at a slightly higher concentration of 1.25 mg/mL, but only in the growth curve analysis. Ctrl-R2 demonstrated better growth compared to its evolved lineage in the drug-free medium. And this appeared in both growth curve analysis in addition to the AUC. Furthermore, Ctrl-R6 showed enhanced growth at a concentration of 1.25 mg/mL in the absence of the drug when compared to the evolved population Met-R6 itself, which appeared only in the AUC not the growth curve analysis (Figure 4-7 and Figure 4-8)

Table 4-3: The significant *p*-values resulted for the unpaired t-test of the pairwise comparisons of changes in the area under the curve (AUC) and the RM-ANOVA of the growth curve analysis of the evolved lines and its corresponding control against different concentrations of metformin in *S. aureus*

S. aureus			
Concentration (mg/mL)	**Pairwise comparison**	***p*-value (t-test)**	***p*-value (RM-ANOVA)**
0	Met-R2 vs Ctrl-R2	0.0277	0.023
0	Met-R4 vs Ctrl-R4	0.0135	0.022
1.25	Met-R4 vs Ctrl-R4	-	0.027
1.25	Met-R6 vs Ctrl-R6	0.0091	-
2.5	Met-R4 vs Ctrl-R4	0.0094	0.045

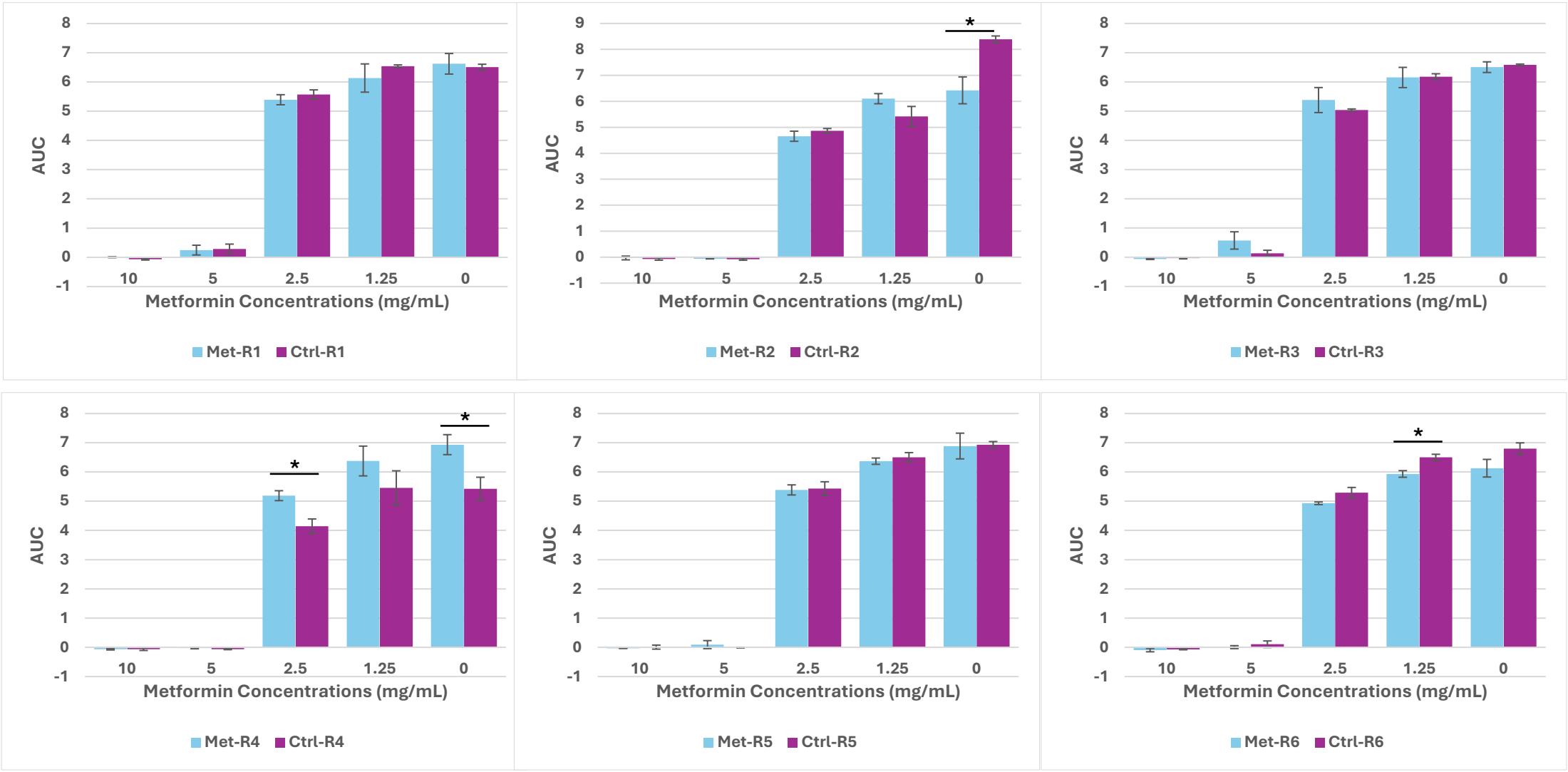

Figure 4-7: Area under the curve (AUC) analysis of the evolved lines and their controls of *S. aureus* NCTC 6571 in the presence of metformin.
AUCs derived from the growth curves of the evolved lines (Met-R1- Met-R6) and their controls (Ctrl-R1-Ctrl-R6) of *S. aureus* NCTC 6571 in the presence of different concentrations of metformin (10, 5, 2.5, and 1.25 mg/mL) along with the negative control; where the error bars represent mean AUC values ± standard deviation and the asterisks '*' represents statistical significance with $p \leq 0.05$ analysed by the unpaired t-test. Each set of the experiment was done in three biological replicate (n=3).

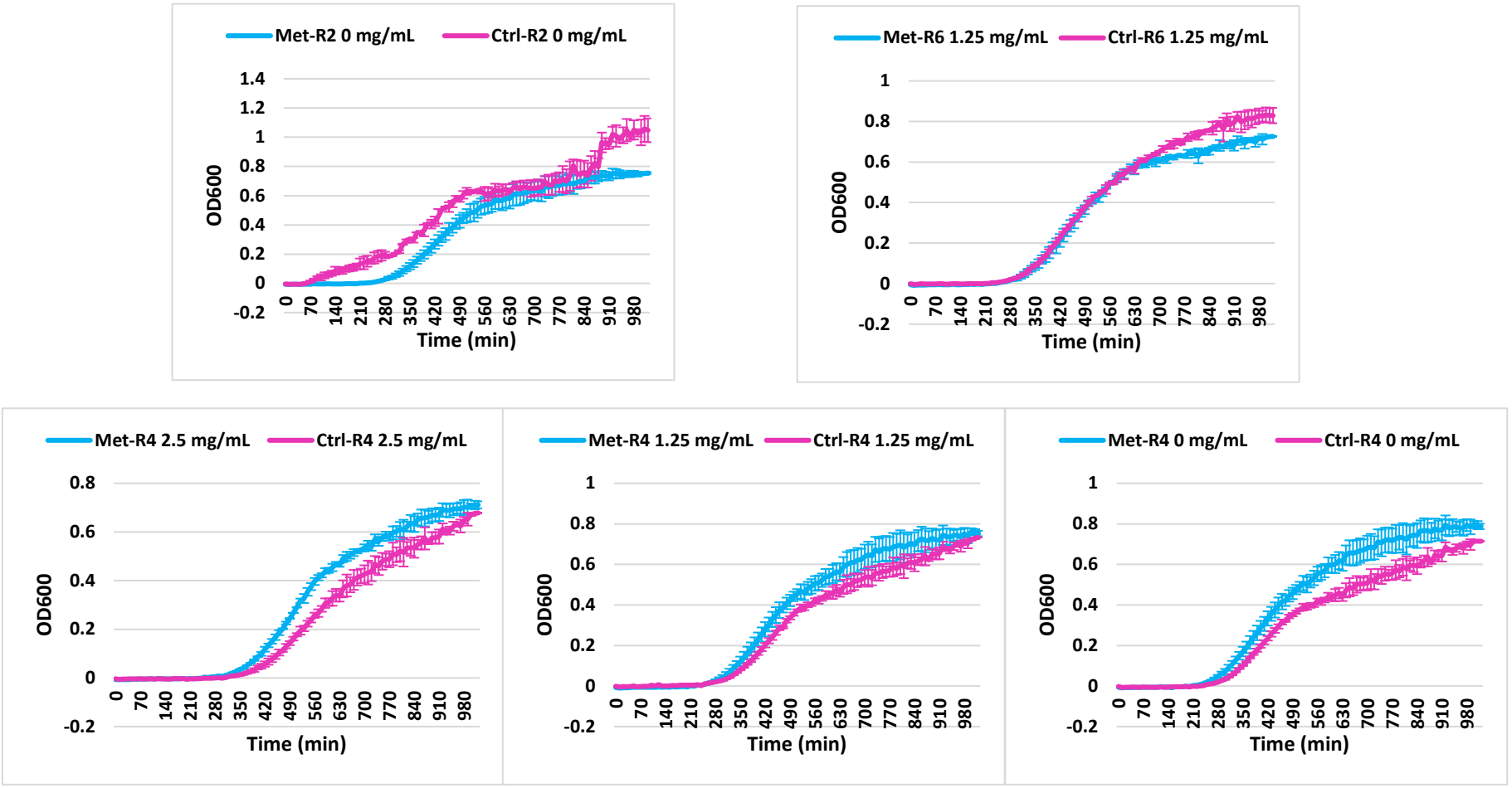

Figure 4-8: Growth profiles of the evolved population Met-R2, R4 and R6 and their controls Ctrl-R2, R4 and R6 of *S. aureus* NCTC 6571 in the presence of different concentrations of metformin

The drug-free broth was used as negative control; where the curves represent mean of OD_{600} ± standard deviation (error bars). Each set of the experiment was done in three biological replicates (n=3).

4.2.2.2. The effect of metformin on protease activity

The changes in protease activity of both *P. aeruginosa* and *S. aureus* between the evolved populations and their controls were examined, along with alterations in the effect of various concentrations of metformin using the skimmed agar method.

For *P. aeruginosa*, the protease activity of the evolved lines did not show any significant difference compared to their controls; however, the effect of metformin on the inhibition of protease activity significantly changed in all metformin-exposed evolved populations except Met-R3. For Met-R1, the inhibition caused by metformin on protease activity was significantly higher compared to the control at the highest concentration tested. However, at the same concentration, Met-R4, R5, and R6 showed a decrease in metformin's inhibition of protease activity. The same occurred at concentrations of 1.25 mg/mL and 5 mg/mL for Met-R4 and only at 1.25 mg/mL for Met-R2 (Figure 4-9) (Table 4-4).

Table 4-4: The significant *p*-values resulted for the unpaired t-test and their corresponding *p*-values from Mann-Whitney U of the pairwise comparisons of changes in diameter of the proteolytic zones of the mutant and its corresponding control against different concentrations of metformin in *P. aeruginosa*

P. aeruginosa

Concentration (mg/mL)	Pairwise comparison	*p*-value from unpaired t-test	*p*-value from Mann-Whitney U
10	Met-R1 vs Ctrl-R1	0.0424	0.2207
10	Met-R4 vs Ctrl-R4	0.0374	0.2207
10	Met-R5 vs Ctrl-R5	< 0.00001	0.1939
10	Met-R6 vs Ctrl-R6	0.0424	0.2207
5	Met-R4 vs Ctrl-R4	0.0374	0.2207
1.25	Met-R2 vs Ctrl-R2	< 0.00001	0.1939
1.25	Met-R4 vs Ctrl-R4	0.0489	0.2207

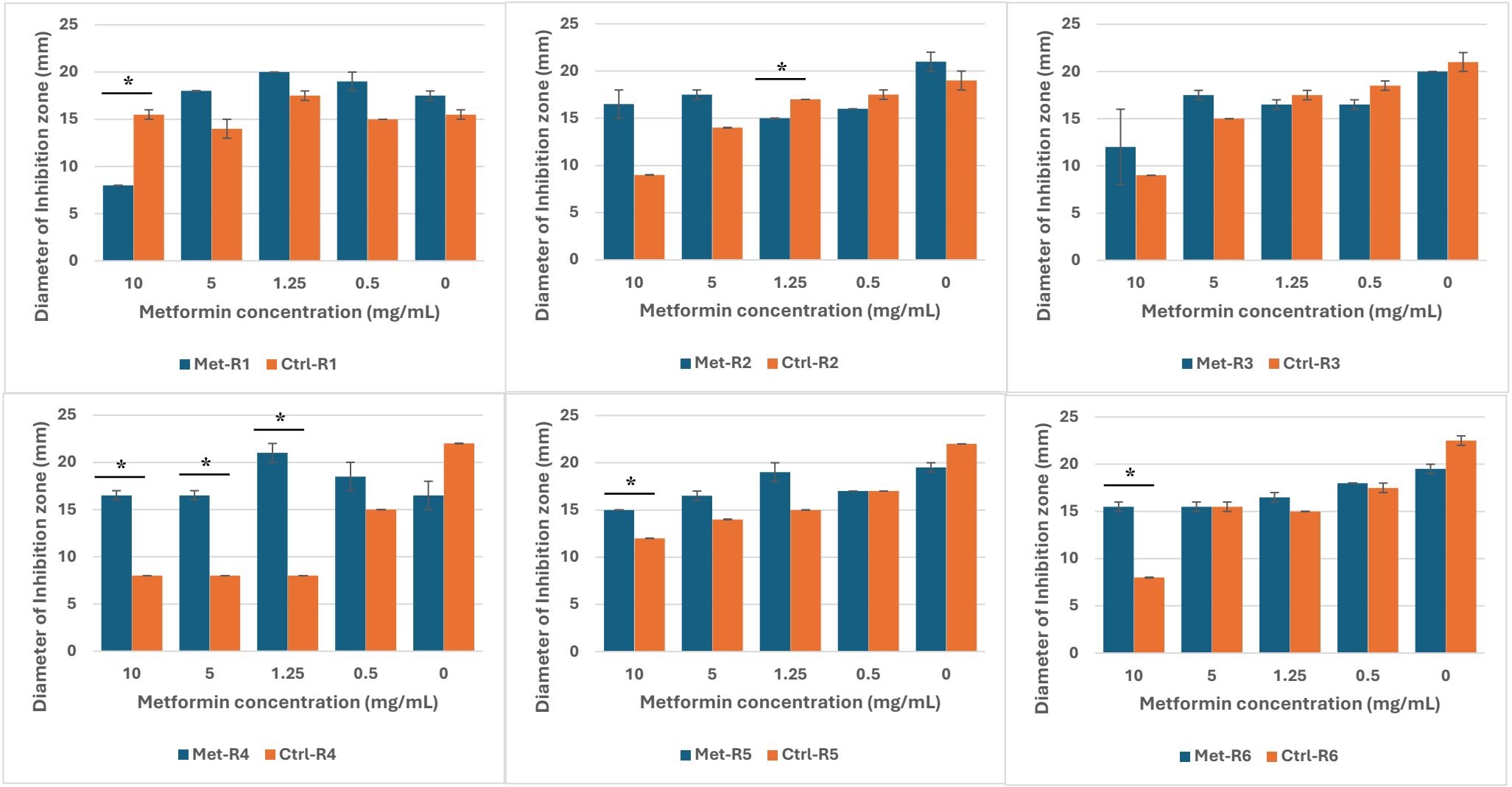

Figure 4-9 : The inhibitory effect of different concentrations of metformin 10, 5, 1.25 and 0.5 mg/mL on the protease activity of the evolved lines (Met-R1- Met-R6) and their controls (Ctrl-R1-Ctrl-R6) of *P. aeruginosa* ATCC 27853 along with the negative control,
The error bars represent the mean of the proteolytic inhibition zone diameter values ± standard deviation and the asterisks '*' represents statistical significance with $p \leq 0.05$ as analysed by the unpaired t-test. Each set of the experiment was done in two biological replicates (n=2), and two technical replicates for each.

For *S. aureus*, there was a significant change in proteolytic activity in Met-R2, R4, and R6 compared to their controls. In Met-R2 and R4, proteolytic activity increased, while Met-R6 exhibited a decrease relative to its corresponding control. In the presence of metformin, notable changes were observed for Met-R2 and R5 across all tested concentrations. For Met-R2, metformin's inhibition intensified at the concentration of 5 mg/mL, whereas the opposite effect was noted at concentrations of 1.25 and 0.5 mg/mL. For Met-R5, there was a slight reduction in metformin's effect at the highest concentration tested, alongside another decrease at 5 mg/mL. However, the effect of metformin on protease activity increased at the concentration of 1.25 mg/mL. (Figure 4-10) (Table 4-5)

Table 4-5: The significant p-values resulted for the unpaired t-test and their corresponding p-values from the Mann-Whitney U of the pairwise comparisons of changes in diameter of the proteolytic zones of the mutant and its corresponding control against different concentrations of metformin in S. aureus

S. aureus

Concentration (mg/mL)	Pairwise comparison	p-value from unpaired t-test	p-value from Mann-Whitney U
10	Met-R5 vs Ctrl-R5	< 0.00001	0.1939
5	Met-R2 vs Ctrl-R2	< 0.00001	0.1939
5	Met-R5 vs Ctrl-R5	< 0.00001	0.1939
1.25	Met-R2 vs Ctrl-R2	< 0.00001	0.1939
1.25	Met-R5 vs Ctrl-R5	< 0.00001	0.1939
0.5	Met-R2 vs Ctrl-R2	< 0.00001	0.1939
0	Met-R2 vs Ctrl-R2	< 0.00001	0.1939
0	Met-R4 vs Ctrl-R4	< 0.00001	0.1939
0	Met-R6 vs Ctrl-R6	< 0.00001	0.1939

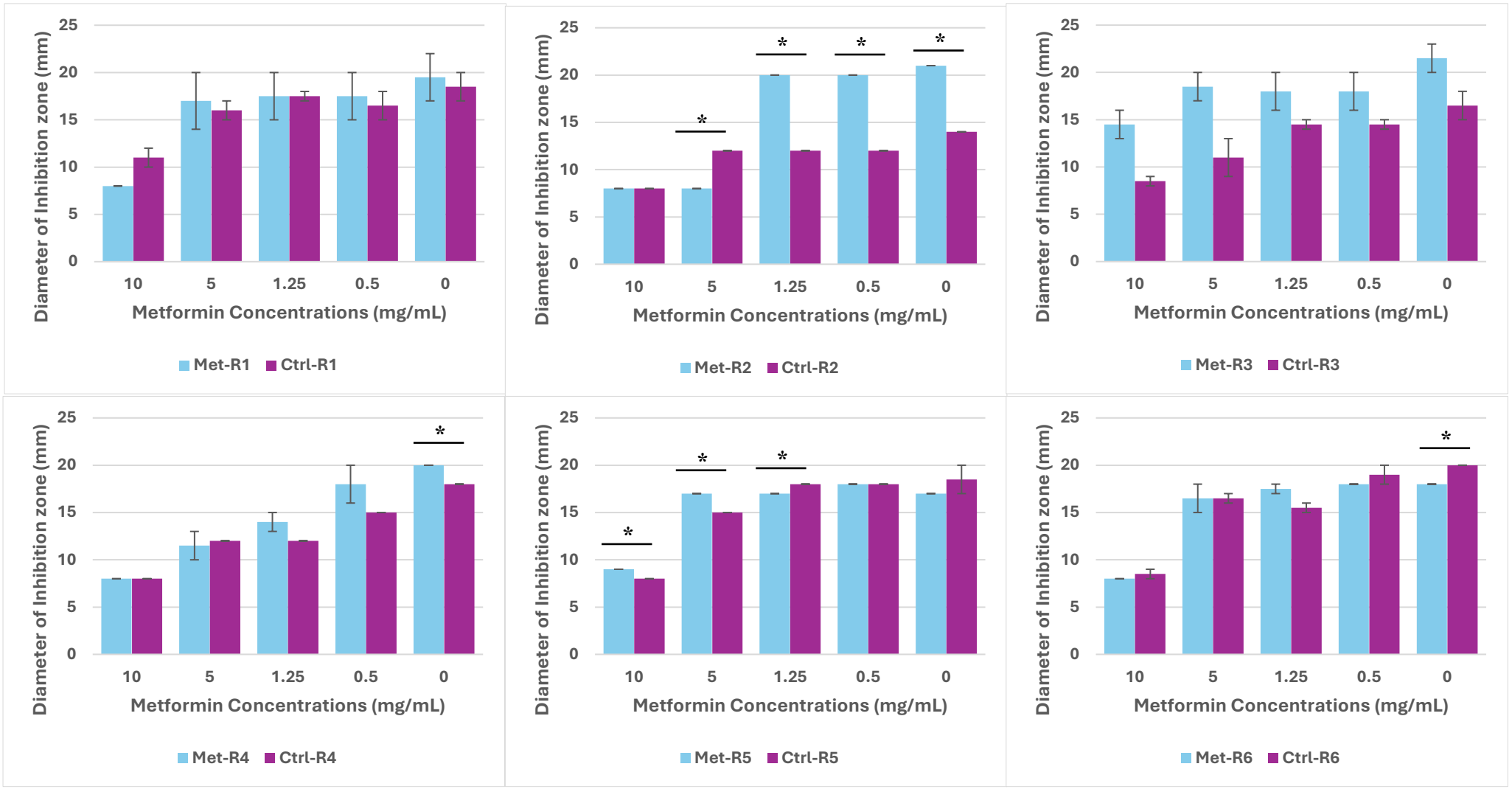

Figure 4-10: The inhibitory effect of different concentrations of metformin 10, 5, 1.25 and 0.5 mg/mL on the protease activity of the evolved lines (Met-R1- Met-R6) and their controls (Ctrl-R1-Ctrl-R6) of *S. aureus* NCTC 6571 along with the negative control.
The error bars represent the mean of the proteolytic inhibition zone diameter values ± standard deviation and the asterisks '*' represents statistical significance with $p \leq 0.05$ analysed by the unpaired t-test. Each set of the experiment was done in two biological replicate (n=2), and two technical replicates for each.

4.2.2.3. The effect of metformin on biofilm formation

The effect of metformin on biofilm formation of the metformin-exposed evolved populations compared to the controls was investigated using the crystal violet assay in the presence of a range of metformin concentrations.

Generally, for *P. aeruginosa*, the presence of metformin resulted in increased biofilm formation, which increased with higher concentrations of the drug in both the evolved lines and their controls. Only Met-R2 and Met-R6 exhibited statistically significant changes compared to their controls in the absence of the drug. The biofilm formation of Met-R2 ($p = 0.0334$) was significantly higher than that of its control, whereas in Met-R6 ($p = 0.0231$), the biofilm formation was lower compared to the control. (Figure 4-11)

For *S. aureus*, the presence of metformin primarily resulted in a reduction of biofilm formation. However, following the statistical analysis, no statistically significant differences were observed between the evolved lines and their controls. (Figure 4-12)

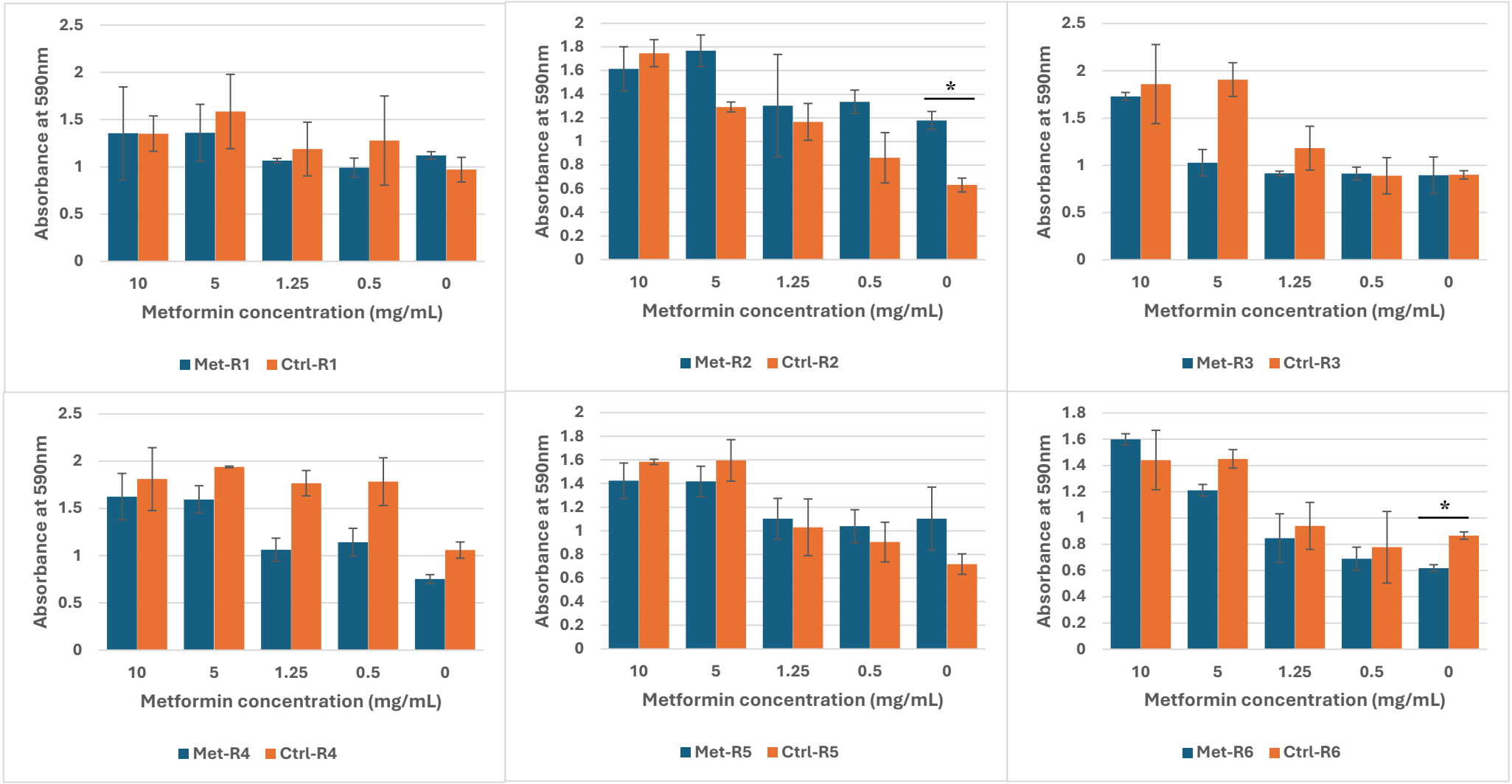

Figure 4-11: The inhibitory effect of different concentrations of metformin 10, 5, 1.25 and 0.5 mg/mL on the biofilm formation of the evolved lines (Met-R1- Met-R6) and their controls (Ctrl-R1-Ctrl-R6) of *P. aeruginosa* ATCC 27853, along with the negative control.
The error bars represent the mean of the absorbance values of the crystal violet at 590 nm ± standard deviation and the asterisks '*' represents statistical significance with $p \leq 0.05$ as analysed by the unpaired t-test. Each set of the experiment was done in two biological replicates (n=2), and two technical replicates for each.

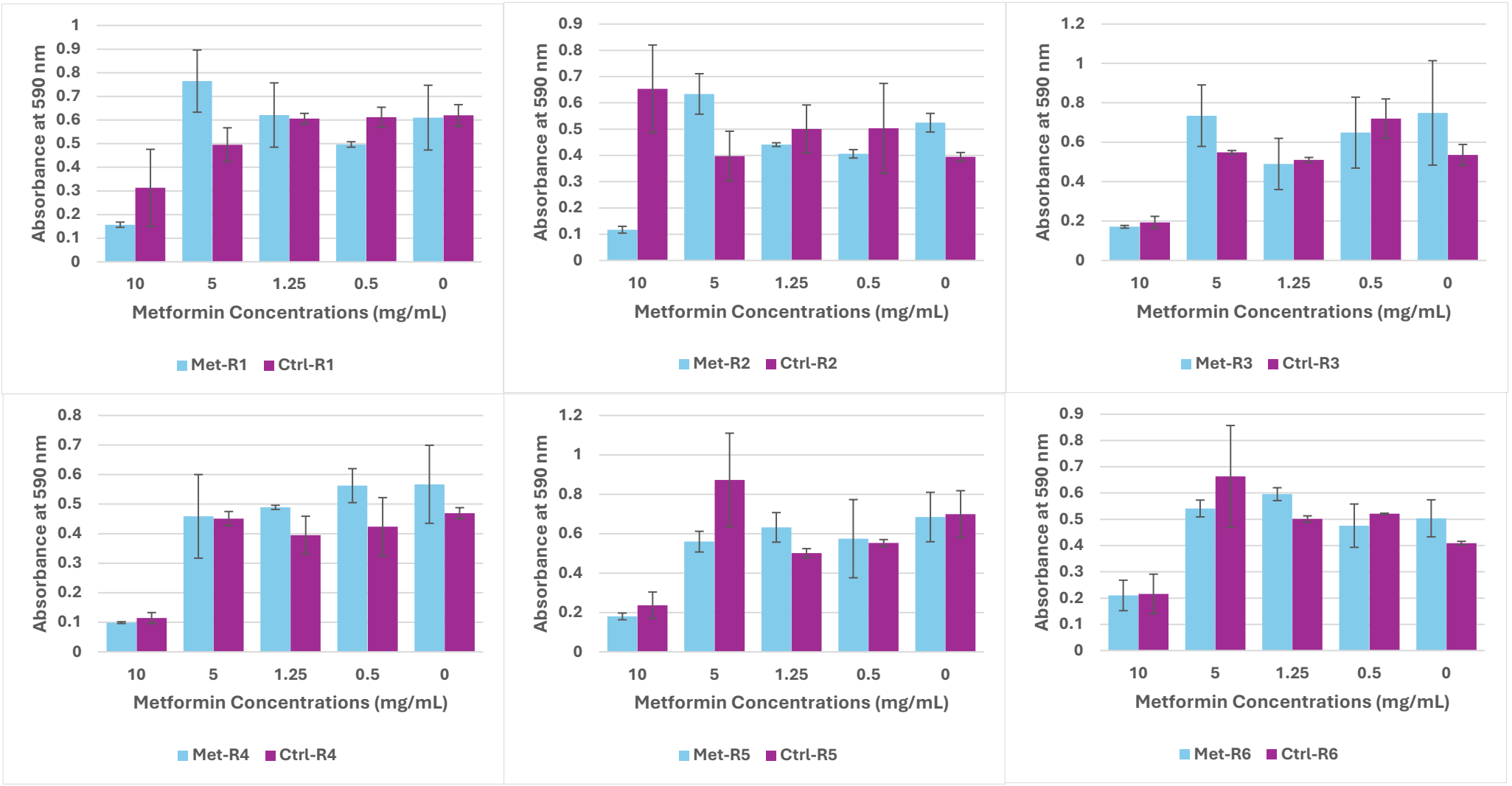

Figure 4-12: The inhibitory effect of different concentrations of metformin 10, 5, 1.25 and 0.5 mg/mL on the biofilm formation of the evolved lines (Met-R1- Met-R6) and their controls (Ctrl-R1-Ctrl-R6) of *S. aureus* NCTC 6571 along with the negative control.
The error bars represent the mean of the absorbance values of the crystal violet at 590 nm ± standard deviation. Each set of the experiment was done in two biological replicates (n=2), and two technical replicates for each.

4.2.2.4. Investigating the changes in bacterial growth in different antibiotics

To investigate the changes between the evolved lines and their controls of both strains for *S. aureus* and *P. aeruginosa*, MICs of different antibiotics were tested using the broth microdilution method.

For either *P. aeruginosa* or *S. aureus* mutants, the MICs of the different antibiotics tested were almost similar between the evolved lines and their controls, and sometimes with a change in one fold dilution as shown in Table 4-6 and Table 4-7.

Table 4-6: MICs of the different antibiotics of the mutants and their controls of *P. aeruginosa* ATCC 2785

M: Metformin-evolved, C: Control, CIP: Ciprofloxacin, GEN: Gentamicin, COS: Colistin, CEF: Ceftazidime

P. aeruginosa

AB	Parent	M1	C1	M2	C2	M3	C3	M4	C4	M5	C5	M6	C6
	MIC (µg/mL)												
CIP	0.125	0.125	0.125	0.125	0.125	0.125	0.125	0.125	0.125	0.125	0.125	0.125	0.125
GEN	2	2	2	2	2	2	2	2	2	4	2	4	2
COS	0.125	0.125	0.125	0.25	0.125	0.125	0.125	0.25	0.25	0.25	0.25	0.25	0.25
CEF	8	8	8	8	8	8	8	8	8	8	8	8	8

Table 4-7: MICs of the different antibiotics of the mutants and their controls of *S. aureus* NCTC 6571

S. aureus

AB	Parent	M1	C1	M2	C2	M3	C3	M4	C4	M5	C5	M6	C6
	MIC (µg/mL)												
ERY	2	2	2	0.25	1	0.25	1	0.25	1	0.5	0.25	4	2
DOX	0.125	0.125	0.125	0.125	0.125	0.125	0.125	0.125	0.125	0.125	0.125	0.125	0.125
GEN	1	0.5	1	0.5	0.5	1	1	1	0.5	0.5	1	1	0.5
CIP	0.125	0.125	0.125	0.125	0.125	0.0625	0.0625	0.125	0.125	0.0625	0.125	0.125	0.125
LIN	1	1	1	1	1	1	1	2	1	1	2	1	2
VAN	1	0.5	0.5	1	0.5	0.5	1	0.5	0.5	0.5	0.5	0.5	0.5

M: Metformin-evolved, C: Control, ERY: Erythromycin, DOX: Doxycycline, GEN: Gentamycin, CIP: Ciprofloxacin, LIN: Linezolid, VAN: vancomycin

In addition to MICs, the growth curve method was used to further investigate any changes in the growth of the evolved populations compared to their controls in the presence of different antibiotics.
Due to time constraints, each growth curve assay was only replicated once for each antibiotic. So, in the individual graphs for each antibiotic, there could not be error bars. Therefore, to show the collective response of all evolved lines compared to their controls at each antibiotic tested, the proportional AUC was calculated for each evolved line against its control. Hence, Figure 4-13 and Figure 4-14 have shown the average of the proportional AUC of evolved *P. aeruginosa* and *S. aureus* lines relative to their corresponding controls across increasing antibiotic concentrations for the different antibiotics tested, where a proportional AUC of 1 indicates equivalent growth between evolved lines and controls, lower than 1 means worse growth and greater than 1 better growth compared to the control.

For *P. aeruginosa*, the proportional AUCs at the four lowest concentrations of all antibiotics were nearly identical across all evolved lines. In contrast, there were variations among the antibiotics at the other concentrations. For three of the four drugs (gentamycin, ciprofloxacin, and colistin), the evolved lines seemed to grow better than controls at mid-range concentrations; however, this only reached significance for ciprofloxacin. For ciprofloxacin, the proportional AUC was significantly greater than 1 at concentrations C (0.5 µg/mL) and D (0.25 µg/mL), indicating that the growth of the evolved lines was significantly higher than that of their controls. Conversely, at concentration E (0.125 µg/mL), the proportional AUC was significantly lower than 1. For gentamycin, the proportional AUC was significantly higher than 1 at concentration H (0.0625 µg/mL). (Figure 4-13)

For *S. aureus,* almost the same pattern as in *P. aeruginosa* was observed, as the proportional AUCs were almost the same for all antibiotics for all evolved lines at the six lowest concentrations tested. There was no statistically significant change in the rest. However, there were huge variations within the evolved lines at the first concentration A for gentamycin and linezolid antibiotics (0.5 and 1 µg/mL, respectively). The same happened at the second concentration B (0.25 µg/mL) of gentamycin and ciprofloxacin antibiotics. This demonstrates that the different evolved lines varied in their response to higher concentrations of the tested antibiotic. (Figure 4-14)

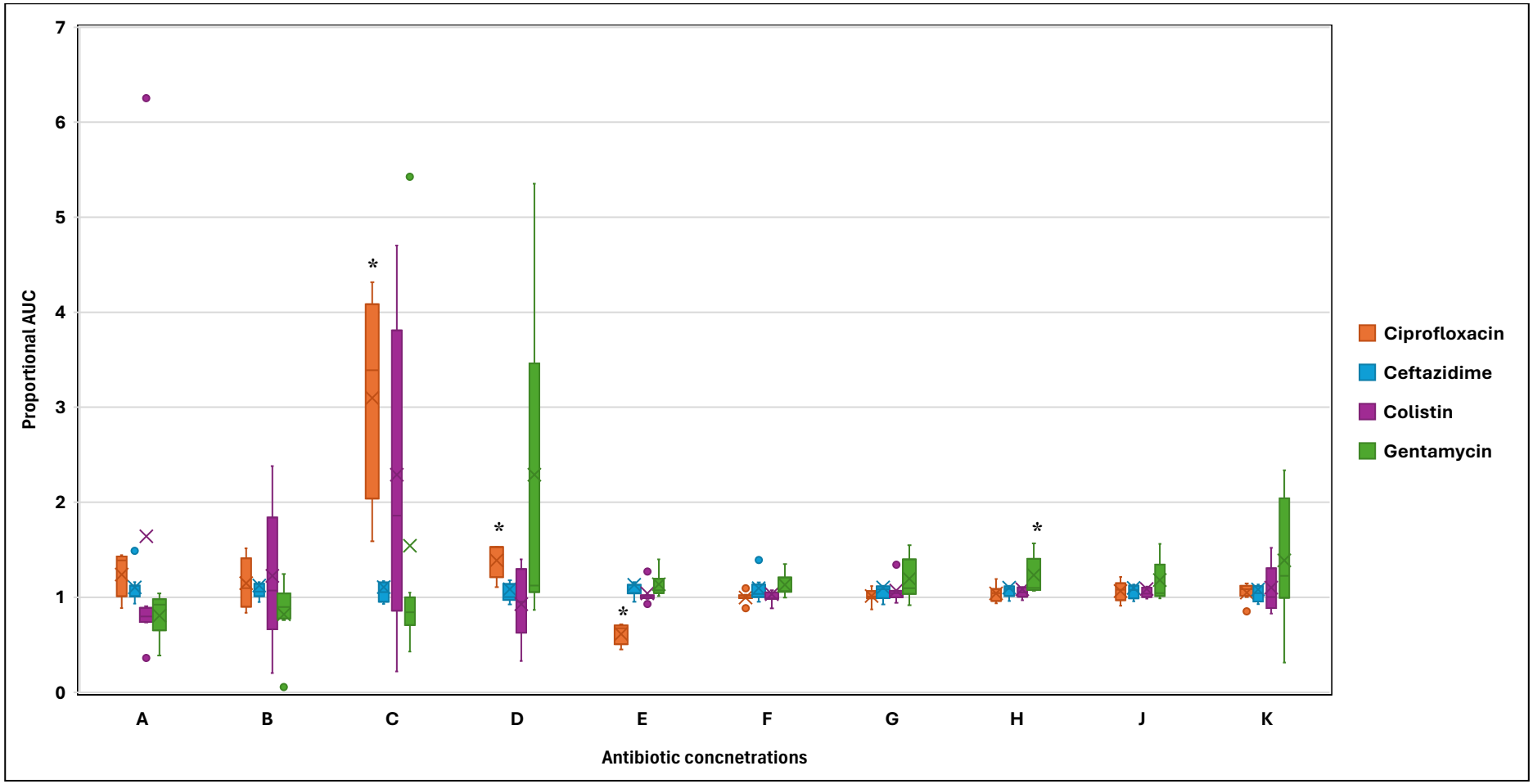

Figure 4-13: Proportional AUC changes across the evolved *P. aeruginosa* Lineages under multiple antibiotics with different concentrations.
Box plot illustrating the changing in the proportional AUC (AUC of evolved line /AUC of control) across all the evolved lineages of *P. aeruginosa* ATCC 27853 with the different concentrations (A-J) tested for each antibiotic of ciprofloxacin, ceftazidime, colistin and gentamycin along with the negative control (K); where A is the highest concentration and J is lowest one, the whiskers represent the distribution of the data, the horizontal line represents the median of the data, 'x' symbol represents the mean of the data, and asterisks '*' represents statistical significance with $p \leq 0.05$. The concentrations tested for ciprofloxacin and ceftazidime were (2 - 0.0078125 µg/mL), for gentamycin (8 - 0.03125 µg/mL) and for colistin (0.5-0.001935 µg/mL)

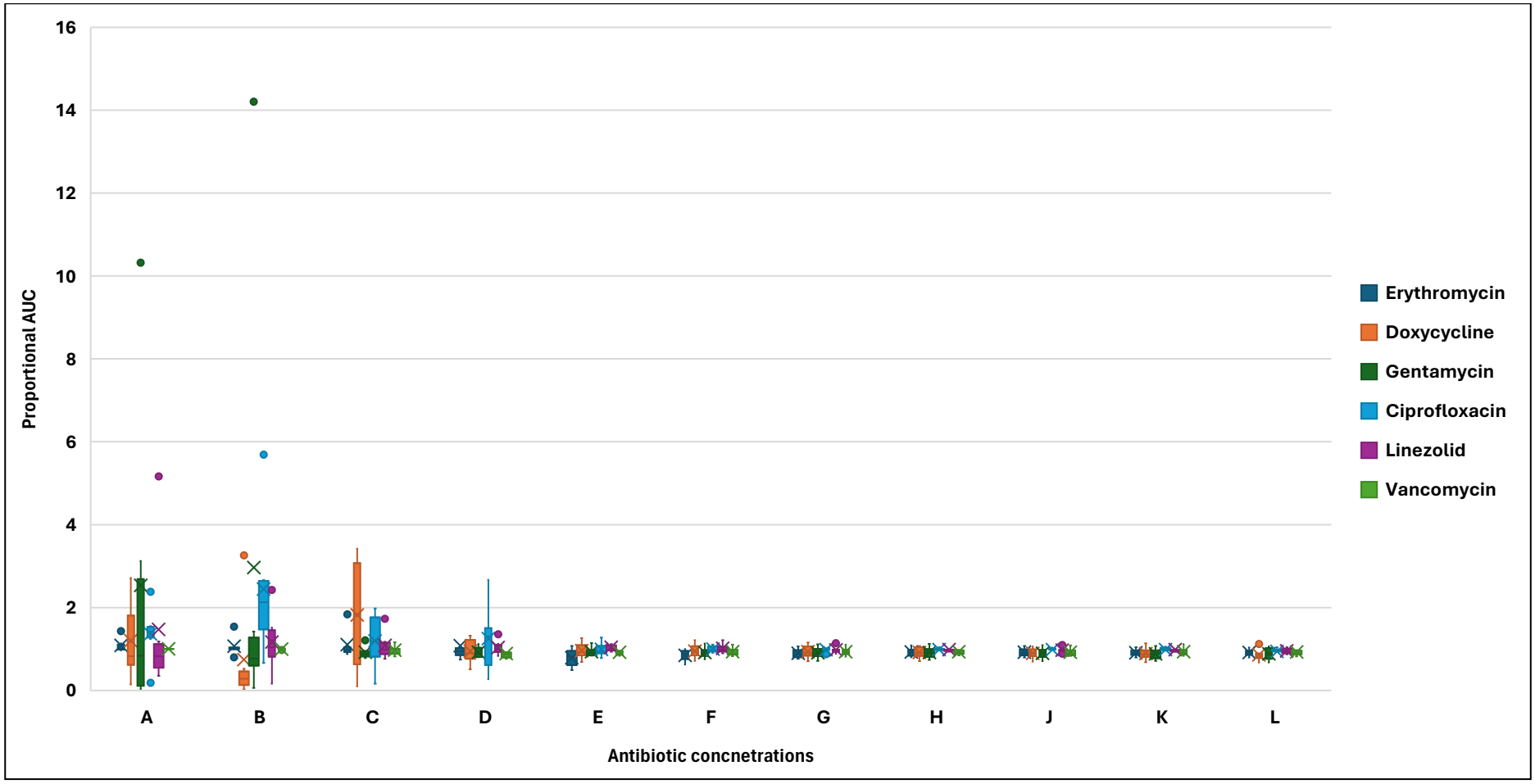

Figure 4-14: Proportional AUC changes across the evolved *S. aureus* Lineages under multiple antibiotics with different concentrations.
Box plot illustrating the changing in the proportional AUC (AUC of evolved line/AUC of control) across all the evolved lineages of *S. aureus* NCTC 6571 with the different concentrations (A-K) tested for each antibiotic of ciprofloxacin, erythromycin, doxycycline, linezolid, vancomycin and gentamycin along with the negative control (L); where A is the highest concentration and K is lowest one, the whiskers represent the distribution of the data, the horizontal line represents the median of the data and 'x' symbol represents the mean of the data. The concentrations tested for erythromycin were (2-0.003 µg/mL), doxycycline (0.125-0.0002 µg/mL), gentamycin and ciprofloxacin (0.5 – 0.0009 µg/mL), linezolid (1 - 0.0019 µg/mL) and vancomycin (2-0.003 µg/mL).

Then, the changes in the AUC of the evolved line compared to its corresponding control were analysed individually for each antibiotic.

For the *P. aeruginosa* strain, the concentrations of (2 - 0.0078125 µg/mL) of ciprofloxacin were tested (Figure 4-15) where Met-R1, R3, and R4 showed increased growth compared to their controls, particularly at the two lowest concentrations.

Additionally, all evolved lines and controls were investigated against gentamicin at concentrations of (8 - 0.015625 µg/mL). Figure 4-16 shows that Met-R1 and R4 exhibited increased growth in all subinhibitory concentrations of gentamicin compared to their controls. Met-R3 and R5 demonstrated decreased gentamicin activity compared to their controls at concentrations of 0.015625 and 1 µg/mL, respectively.

Colistin was tested at concentrations ranging from 0.5 to 0.0009 µg/mL (Figure 4-17), where Met-R1 and R4 exhibited a significant decrease in susceptibility at sub-inhibitory concentrations compared to their controls. Met-R2 and R3 demonstrated increased susceptibility at a concentration of 0.0625 µg/mL.

Lastly, all mutants and controls were tested against ceftazidime concentrations of 2 - 0.003 µg/mL (Figure 4-18). Only Met-R4 showed a clear decrease in susceptibility to the drug.

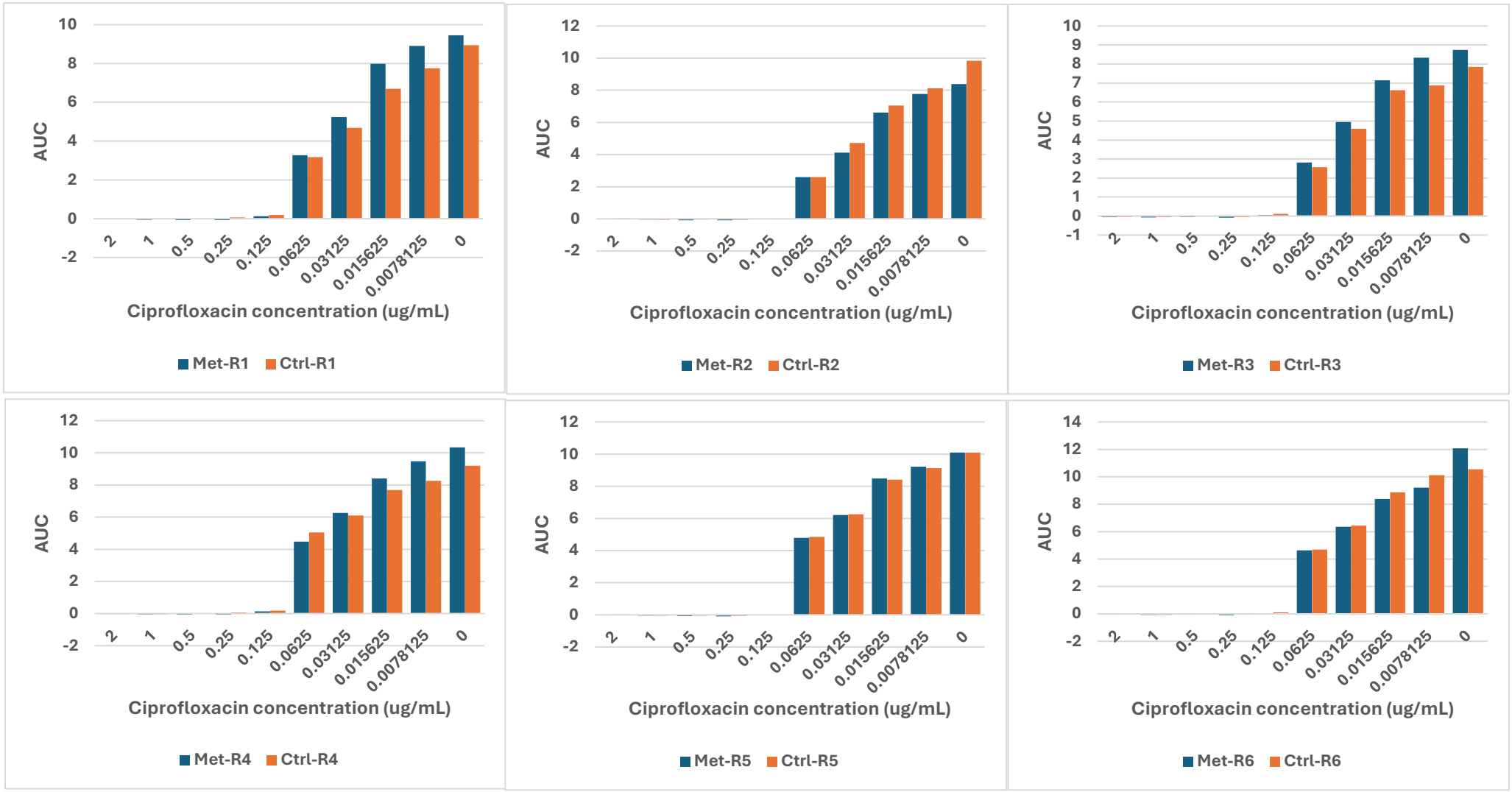

Figure 4-15: Area under the curve (AUC) from the growth curves of the evolved lines (Met-R1- Met-R6) and their controls (Ctrl-R1-Ctrl-R6) of *P. aeruginosa* ATCC 27853 in the presence of different concentrations of ciprofloxacin (2 - 0.0078125 µg/mL) along with the negative control.

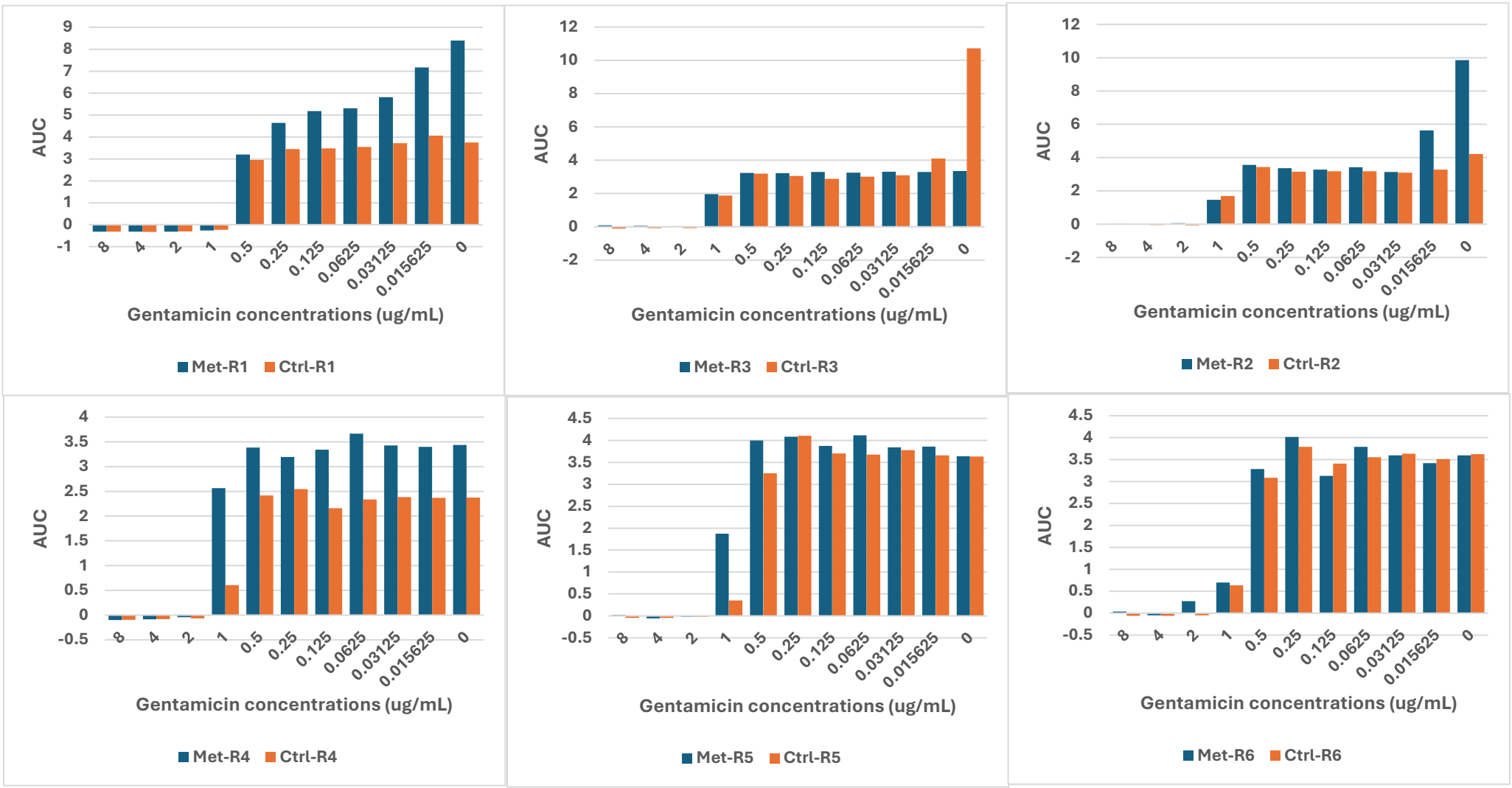

Figure 4-16: Area under the curve (AUC) from the growth curves of the mutants (1-6) and their controls of *P. aeruginosa* ATCC 27853 in the presence of different concentrations of gentamycin (8 - 0.015625 µg/mL) along with the negative control.

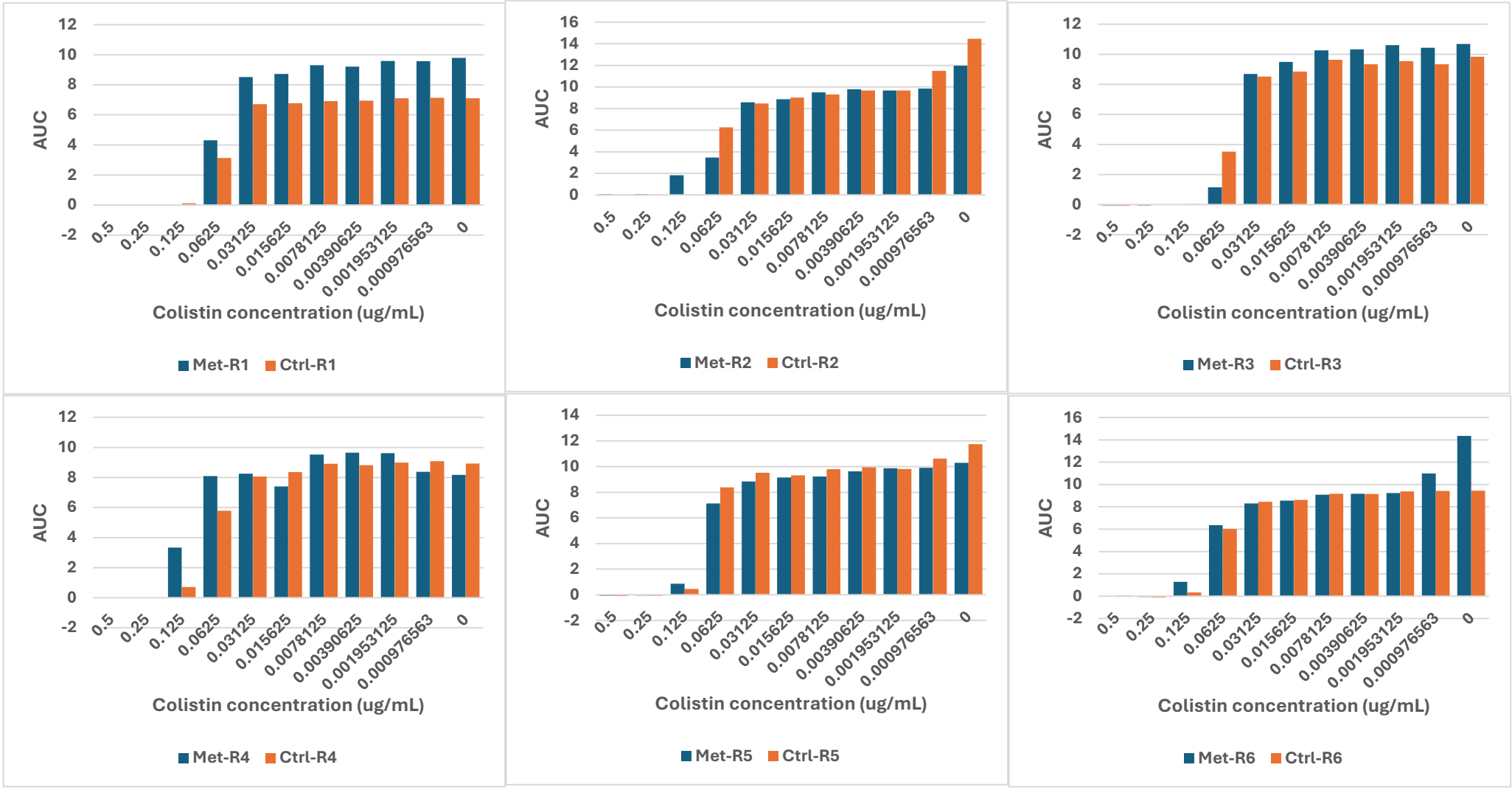

Figure 4-17: Area under the curve (AUC) from the growth curves of the evolved lines (Met-R1- Met-R6) and their controls (Ctrl-R1-Ctrl-R6) of *P. aeruginosa* ATCC 27853 in the presence of different concentrations of colistin (0.5-0.0009 µg/mL) along with the negative control.

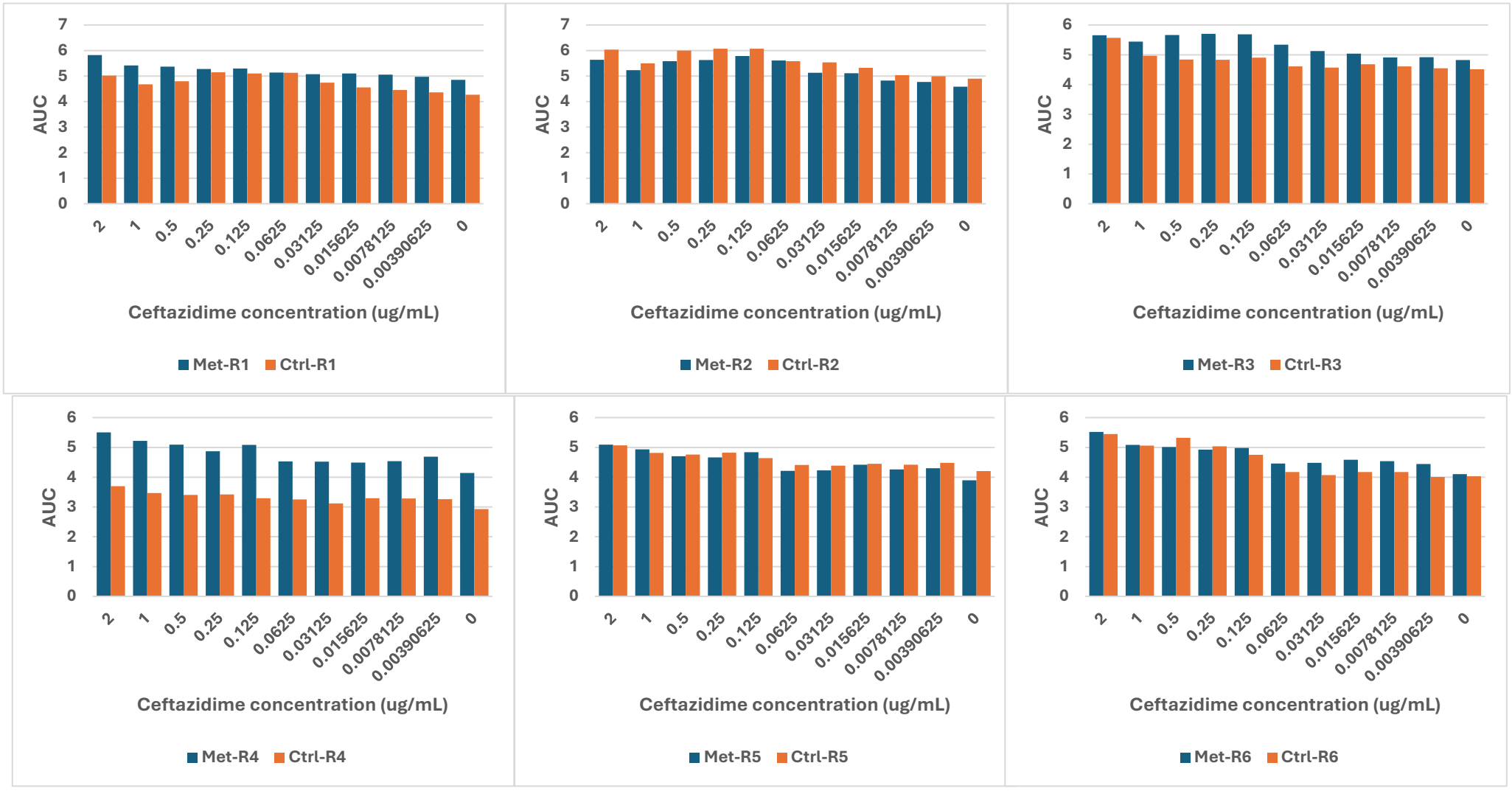

Figure 4-18: Area under the curve (AUC) from the growth curves of the evolved lines (Met-R1- Met-R6) and their controls (Ctrl-R1-Ctrl-R6) of *P. aeruginosa* ATCC 27853 in the presence of different concentrations of ceftazidime (2 - 0.003 µg/mL) along with the negative control.

For the *S. aureus* strain, starting with erythromycin, 2-0.003 µg/mL concentrations were tested. Met-R1, R2 and R3 showed an increase in susceptibility to the drug compared to their corresponding controls, especially at the concentrations 0.125-0.003 µg/mL. Met-R4 and R6 showed less susceptibility in the last four concentrations of Met-R4 and the first four concentrations of Met-R6. (Figure 4-19)

Doxycycline with concentrations of 0.125-0.0002 µg/mL was tested. Like erythromycin, Met-R1, R2 and R3 showed the same pattern of increase in susceptibility compared to their controls. Met-R4 and R5 showed less susceptibility, especially at concentrations of 0.031-0.0002 µg/mL for both of them. Met-R6 showed a slight increase in susceptibility in the lowest three concentrations. (Figure 4-20)

Furthermore, gentamycin with concentrations 0.5 – 0.0009 µg/mL was tested. Met-R1, R2 and R3 showed less growth at all concentrations compared to their controls. Met-R6 showed a slight increase in growth at all subinhibitory concentrations compared to the control. (Figure 4-21)

In addition, ciprofloxacin at concentrations of 0.5 – 0.0009 µg/mL was investigated. Met-R1 and R6 showed an increase in growth at concentrations 0.031 and 0.015 µg/mL. Met-R3 showed more susceptibility at the subinhibitory concentrations compared to its control. (Figure 4-22)

At the concentrations of 1 - 0.0019 µg/mL, linezolid was tested, and there was a slight increase in susceptibility among Met-R1, R2, R3 and R5. However, Met-R4 and R6 demonstrated the opposite trend, particularly at concentrations of 1 - 0.031 µg/mL for Met-R4. (Figure 4-23)

Lastly, when vancomycin at the concentrations of 2-0.003 µg/mL was tested, mutants Met-R1, R2, R3 and R6 showed less growth compared to their controls. While Met-R4 showed a decrease in susceptibility towards the drug. (Figure 4-24)

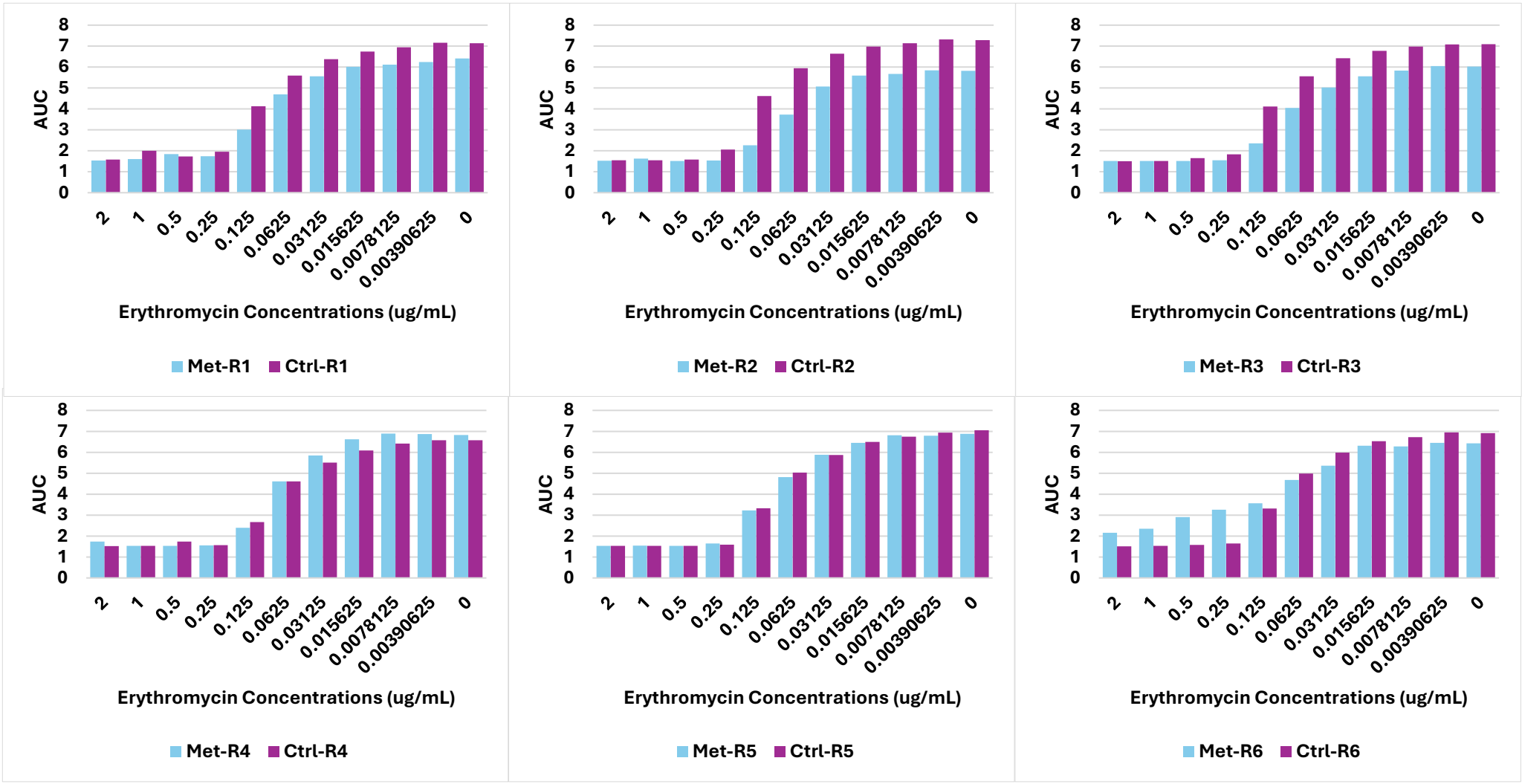

Figure 4-19: Area under the curve (AUC) from the growth curves of the evolved lines (Met-R1- Met-R6) and their controls (Ctrl-R1-Ctrl-R6) of *S. aureus* NCTC 6571 in the presence of different concentrations of erythromycin (2 - 0.003 µg/mL) along with the negative control

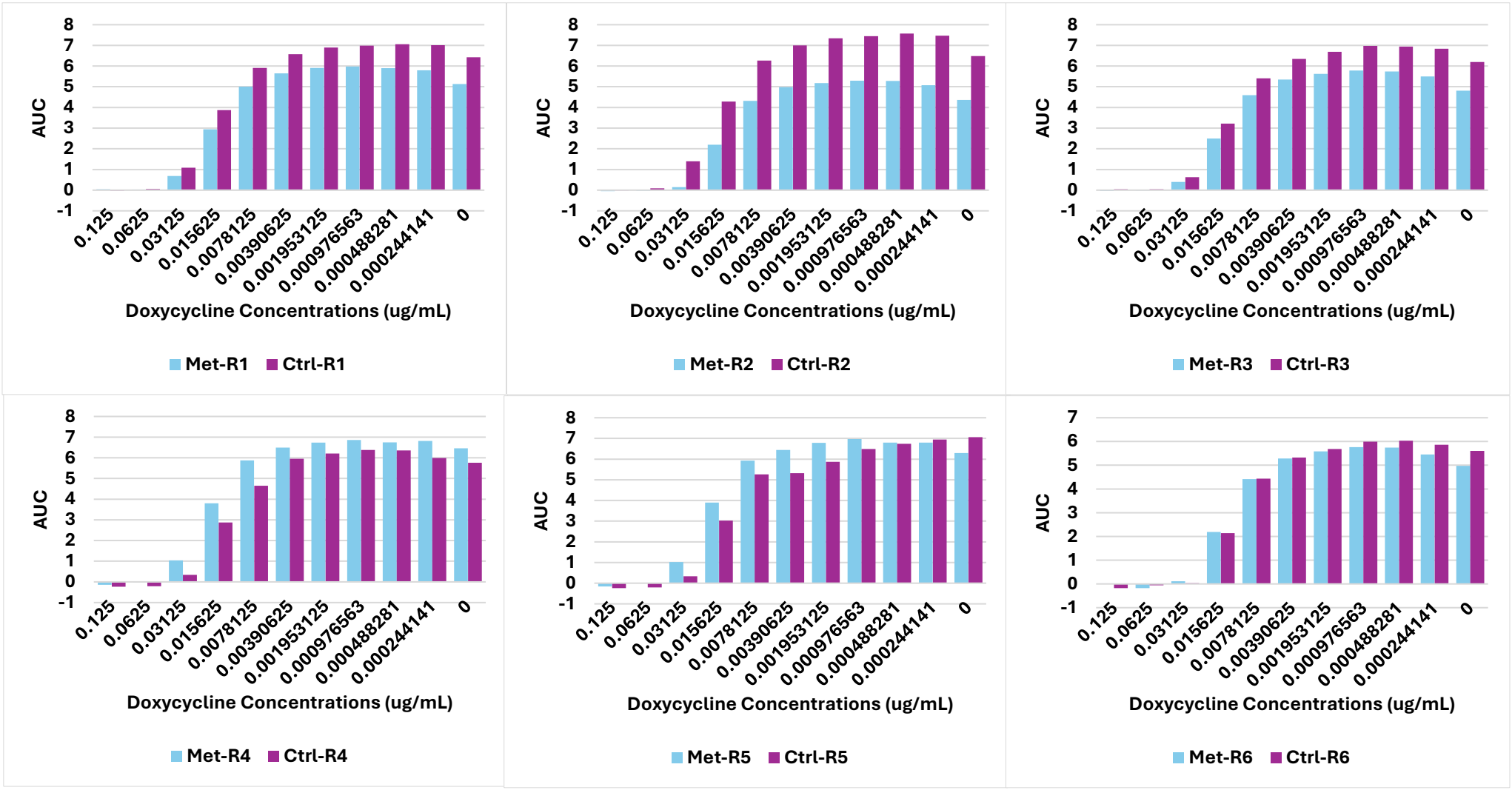

Figure 4-20: Area under the curve (AUC) from the growth curves of evolved lines (Met-R1- Met-R6) and their controls (Ctrl-R1-Ctrl-R6) of *S. aureus* NCTC 6571 in the presence of different concentrations of doxycycline (0.125-0.0002 µg/mL) along with the negative control.

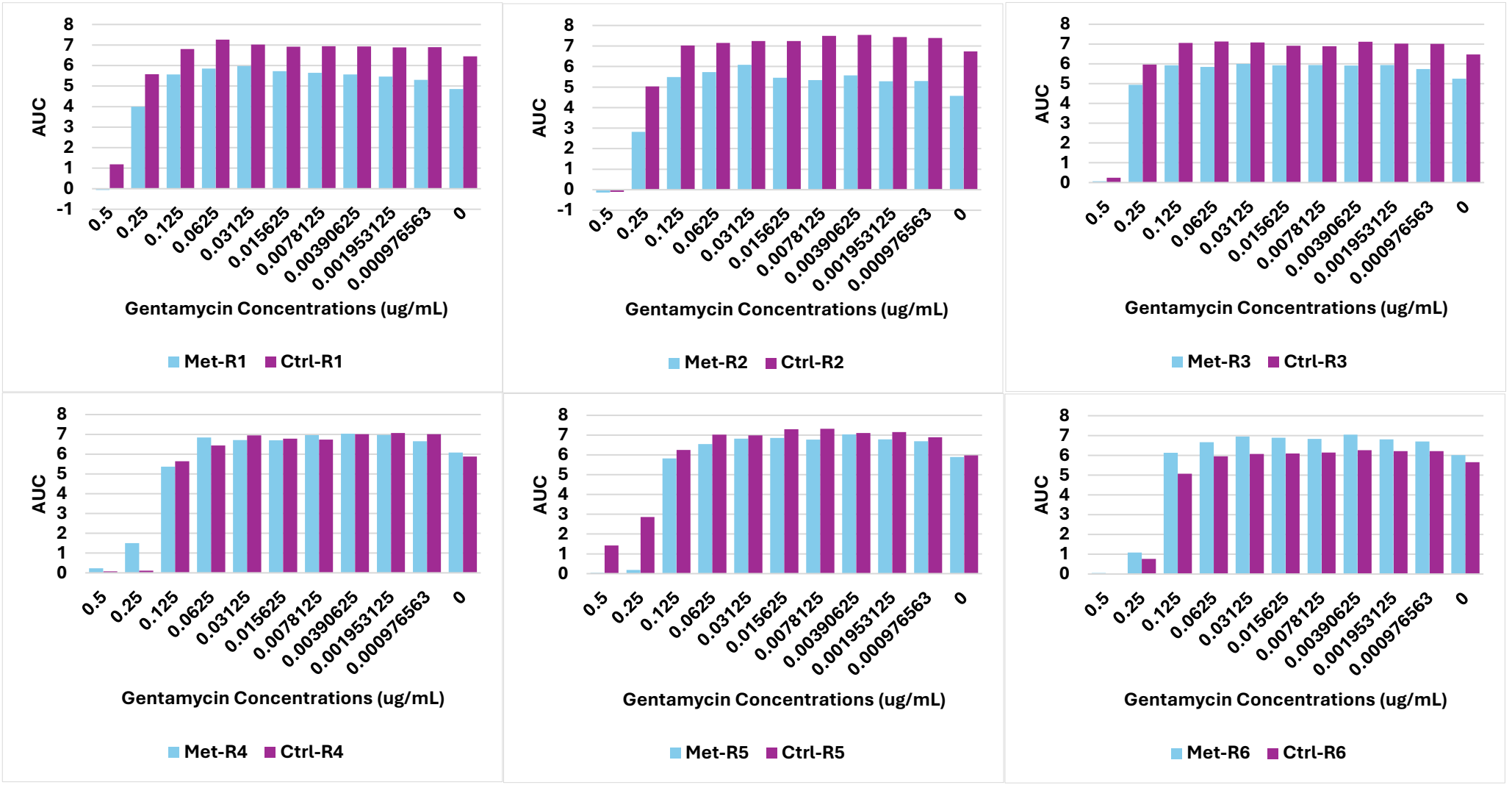

Figure 4-21: Area under the curve (AUC) from the growth curves of the evolved lines (Met-R1- Met-R6) and their controls (Ctrl-R1-Ctrl-R6) of S. aureus NCTC 6571 in the presence of different concentrations of gentamycin (0.5 – 0.0009 µg/mL) along with the negative control

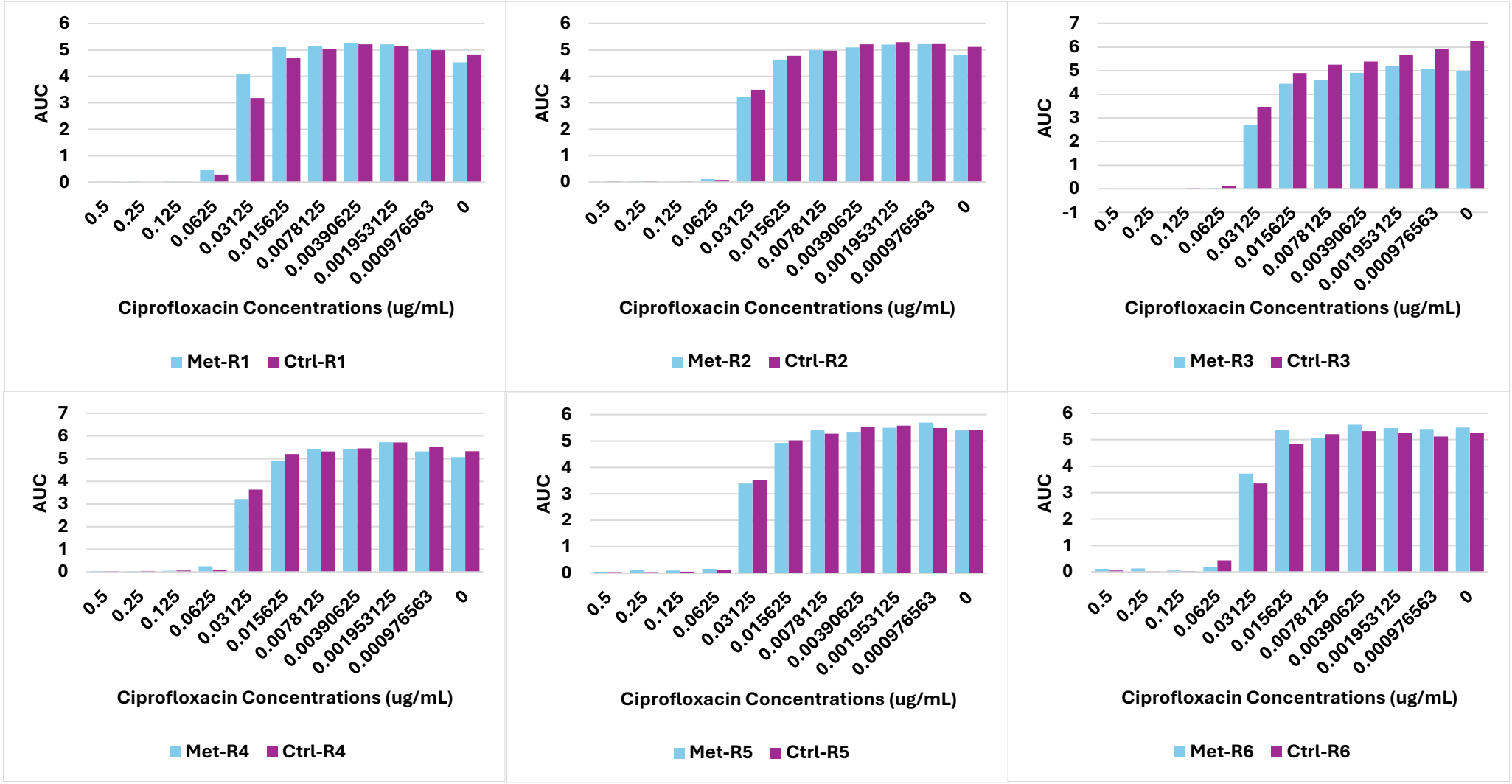

Figure 4-22: Area under the curve (AUC) from the growth curves of the evolved lines (Met-R1- Met-R6) and their controls (Ctrl-R1-Ctrl-R6) of *S. aureus* NCTC 6571 in the presence of different concentrations of ciprofloxacin (0.5 – 0.0009 µg/mL) along with the negative control

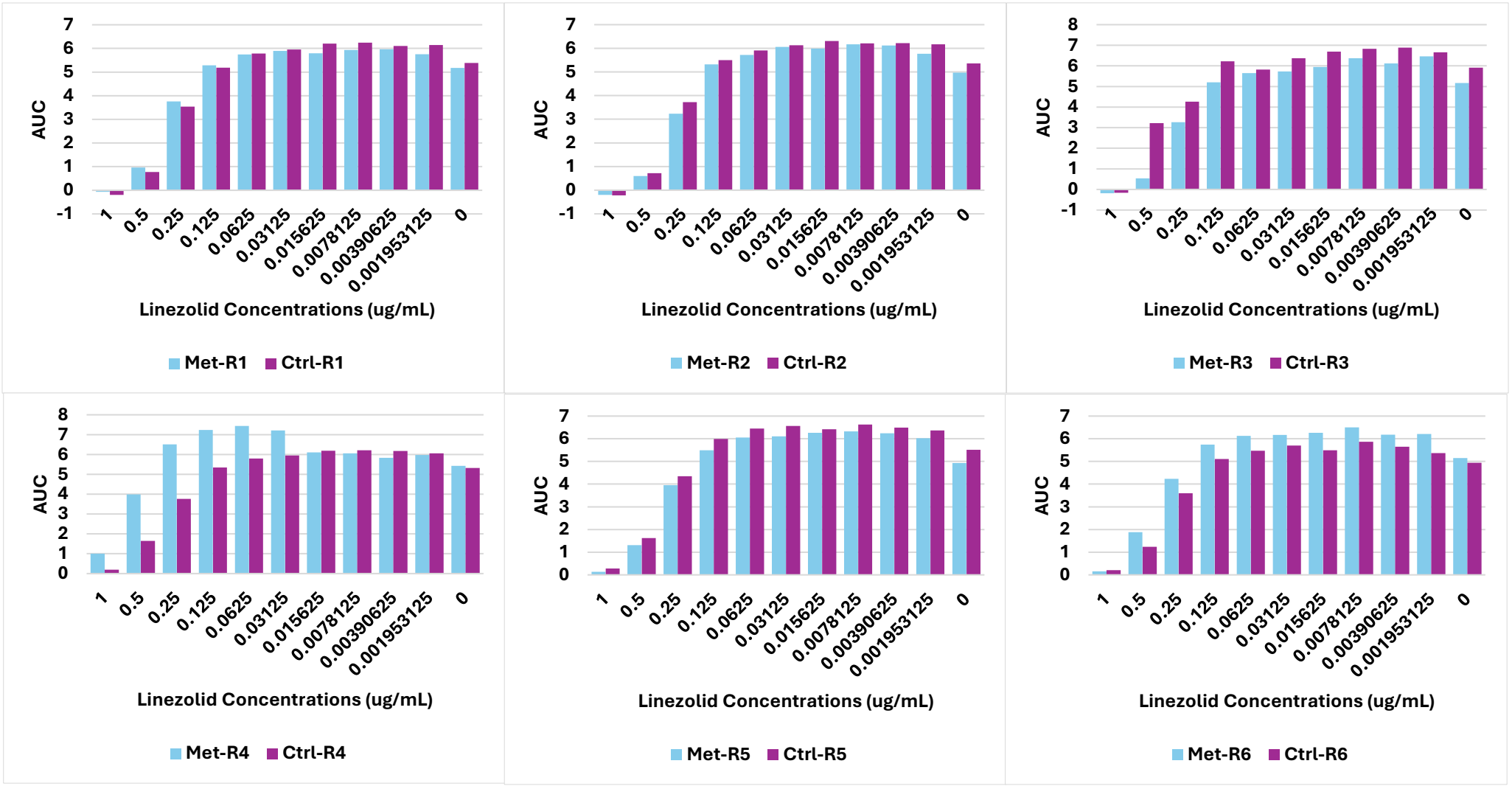

Figure 4-23: Area under the curve (AUC) from the growth curves of the evolved lines (Met-R1- Met-R6) and their controls (Ctrl-R1-Ctrl-R6) of *S. aureus* NCTC 6571 in the presence of different concentrations of linezolid (1 - 0.0019 µg/mL) along with the negative control

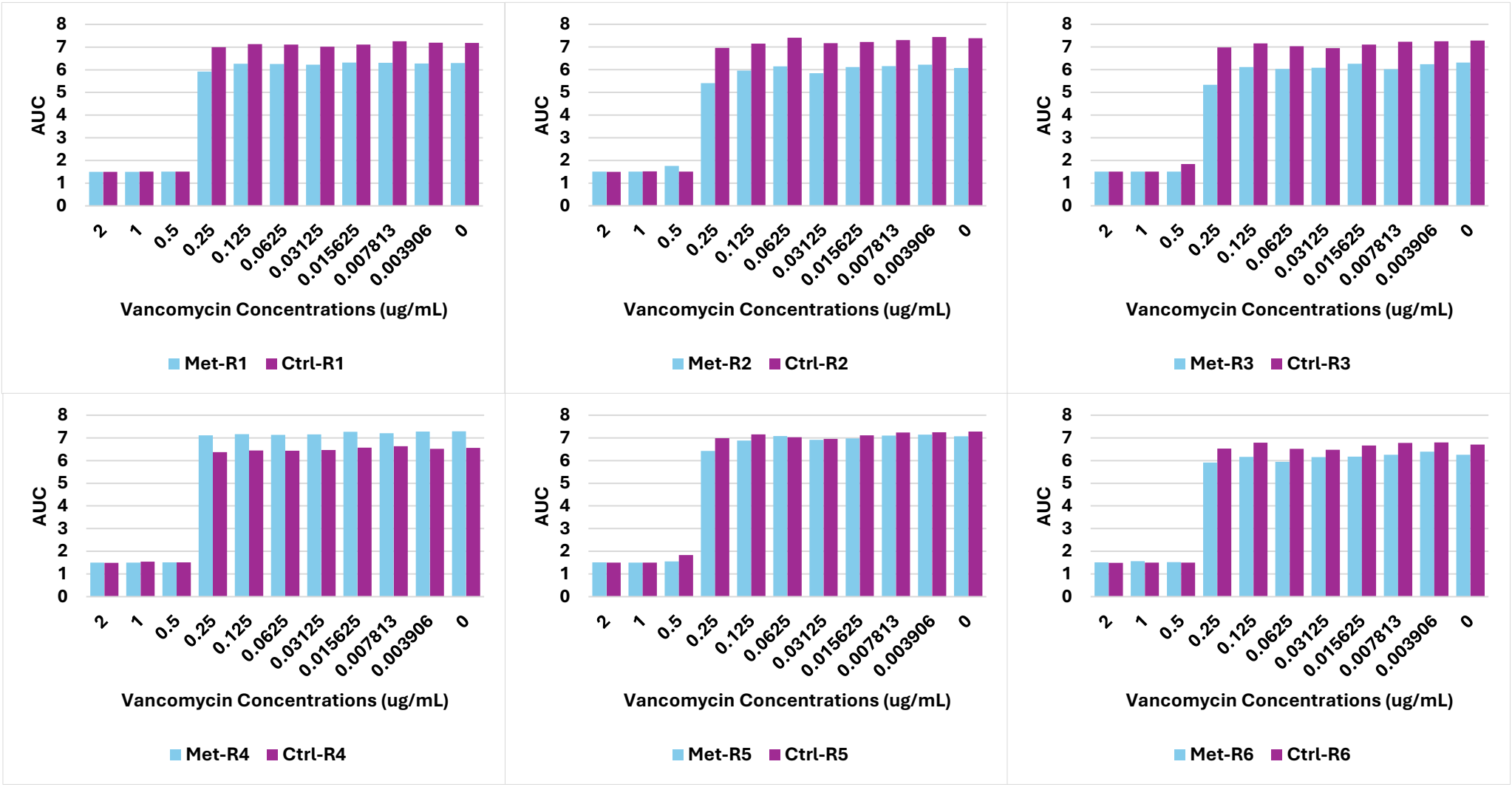

Figure 4-24: Area under the curve (AUC) from the growth curves of the evolved lines (Met-R1- Met-R6) and their controls (Ctrl-R1-Ctrl-R6) of *S. aureus* NCTC 6571 in the presence of different concentrations of vancomycin (2-0.003 µg/mL) along with the negative control

4.2.3. Study the molecular changes in the metformin-exposed evolved populations

To detect the genetic mutations that occur in the evolved populations compared to their parents, the genomic DNA of all evolved lines and their controls was sequenced using short-read and long-read techniques and analysed against the parents for both tested strains of *S. aureus* and *P. aeruginosa*. The analysis has been divided into two parts: the characterization of SNPs and INDELs and the characterization of structural variations.

4.2.3.1. The characterization of SNPs and INDELs

Upon the analysis of the sequenced data using breseq and snippy, all the mutations found only in the metformin-evolved lines are shown in Table 4-8and Table 4-9 for *S. aureus* and *P. aeruginosa,* respectively, and all the mutations found either in both evolved lines and controls or in controls only are shown in the supplementary tables in the appendix.

For *S. aureus*, there were different mutations observed in all evolved lines except Met-R6. In three evolved lines out of six, there were two types of mutations that occurred in the Fibronectin-binding protein A gene (*fnbA*), which is generally responsible for the adhesions of the bacteria to the cells and normal formation of biofilm (Herman-Bausier et al., 2015). one (P881_P883del) was deletion at the position of 9 nucleotides, resulting in the frame deletion of 3 consecutive proline amino acids in Met-R4 and R5. And one of the mutations (T879T) was a synonymous substitution of one base pair that results in the same amino acid, threonine, and it was found in the Met-R1, R4 and R5.

In addition, there was a missense mutation (C288Y) found in Met-R1 as a substitution of one base pair resulting in changing the amino acid from cysteine to tyrosine in the *gatD_1* gene that encodes for galactitol 1-phosphate 5-dehydrogenase which is responsible for the metabolism of galactitol in the bacterial cells which play role in bacterial growth use galactitol as a carbon source (Nolle et al., 2017) .

In addition, there were three different mutations found in the *apt* gene in three evolved lines out of six that encodes for adenine phosphoribosyltransferase that catalyzes adenine metabolism and producing AMP in an energy efficient way. These mutations were a missense mutation at the position of 102 (T102K) in Met-R2, and at the position 124 (G124D) in mutant 3. However, in mutant 4, there was a substitution of base pair in the same gene at position 5 (Q5*) resulting in changing the amino acid from glutamine to a stop codon which resulted in an early stop translating the protein.

Furthermore, there were mutations happened in the intergenic area between two genes encodes for t-RNA for Met-R2 and R3, wherein Met-R2, it was one base pair deletion in the intergenic area of tRNA of methionine and tRNA of alanine. For Met-R3, there were 2 base pair deletion in the intergenic area

of tRNA of leucine and tRNA of glycine, in addition to a substitution of one base pair in the same intergenic area.

Table 4-8: Mutations found only in the metformin-exposed evolved lines of *S. aureus* NCTC 6571 as a result of the whole genome sequencing analysis for the short and long reads samples using Breseq and Snippy

Strain	Gene	Mutation	Annotation	Type	Effect	Product
Met-R1	*P_02504* →	C→A	T267N	SUB	Missense	hypothetical protein
	gatD_1 →	G→A	C288Y	SUB	Missense	Galactitol 1-phosphate 5-dehydrogenase
	**fnbA* →	A→G	T879T	SUB	synonymous	Fibronectin-binding protein A
	**P_01585* ←	A→G	D768D	SUB	synonymous	hypothetical protein
Met-R2	*P_02621* ← / ← *P_02622*	Δ1 bp	intergenic (-20/+2)	DEL	Intergenic	tRNA-Met/tRNA-Ala
	* *P_01320*→	G→A	K530K	SUB	synonymous	Staphylocoagulase
	* *P_01320*→	C→T	N535N	SUB	synonymous	Staphylocoagulase
	* *P_01320*→	T→C	Y537Y	SUB	synonymous	Staphylocoagulase
	**apt*→	C→A	T102K	SUB	Missense	Adenine phosphoribosyltransferase
Met-R3	*P_02625* ← / ← *P_02626*	Δ2 bp	intergenic (-2/+8)	DEL	Intergenic	tRNA-Leu/tRNA-Gly

	P_02625 ← / ← P_02626	Δ1 bp	intergenic (-5/+6)	DEL	Intergenic	tRNA-Leu/tRNA-Gly
	P_02625 ← / ← P_02626	A→T	intergenic (-8/+3)	SUB	Intergenic	tRNA-Leu/tRNA-Gly
	**apt→*	G→A	G124D	SUB	Missense	Adenine phosphoribosyltransferase
Met-R4	*apt →*	C→T	Q5*	SUB	Stopgain	Adenine phosphoribosyltransferase
	**fnbA→*	Δ9 bp	P881_P883del	DEL	Conservative inframe deletion	Fibronectin-binding protein A
	**fnbA→*	A→G	P886P	SUB	synonymous	Fibronectin-binding protein A
	* *P_01728*	G→A	L22L	SUB	synonymous	hypothetical protein
Met-R5	**fnbA→*	Δ9 bp	P881_P883del	DEL	Conservative inframe deletion	Fibronectin-binding protein A
	**fnbA→*	A→G	P886P	SUB	synonymous	Fibronectin-binding protein A

(*) indicates the mutation was found due to the alignments of the hybrid short-long read analysis. If the mutation is blue colour, it means missense, green means synonymous and red means nonsense. '→' besides the gene name means that it is on the forward strand, and '←' means that the gene is on the reverse one. 'Δ' means that there is deletion at this position.

For *P. aeruginosa*, mutations were also detected in intergenic regions. In Met-R1, there was a substitution mutation in the intergenic area downstream the *typA* gene with 61 bp which encodes for GTP-binding protein TypA/BipA. TypA (or BipA) is considered as ribosome-binding GTPases, which is important in the initiation of the protein translation and ribosome assembly, and it was found that it has a crucial role in biofilm formation and swarming motility in *P. aeruginosa* (Neidig et al., 2013). In addition, there was an insertion of 75 bp upstream 600bp of the *mip* gene which encodes for Peptidyl-prolyl cis-trans isomerase Mip that is important in protein folding inside that bacteria and it was found to have a role in the virulence of the bacteria and their corresponding response to the stress (Janet-Maitre et al., 2024). In the same gene there were three substitution mutations in the intergenic area upstream of 602, 612, and 614 bp in Met-R3 and R6. Those substitution mutations were also found in Ctrl-R2 and R4, so they are not unique to the drug-exposed condition. Also in Met-R1, there were two mutations in hypothetical proteins – one was missense (G53P) and the other was synonymous (G26G), which was also noticed in Met-R2 and R6.

Furthermore, in both Met-R2 and R3, there was another substitution mutation in the intergenic area upstream of the *acnM* gene with 120 bp and downstream of the *prpC_2* gene with 11 bp, which encode for Aconitate hydratase A and 2-methylcitrate synthase, respectively. Aconitate hydratase A is important in catalysing the isomerization between citrate and isocitrate in the tricarboxylic cycle (TCA), as well as the conversion of 2-methylcitrate to 2-methylisocitrate in the 2-methylcitrate cycle (2-MCC). This is crucial for the aerobic respiration of the bacteria and energy generation, while 2-methylcitrate synthase converts Propionyl-CoA and oxaloacetate from TCA into 2-methylcitrate, facilitating entry into the 2-MCC, which plays an important catabolic role in regulating the amount of propionate short-chain fatty acid. Thus, AcnM and PrpC are interrelated and vital for bacterial metabolism(Brämer et al., 2002). In Met-R2, there were four additional missense mutations in three different genes. One was in *the acdS* gene (G204V), which encodes for 1-aminocyclopropane-1-carboxylate (ACC) deaminase, demonstrating catabolic activity on ACC, predominantly in plant–microbe interactions, but it has also been found to be significant for bacteria in tolerating stressful environments(Singh et al., 2015). The other mutation was in *argJ* (A86E), which encodes for the arginine biosynthesis bifunctional protein ArgJ that catalyses two steps in the synthesis of arginine in the bacterial cell: N-acetylglutamate and ornithine synthesis(Yee et al., 2020). The other two mutations (E32D and L34R) were in the same hypothetical protein.

In Met-R3, it was noticed a missense mutation with a substitution of one bp of the *pntB* gene that encodes NAD(P) transhydrogenase subunit beta. NAD(P) transhydrogenase works as a proton pump in the cell membrane, which helps in controlling the redox activity and proton motive force in the cell, which can energise ATP synthesis (Nikel et al., 2016). The other mutation in the same evolved line was a

synonymous mutation in *hcnB_2,* which upon translation produces Hydrogen cyanide synthase subunit HcnB, a membrane protein that catalyses a respiratory chain reaction to produce cyanide, which helps in increasing the tolerance of the bacteria against some of the oxidative stresses.
In Met-R4, there were two mutations (D203Y and L256R) in two genes encoding HTH-type transcriptional regulators; one was a putative type, and the other was the TrpI regulator. These regulators are DNA-binding proteins that are important in gene regulation, especially for virulence expression and stress response(Wang et al., 2023). The TrpI protein is known to regulate the transcription of *trpBA,* which is responsible for tryptophan metabolism that is vital for the production of many proteins and enzymes in the bacteria (Gao & Gussin, 1991). In addition, there was another missense mutation (L504R) in *the acoR* gene, which encodes for the Acetoin catabolism regulatory protein, regulating the metabolism of acetoin as a carbon source when there is a deficiency in the environment of other carbon sources, such as glucose and succinate.

In Met-R5, there was one substitution missense mutation (E119A) in *mexD* which was annotated in the automated annotator used as *acrB_1*. The genes in this operon initially annotated as *acrA* and *acrB* within the same operon containing *oprJ*. However, based on gene organization and mapping against BLAST data base, this system corresponds to a MexCD-OprJ-type RND efflux pump, rather than AcrAB*,* which is generally a known way to protect the cells against many different toxic compounds including antibiotics.

In Met-R6, in addition, there was a missense mutation (T31P) in the *dsbD_2* gene that resulted in the Thiol:disulfide interchange protein DsbD, which is important in the formation of the disulfide bonding process in the Dsb system, where the DsbD plays a role in the electron transportation through the cell membrane (Łasica & Jagusztyn-Krynicka, 2007).

Table 4-9: Mutations found only in the metformin-exposed evolved lines of *P. aeruginosa* ATCC 27853 as a result of the whole genome sequencing analysis for the short and long reads samples using Breseq and Snippy

Strain	Gene	Mutation	Annotation	Type	Effect	Product
Met-R1	*typA* → / –	G→T	intergenic (+61/–)	SUB	Intergenic	GTP-binding protein TypA/BipA/–
	– / → *mip*	+75 bp	intergenic (–/-600)	INS	Intergenic	–/Peptidyl-prolyl cis-trans isomerase Mip
	P_02645 →	G→C	G26G	SUB	Synonymous	hypothetical protein
	**P_05599* ←	T→G	G53P	SUB	Missense	hypothetical protein
Met-R2	*P_02645* →	G→C	G26G	SUB	Synonymous	hypothetical protein
	acdS ←	C→A	G204V	SUB	Missense	1-aminocyclopropane-1-carboxylate deaminase
	acnM ← / ← *prpC_2*	C→G	intergenic (-120/+11)	SUB	Intergenic	Aconitate hydratase A/2-methylcitrate synthase
	**argJ*←	G→T	A86E	SUB	Missense	Arginine biosynthesis bifunctional protein ArgJ
	**P_04871*→	A→C	E32D	SUB	Missense	hypothetical protein
	**P_04871*→	T→G	L34R	SUB	Missense	hypothetical protein
Met-R3	*acnM* ← / ← *prpC_2*	C→G	intergenic (-120/+11)	SUB	Intergenic	Aconitate hydratase A/2-methylcitrate synthase
	**pntB* →	T→G	F288V	SUB	Missense	NAD(P) transhydrogenase subunit beta

	**hcnB_2* →	C→T	A196A	SUB	Synonymous	Hydrogen cyanide synthase subunit HcnB
Met-R4	*P_00002* ←	C→A	D203Y	SUB	Missense	putative HTH-type transcriptional regulator
	**acoR* →	T→G	L504R	SUB	Missense	Acetoin catabolism regulatory protein
	**trpI_1* →	T→G	L256R	SUB	Missense	HTH-type transcriptional regulator TrpI
Met-R5	**mexD* →	A→T	E119A	SUB	Missense	Multidrug efflux pump subunit MexD
Met-R6	*glyA_2* →	C→T	H29H	SUB	Synonymous	Serine hydroxymethyltransferase
	glyA_2 →	G→C	R25R	SUB	Synonymous	Serine hydroxymethyltransferase
	P_02645 →	G→C	G26G	SUB	Synonymous	hypothetical protein
	**dsbD_2* →	A→C	T31P	SUB	Missense	Thiol:disulfide interchange protein DsbD

(*) indicates the mutation was found due to the alignments of the long read sequencing only. If the mutation is blue colour, it means missense, green means synonymous and red means nonsense. '→' besides the gene name means that it is on the forward strand, and '←' means that the gene is on the reverse one. 'Δ' means that there is deletion at this position.

4.2.3.2. The characterization of structural variations

For *S. aureus*, upon running SVIM-asm for detecting any structural variations in the assembled genome compared to the controls Table 4-10, it was found that in Met-R2, there were two deletions. One was of 165 bp, which includes two genes encoding t-RNAs – one that carries asparagine and the other that carries glutamic acid, and the other was of 57 bp in *ssl3* that encodes Staphylococcal superantigen-like 3. There was also an insertion of 612 bp in a hypothetical protein. In Met-R3, there was an insertion of 170 bp, which was found in the intergenic area between the gene that encodes a tRNA that carries tyrosine and the gene encoding a tRNA that carries glycine. Another deletion of 231 bp was found in the *ebh* gene that encodes for Extracellular matrix-binding protein Ebh in Met-R5.

The assembled genome of *S. aureus* samples was not in a single contig; therefore, using Socru to identify the changes around the ribosomal operons was not applicable. This tool requires the genome to be fully assembled as one chromosome, not as contigs; otherwise, it may produce false results.

Table 4-10: The structural variations found in *S. aureus* evolved lines as result of running SVIM-asm on the whole genome sequenced data

Strain	Contig	Position	Type	Length
Met-R2	Contig_2	670341	DEL	165 bp
	Contig_3	322250	DEL	57 bp
	Contig_4	82411	INS	612 bp
Met-R3	Contig_2	670703	INS	170 bp
Met-R5	Contig_1	432823	DEL	231 bp

For *P. aeruginosa*, upon using SVIM-asm on the sequenced samples, no structural variations of large insertions, deletions, inversions, translocations or duplications compared with the parent strain were found. Also, upon running the Socru tool, no change in the order and orientation of the genomes around the ribosomal operons compared to the parent strain were identified.

\

Table 4-11: A summarised table for all changes that occurred in the six evolved strains resulting from the evolutionary experiment of *S. aureus* with the continuous exposure to 1.25 mg/mL metformin

	Met-R1	**Met-R2**	**Met-R3**	**Met-R4**	**Met-R5**	**Met-R6**
Growth profile	NS	-	NS	+	NS	+
Protease activity	NS	+	NS	+	+	-
Biofilm	NS	NS	NS	NS	NS	NS
Erythromycin	-	-	-	+	NC	+
Doxycycline	-	-	-	+	+	NC
Gentamycin	-	-	-	+	-	+
Ciprofloxacin	+	NC	-	NC	NC	+
Linezolid	NC	NC	-	+	NC	+
Vancomycin	-	-	-	+	NC	-
Gene had Mutations	*- gatD_1* (galacitol metabolism and glycolysis)	*- apt* (adenine metabolism and AMP production) *-trna (intergenic & deletions)* (protein synthesis and transcriptional regulator) *-ssl3* immune protectant	*-apt* (adenine metabolism and AMP production) *-trna (intergenic)* (protein synthesis and transcriptional regulator)	*-apt* (adenine metabolism and AMP production) *-fnbA* (bacterial adhesions and biofilm)	*-fnbA* (bacterial adhesions and biofilm) *-ebh* (bacterial adhesion)	

Notes: NS: Not applicable due to the absence of statistical significance, + : Greater effect/growth compared to control/parent strain, - : Lower effect/growth compared to control/parent strain. For the growth in the different antibiotics, the symbols depend on the visualisation of the data as a general effect, not the statistical analysis, and NC means no change.

Table 4-12: A summarised table for all changes that occurred in the six evolved strains resulting from the evolutionary experiment of *P. aeruginosa* with the continuous exposure to 1.25 mg/mL metformin

	Met-R1	**Met-R2**	**Met-R3**	**Met-R4**	**Met-R5**	**Met-R6**
Growth profile	+	-	NS	+	NS	NS
Protease activity	-	-	NS	+	+	+
Biofilm	NS	+	NS	NS	NS	-
Ciprofloxacin	+	NC	+	+	NC	NC
Gentamicin	+	NC	-	+	-	NC
Colistin	+	-	-	+	NC	NC
Ceftazidime	NC	NC	NC	+	NC	NC
Gene had Mutations	*-typA (intergenic)* protein synthesis *-mip (intergenic)* protein folding and bacterial virulence	*-acnM (intergenic)* citrate metabolism and TCA *-acdS* tolerating stressful environments *-argJ* arginine biosynthesis	*-acnM (intergenic)* citrate metabolism and TCA *- pntB* Controlling of redox and PMF	*-trpI* tryptophan regulatory protein *-acoR* acetoin regulatory protein	*-mexD* efflux pump	*-dsbD* electron transportation in cell membrane

Notes: NS: Not applicable due to the absence of statistical significance, + : Greater effect/growth compared to control/parent strain, - : Lower effect/growth compared to control/parent strain. For the growth in the different antibiotics, the symbols depend on the visualisation of the data as a general effect, not the statistical analysis, and NC means no change.

4.3. DISCUSSION

The continuous exposure of bacteria to sublethal doses of antimicrobial agents can lead to an increase in the tolerance of these bacteria and the evolution of multidrug-resistant strains (Kohanski et al., 2010). Therefore, it was crucial to investigate how bacteria responded to continuous exposure to one of the physiological concentrations of metformin, which was considered a sublethal concentration for both *P. aeruginosa* and *S. aureus* strains tested. It is reported that the metformin concentration in plasma ranges from 1-113 mg/L, with an average therapeutic concentration of 1-2 mg/L; however, it has been noted that the concentration of the drug is over 30-300 times higher in tissues such as the liver, intestine, and kidneys (J.-D. Lalau et al., 2011; Lee et al., 2021). Therefore, the concentration of 1.25 mg/mL was selected for the evolutionary experiment, which represents around 1/10 MIC for *P. aeruginosa* and ¼ MIC for *S. aureus*.

4.3.1. Characterisation of the metformin-exposed evolved populations growth profile

The evolutionary experiment with the two tested strains showed that the MIC of metformin did not change before and after the experiment for all drug-evolved population lines, remaining at 40 mg/mL for *P. aeruginosa* and 10 mg/mL for *S. aureus*. However, it is known that bacteria can adapt to the presence of antibiotics not by becoming typically resistant, but by becoming tolerant and persistent, which is reflected in their growth profiles. They may also tolerate bactericidal agents, even though their MICs did not change (Sulaiman & Lam, 2021). Therefore, dose-response growth curves were performed.

The results showed that two out of six evolved lines of *P. aeruginosa* exhibited improved growth in the presence of all tested concentrations of metformin compared to the control. For *S. aureus*, there was a a drug-exposed evolved line that grew better at one concentration tested (2.5 mg/mL). And for both species, the growth curve analysis showed the effect here was accelerated entry into and progression through the exponential phase rather than by increases in final biomass alone. This may indicate that metformin could select for an increase in antimicrobial tolerance by modifying the growth kinetics in bacteria to some extent, but in different patterns and strain dependence. This could align with a study that showed that continuous exposure of *E. coli* to sublethal concentrations of metformin in wastewater could induce antibiotic resistance due to chromosomal mutagenesis (Wei et al., 2022). And generally, there are some studies showed that the prolonged exposure to some antimicrobials could affect the cell divisions in the exponential phase without having a huge effect on the final biomass (Bertrand, 2019).

On the other hand, there was one evolved population of *P. aeruginosa* and other two populations of *S. aureus* that exhibited slower growth with extended lag phases and slower exponential growth, especially in the absence of the drug or low drug concentration, compared to their control. This could be explained by the fact that the mutations that arose in response to the stress caused a fitness cost to the mutated

strains. This can lead to a decrease in the growth rate compared to the parent strain, especially in the absence of the drug (Pal & Andersson, 2024).

As mentioned in Chapter 3, section 3.3.1, the combination of the AUC and growth-curve analysis was crucial for a more comprehensive understanding of the growth curves and the differences between the drug-evolved populations and their controls. This was evident in one of the *P. aeruginosa* lineages, where the evolved population exhibited reduced growth relative to the control during the exponential phase under metformin exposure, particularly towards the end of exponential growth, but recovered later and reached a comparable final optical density, with the curves overlapping and the final OD slightly exceeding that of the control. As a result, these differences were not reflected in the AUC analysis. In contrast, another evolved lineage showed a slight improvement in growth in the absence of metformin, detectable in the growth-curve analysis but not large enough to be detected with the AUC. This was also observed in one of the *S. aureus* evolved lineages. Together, these findings demonstrate that adaptation to metformin can affect the timing and rate of growth phases without necessarily altering total growth output.

4.3.2. Characterisation of the metformin-exposed evolved populations virulence factors

To assess any changes in the virulence factors, the protease activity of the evolved lines in the presence and absence of metformin was investigated. It was noted that metformin stress caused changes in the protease activity of the cells. Despite the protease activity in the absence of the drug not showing a significant difference compared to controls, there was a general trend of decrease in the metformin's effect on the inhibition of proteolytic activity on *P. aeruginosa* evolved lines compared to their controls. This occurred in three out of six of the evolved lines at different concentrations of metformin. One of these evolved lines was the same one that showed better growth in the growth profile. In *S. aureus,* three evolved lines had changes in proteolytic activity in the absence of the drug, and these were the same evolved lines that exhibited changes in their growth profile. In two of them, the change was an increase in protease activity. In one of those evolved lines, the effect of metformin was significantly less at low concentrations compared to its control. This could suggest that one of the adaptation mechanisms to the metformin stress was the increase in the production of protease, which is one of the virulence factors. This is aligned with the reported effect of the sub-inhibitory concentrations of antimicrobial peptides (Vasilchenko & Rogozhin, 2019). This was in contrast to what was found in other antibacterial agents like ciprofloxacin, where it is reported that the continuous usage of sub-inhibitory concentrations decreases the production of virulence factors, including protease (Ahmed et al., 2020). While there are not enough studies about the effect of continuous exposure of bacteria to metformin on protease activity, there is a paper that has studied its continuous use in an *in vivo* study on fish larvae, where it was shown that because of the continuous exposure of the bacteria in the larvae gut to metformin, there was an over-

expression of many virulence genes that are responsible of adhesions, toxins and lipases (Rogall et al., 2020), which supporting the findings of this study.

The crystal violet assay revealed that one of the *P. aeruginosa* evolved lines showed an increase in biofilm formation compared to its evolved lines in drug-free medium, which was the evolved lines that exhibited a decrease in growth and a decrease in protease activity. It is known that the exposure of the bacteria to continuous stress, like antibiotics, may induce phenotypic changes that can lead to a decrease in the metabolism inside the cells and change them to less active cells to adapt to the stress (Cabral et al., 2018). Therefore, this could explain the findings of this study where, one of the mechanisms to tolerate the stress due to continuous exposure to metformin was by entering a more dormant stage, indicated by increased biofilm formation and decreased active processes like growth and enzyme production. This is aligned with several studies in the literature that investigate the continuous exposure to different antibiotics. A study performed on *H. pylori* showed an increase in biofilm-like phenotype after exposure to levofloxacin and metronidazole (Krzyżek et al., 2024). Another study found that continuous exposure of *A. baumannii* to sub-inhibitory concentrations of ciprofloxacin and tetracycline leads to an increase in the formation of biofilm formation (Penesyan et al., 2019).

4.3.3. Characterisation of the metformin-exposed evolved populations susceptibility to different antibiotics

It was important to investigate any changes in the susceptibility of the evolved lines generated from both strains to various selected antibiotics. For *P. aeruginosa* evolved lines, the collective response of all evolved lines indicated an increased tolerance to sub-inhibitory concentrations of gentamicin, ciprofloxacin, and colistin. While analysing the data of individual evolved lines compared to their corresponding controls, it showed that primarily two evolved lines (Met-R1 and R4) demonstrated a decrease in susceptibility to these three antibiotics, particularly at sub-inhibitory concentrations. Interestingly, these two evolved lines were the same ones that exhibited a decrease in susceptibility to metformin in the growth profile analysis. For the *S. aureus* strain, one evolved line (Met-R4) displayed a reduction in susceptibility to erythromycin, doxycycline, linezolid, and vancomycin at sub-inhibitory concentrations, and it was also the evolved line that showed increased growth in the sub-inhibitory concentration of metformin. This could generate the hypothesis that the bacteria's strategy to tolerate continuous exposure to metformin stress might also lead to tolerance to other antibiotics to some extent. Some studies in the literature have found that continuous exposure to metformin may lead to cross-resistance with other antibiotic. the study by Wei *et al* (2022) that showed the up-regulation of the antibiotic efflux pumps in *E. coli* after continuous exposure to low concentrations of metformin explains the reduced susceptibility towards cefoxitin, ampicillin, cefazolin, azithromycin, and polymyxin B (Wei et al., 2022). Another study by Kim *et al* (2024) also showed the overexpression of the efflux pump

genes in the gut microbiome of diabetic patients taking metformin as an antidiabetic drug compared to the controls without metformin (Kim et al., 2024). Therefore, it was worth investigating the transcriptomic analysis of the two bacterial species and analysing the differential gene expression due to the exposure to metformin, which would be discussed in Chapter 5.

4.3.4. The genetic characterisation of the metformin-evolved populations

Following phenotypic characterisation, the genetic changes have been investigated through whole-genome sequencing. For *S. aureus*, there were five mutations found in the tested evolved lines. One of those mutations was in *fnbA* as an in-frame deletion in Met-R4 and R5. FbnA is an important protein that is involved in the formation of biofilm in *S. aureus* and helps in the adhesion of the cells and the virulence of the bacteria (Herman-Bausier et al., 2015). Despite being an in-frame deletion, it may have an effect on the function of the protein itself and the bacterial phenotype. This phenomenon has been identified in other genes, where it was found that the conserved in-frame deletion of *mtrB* in *M. tuberculosis* may affect the growth rate and can affect amikacin tolerance, though it does not cause a frame-shift in the protein reading frame (Park et al., 2025). In one study, the mutation of *fbnA* showed less affinity to elastin and fibrinogen binding (O'Neill et al., 2008). Therefore, the mutation of *fbnA* could affect the biofilm formation and the adaptation to metformin. As the biofilm results did not show any statistical significance, which may be a result of high experimental variations and a small number of replicates, which is one of the limitations of this study, it could not be confirmed whether this mutation affects the biofilm or not. But from the other phenotypic data, the mutation could lead to the decrease of biofilm that was reflectd on the increase in growth and protease.

In addition, there was a missense mutation in the *gatD* gene in one evolved line (Met-R1) of *S. aureus*, which encodes the NAD+-dependent galactitol dehydrogenase and plays an important role in the utilisation of galactitol within bacterial cells, forming metabolic intermediates that enter glycolysis (Nolle et al., 2017). Thus, the existence of the mutation due to continuous exposure to metformin may indicate that blocking this pathway could be beneficial for the adaptation of bacterial cells under stress. The hypothesis of this study is that metformin could affect the respiration and metabolic functions of the bacteria, and this finding may align with the hypothesis through modification of the metabolic pathway. A study on the continuous exposure of *Salmonella Typhimurium* to sub-inhibitory concentrations of ciprofloxacin found that it could lead to a mutation in *gatR,* the regulator of the *gat* operon, causing down-regulation of *gatD* and resulting in increased resistance of this evolved line (Chen et al., 2024).

Three different mutations were found in the *apt* gene in three evolved lines (Met-R2, R3, and R4) of *S. aureus*. The Apt enzyme plays an important role in the nucleotide salvage pathway, which is a more

energy-efficient way than the *de novo* synthesis of purines. It is known to help bacterial cells survive under stress. It has been reported that mutations in this gene, resulting from the evolutionary adaptation of *S. aureus* to nafcillin, lead to increased tolerance to antibiotics (Salazar et al., 2020). Additionally, it was found that the presence of these mutations could help *S. aureus* adapt to vancomycin by affecting cell wall metabolism (Lamichhane-Khadka et al., 2021).

Four mutations were found in the intergenic area between two tRNA genes in two evolved lines (Met-R2 and R3) of *S. aureus*, alongside greater structural variation in another intergenic area of tRNA genes (Met-R3). It is known that tRNA genes are important for protein translation and act as transcriptional regulators for some virulence genes (Koh & Sarin, 2018). A study on *E. coli* and the effects of continuous exposure to ciprofloxacin has revealed that exposure to sub-inhibitory concentrations of ciprofloxacin leads to oxidative stress. One of the bacterium's mechanisms to adapt involves modifications in the region near the tRNA genes, resulting in the overexpression of tRNA. This overexpression helps regulate protein synthesis, allowing the production of more proteins to repair the impaired components due to antibiotic stress (Fang et al., 2022). Therefore, this could explain the advantage of these mutations in adapting to metformin stress. On the other hand, upon investigating the structural variations that occurred in the genomes, it was found that there was a deletion of two other tRNA encoding genes in Met-R2. A study in *Burkholderia spp.* showed that the disruption of tRNA-Asp could lead to persistent cell formation as a response to ampicillin and meropenem stress, resulting in a decrease in the growth rate of this evolved line (Fang et al., 2022). That may explain the reduction of the growth profile of Met-R2 compared to its control, and that could be the explanation of the decrease in the AUC of the different antibiotics tested against this evolved line. In addition, the persisters are found to have less production of many virulence factors, adhesions, and immune factors (Huemer et al., 2021). In the same evolved lineof *S. aureus*, it was noticed that there was a large deletion in the *ssl3* gene, which encodes the staphylococcal super-like antigen 3. SSLs are important proteins for the bacteria to protect themselves from the host immune response through inhibition of cytokine production (Yokoyama et al., 2012). This could support the idea that this evolved line tends to enter the dormant stage as a response to the metformin stress, reducing energy-consuming processes like the production of SSL proteins.

In *P. aeruginosa*, there was a mutation downstream of the *typA* gene in Met-R1, which is known to play a role in the regulation of stress responses and some virulence factors in Gram-negative species like *E. coli, Salmonella spp.,* and *P. aeruginosa*. Additionally, it is important for biofilm formation and confers tolerance to various antibiotics (Neidig et al., 2013). However, literature indicates that intergenic mutations mainly affect downstream genes, not upstream ones (Mateus et al., 2021). In the same evolved line, there was another intergenic mutation upstream of the *mip* gene, which pertains to the *mipAB*

operon, recognised as significant in response to exposure to certain antibiotics like polymyxins by activating the associated efflux pump (Janet-Maitre et al., 2024). The third intergenic mutation was identified in two of the six evolved lines (Met-R2 and R3), downstream of *prpC* and upstream of *acnM*, which are part of the same *prp* operon that is vital for the degradation of propionate and its utilisation as a carbon source for energy production. Furthermore, it is known that metformin impacts energy production, suggesting that the regulation of those genes could be a possible bacterial adaptation to metformin stress.

In Met-R2, there is a mutation in *argJ*, which is important in arginine biosynthesis. A study performed on an *S. aureus* strain revealed that the *argJ* gene is crucial for the formation of the persistent form of the bacterium under antibiotic stress (Yee et al., 2020). As the mutation was in the coding sequence gene, this mutation could affect the activity of the ArgJ and the presister formation that could be increasing of its activity that may explain adaptation to metformin exposure, which aligns with the evolved line 's phenotypic properties and reduced growth.

Met-R3 had a mutation in the *pntB* gene, which is known for maintaining redox balance by preventing the excess presence of NADH and converting it to NADPH while functioning as a proton pump into the bacterial cell (Nikel et al., 2016). Therefore, this can be explained by the hypothesis of this study that metformin could cause redox imbalance by inhibiting the respiratory chain in mitochondria. If this gene were activated more, it would lead to a rebalancing of redox homeostasis in the bacteria.

There were two mutations in two transcriptional activators in Met-R4. One was for the activation of tryptophan biosynthesis, *trpI*. A study investigated the negative effect the mutation in *trpI* gene on the activation of *trpBA* genes that. Are responsible for tryptophan biosyntheis (Gao & Gussin, 1991). The other gene was a regulatory gene, *acoR* in *P. aeruginosa* PAO1, which activates acetoin catabolism by activating *acoAB* and converting it to acetyl-CoA, which then enters the TCA cycle to produce energy (Liu et al., 2018). However, upon the manual investigation of the *P. aeruginosa* strain, it showed the absence of those genes. This may indicate that the *acoR* gene regulates other gene sets that could be related to acetoin metabolism or something similar.

A mutation in the multidrug efflux pump gene *mexD* was identified in Met-R5, which is the part of the RND efflux pump, MexCD-OprJ. It is known that this efflux pump eliminates many antimicrobial agents and toxins from the cell. Despite there was no enough reported studies for the mutation in this efflux pump itself, there are some studies discovered mutations in the regulator of this pump, *nfxB*, that could enhance its activity in pumping out its substrates like triclosan antimicrobial and fluoroquinolones

(Chuanchuen et al., 2001; Monti et al., 2013). Though the exact mutation has not been mentioned in the literature, this could support the notion that one mechanism of adaptation to metformin involves increasing the expression of the efflux pump, aligning with published data regarding the effect of metformin on the overexpression of efflux genes in the gut microbiota (Kim et al., 2024).

A substitution mutation in *the dsbD* gene was found in Met-R6. DsbD is an important transmembrane protein that assists in proper protein folding by using an electron transport shuttle between the cytoplasm and periplasm. This function aids in producing functional proteins even under redox stress; consequently, *dsb*-deficient bacteria are less virulent (Łasica & Jagusztyn-Krynicka, 2007). Considering the effect of metformin on redox homeostasis in bacterial cells, he changes in the activity of this gene could provide another means of adaptation to metformin stress.

In conclusion, the continuous exposure of *P. aeruginosa* and *S. aureus* to low concentrations of metformin resulted in different adaptation mechanisms between the evolved lines. Some of the adapted bacteria had an increase in their growth and virulence like protease that reflected on the decrease the susceptibility of metformin and other antibiotics, and some may explain their adaptation by the formation of presister like cells that showed apparently decrease in their growth and tolerance towards antibiotic; however, this could be a prolonged growth with slower rate.

CHAPTER 5-

Further Molecular Mechanisms of Metformin Action in Bacteria

5. Further Molecular Mechanisms of Metformin Action in Bacteria

5.1. INTRODUCTION

Although clinical and cellular studies have described the effects of metformin in eukaryotic systems, its molecular mechanism of action in bacteria remains poorly defined. While several studies have reported that metformin can affect bacterial growth, metabolism, and the gut microbiota (Abbas et al., 2017; Wu et al., 2017), these observations provide limited insight into the underlying molecular targets and pathways involved. To date, there is insufficient information on how metformin inhibits bacteria and on its molecular targets. Therefore, following the phenotypic characterisation of metformin exposure and the analysis of adaptive responses arising during prolonged treatment in the previous chapters, it was crucial to investigate metformin's mechanism of action at the molecular level.

Transcriptomic analysis using RNA-seq was used to investigate gene expression changes associated with metformin exposure. This approach enables the identification of differentially expressed genes, affected metabolic and stress-response pathways, and the regulatory networks that could be linked to phenotypic adaptation to drug exposure, whether in the short or long term. This approach is efficient with large datasets of information linked to coding sequence regions, and it offers high sensitivity and genome-wide coverage, compared with other techniques (Croucher & Thomson, 2010). Therefore, RNA-seq was performed on the two strains tested in the previous chapter (*S. aureus* and *P. aeruginosa*) at high and low metformin concentrations. Additionally, one evolved line and its corresponding control from each strain were tested to investigate changes that occurred as an adaptive response to long-term metformin exposure.

In parallel, transposon mutagenesis using the TraDIS-Xpress approach was used to identify genes that contribute to bacterial fitness in the presence of metformin, thereby providing functional insight into genetic targets of tolerance or susceptibility. TraDIS-Xpress involves sequencing a high-density transposon library with an outward-facing promoter within the transposon. This design enables the identification of genes that are essential or conditionally essential under metformin exposure with reduced experimental complexity than the traditional method (Yasir et al., 2020). Therefore, the transposon library was constructed using the same *P. aeruginosa* strain as the other data to ensure comparability and was then exposed to different concentrations of metformin, providing a comprehensive view of gene–drug interactions and offering additional mechanistic insight into how metformin works in bacteria.

In eukaryotic cells, metformin is well established as an inhibitor of mitochondrial respiratory chain Complex I, thereby reducing oxidative phosphorylation and altering cellular energy balance (Luengo et

al., 2014). Given the close relationship between mitochondria and the respiratory electron transport chain in bacteria (Andersson et al., 1998), it has been hypothesised that metformin may similarly interfere with bacterial respiratory components. However, experimental evidence supporting this hypothesis in bacterial systems remains limited, and the extent to which bacterial electron transport chains are direct targets of metformin is still unclear. Therefore, the effect of metformin on bacterial respiration was examined using Mitoplates and a Biolog system against the different bacterial species used in Chapter 1, enabling comparative analysis with established mitochondrial respiratory inhibitors and direct assessment of respiratory chain activity to see the different pattern of the metformin activity and the interaction on the different bacterial species.

Together, these approaches were integrated to address the existing knowledge gap on the molecular basis of metformin's action in bacteria and to link phenotypic adaptation with transcriptional regulation, gene essentiality, and respiratory function.

5.2. RESULTS:

5.2.1. The transcriptomic analysis of the RNA-seq data

5.2.1.1. Detection of the effect of metformin on differential gene expression (DGE)

5.2.1.1.1. Detection of the effect of metformin on DGE compared to no drug in P. aeruginosa:

The differential expression analysis of the *P. aeruginosa* ATCC 27853 parent samples in the presence of 1.25 mg/mL of metformin compared to the control showed no significant difference. The samples exposed to 10 mg/mL metformin showed significant upregulation of 24 genes (Figure 5-1). Of particular note are upregulated genes in the *arn* operon with logFC 1.7-2.1 (*arnA, arnB, arnC_2, arnD and arnT_2*), which is responsible for modifying the lipid A part of the lipopolysaccharides of the cell membrane (Lo Sciuto et al., 2020). Another overexpressed gene, *rkpK* gene that involves in the lipopolysaccharide biosynthesis. Another operon containing several overexpressed genes was the *puu* operon with logFC 1.7-2.2, including *puuA, puuB* and *puuP*, which is important in utilizing putrescine, a polyamine compound, as a carbon and nitrogen source (Chou et al., 2008). GO enrichment analysis mapped seven genes to the database and revealed that the overexpressed genes were involved mainly in glutamine and asparagine metabolic and biosynthetic processes (Figure 5-2and Figure 5-3). For further investigation of the pathways, KEGG analysis was used and resulted in 16 mapped overexpressed genes (Figure 5-4). It showed that all the genes in *arn* operon are responsible for cationic antimicrobial peptide resistance. Also, *asnB*, *glnA* and *puuA* are involved in aspartate, glutamate, arginine and nitrogen metabolism. In addition, it was revealed that *mexC*, *mexD*, *oprJ*, *smvA* and P_02711 (*emrE*) represent multi-drug resistant efflux pumps with the highest logFC among all the genes, which was around 3-4.5 after exposure to metformin comparing to no drug. The *emrE* gene is a putative gene for efflux pump

which was not annotated using the used annotator (Prokka), so it was presented as locus tag then it was found with the further annotation for KO annotations.

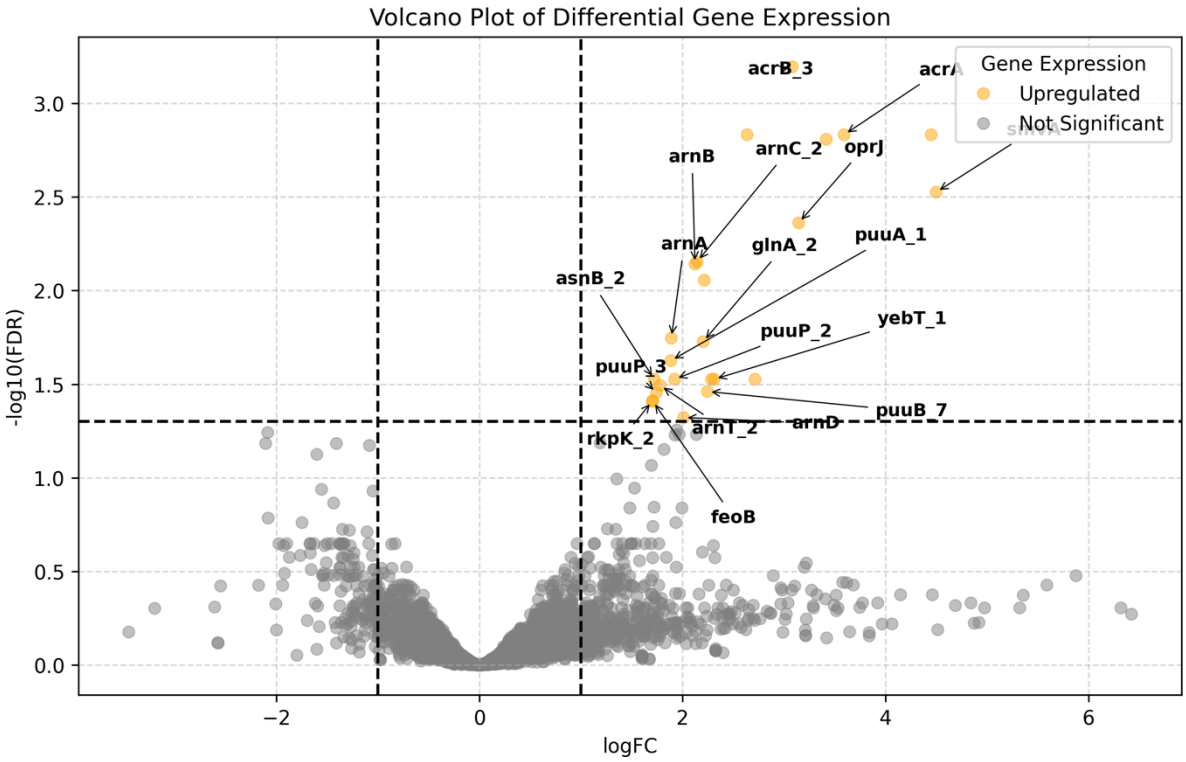

Figure 5-1: Volcano plot showing the differential expression gene analysis upon the exposure of *P. aeruginosa* ATCC 27853 to 10 mg/mL of metformin.
The significantly changed genes with false discovery rate (FDR) ≤ 0.05 and log fold of change (logFC) ≥ |1| indicated by dashed lines on the y and x axes respectively. The significantly upregulated genes are represented in yellow, and the non-significant ones in grey. The highlighted genes are all the significant genes excluding the hypothetical proteins. The experiment was done with three biological replicates (n=3).

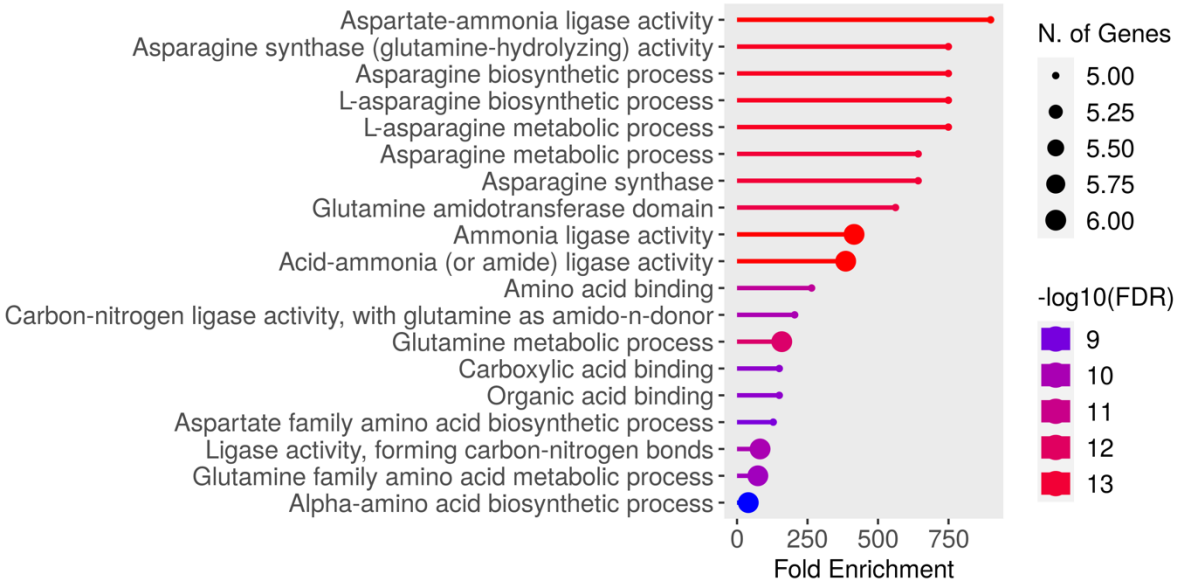

Figure 5-2: Lollipop plot showing the enrichment analysis in GO terms of the seven mapped upregulated genes in *P. aeruginosa* ATCC 27853
The red indicates highly significant enrichment, and blue indicates a less significant one. The head size of the lollipop shows the number of genes involved in the analysis.

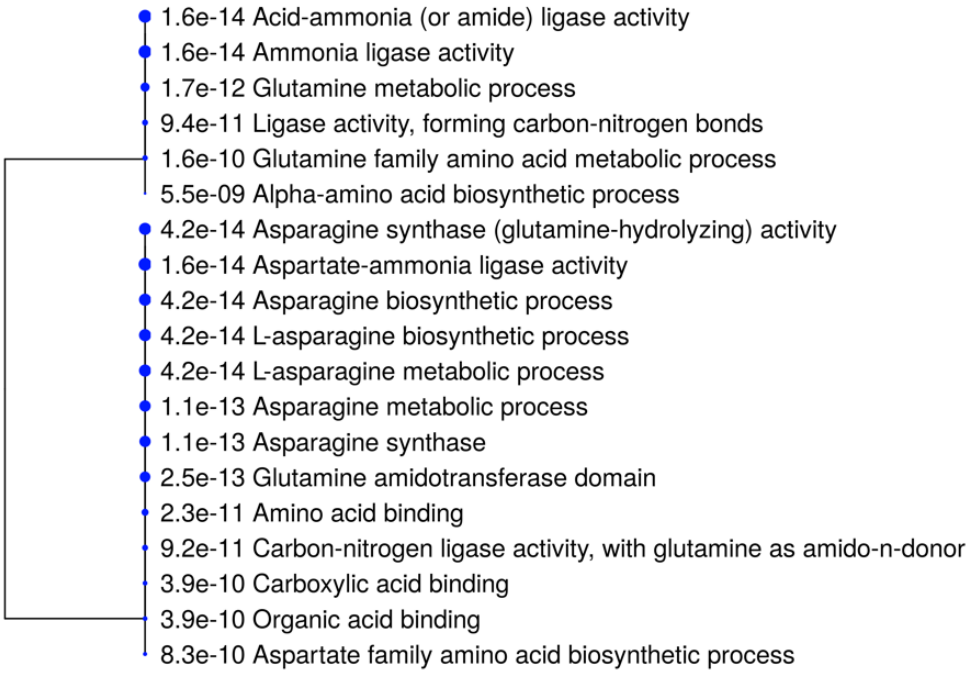

Figure 5-3: Tree plot showing the relation between the different pathways in GO terms involved in the seven mapped overexpressed genes of *P. aeruginosa* ATCC 27853.
The larger the circle next to each term, the higher the significance according to their p values next to them

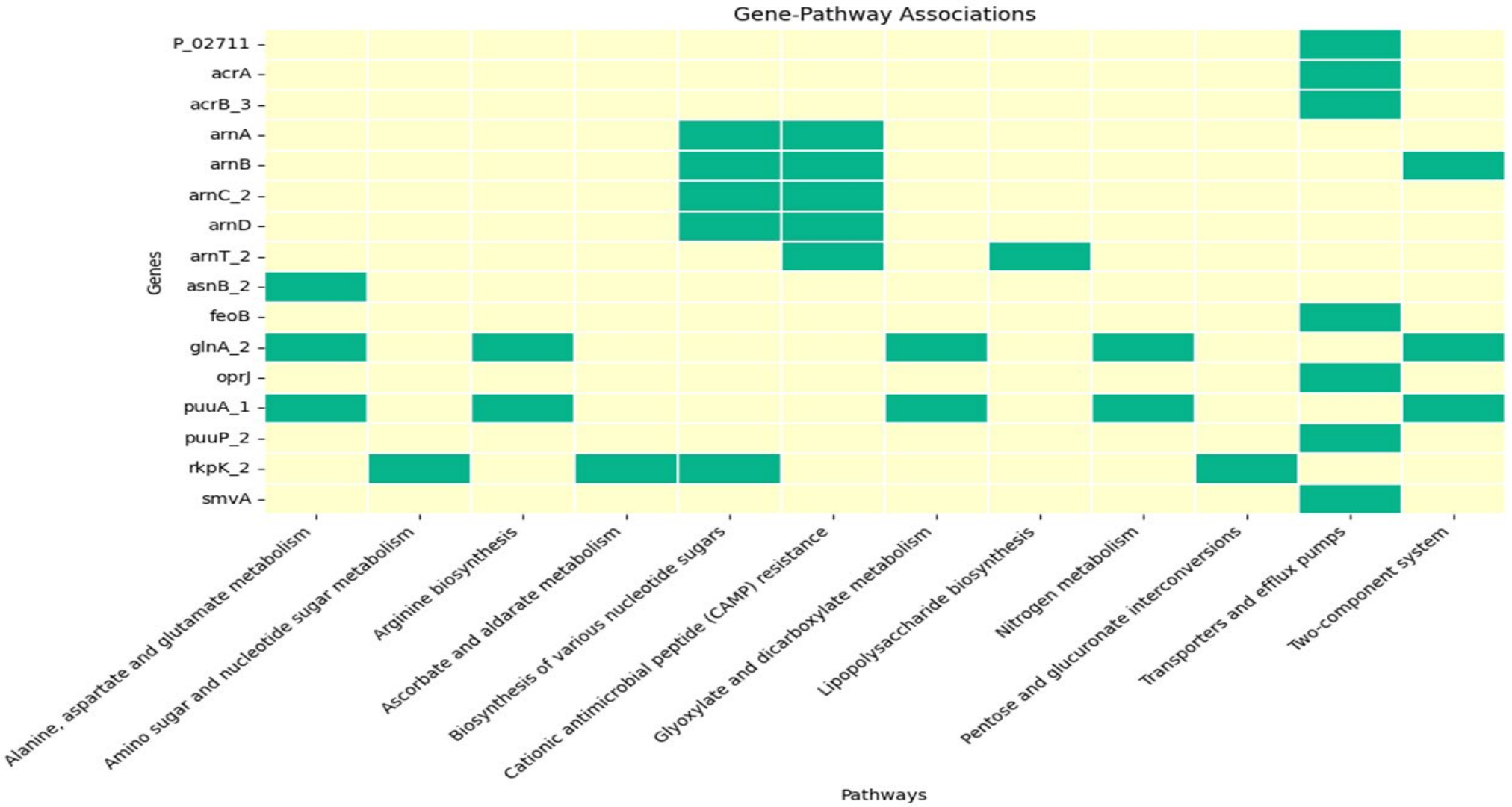

Figure 5-4: Illustration showing the gene-pathway associations of the 16 mapped overexpressed genes of *P. aeruginosa* ATCC 27853 upon analysis using the KEGG database.
The green blocks show the presence of the gene (y-axis) in the corresponding pathways (x-axis).

5.2.1.1.2. Detection of the effect of metformin on DGE compared to no drug in S. aureus:

The DGE analysis for the parent samples of *S. aureus* NCTC 6571 showed no difference upon exposure to a concentration of 1.25 mg/mL of metformin, as seen with *Pseudomonas* above. However, 270 genes were upregulated, and 344 genes were downregulated due to exposure to 5 mg/mL of metformin (Figure 5-5). To detect the most prominent pathways involved, the overexpressed genes were analysed using ShinyGO and 87 of them were matched to the GO database for enrichment analysis. It was revealed that the main pathway involved is nitrogen compound metabolism, which includes 66 genes and is linked to other pathways like organic cyclic compound metabolism (Figure 5-6and Figure 5-7). The genes then underwent KEGG analysis to identify specifically which biochemical pathways are involved (Figure 5-8). Notably, a significant number of genes are involved in amino acid metabolism, primarily histidine (the *his* operon containing *hisF*, *hisG*, and *his*Z genes, along with the *hisS* gene, which is responsible for histidine-tRNA ligase, an important enzyme in loading histidine onto t-RNA). Similarly, genes related to tryptophan were also overexpressed, including the *trp* operon (*trpA*, *trpB,* and *trpF)*. Furthermore, another group of genes involved in the metabolism of cofactors and vitamins included biotin biosynthesis genes in the *bio* operon (*bioD*, *bioK*, P_00755 (*bioF), and bioW*, which are responsible for biotin production, along with *bioY*, which acts as a biotin transporter), as well as the *birA* gene, known as a repressor of the *bio* operon, *bioY* and the *yhfS* gene that plays role in fatty acid synthesis, and was also overexpressed after exposure to metformin. (Satiaputra et al., 2018). Additionally, there was significant upregulation in both the large (*rplA*, *rplR*, *rplT*, *rplU*) and small (*rpsN2*, *rpsQ*) ribosomal proteins responsible for protein synthesis. It was also noted that the *mecA* gene, responsible for methicillin resistance in *Staphylococcus* spp, was upregulated as well. Also, it was noticeable that the *mprAEF* genes encoding the Na(+)/H(+) antiporter get upregulated.

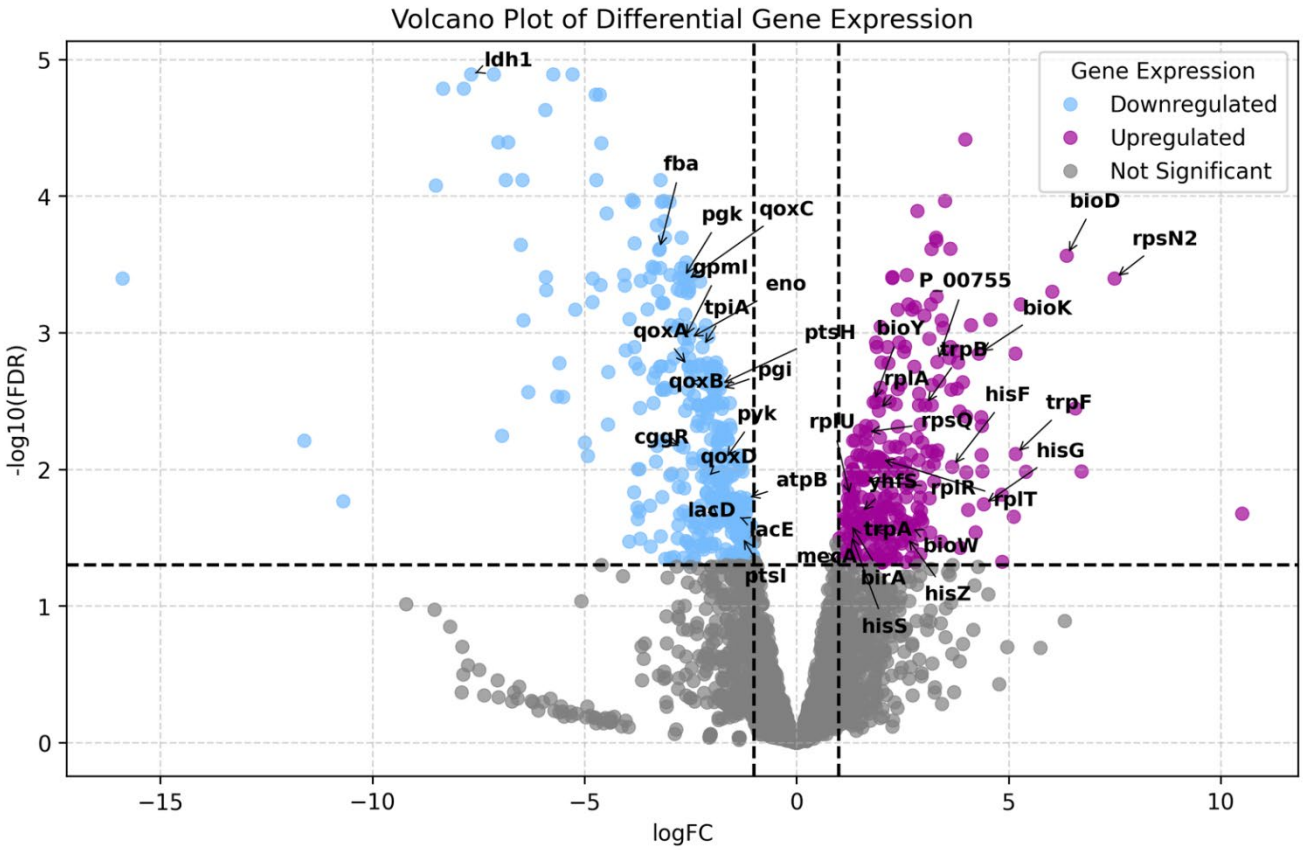

Figure 5-5: Volcano plot showing the differential expression gene analysis upon the exposure of S. aureus NCTC 6571 to 5 mg/mL of metformin.
The significantly changed genes with false discovery rate (FDR) ≤ 0.05 and log fold of change (logFC) ≥ |1| indicated by dashed lines on the y and x axes, respectively. The significantly upregulated genes are represented in purple, the downregulated ones in light blue and the non-significant ones in grey. The highlighted genes are the selected genes further analysed and interpreted.

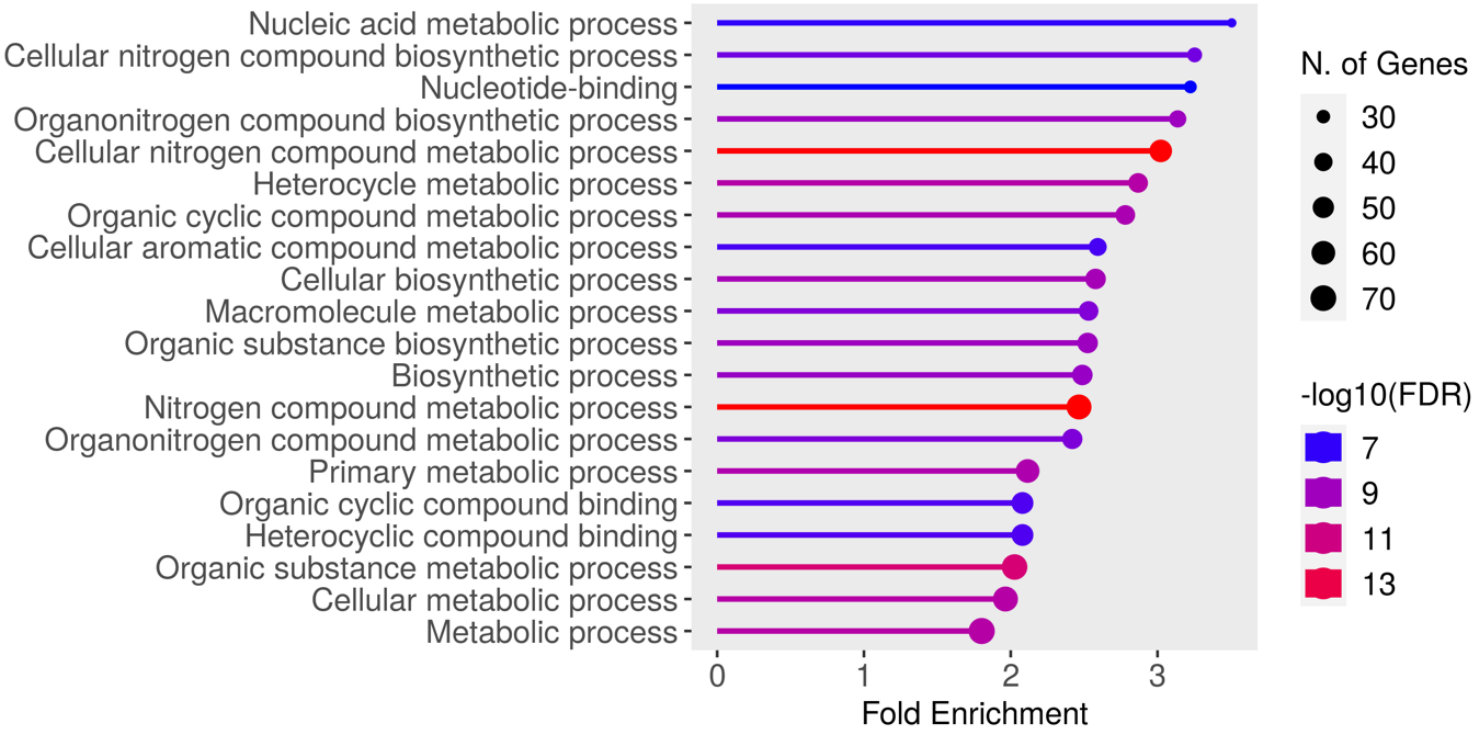

Figure 5-6: Lollipop plot showing the enrichment analysis in GO terms of the 87 mapped upregulated genes in *S. aureus* NCTC 6571.
Red indicates highly significant enrichment, and blue indicates a less significant one. The head size of the lollipop shows the number of genes involved in the analysis.

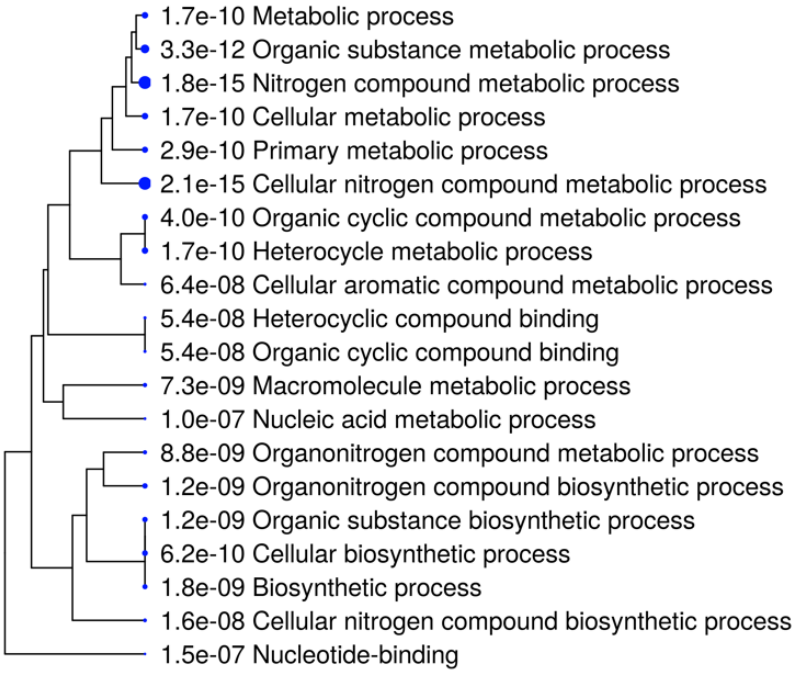

Figure 5-7: Tree plot showing the relation between the different pathways in GO terms involved in the 87 mapped overexpressed genes of *S. aureus* NCTC 6571.
The larger the circle next to each term, the more significant one.

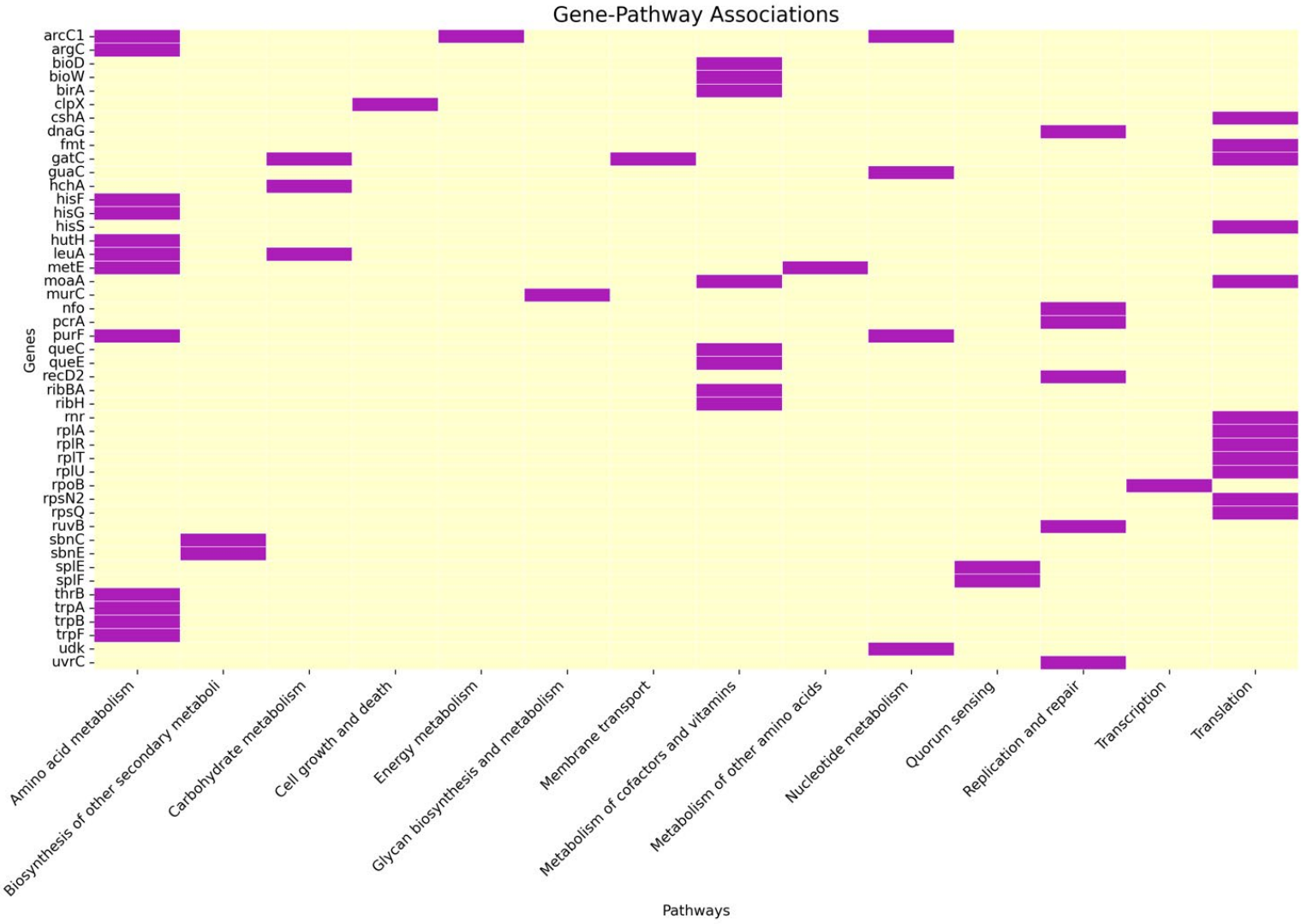

Figure 5-8 : Illustration showing the gene-pathways associations of the selected overexpressed genes of *S. aureus* NCTC 6571 upon the analysis using the KEGG database.
The purple blocks show the presence of the gene (y-axis) in the corresponding pathways (x-axis).

To detect the most prevalent pathways the downregulated genes belong to, GO enrichment analysis was performed, where 110 genes were mapped to the GO database (Figure 5-9 and Figure 5-10). By focusing on the highly significantly enriched (according to the p values), more specific pathways (rather than the general ones), it was revealed that the downregulated genes were mainly associated with energy production through ATP metabolism, glycolysis and phosphorylation. There were 30 genes in these pathways, so for further understanding of the relationships between these, they were mapped to the KEGG database (Figure 5-11). The main pathways of the downregulated genes were carbohydrate and energy metabolism. The first group of genes is the *pts* genes (*ptsG, ptsH, ptsI*), which are the first step in glycolysis by phosphorylation of glucose to glucose-6-phosphate. Then, the *pgi* gene converts glucose-6-phosphate to fructose-6-phosphate. Following this, the *pfk* gene is responsible for fructose bisphosphate. Then, the *fba* gene converts this to glyceraldehyde phosphate. The next set of identified genes represents the glycolytic operon, which consists of *tpiA, gapA, pgk, eno,* and *gpmI*, which are important to complete glycolysis and formation of the high-energy compound phosphoenolpyruvate

(PEP). The *pyk* gene converts PEP to pyruvate and generates ATP (Yamamoto et al., 2012). Furthermore, the *pdhA* and *pdhB* genes, which encode the pyruvate dehydrogenase enzyme complex that converts pyruvate into acetyl-CoA, were downregulated. In addition to the *cggR* gene, which is the regulatory gene for this operon. Furthermore, the presence of metformin leads to the downregulation of some genes of the *lac* operon (*lacC* and *lacD*), which are responsible for lactose metabolism, and *lacE,* which is responsible for the transportation of lactose inside the bacterial cell. Also, *ldh1* was downregulated, which is codes for the lactate dehydrogenase enzyme that converts lactate to pyruvate. It was noticeable that amongst the downregulated genes was the *qoxABCD* operon, which encodes quinol oxidases that are important in aerobic respiration. Along with that is the *atpB* gene, which encodes for ATP synthase, a crucial enzyme for ATP production. Also, the *ndhB* gene was downregulated which encodes for one of the subunits of the type I NADH dehydrogenase.

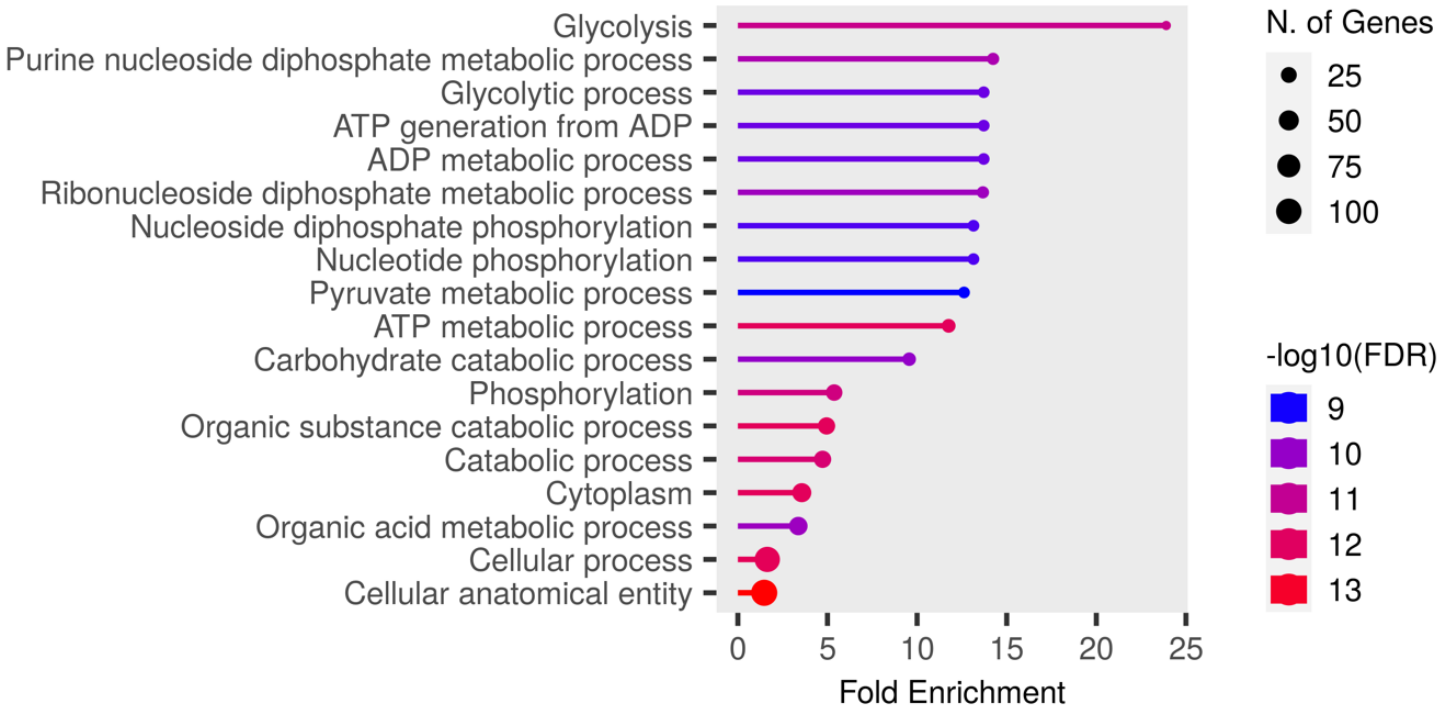

Figure 5-9: Lollipop plot showing the enrichment analysis in GO terms of the 110 mapped downregulated genes in *S. aureus* NCTC 6571.
Red indicates highly significant enrichment, and blue indicates a less significant one. The head size of the lollipop shows the number of genes involved in the analysis.

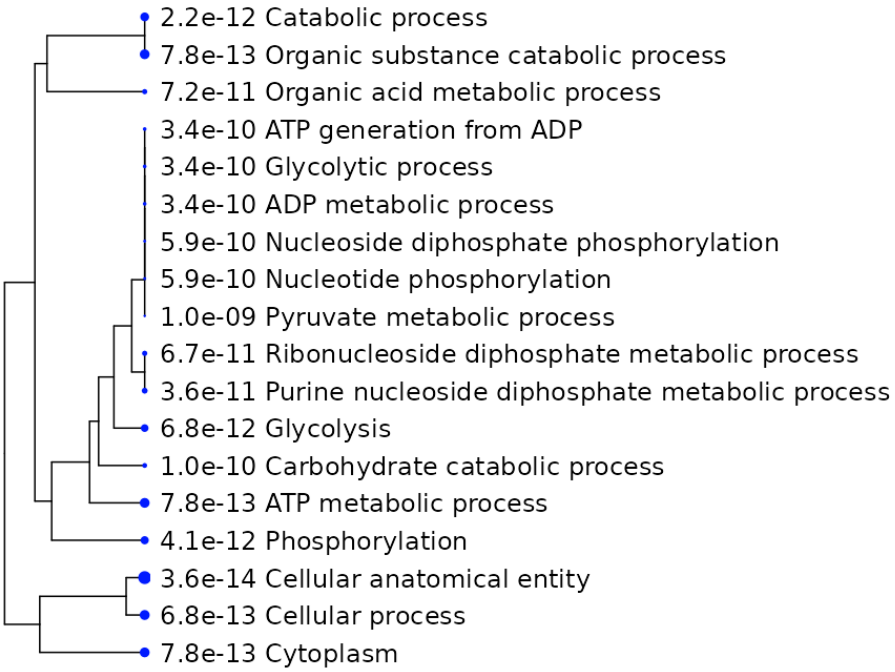

Figure 5-10: Tree plot showing the relation between the different pathways in GO terms involved in the 110 mapped downregulated genes of *S. aureus* NCTC 6571,
The larger the circle next to each term, the more significant one.

Figure 5-11: Illustration showing the gene-pathways associations of the selected downregulated genes of *S. aureus* NCTC 6571 upon the analysis using the KEGG database.
The purple blocks show the presence of the gene (y-axis) in the corresponding pathways (x-axis).

5.2.1.2. Detection of changes in differential gene expression (DGE) in metformin-evolved populations from the evolutionary experiment

5.2.1.2.1. Detection of the changes in the DGE of the metformin-evolved populations from the evolutionary experiment compared to the parent without the drug:

5.2.1.2.1.1 Detection of the changes in the DGE of the metformin-evolved populations from the evolutionary experiment compared to the parent without the drug in P. aeruginosa:

For the *P. aeruginosa* ATCC 27853, the DGE of Met-R4 samples was analysed in the absence of metformin compared to the parent samples, and no significant change was found between them.

5.2.1.2.1.2 Detection of the changes in the DGE of the metformin-evolved populations from the evolutionary experiment compared to the parent without the drug in S. aureus:

For *S. aureus* NCTC 6571, the DGE of Met-R3 samples was analysed in the absence of metformin compared to the parent samples (Figure 5-12). It was found that two genes of the *deo* operon (*deoB and deoC*), which are responsible for encoding the enzymes for nucleotide metabolism and using them as a carbon and energy source, were significantly upregulated in the evolved strain compared to the parent one. On the other hand, the evolved strains showed downregulations in *hlgB* and *hlgC,* which are responsible to form the γ-hemolysin toxin active complex BC. Another gene that got downregulated was *wbpI*, which represents nucleotide sugar biosynthesis. The final gene was *brnF*, which is responsible for the transporting of the branched-chain amino acids.

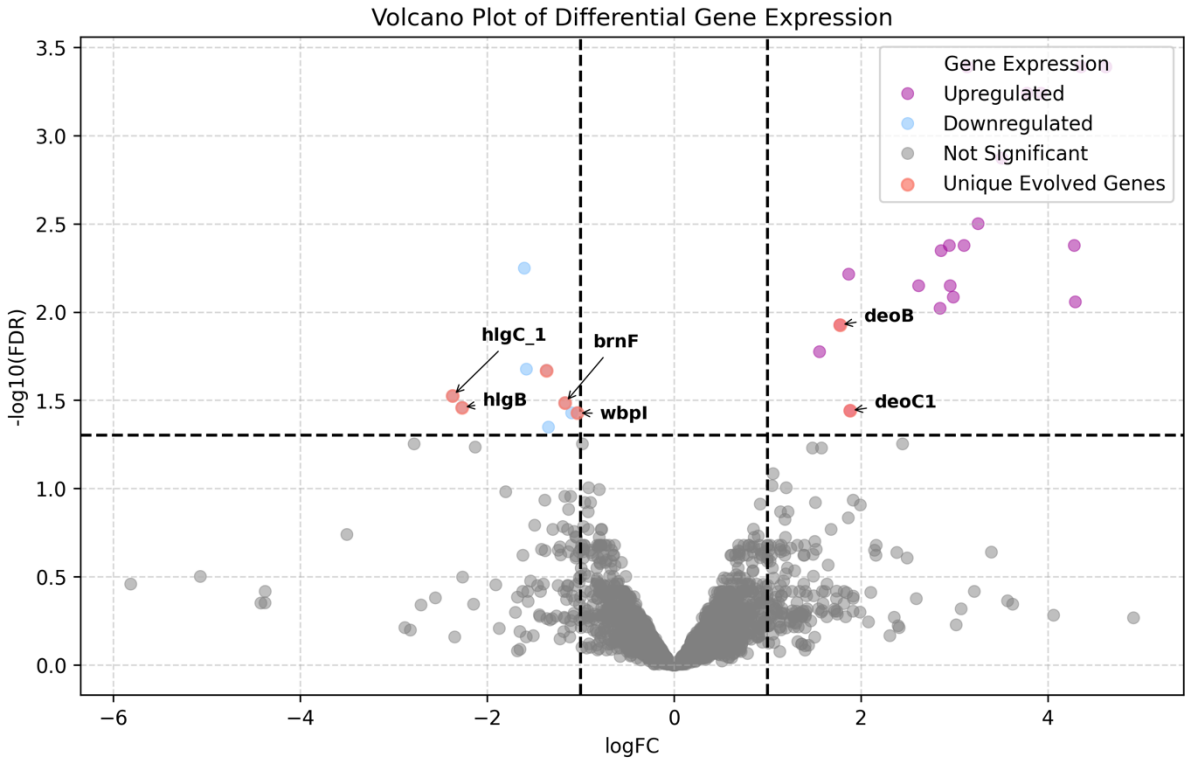

Figure 5-12: Volcano plot showing the differential expression gene analysis of Met-R3 from the evolutionary experiment of *S. aureus* NCTC 6571 compared to its parent.
The significantly changed genes with false discovery rate (FDR) ≤ 0.05 and log fold of change (logFC) ≥ |1| indicated by dashed lines on the y and x axes, respectively. The significantly upregulated genes are represented in purple, the downregulated ones in light blue, the non-significant ones in grey and the unique genes presented in the evolved strain and not in control in orange. The highlighted genes are all the significant genes excluding the hypothetical proteins. The experiment was done with three biological replicates (n=3).

5.2.1.2.2. Detection of the changes in the DGE of the metformin-evolved populations from the evolutionary experiment after exposure to metformin compared to the parent:

5.2.1.2.2.1 Detection of the changes in the DGE of the metformin-evolved populations from the evolutionary experiment after exposure to metformin compared to the parent in P. aeruginosa:

The comparison of the DGE of the samples of Met-R4 of *P. aeruginosa* ATCC 27853 in the presence and absence of 10 mg/mL metformin, compared to the DGE of the parent samples, revealed that there were two genes of the *arn* operon (*arnF* and *arnE)* that are overexpressed uniquely in the evolved strains and not the controls. In addition, *pyrC* was upregulated in the evolved strain as well, which plays a role in pyrimidine metabolism (Figure 5-13). It was noticeable that the genes representing the multi drug-resistant efflux pump *mexC*, *mexD* and *oprJ* did not get upregulated in the evolved strain upon exposure to metformin compared to what happened in the parent strain.

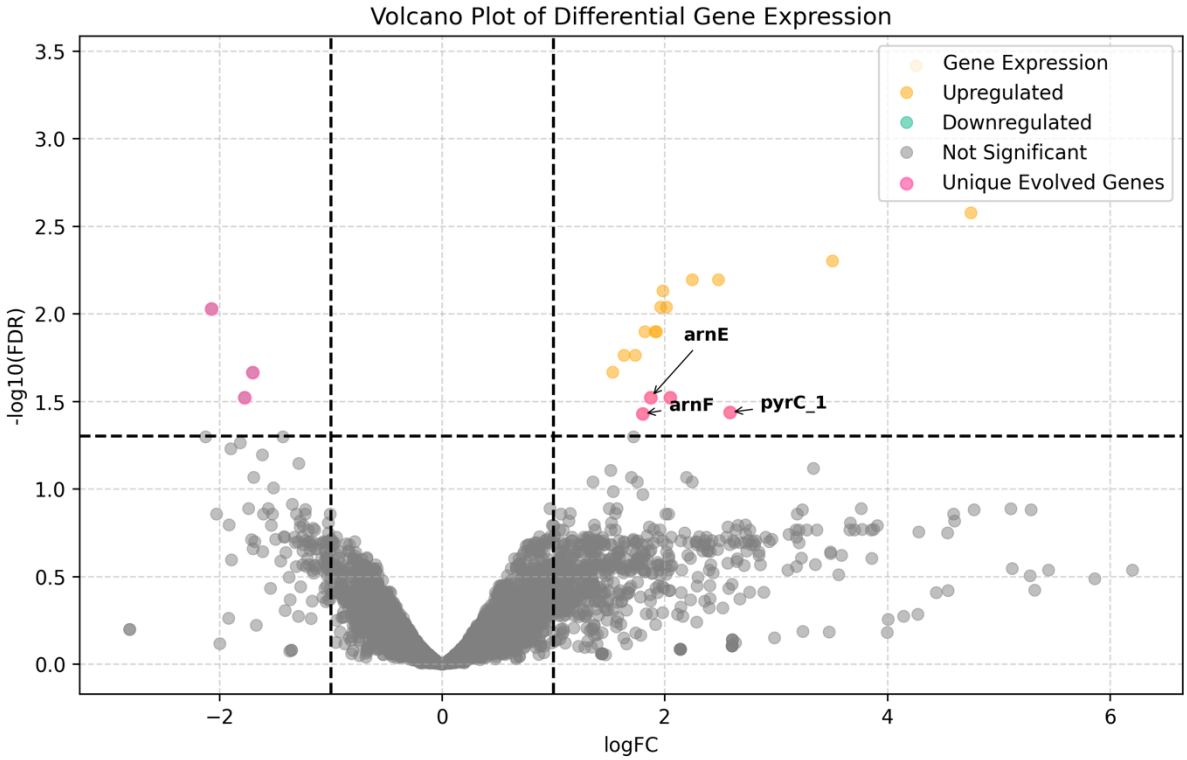

Figure 5-13: Volcano plot showing the differential expression gene analysis of Met-R4 from the evolutionary experiment of *P. aeruginosa* ATCC 27853 in the presence and absence of 10 mg/mL metformin.
The significantly changed genes with false discovery rate (FDR) ≤ 0.05 and log fold of change (logFC) ≥ |1| indicated by dashed lines on the y and x axes, respectively. The significantly upregulated genes are represented in yellow, the non-significant ones in grey, and the unique genes presented in the evolved strain compared to the parent strain and not in the control in pink. The highlighted genes are all the significant genes excluding the hypothetical proteins. The experiment was done with three biological replicates (n=3).

5.2.1.2.2.2 Detection of the changes in the DGE of the metformin-evolved populations from the evolutionary experiment after exposure to metformin compared to the parent in S. aureus:

The comparison of the DGE of Met-R3 samples of *S. aureus* NCTC 6571 in the presence and absence of 5 mg/mL metformin compared to the parent strain revealed that 85 genes were overexpressed and 86 genes were downregulated (Figure 5-14). For the upregulated genes, two other genes of the *trp* operon (*trpE* and *trpG*) were noticed, besides the other genes in the operon, in the parent samples. Also, only *hisG* from *his* operon that got overexpressed as in the parent strain, but no significant change in the rest of the genes. There was no significant change in the expression of *birA* and *yhfS* genes relating to biotin metabolism. For further analysis of the upregulated genes, GO enrichment analysis was performed, but did not identify significantly enriched pathways with an FDR cut-off of 0.05. After performing KEGG analysis (Figure 5-15), 21 genes were mapped to the database. It was noticed that *bceA* was overexpressed in the evolved strain, which an ABC transporter that is responsible for encoding the bacitracin efflux pump. Another ABC transporter is *potA,* which plays a role in the transport of polyamine compounds like putrescine. Furthermore, *gatD* was upregulated, which is responsible for galactitol 1 phosphate 5 dehydrogenase which is responsible for the metabolism of galactitol.

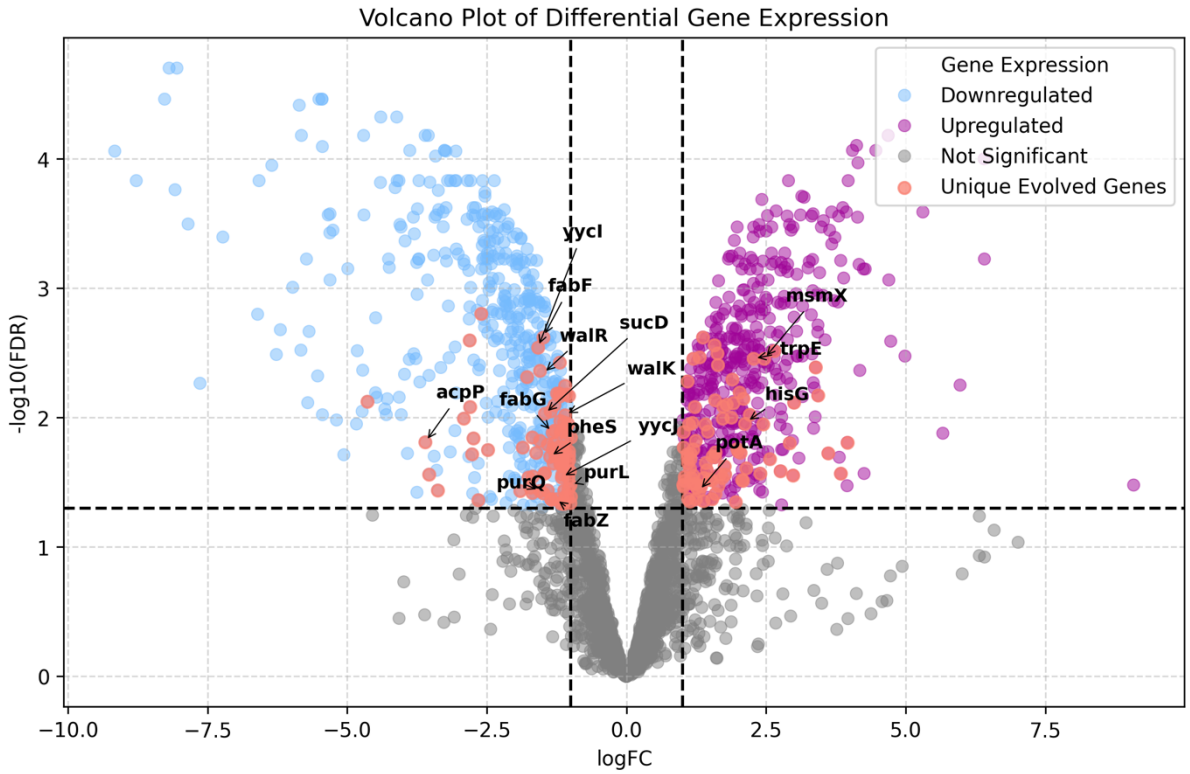

Figure 5-14: Volcano plot showing the differential expression gene analysis of Met-R3 from the evolutionary experiment of *S. aureus* NCTC 6571 in the presence and absence of 5 mg/mL metformin.
The significantly changed genes with false discovery rate (FDR) ≤ 0.05 and log fold of change (logFC) ≥ |1| indicated by dashed lines on the y and x axes, respectively. The significantly upregulated genes are represented in purple, the downregulated ones in light blue, the non-significant ones in grey and the unique genes presented in the evolved strain and not in control in orange. The highlighted genes are selected significant genes. The experiment was done with three biological replicates (n=3).

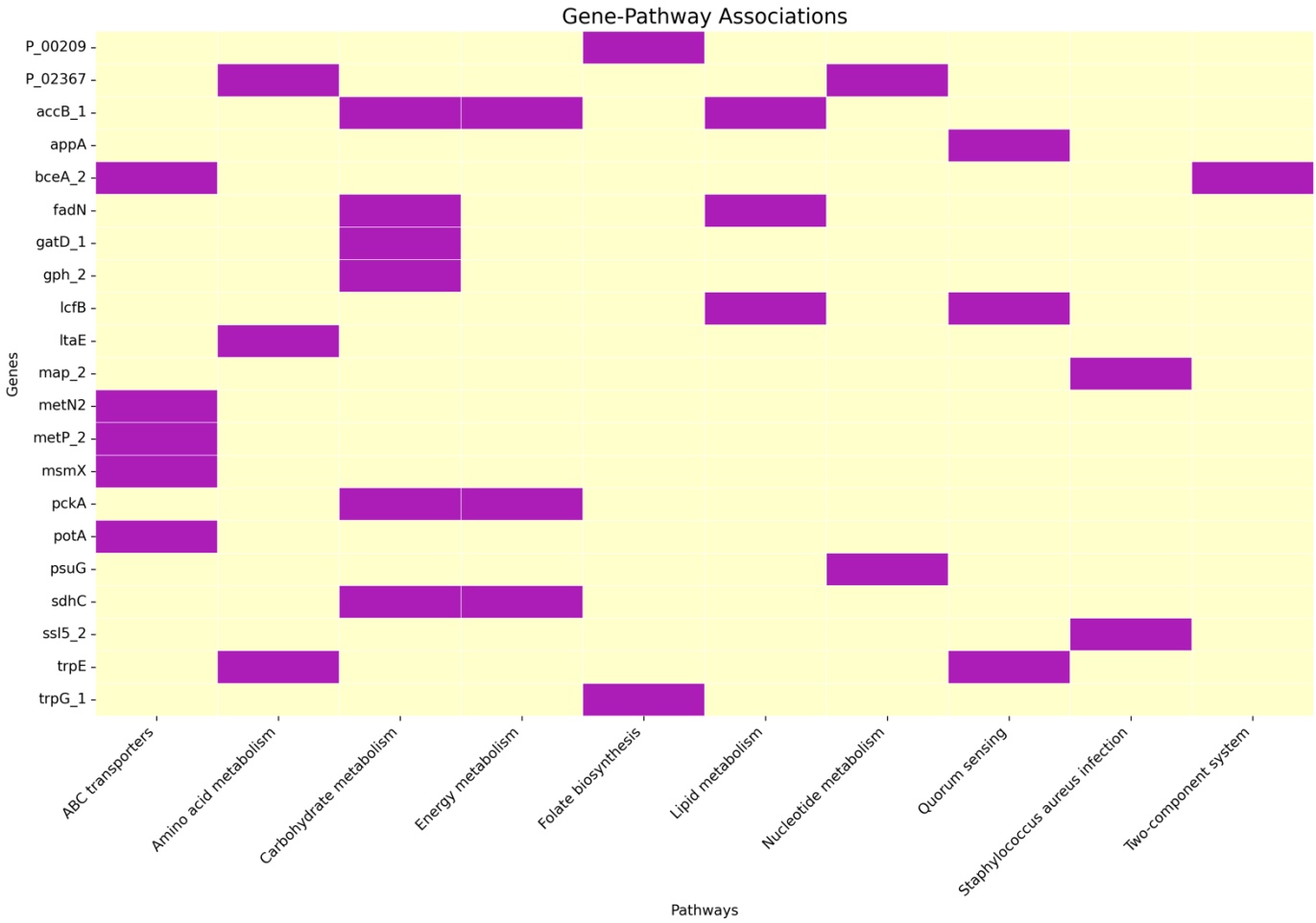

Figure 5-15: Illustration showing the gene-pathways associations of the selected upregulated genes of Met-R3 from the evolutionary experiment of *S. aureus* NCTC 6571 compared to its parent upon the analysis using the KEGG database.
The purple blocks show the presence of the gene (y-axis) in the corresponding pathways (x-axis).

For the downregulated genes, it was noticed that *cggR* and *atpB* were not changed upon the exposure to metformin compared to what happened in the parent strain, but the rest of the glycolytic genes were downregulated like in the parent strain. Also downregulated was the *agrA* gene, which is an important part of the accessory gene regulator (agr) system that acts as a quorum-sensing system that regulates the expression of the virulence factors. For further investigation, 27 genes were mapped to the GO database for the enrichment analysis (Figure 5-16 and Figure 5-17). It was revealed that exposure of the evolved strain to metformin uniquely caused a decrease in the highly enriched pathways of lipid and oligosaccharide biosynthetic processes and ribonuclease activity. For deeper analysis, these 27 genes were analysed using the KEGG database (Figure 5-18). It was noticed that *sucD*, which encodes an important enzyme in the TCA was downregulated. Also downregulated were *purQ* and *purL* that encode phosphoribosylformylglycinamidine synthase, which is a crucial enzyme in purine metabolism involved in DNA synthesis and energy production. Part of the *fab* gene cluster, including *fabF, fabG, and fabZ,* were downregulated, which are responsible for fatty acid biosynthesis. Also, it was noticed that *acpP*

plays a crucial role in the biosynthesis relating to the *fab* operon by encoding the acyl carrier protein that carries the fatty acids building blocks and is located next to the *fab* genes, forming the *fab-acpP* locus (My et al., 2013). Furthermore, there was downregulation in the *walK* gene along with its partner *walR,* which together form the two-component system WalKR that plays a role in cell wall metabolism and biofilm formation. In addition, it was noticed that there is a downregulation in *yycI,* which is the regulator of the WalKR system, as it causes its activation to work. Another gene from *yyc* operon, *yycJ,* that plays role in biofilm formation as well, was downregulated. Also, the *map* gene is responsible for encoding the Map protein that plays a role in cell adhesions and infection. Additionally, *pheS* got downregulated after exposure to metformin, where it encodes enzyme phenylalanyl-tRNA synthetase that is important in protein synthesis and cell growth.

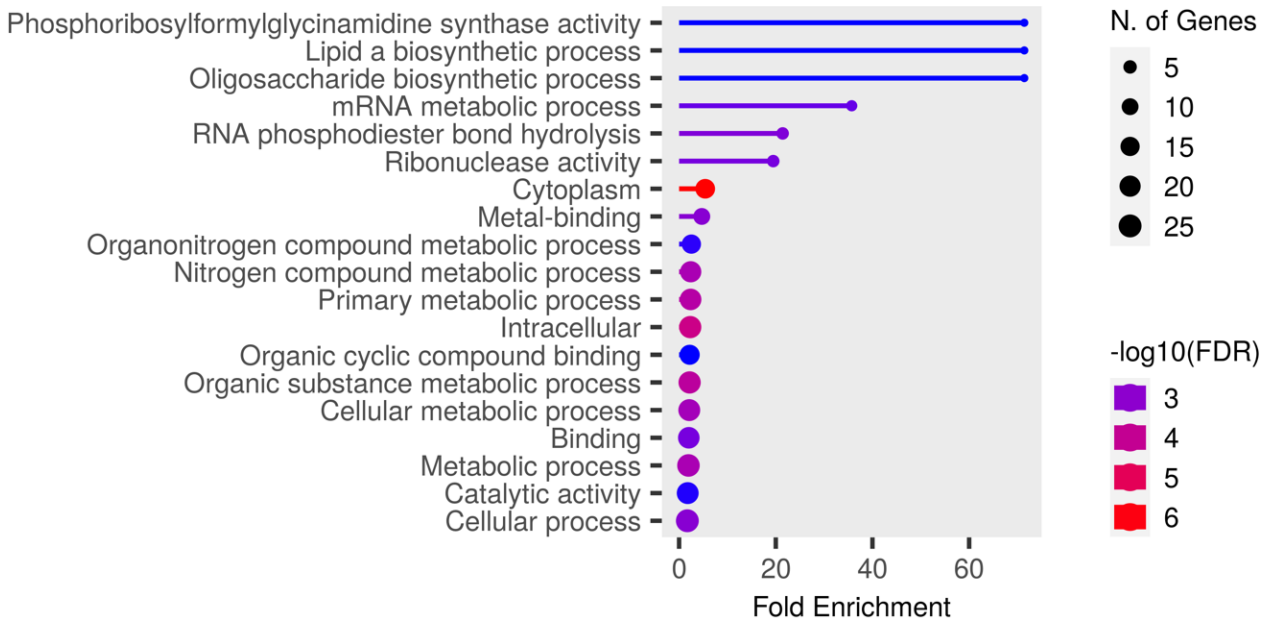

Figure 5-16: Lollipop plot showing the enrichment analysis in GO terms of the 27 mapped downregulated genes in Met-R3 from the evolutionary experiment of *S. aureus* NCTC 6571 compared to its parent.
Red indicates highly significant enrichment, and blue indicates a less significant one. The head size of the lollipop shows the number of genes involved in the analysis.

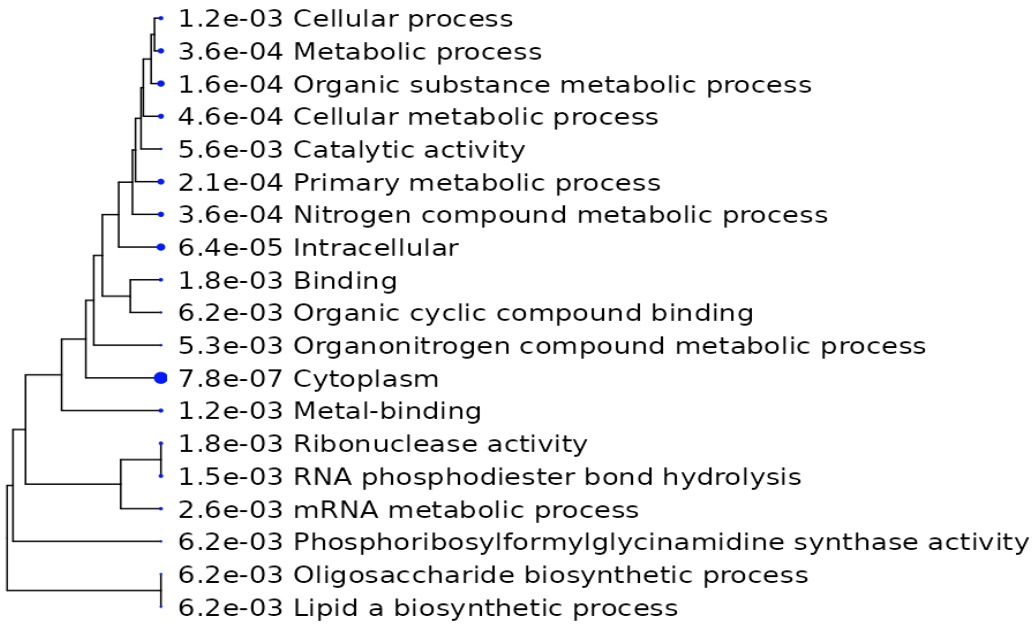

Figure 5-17: Tree plot showing the relation between the different pathways in GO terms involved in the 27 mapped downregulated genes in Met-R3 from the evolutionary experiment of *S. aureus* NCTC 6571.
The larger the circle next to each term, the more significant one.

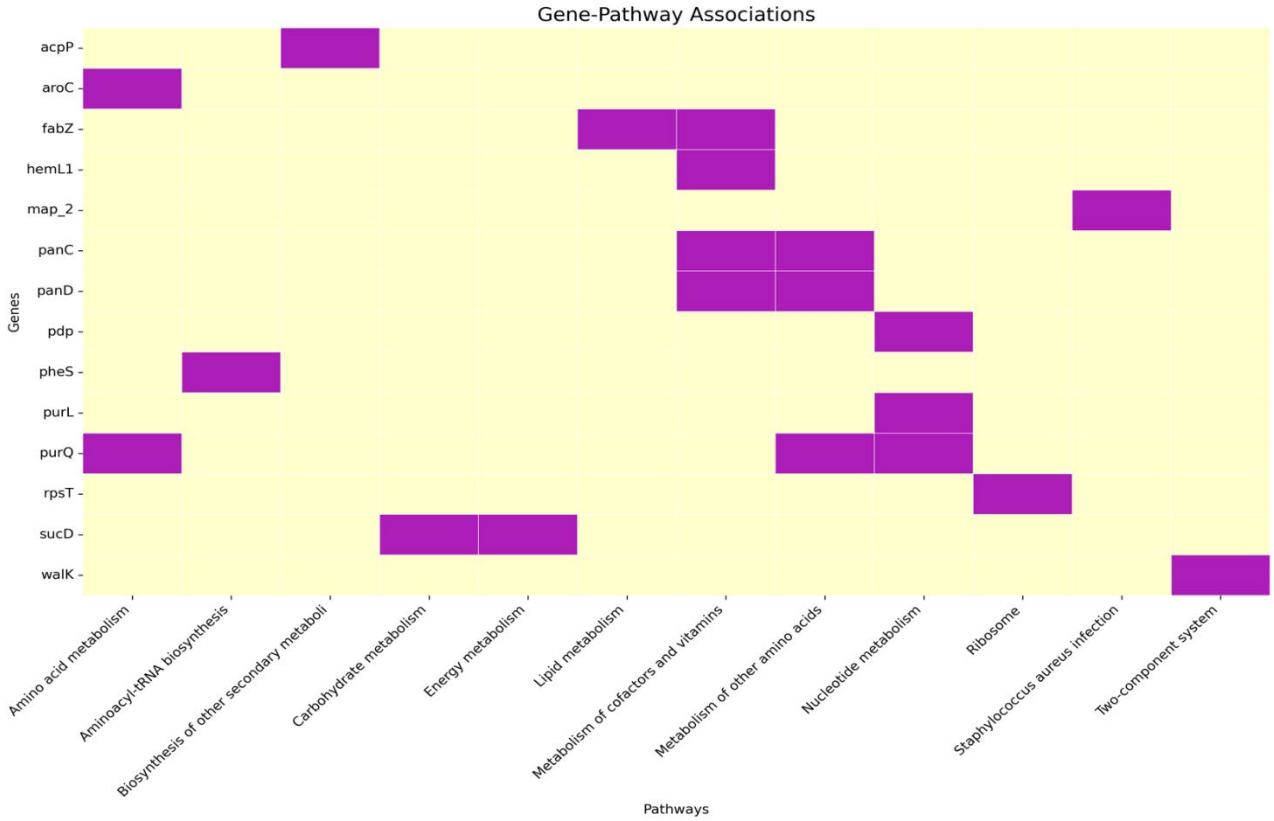

Figure 5-18: Illustration showing the gene-pathways associations of the selected downregulated genes of Met-R3 from the evolutionary experiment of *S. aureus* NCTC 6571 compared to its parent upon the analysis using the KEGG database.
The purple blocks show the presence of the gene (y-axis) in the corresponding pathways (x-axis).

5.2.2. Transposon Mutagenesis Analysis:

The sequenced data from the transposon library of *P. aeruginosa* ATCC 27853, exposed to various concentrations of metformin alongside the control, were analysed using AlbaTradis to compare the different conditions with the control.

The analysis revealed that there was no significant change in the transposon library exposed to 1.25 mg/mL metformin compared to the control. However, following exposure to 10 mg/mL (0.25x MIC) metformin, 11 genes exhibited significant changes ($q \leq 0.001$) in their knockout insertions of the transposons. Furthermore, after exposure to 20 mg/mL (0.5x MIC), there were 51 genes that significantly changed. Additionally, 90 genes showed significant changes in the knockout transposon insertions compared to the control following exposure to 40 mg/mL (1x MIC) metformin.

The genes that commonly exhibited a decrease in the knockout at 0.25 and 0.5x MIC compared to the control include the operon *carAB*, which is essential for arginine metabolism. Additionally, a decrease in the knockout of the *oprM* gene, part of the *mexAB-oprM* operon that encodes the multidrug-resistant efflux pump MexAB-OprM, was noted. Notably, the other genes in this operon (*mexA* and *mexB*) had fewer knockouts compared to the control. However, there was a significant increase in the *mexR* gene, the repressor of this operon, upon exposure to 1x MIC of metformin. Furthermore, a significant decrease in knockouts was observed at 0.25 and 0.5x MIC for *degP,* which encodes a protease involved in degrading misfolded proteins. A similar response was observed in the *hflK* gene, which regulates the activity of the FtsH protease that plays a crucial role in degrading misfolded proteins. Additionally, the *hflC* gene, the other component of the *hflCK* operon, showed significantly fewer knockouts compared to the control at 0.5x MIC. (Appendix Figure 7-2)

Upon exposure to 0.5x and 1x MIC, a significant selection occurred in the knockouts of the *aguA* gene, which encodes the agmatine deiminase enzyme that converts agmatine to putrescine. Additionally, there was a notable increase in the knockouts of the transposon insertions in the *tetC* gene, responsible for encoding tetracycline efflux pumps. (Appendix Figure 7-3)

After the transposon library was exposed to 1x MIC, the knockouts in the *pgi* and *tpiA* genes, which are important enzymes in glycolysis for reaching pyruvate, were enriched compared to the control. In addition, the insertions in the *aceE* and *aceF* genes were dominant in the drug. These genes are part of the pyruvate dehydrogenase (PDH) complex, which catalyzes the conversion of pyruvate into acetyl-Coa. Furthermore, the knockouts in the *gltA* gene, which encodes citrate synthase that converts acetyl-Coa to citrate, were also observed. Additionally, transposon insertions in the *icd_1* gene were more

prevalent in the library exposed to the drug compared to the control. This gene plays a crucial role in the TCA cycle, converting isocitrate to ketoglutarate. (Appendix Figure 7-4)

Moreover, there was enrichment in the knockouts related to the cytochromes after exposure to 1x MIC of metformin. Starting with the *petABC* operon, which encodes the cytochrome bc1 complex, known as complex III in the electron transport chain. Additionally, there was an increase in the insertion of the transposon in the *nuoB* gene, which is part of the *nuo* operon responsible for the formation of complex I in the electron transport chain and ATP production. Another enrichment was observed in the *ccm* operon, including *ccmA, ccmB, ccmC*, *ccmE,* and *ccmF,* which are responsible for the maturation of cytochrome c. (Appendix Figure 7-5)

The exposure to 1x MIC selected mutants of the biotin synthesis gene operon, which also plays a role in fatty acid biosynthesis, including *bioA, bioB, bioC, bioD,* and *bioF*. Additionally, there was further selection for mutants in the Mla pathway (Maintenance of lipid asymmetry) genes *mlaABCDEF,* which balance the lipopolysaccharides in the outer membrane and transport mislocalized glycerophospholipids to the cytoplasm. (Appendix Figure 7-6)

A representative example of the corresponding TraDIS insertion profiles across some genes of *aguA, tetC, mexR, mexA, mexB* and *oprM* illustrating the range of the insertion patterns under different concentrations of metformin is shown in (Figure 5-19).

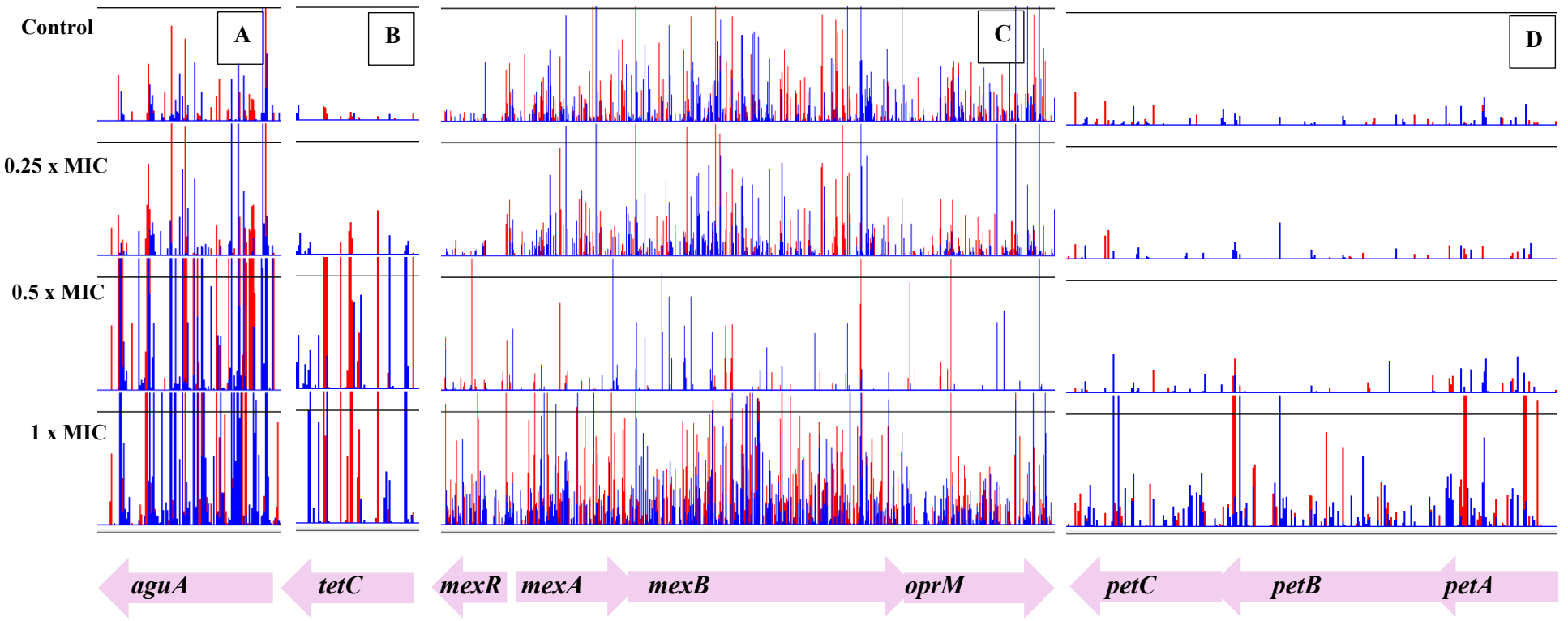

Figure 5-19: Transposon insertion pattern for A)*aguA* gene, B) *tetC* gene, C) *mexR, mexA, mexB, and oprM* genes, D) *petA, petB and petC* genes.
Genetic map of the gene names is shown at the bottom of the panel; indicating gene positions and transcriptional orientation using pink arrows. The top row in each plot shows untreated control cultures; the three rows below are for cultures grown in the presence of 0.25x, 0.5x, and 1x the MIC of metformin. Each row of vertical red or blue lines indicates the position of mapped reads, and the height of the bar represents the relative number of reads mapped. The red inserts indicate the transposon insertions from left to right (→), and the blue inserts indicate the transposon insertions from right to left (←).The representing data has a significance cut-off of $q \leq 0.001$ for two independent experiments for each concentration (n=2). However, only one repeat of each concentration is displayed for clarity.

5.2.3. Investigating the effect of metformin on bacterial metabolic activity in combination with known mitochondrial inhibitors

The effect of 10 mg/mL metformin was tested in combination with 22 different known mitochondrial inhibitors on the metabolic activity of the eight tested strains: *S. aureus, P. aeruginosa, E. coli,* and *K. pneumoniae*. This was done alongside controls consisting of only metformin, only inhibitors, and drug-free negative controls.

For *S. aureus* NCTC 6571, the percentage reduction of metformin alone on the AUC of the metabolic curve compared to the control was, on average, 46.4%. A significant synergy was observed ($p \leq 0.05$) after calculating the expected combination effect on the % reduction using the Bliss independence equation for alexidine ($p = 0.0044$), nordihydroguaiaretic acid ($p = 0.0068$), and trifluoperazine ($p = 0.0043$). The expected percentage reduction from combining metformin with alexidine, nordihydroguaiaretic acid, and trifluoperazine was 52.6%, 47.7%, and 69.5%, respectively, while the actual % reductions were 75.4%, 70.2%, and 76.1%, respectively. However, the combination with celastrol demonstrated antagonistic action ($p = 0.0198$), with an expected reduction of 66.3% compared to an actual % reduction of 60.3% (Figure 5-20). For the *S. aureus* ATCC 25923 strain, the percentage reduction in AUC for metformin alone was 31.4%. Similarly to the *S. aureus strain,* the combination with alexidine ($p = 0.0014$) showed significant synergy compared to metformin alone; the expected % reduction was 56.2%, while the actual percentage reduction was 62.3%. Furthermore, the combinations with diclofenac ($p < 0.00001$), trifluoperazine ($p = 0.0002$), and celastrol ($p < 0.00001$) exhibited an additive effect, as the expected percentage reductions were nearly equal to the actual reductions. In contrast, there was an antagonistic effect of the combination with papaverine ($p = 0.0003$) as the expected % reduction was 33% while the actual was 19% (Figure 5-21).

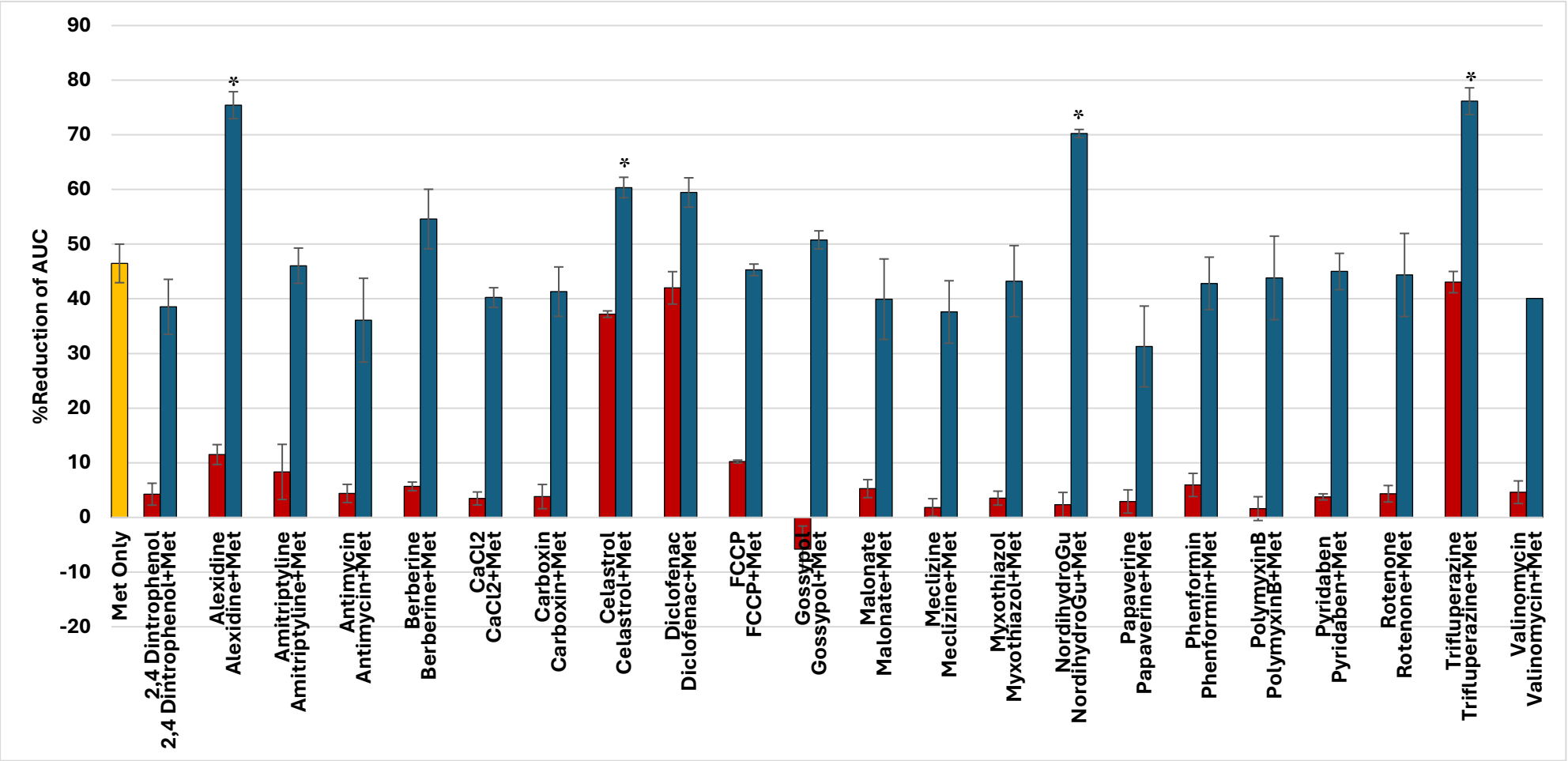

Figure 5-20: Effect of metformin and mitochondrial inhibitors on *S. aureus* NCTC 6571 metabolic inhibition, as measured by the reduction in area under the curve (AUC). A bar plot illustrates the effect of 10 mg/mL metformin (Met) alone (yellow bar), different mitochondrial inhibitors in Mito-I1 plates (red bars), and their combinations with metformin (blue bars) on AUC reduction compared to the control of the bacterial strain *S. aureus* NCTC 6571. The x-axis represents the different drugs used, while the y-axis indicates the reduction of AUC. Data represent mean values from two independent biological replicates (n = 2), with error bars showing standard deviation. Statistical significance between combination treatments and metformin alone was calculated using one-way ANOVA followed by Tukey's HSD post hoc test; significance was defined as $p \leq 0.05$ and indicated by asterisks (*).

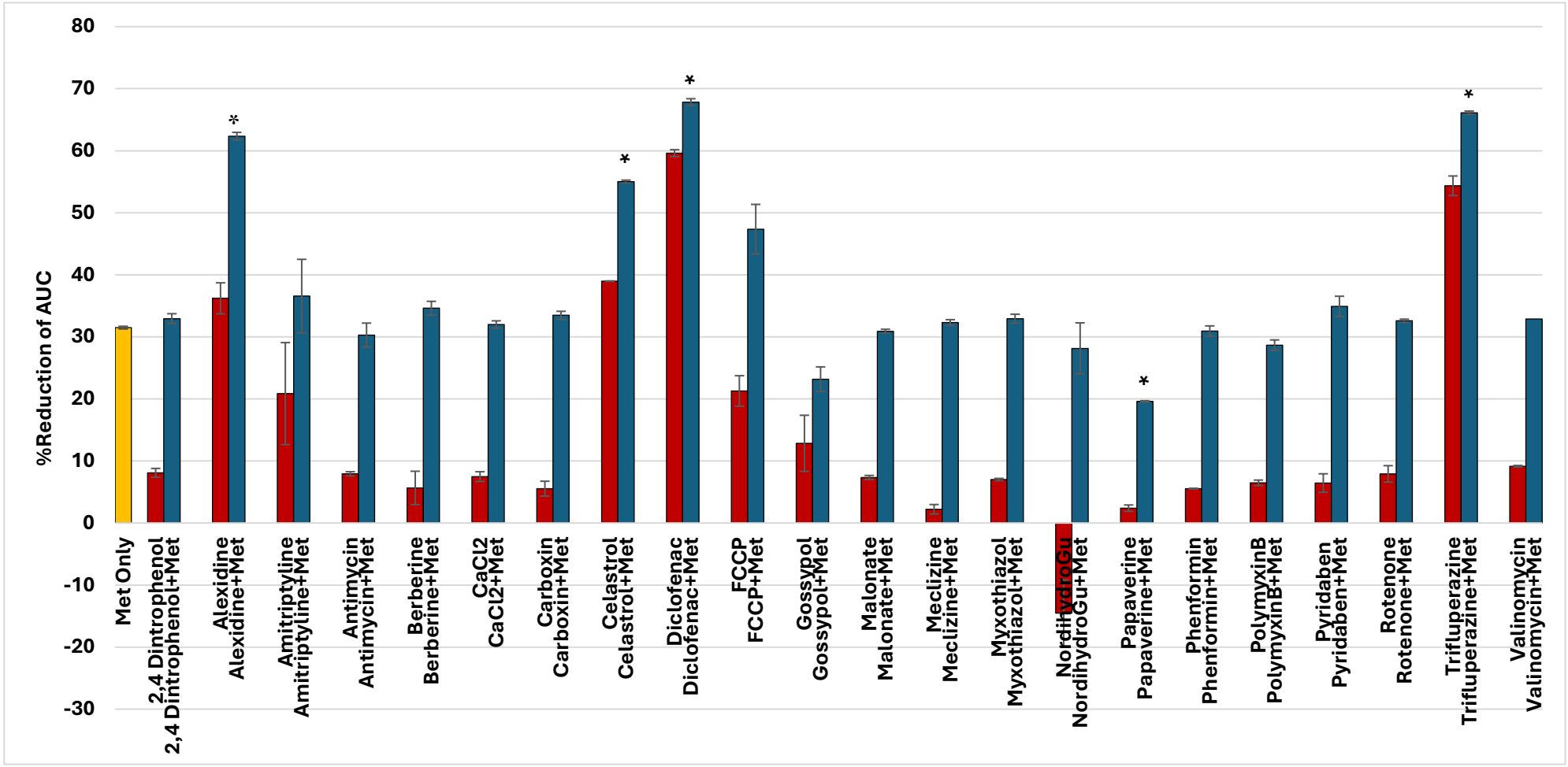

Figure 5-21: Effect of metformin and mitochondrial inhibitors on *S. aureus* ATCC 25923 metabolic inhibition, as measured by the reduction in area under the curve (AUC).
A bar plot illustrates the effect of 10 mg/mL metformin (Met) alone (yellow bar), different mitochondrial inhibitors in Mito-I1 plates (red bars), and their combinations with metformin (blue bars) on AUC reduction compared to the control of the bacterial strain *S. aureus* ATCC 25923. The x-axis represents the different drugs used, while the y-axis indicates the reduction of AUC. Data represent mean values from two independent biological replicates (n = 2), with error bars showing standard deviation. Statistical significance between combination treatments and metformin alone was calculated using one-way ANOVA followed by Tukey's HSD post hoc test; significance was defined as $p \leq 0.05$ and indicated by asterisks (*).

For *P. aeruginosa* NCTC 10662, the percentage reduction of metformin alone on the AUC compared to the control was 32.2%. The analysis revealed a significant difference between the combination with alexidine ($p = 0.0254$) as an additive effect compared to metformin alone. In contrast, the combination with polymyxin B ($p = 0.0001$) and phenformin ($p = 0.0205$) showed a significant antagonistic effect compared to metformin alone, with expected percentage reductions of 94.1% and 39.05%, respectively. However, the actual percentage reductions for these combinations were 85.08% and 23.08%, respectively (Figure 5-22). For the other *P. aeruginosa* strain, ATCC 27853, there was a synergistic effect between the combinations of alexidine ($p < 0.00001$) and trifluoperazine ($p < 0.00001$) compared to metformin, with actual percentage reductions in AUC of 53.5% and 40.9%, respectively, against the expected calculated values of 46.19% and 29.1%, respectively. Furthermore, the combinations of FCCP ($p = 0.0376$), CaCl2 ($p = 0.0085$), gossypol ($p = 0.0372$), and amitriptyline ($p = 0.0002$) demonstrated an additive effect compared to metformin alone. In contrast, combinations of nordihydro-guaiaretic acid ($p = 0.0082$), polymyxin B ($p < 0.00001$), and papaverine ($p = 0.0092$) displayed an antagonistic effect compared to metformin alone, with actual percentage reductions of 21.1%, 85.4%, and 10.5%, respectively, in comparison to the expected reductions of 26.7%, 92.9%, and 17.4%, respectively (Figure 5-23).

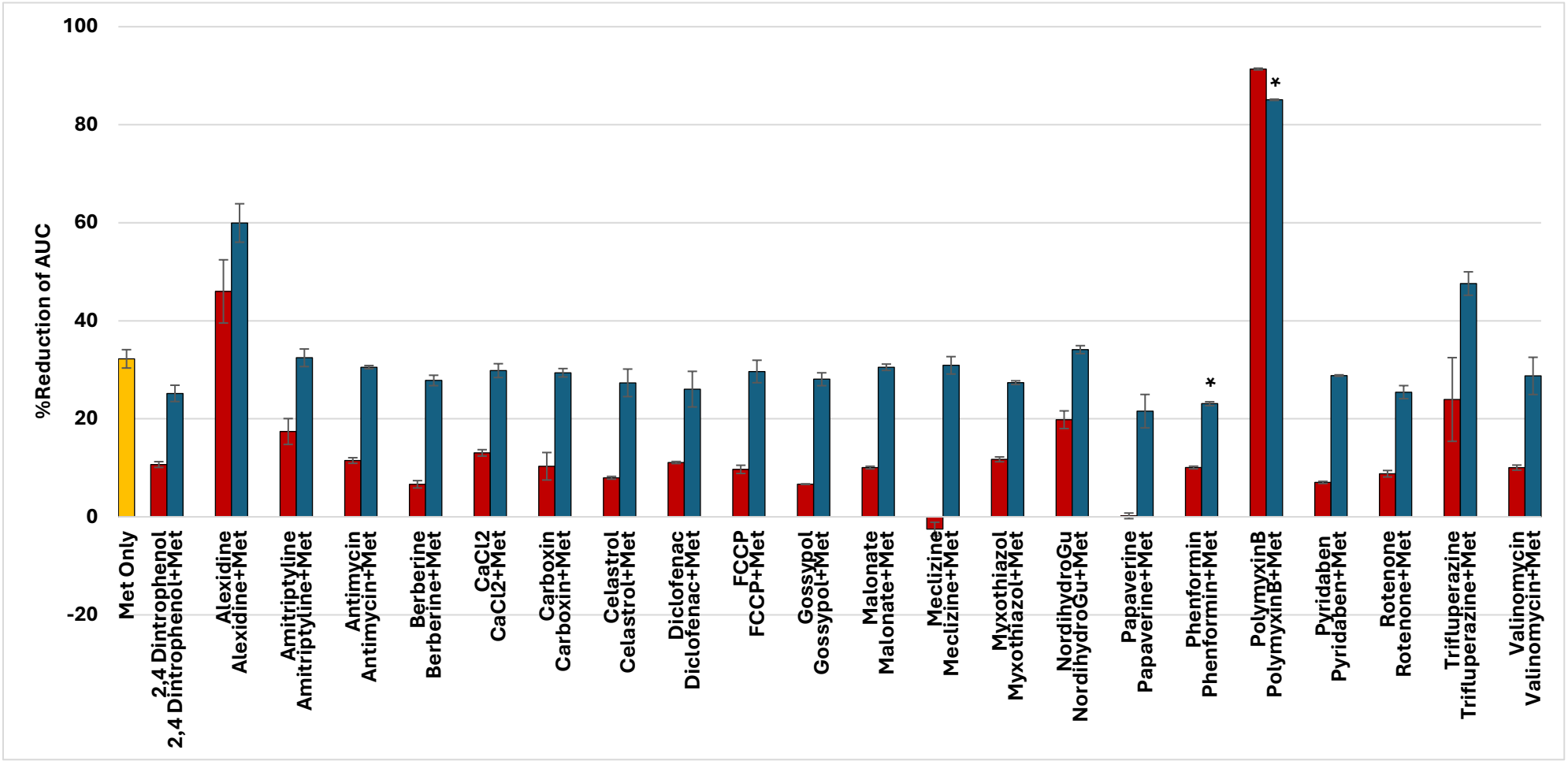

Figure 5-22: Effect of metformin and mitochondrial inhibitors on *P. aeruginosa* NCTC 10662 metabolic inhibition, as measured by the reduction in area under the curve (AUC).
A bar plot illustrates the effect of 10 mg/mL metformin (Met) alone (yellow bar), different mitochondrial inhibitors in Mito-I1 plates (red bars), and their combinations with metformin (blue bars) on AUC reduction compared to the control of the bacterial strain *P. aeruginosa* NCTC 10662. The x-axis represents the different drugs used, while the y-axis indicates the reduction of AUC. Data represent mean values from two independent biological replicates (n = 2), with error bars showing standard deviation. Statistical significance between combination treatments and metformin alone was calculated using one-way ANOVA followed by Tukey's HSD post hoc test; significance was defined as $p \leq 0.05$ and indicated by asterisks (*).

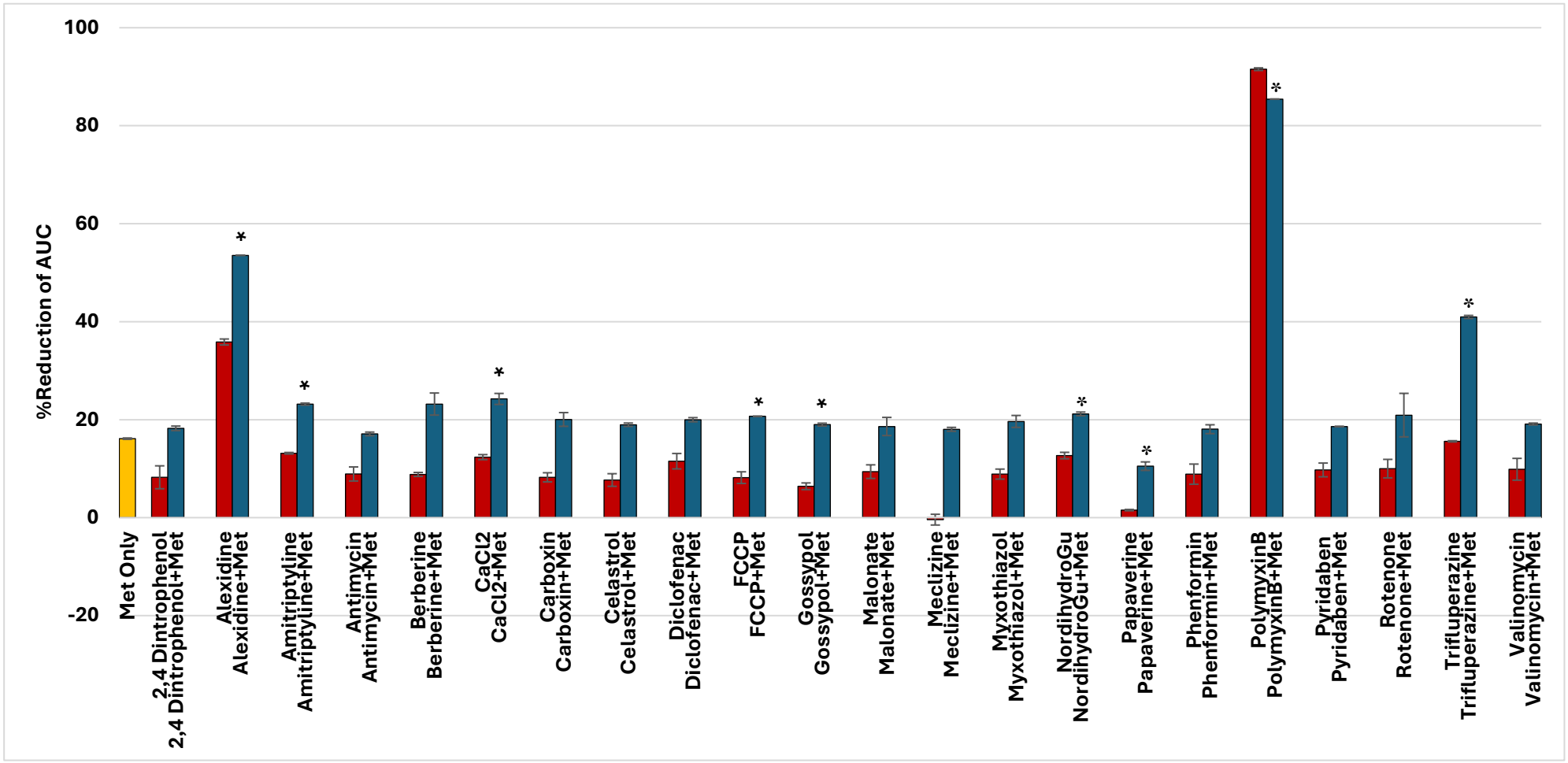

Figure 5-23: Effect of metformin and mitochondrial inhibitors on *P. aeruginosa* ATCC 27853 metabolic inhibition, as measured by the reduction in area under the curve (AUC).
A bar plot illustrates the effect of 10 mg/mL metformin (Met) alone (yellow bar), different mitochondrial inhibitors in Mito-I1 plates (red bars), and their combinations with metformin (blue bars) on AUC reduction compared to the control of the bacterial strain *P. aeruginosa* ATCC 27853. The x-axis represents the different drugs used, while the y-axis indicates the reduction of AUC. Data represent mean values from two independent biological replicates (n = 2), with error bars showing standard deviation. Statistical significance between combination treatments and metformin alone was calculated using one-way ANOVA followed by Tukey's HSD post hoc test; significance was defined as $p \leq 0.05$ and indicated by asterisks (*).

For the *E. coli* NCTC 10418 strain, the exposure to metformin alone caused reduction in AUC with 90.8% compared to the control. The analysis showed that the combinations of CaCl2 ($p = 0.0001$), trifluoperazine ($p = 0.0064$), and polymyxin B ($p = 0.0016$) had an antagonistic effect compared to metformin alone because their expected calculated percentages of reduction were 86.7%, 98.02%, and 99.01%, respectively, while the actual percentages of reduction were -3.1%, 85.7%, and 81.8%, respectively (Figure 5-24). For the other *E. coli* strain ATCC 25922, the percentage of reduction in AUC was 14.3% in the case of metformin alone. However, there was a synergistic effect in the combinations of alexidine ($p = 0.0008$), nordihydroguaiaretic acid ($p = 0.0014$), amitriptyline ($p = 0$), and papaverine ($p = 0.0113$), as the actual percentage reductions were 84.07%, 51.5%, 68.2%, and 30.8%, respectively; however, the calculated percentages were 70.2%, 24.2%, 59.09%, and 20.1%, respectively. The combination with trifluoperazine ($p = 0$) showed an additive effect on the reduction of the AUC compared to metformin alone. However, the combination with polymyxin B ($p = 0$) showed an antagonistic effect, as its expected reduction was 92.9%, but the actual reduction was 86.6% (Figure 5-25).

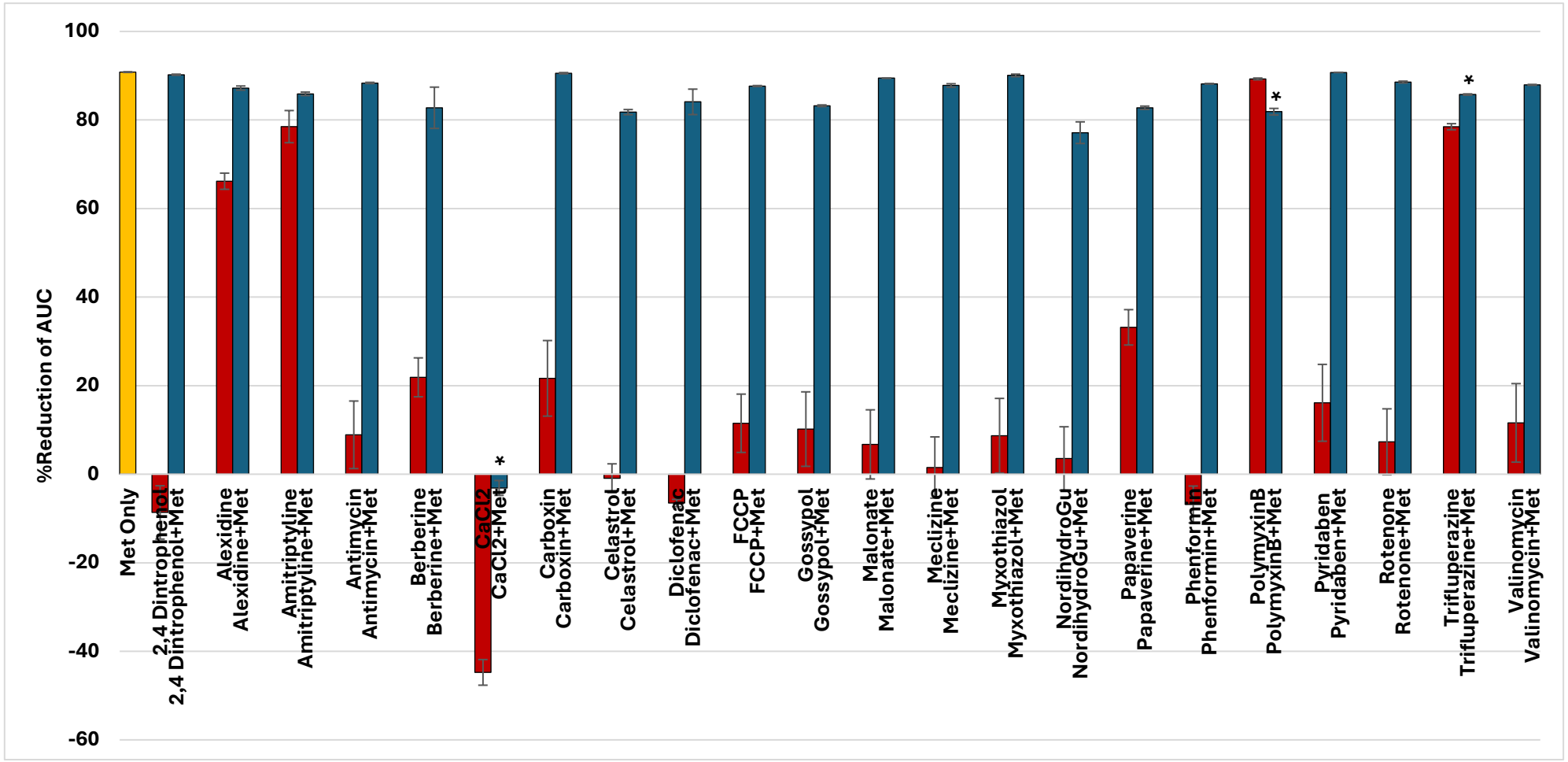

Figure 5-24: Effect of metformin and mitochondrial inhibitors on *E. coli* NCTC 10418 metabolic inhibition, as measured by the reduction in area under the curve (AUC). A bar plot illustrates the effect of 10 mg/mL metformin (Met) alone (yellow bar), different mitochondrial inhibitors in Mito-I1 plates (red bars), and their combinations with metformin (blue bars) on AUC reduction compared to the control of the bacterial strain *E. coli* NCTC 10418. The x-axis represents the different drugs used, while the y-axis indicates the reduction of AUC. Data represent mean values from two independent biological replicates (n = 2), with error bars showing standard deviation. Statistical significance between combination treatments and metformin alone was calculated using one-way ANOVA followed by Tukey's HSD post hoc test; significance was defined as $p \leq 0.05$ and indicated by asterisks (*).

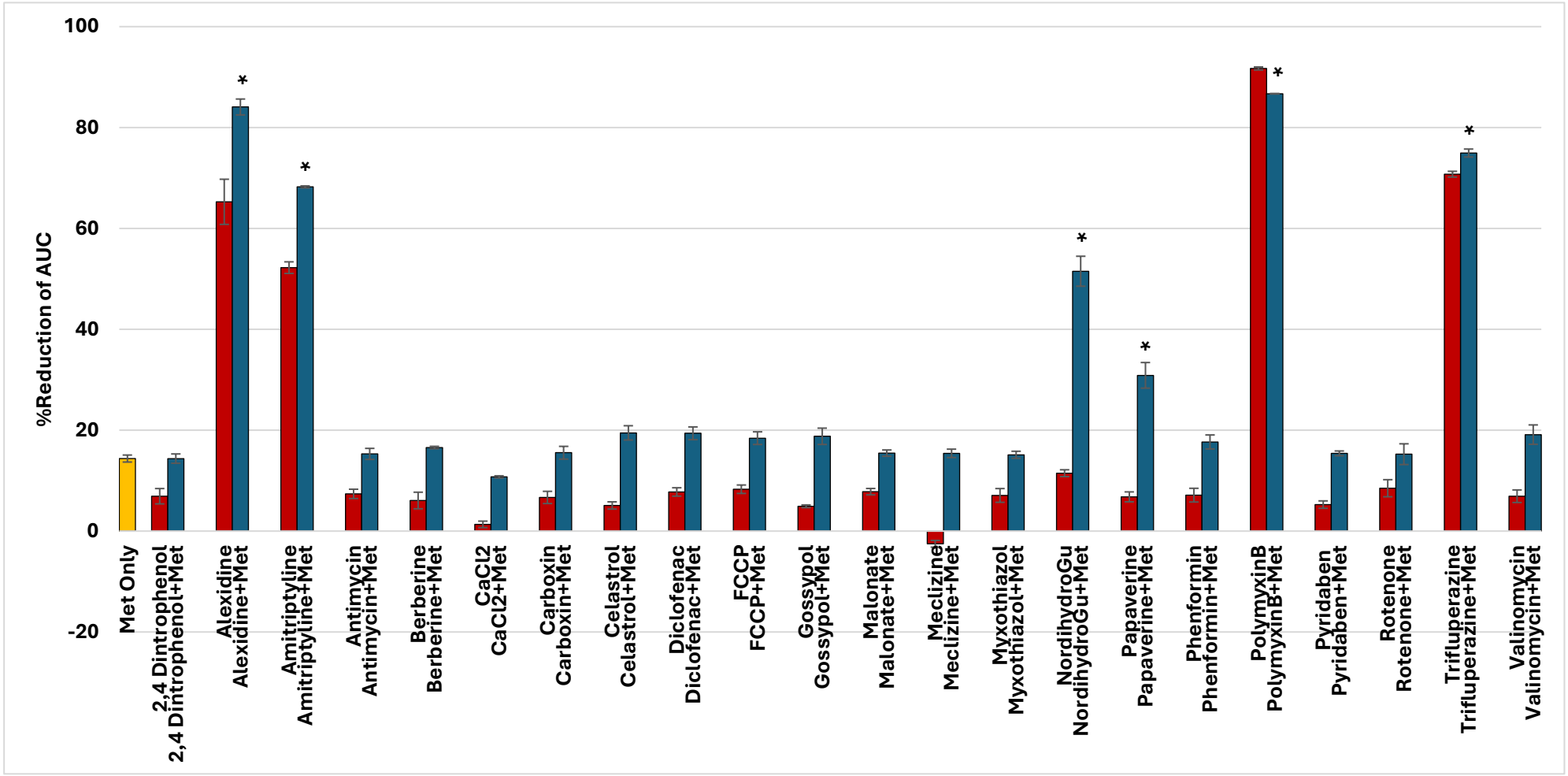

Figure 5-25: Effect of metformin and mitochondrial inhibitors on *E. coli* ATCC 25922 metabolic inhibition, as measured by the reduction in area under the curve (AUC). A bar plot illustrates the effect of 10 mg/mL metformin (Met) alone (yellow bar), different mitochondrial inhibitors in Mito-I1 plates (red bars), and their combinations with metformin (blue bars) on AUC reduction compared to the control of the bacterial strain *E. coli* ATCC 25922. The x-axis represents the different drugs used, while the y-axis indicates the reduction of AUC. Data represent mean values from two independent biological replicates (n = 2), with error bars showing standard deviation. Statistical significance between combination treatments and metformin alone was calculated using one-way ANOVA followed by Tukey's HSD post hoc test; significance was defined as $p \leq 0.05$ and indicated by asterisks (*).

For *K. pneumoniae* ATCC 700721 strain, the reduction in AUC with metformin alone was 12.8%. In addition, the combination of metformin with alexidine ($p = 0.0039$), diclofenac ($p = 0.0251$), valinomycin ($p = 0.0321$), celastrol ($p = 0.0032$), trifluoperazine ($p = 0.0018$), and polymyxin B ($p < 0.00001$) showed only an additive effect. In contrast, the combinations with phenformin ($p = 0.0208$), CaCl2 ($p = 0.0113$), and amitriptyline ($p = 0.0008$) exhibited an antagonistic effect compared to metformin alone because the expected percentage reductions were 21.06%, 22.4%, and 41.8%, respectively; however, the actual percentage reductions were 15.7%, 16.7%, and 36.1%, respectively (Figure 5-26). For the other *K. pneumoniae* strain ATCC 700603, metformin reduced the AUC by 11.6% compared to the control. It was found that there was a synergistic effect with the combinations of trifluoperazine ($p = 0.0009$) as the actual percentage reductions were 35.5% compared to the expected reductions of around 27%. Furthermore, an additive effect was observed with the combinations of alexidine ($p = 0.0014$), FCCP ($p = 0.0204$), valinomycin ($p = 0.0064$), CaCl2 ($p = 0.0023$), celastrol ($p = 0.0312$), and polymyxin B ($p = 0.0003$). In contrast, the combinations with diclofenac ($p = 0.0022$) and nordihydroguaiaretic acid ($p = 0.0447$) displayed an antagonistic effect, as the actual percentage reductions were 14.3% and 15.2%, respectively, while the expected reductions were around 21% for both(Figure 5-27).

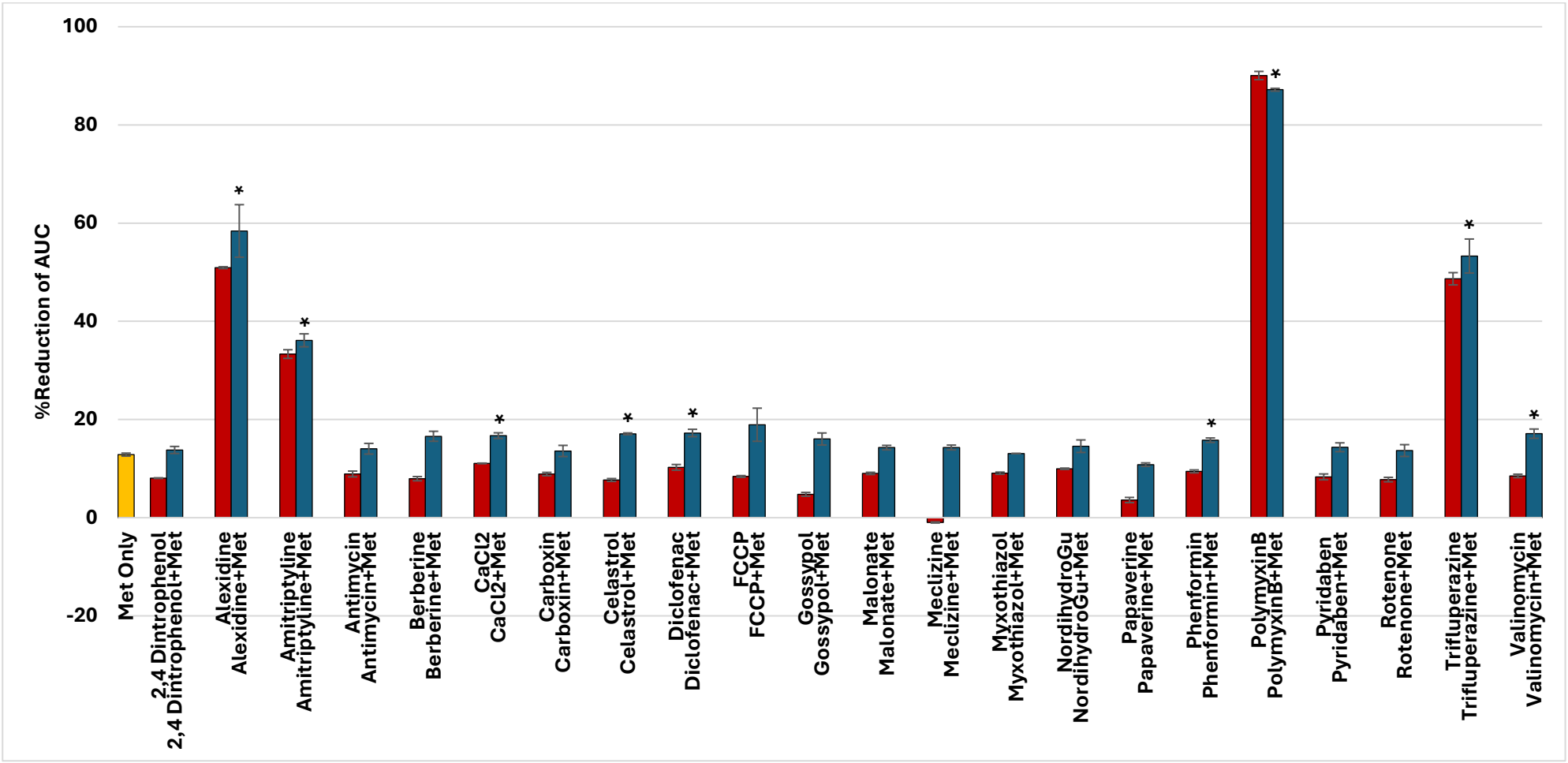

Figure 5-26: Effect of metformin and mitochondrial inhibitors on *K. pneumoniae* ATCC 700721 metabolic inhibition, as measured by the reduction in area under the curve (AUC).

A bar plot illustrates the effect of 10 mg/mL metformin (Met) alone (yellow bar), different mitochondrial inhibitors in Mito-I1 plates (red bars), and their combinations with metformin (blue bars) on AUC reduction compared to the control of the bacterial strain *K. pneumoniae* ATCC 700721. The x-axis represents the different drugs used, while the y-axis indicates the reduction of AUC. Data represent mean values from two independent biological replicates (n = 2), with error bars showing standard deviation. Statistical significance between combination treatments and metformin alone was calculated using one-way ANOVA followed by Tukey's HSD post hoc test; significance was defined as $p \leq 0.05$ and indicated by asterisks (*).

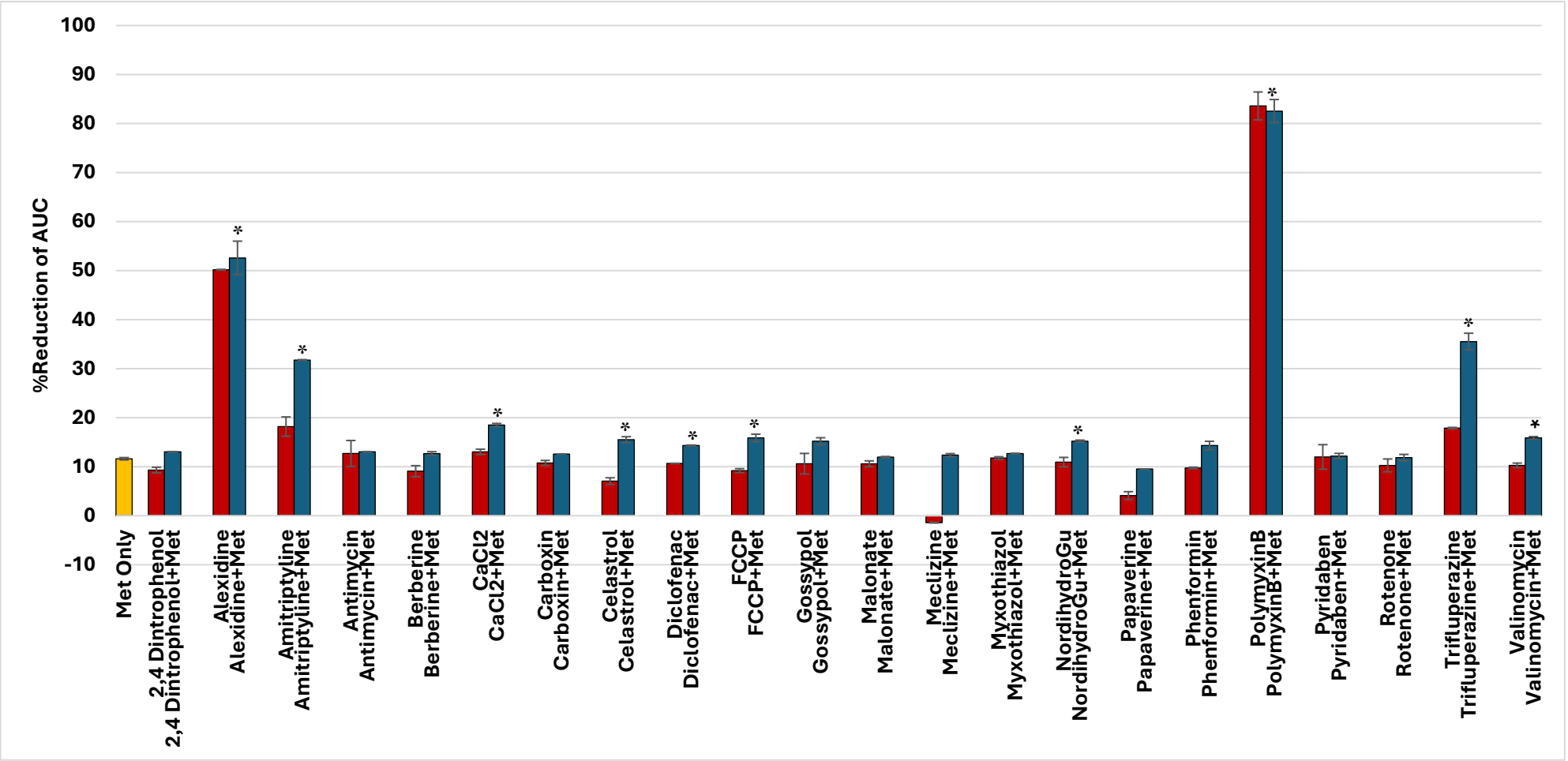

Figure 5-27: Effect of metformin and mitochondrial inhibitors on *K. pneumoniae* ATCC 700603 metabolic inhibition, as measured by the reduction in area under the curve (AUC).
A bar plot illustrates the effect of 10 mg/mL metformin (Met) alone (yellow bar), different mitochondrial inhibitors in Mito-I1 plates (red bars), and their combinations with metformin (blue bars) on AUC reduction compared to the control of the bacterial strain *K. pneumoniae* ATCC 700603. The x-axis represents the different drugs used, while the y-axis indicates the reduction of AUC. Data represent mean values from two independent biological replicates (n = 2), with error bars showing standard deviation. Statistical significance between combination treatments and metformin alone was calculated using one-way ANOVA followed by Tukey's HSD post hoc test; significance was defined as $p \leq 0.05$ and indicated by asterisks (*).

All the results of the interaction between the different mitochondrial inhibitors and metformin on the metabolic activity on the all tested bacterial strains were collected in (Table 5-1), where it shows the significantly synergistic, additive and antagonistic interactions indicated with arrows described in the table's footnote.

Table 5-1: Summarising the interaction between metformin and mitochondrial inhibitors on bacterial metabolic activity, as measured by the reduction in the area under the curve (AUC)

Inhibitor	*S. aureus* NCTC 6571	*S. aureus* ATCC 25923	*P. aeruginosa* NCTC 10662	*P. aeruginosa* ATCC 27853	*E. coli* NCTC 10418	*E. coli* ATCC 25922	*K. pneumoniae* ATCC 700721	*K. pneumoniae* ATCC 700603
2,4-Dinitrophenol	ns	ns	ns	ns	ns	ns	ns	ns
Alexidine	↑↑	↑↑	↑	↑↑	ns	↑↑	↑	↑
Amitriptyline	ns	ns	ns	↑	ns	↑↑	↓	ns
Antimycin A	ns	ns	ns	ns	ns	ns	ns	ns
Berberine	ns	ns	ns	ns	ns	ns	ns	ns
$CaCl_2$	ns	ns	ns	↑	↓	ns	↓	↑
Carboxin	ns	ns	ns	ns	ns	ns	ns	ns
Celastrol	↓	↑	ns	ns	ns	ns	↑	↑
Diclofenac	ns	↑	ns	ns	ns	ns	↑	↓
FCCP	ns	ns	ns	↑	ns	ns	ns	↑
Gossypol	ns	ns	ns	↑	ns	ns	ns	ns
Malonate	ns	ns	ns	ns	ns	ns	ns	ns
Meclizine	ns	ns	ns	ns	ns	ns	ns	ns
Myxothiazol	ns	ns	ns	ns	ns	ns	ns	ns
Nordihydroguaiaretic acid	↑↑	ns	ns	↓	ns	↑↑	ns	↓
Papaverine	ns	↓	ns	↓	ns	↑↑	ns	ns
Phenformin	ns	ns	↓	ns	ns	ns	↓	ns
Polymyxin B	ns	ns	↓	↓	↓	↓	↑	↑
Pyridaben	ns	ns	ns	ns	ns	ns	ns	ns
Rotenone	ns	ns	ns	ns	ns	ns	ns	ns
Trifluoperazine	↑↑	↑	ns	↑↑	↓	↑	↑	↑↑
Valinomycin	ns	ns	ns	ns	ns	ns	↑	↑

Notes: Symbols indicate the change in the percentage reduction of AUC relative to metformin treatment alone, where ↑↑ = synergistic interaction; ↑ = additive interaction; ↓ = antagonistic interaction; ns = no significant change.

5.3. DISCUSSION

5.3.1. The effect of the exposure of the bacteria to metformin on the regulation of different genes.

After the exposure of *P. aeruginosa* ATCC 27853 to 10 mg/mL metformin, it was noticed that there was overexpression of the *arnABCDT* genes which are responsible for adding 4-amino-4-deoxy-L-arabinose (L-Ara4N) to the lipid A moiety of the outer membrane (Lo Sciuto et al., 2020). The lipid A part is the hydrophobic part of the lipopolysaccharide (LPS) layer, which is the major part of the outer membrane of the Gram-negative cell membrane acting as the anchor between the LPS and the outer membrane

(Hankins et al., 2013). Therefore, by aminoarabinosylation of the lipid A part, it leads to a decrease in the negative charge on the cell membrane and decreases the affinity to cationic antimicrobial agents, including antimicrobial peptides (Kim et al., 2016), and polymyxins (like polymyxin B and colistin) (Lo Sciuto et al., 2020), thus increasing the bacterial resistance to them. This may be explained here as metformin is a cationic compound in physiological solutions due to the presence of biguanide groups (Foretz et al., 2014), suggesting that bacteria may adapt to its exposure by decreasing permeability. It may also indicate that the interaction between the cationic part of metformin and the negative charge of the LPS is a mechanism for entry into the cell.

Furthermore, exposure to metformin led to the induction of various multidrug- resistant genes such as *mexCD, oprJ, smvA,* and *emrE*. The *mexCD* gene encodes the MexCD-OprJ efflux pump, which is known to expel different hydrophobic and amphiphilic molecules, contributing to resistance against many antibiotics including tetracycline, chloramphenicol, fluoroquinolones, β- lactams, erythromycin, antimicrobial peptides, and other toxic compounds like triclosan (Elkins & Nikaido, 2002; Masuda et al., 2000; Ruiz & Levy, 2013). SmvA is another efflux pump that expels various antibiotics, including cationic compounds (Ruiz & Levy, 2013), which aligns with metformin' s case. EmrE, a putative small drug resistance efflux pump, has been found to play a role in aminoglycoside resistance in *P. aeruginosa* (Li et al., 2003). A study conducted in 2024 (Kim et al., 2024) found that the metagenomic analysis of the gut microbiome in diabetic individuals treated with metformin showed an increased prevalence of multidrug resistance genes, particularly in *E. coli,* including the same efflux pumps identified in this research. Additionally, it was reported (Wei et al., 2022) that exposure to metformin as a water pollutant at low concentrations of 10 mg/L led to the upregulation of various efflux pump genes such as *emrK*, *emrY, acrA,* and *acrB* in *E. coli,* suggesting an increase in multidrug resistance toward different antibiotics. Conversely, it was found that metformin can act as an efflux pump inhibitor in *K. pneumoniae* at a concentration of 50 mg/mL, where it was suggested that these pumps were AcrAB based on their presence in PCRs (Abbas et al., 2021a). A possible explanation is that metformin can inhibit different efflux pumps than those stated by Abbas et al. (2021), especially since they did not confirm exactly which efflux pumps were affected by metformin. There was also a report indicating that metformin could restore doxycycline resistance at various concentrations of 1-5 mg/mL by downregulating the *tetA* gene responsible for the tetracycline efflux pump (Liu et al., 2020a).

The exposure to metformin also causes upregulation of some *puu* genes, which are responsible for the utilisation of putrescine in certain bacteria, such as *E. coli* and *P. aeruginosa*. Putrescine is one of the important polyamine compounds significant for cellular growth, protecting DNA from oxidative stress, and playing a role in RNA polymerase activity, protein synthesis, membrane stability and functioning of

ion channels. Additionally, it has been found that bacteria can use these compounds as carbon and nitrogen sources. Among these genes, the gene for PuuP is responsible for transporting putrescine into the cell. Furthermore, PuuA and PuuB are the first two enzymes involved in the putrescine utilization pathway. Moreover, it has been reported that the presence of exogenous polyamines overexpresses the *puu* genes to achieve balance and prevent toxic effects from the accumulation of these compounds inside the cell (Chou et al., 2008; Yao et al., 2011). Therefore, this overexpression can be explained by the structure of metformin (a biguanide compound), which resembles putrescine (a polyamine compound); thus, the bacteria may sense the presence of metformin as an excess of putrescine, activating its utilisation. However, there is no excess putrescine, suggesting an increase in its catabolism, which may be one of the mechanisms by which metformin affects bacterial growth.

As a response to the exposure of *S. aureus* NCTC 6571 to 5 mg/mL metformin, some genes of it*s* operon, which are responsible for histidine biosynthesis, got upregulated. Histidine is an important amino acid that is considered a building block in many proteins. Also, it plays a role in some cellular functions and helps overcome different stress responses (Wang, Wang, et al., 2020). For instance, it is found that histidine biosynthesis is overexpressed to help *S. aureus* grow under acidic stress (Beetham et al., 2023). Another paper showed that *Litsea cubeba* essential oil, known for its antimicrobial activity, causes the overexpression of histidine biosynthesis in *S. aureus* due to cellular stress at sub-MIC concentrations (Yang et al., 2020). In addition, there was upregulation of *trp* operon, which is responsible for another amino acid biosynthesis, tryptophan. Tryptophan is an important amino acid which is known to be in the polypeptide chains of many bacterial enzymes, and it helps the bacteria to balance their redox homeostasis (Roager & Licht, 2018). A study investigating *Mycobacterium tuberculosis* showed that one of the cellular changes to overcome the stress caused by the host immunity is by upregulation of *trp* genes to overproduction of tryptophan amino acid (Zhang et al., 2013). The same was observed for *S. aureus* during their adaptation in the lung in the study (Chaffin et al., 2012). Furthermore, there was overexpression of some of the ribosomal proteins for large and small subunits, which may be explained by the fact that the bacteria tend to adapt to different stress responses by increasing protein synthesis (Njenga et al., 2023). Thus, this potentially suggests that the effect of metformin can induce a stress response in the bacterial cell, which attempts to counteract this by overproducing histidine and tryptophan amino acids.

Also, there was an overexpression of the genes forming the *bio* operon, which are responsible for biotin biosynthesis. Biotin is essential for bacteria as it enables biotin-dependent enzymes to function, including those important in fatty acid biosynthesis and the TCA cycle. The bacteria need to achieve an efficient balance between the demand for biotin and its supply, so in the presence of sufficient biotin,

the BirA enzyme acts as a repressor of *bio* operon expression because biotin synthesis is energy costly. Additionally, it works as an activator for biotin-dependent enzymes by catalysing the ligation of biotin to the enzymes (Satiaputra et al., 2018). In this study, exposure of the bacteria to metformin resulted in the overexpression of *bio* genes, as well as the *birA* gene, which represents two opposing effects. This may suggest that metformin inhibits the function of the BirA enzyme, leading to a lack of repression on the *bio* genes, which observed as their overexpression, and the bacteria attempt to compensate for the impaired function of BirA by overexpressing its encoding gene. There is no published data on metformin affecting that enzyme. However, biotin ligase (BirA) is a targetable drug for developing antimicrobial agents against *S. aureus* (Soares da Costa et al., 2012) and *M. tuberculosis* (Duckworth et al., 2011).

The *mecA* gene was overexpressed significantly in the treated samples compared to the control, which encodes for penicillin-binding protein 2A (PBP_{2a}) that has a lower affinity to β-lactam antibiotics (Wielders et al., 2002). This may suggest that metformin could induce cell wall stress similar to that caused by penicillins, so the bacteria respond with overexpression of the resistance gene. Liu *et al.* (2020) suggested that metformin disrupts the outer membrane of Gram-negative bacteria (Liu et al., 2020a). Furthermore, the previously mentioned effect of metformin on its interaction with the LPS of *P. aeruginosa* strengthens this hypothesis.

Conversely, it was observed that the exposure of *S. aureus* NCTC 6571 to metformin led to the downregulation of genes involved in glycolysis (*pts*, *pgi*, *pfk*, *tpiA*, *gapA*, *pgk, eno*, *gpmI*, *pyk*, *pdhA, pdhB*) and several components of the electron transport chain (*ndhB*, *qoxABCD,* and *atpB*). Glycolysis is the initial part of aerobic respiration, producing NADH and ATP, and culminating in the conversion of pyruvate to acetyl- Coa, followed by the TCA cycle, which generates additional NADH molecules that serve as electron donors for the next step in aerobic respiration: the electron transport chain (ETC). The bacterial ETC is structurally similar to the mitochondrial one, but it resides in the cell membrane. It consists of the NADH dehydrogenase complex, ubiquinone, cytochrome b- c1 complex, cytochrome c, cytochrome oxidase complex (including cytochrome aa_3 oxidase), and ATP synthase (Figure 5-28). In the ETC, the NADH molecule is oxidised to form NAD +, electrons are transported through various complexes reaching the final electron acceptor (O 2), and protons (H^+) are pumped outside the cell, resulting in the establishment of a proton motive force (PMF) across the cell membrane, which drives ATP synthase to pump H + back into the cytoplasm, forming water with O 2. The redox balance of the NAD +/NADH ratio plays a crucial role in regulating all aerobic processes (Ahmad et al., 2025; Alberts et al., 2002; Kracke et al., 2015). Metformin is known to inhibit mitochondrial complex I within the ETC in humans (Fontaine, 2018). Therefore, this study hypothesizes that metformin could also inhibit the ETC in bacteria, causing ATP depletion. This might explain the bacterial response observed here, which

involves the shutdown of energy metabolism through the downregulation of glycolysis and certain ETC components. This effect was noted with polymyxin B against *Bacillus subtilis*, which is known to inhibit NADH dehydrogenase and disrupt the PMF, leading to downregulation of glycolytic genes (Yu et al., 2019). The exact mechanism of metformin' s action on the ETC has not yet been published; however, two mechanistic studies have indicated that metformin may disrupt the PMF in *K. pneumoniae* (X. Xiao et al., 2022) and *E. coli* (Liu et al., 2020a). Additionally, it has been reported that the combination of doxycycline and metformin can cause downregulation of certain oxidative phosphorylation genes, including *atp* genes and *nuo* genes, compared to doxycycline alone for *E. coli* (Liu et al., 2020a). Another support to this finding is that another set of genes was upregulated in response to metformin, specifically the *mrpAEF* genes. Mrp is a Na(+)/H(+) antiporter crucial for ion homeostasis and maintaining balanced PMF, which is essential for cell growth (Foreman et al., 2021). Disruption of PMF is known to have broad effects on cellular growth and tolerance (Wan et al., 2024); how this mechanistic insight relates to the phenotypic outcomes described in Chapter 1 is integrated in the General Discussion.

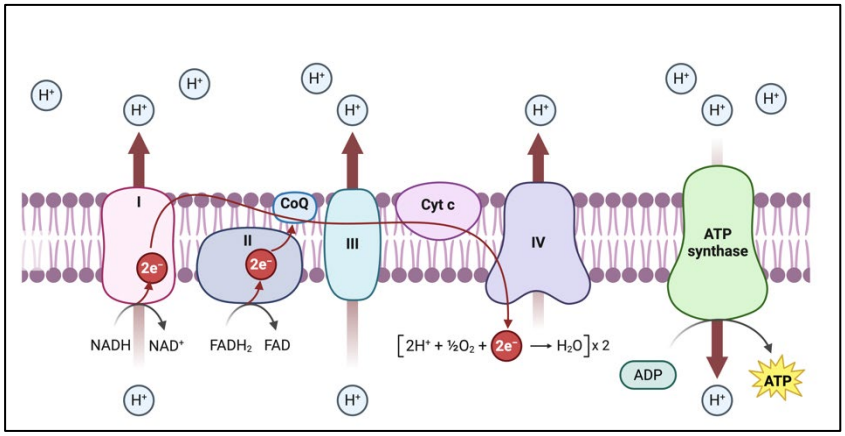

Figure 5-28: Schematic representation of a simplified electron transport chain illustrating main principles of ATP synthesis in bacteria.
Electrons from NADH and $FADH_2$ enter the electron transport chain at Complexes I and II and are transferred via coenzyme Q and cytochrome c to Complex IV, where oxygen is reduced to water. Proton movement at Complexes I, III, and IV generates an electrochemical gradient (the proton motive force, PMF) that drives ATP synthesis by ATP synthase. Imported from https://BioRender.com.

5.3.1.1. Effect of continuous metformin exposure on bacterial gene expression without drug:

The transcriptomics of one evolved line (Met-R3) of the *S. aureus* strain from the evolutionary experiment; section 2.4.2**.** was analysed and compared to the parent. This analysis revealed that two genes belonging to the *deo* operon were upregulated, which is responsible for the deoxyribonucleoside catabolism pathway and the formation of nucleobase and deoxyribophosphate (salvage pathway). This is important for repairing DNA damage that may have occurred due to the drug stress in the evolutionary experiment, as the bacteria needed new nucleotides for that purpose (Carvajal-Garcia et al., 2023; Khil & Camerini-Otero, 2002). In contrast, there was downregulation of the *wbpI* gene, which is responsible

for *de novo* nucleotide sugar biosynthesis. This means that the bacterial cell prefers to obtain new nucleotides through the salvage pathway, as it is more energy-efficient compared to the *de novo* pathway (Nyhan, 2014). This preference could be explained by the hypothesis of this study, which suggests that metformin could cause metabolic and energy stress, so the bacteria tried to adapt by shifting to a less metabolically burdensome mode.

5.3.1.2. Effect of continuous metformin exposure on bacterial gene expression in the presence of drug

The transcriptomic analysis of Met-R4, one of the *P. aeruginosa* strain evolved lines generated from the evolutionary experiment in, showed that after exposure to 10 mg/mL metformin, the genes encoding the efflux pump MexCD-OprJ were no longer overexpressed as they were in the parent strain. However, the *smvA* and *emrE* genes were upregulated in both the evolved and parent strains. This can be explained by the bacterium's tendency to adapt to the presence of the drug by utilising energy more efficiently, focusing on the more specific efflux pumps for cationic compounds like SmvA and EmrE, rather than expressing the broader spectrum pump; MexCD-OprJ, which are known to be energy costly and require PMF to function (Yamaguchi et al., 2015). Another observation was the upregulation of the *arnF* and *arnE* genes in the evolved strain compared to the parent after exposure to metformin, in addition to the *arnABCDT* genes, which together form the *arn* operon responsible for developing resistance against cationic antimicrobial agents. This observation suggests that this may be how the bacteria adapt to metformin and further indicates that the interaction with LPS may be the route through which metformin enters the bacterial cell.

For Met-R3 of *S. aureus*, two additional genes (*trpE and trpG*) involved in tryptophan biosynthesis were overexpressed in the evolved strain compared to the parent strain after exposure to 5 mg/mL metformin. As previously mentioned, tryptophan plays a role in redox homeostasis, which is suggested to be impaired due to the action of metformin on the ETC. Therefore, the bacteria adapted to the continuous exposure to metformin by upregulating more tryptophan biosynthesis genes. Furthermore, *birA,* which encodes the biotin gene repressor, was upregulated in the parent strain only, not in the evolved strain. The hypothesis suggested in this study is that metformin may inhibit the BirA enzyme. Thus, the bacterial cell could adapt to this effect, preventing compensatory upregulation of the gene.
In the evolved strain of *S. aureus*, adaptation to the presence of metformin during the evolutionary experiment was achieved by upregulating two genes encoding ABC transporters to get rid of the drug. One was the BceA efflux pump, which is known as the bacitracin efflux pump, and it was reported that it could be induced with cationic antimicrobial drugs (Pietiäinen et al., 2009). The other was PotA, which imports polyamine compounds into the bacterial cell (Ren et al., 2022). This observation can be

explained, as previously mentioned, since metformin may be structurally related to putrescine, leading to potential misrecognition.

In contrast, there was a downregulation of the *agrA* gene in the evolved strain after exposure to metformin, which did not occur in the parent strain. Agr is known to be the quorum- sensing system and the transcriptional regulator for many virulence- encoding genes in *S. aureus* (Traber et al., 2008). It has been reported that *S. aureus* tends to trade off its virulence under antibiotic stress in favour of increasing resistance genes, like the *mecA* gene, (Painter et al., 2014) which is the case here in response to metformin. The downregulation in the evolved strain can be explained by the adaptation of the bacteria to continuous exposure to metformin. In addition, there was downregulation in some genes of the *fab* cluster, which encodes enzymes important in *de novo* fatty acid biosynthesis, along with *acpP,* which encodes the acyl carrier protein forming the *fab- acpP* locus (My et al., 2013). It is known that the process of fatty acid biosynthesis requires a high amount of energy. Therefore, it is reported that bacterial cells under stress tend to decrease their energy-consuming processes like fatty acid biosynthesis (Garay et al., 2014). This further confirms the hypothesis of this study that metformin causes energy depletion and redox stress, leading the bacteria to adapt by decreasing any energy-consuming processes.

Additionally, in the same evolved line, there was downregulation in another group of genes forming the WalKR complex, which is important for cell homeostasis and growth. It has been reported that the inhibition of WalKR enzymes causes thickening of the cell wall and produces more persistent bacterial cells, increasing their resistance to antibiotics (Tan et al., 2022). Furthermore, there was downregulation of the *yycI* and *yycJ* genes, which are known to be the regulators of *walKR*. Their disruption could cause the downregulation of *walKR*, which is reported to increase vancomycin resistance in *S. aureus* (Cameron et al., 2016). It has also been reported that subinhibitory concentrations of chlorhexidine, a biguanide compound with antimicrobial activity, cause downregulation in the expression of *walKR* genes, suggesting that it works on the cell wall degradation of *S. aureus* (Baseri et al., 2021). This may also explain and confirm the hypothesis of metformin causing cell wall stress in *S. aureus.*

5.3.2. The effect of transposon insertions in P. aeruginosa ATCC 27853 at different concentrations of metformin:

It was noted that the knockouts of *carAB* genes were essential for the growth of the bacteria at the sub-inhibitory concentrations of metformin (0.25x and 0.5xMIC). It is known that *carAB* genes are important for encoding the enzyme that catalyses the synthesis of carbamoylphosphate, the precursor for the arginine amino acid. Therefore, it is crucial for bacterial viability, especially under stress (Butcher et al., 2016). This observation aligns with what was mentioned earlier about the upregulation of amino acid synthesis under the stress of sub-inhibitory concentrations of metformin.

Furthermore, the knockouts of the genes encoding MexAB-OprM efflux pump did not survive under the stress of the sub-inhibitory concentrations of metformin, which indicated that this pump could be essential to get rid of metformin out of the cell and inactivation of this pump led to cell death. In contrast, the knockout of *mexR* was highly selective at 1xMIC of metformin compared to the control. MexAB-OprM efflux pump is one of the most important efflux pumps for different classes of antibiotics including quinolones, macrolides, tetracyclines, lincomycin, chloramphenicol, novobiocin, and most β-lactams in *P. aeruginosa* (Lorusso et al., 2022). This pump is regulated by the *mexR* gene, where the protein encoded downregulates the *mexAB-oprM* expression. Therefore, it was reported that the *mexR* mutant causes overexpression of MexAB-OprM efflux pump in *P. aeruginosa,* leading to increased resistance to several antibiotics (Poole et al., 1996). This may suggest that metformin could be a substrate for the MexAB-OprM efflux pump and the bacteria need it to tolerate it and can generate resistance by overexpressing this pump.

In addition, it was noticed that the knockouts of *degP* and *hflCK* genes could not survive at the subinhibitory concentrations of metformin. The *degP* encodes a protease important to degrade the misfolding proteins, while *hflCK* encodes accessory regulator genes for FtSH enzyme, another protease for the misfolding proteins. Both proteases are important for bacterial growth and withstand the oxidative stress and some antibiotics like aminoglycosides (Hinz et al., 2011; Jones et al., 2001).

In contrast, the concentrations of 0.5xMIC and 1xMIC were highly selective for the knockouts of the *aguA* gene, which encodes the agmatine deaminase enzyme that plays an important role in converting agmatine to putrescine. As mentioned previously, putrescine is an important compound for bacteria, supporting cell growth and many cellular processes. Additionally, it can be converted to succinate through biochemical steps and subsequently enter the TCA cycle to be used as a carbon source for energy production (Chou et al., 2008). Based on transcriptomic analysis of the upregulation of *puu* genes responsible for putrescine utilisation, there can be a hypothesis that metformin may inhibit the AguA enzyme due to the similarity in structure between agmatine and metformin, acting as a competitive inhibitor. This would lead to a decrease in the production of putrescine, while the bacteria would simultaneously overexpress putrescine utilisation as a result of mistaking metformin for a polyamine (Figure 5-29). Thus, with the combined effect, there would be a depletion of putrescine (less production, more utilization), adversely affecting cell growth and functions. Also, there could be toxic metabolites due to the interaction between metformin and agmatine deaminase. It was reported that different types of bacteria could degrade metformin using various types of guanyl urea hydrolases (Martinez-Vaz et al., 2022). Therefore, the knockout of the *aguA* gene resulted in greater resistance to metformin at high

concentrations. In the literature, there are no studies about the effect of metformin on the agmatine deaminase enzyme; however, there is a study reporting that metformin could be a competitive inhibitor to agmatinase that works on converting agmatine to putrescine in *E. coli* (Tassoulas & Wackett, 2024), which resembles the AguA in *P. aeruginosa*. This finding is supported by another observation that the knockout of *puuC* gene was beneficial to survival at 0.5x MIC as this would decrease the excessive utilisation of putrescine. Regarding the hypothesis of that the bacteria could recognize metformin as natural polyamine compound, there are some studies showing that the bacteria can use metformin as nitrogen source in presence of carbon source. Tassoulas & Wackett (2024) showed that using the agmatinase in *E. coli* as mentioned previously in this paragraph (Tassoulas & Wackett, 2024). Later in the same year (2024), the same research group found that the wastewater bacteria could evolve some biodegrading enzymes to degrade metformin and use it as a nitrogen source (Tassoulas et al., 2024). In addition, Hillmann, Katie & Niehaus, Thomas (2022) studied two *Pseudomonas* strains from the wastewater that could use metformin as a nitrogen source as well (Hillmann & Niehaus, 2022). Therefore, this together may confirm the idea of how metformin affects the agmatine deaminase and putrescine production.

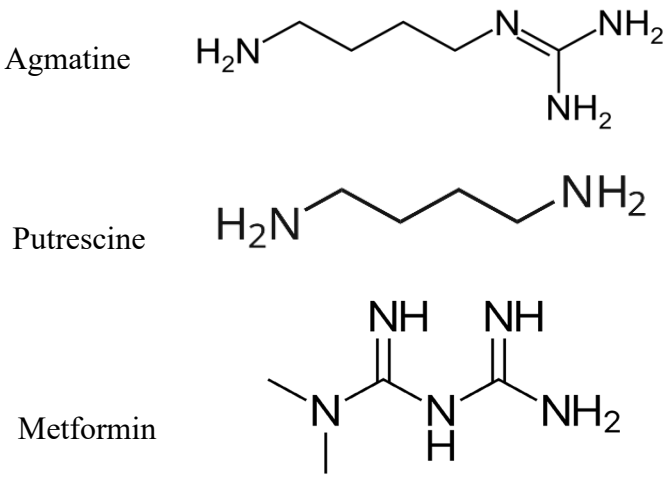

Figure 5-29: The chemical structures of agmatine, putrescine and metformin

Another knockout highly selected in high concentrations of metformin was the one of the *tetC* gene. TetC is one of the most common efflux pumps for the dissemination of tetracycline resistance (Aroca Molina et al., 2024). This observation indicates that the inactivation of the TetC efflux pump is beneficial for bacteria to survive under the stress of metformin. This can be explained by the fact that generally, efflux pumps are energy-consuming, especially if the bacterial cell is under stress, as here (Yamaguchi et al., 2015). Therefore, removing one of the factors causing a burden on the bacterial cell will be beneficial and help it to survive. Another explanation could be that metformin may utilise TetC as a transporter to enter the cell. TetC is from the Major Facilitator Superfamily (MFS) pumps, which are

classified as drug/proton antiporters (Yamaguchi et al., 2015). There was no study about the action of TetC itself for the substrates to influx inside the cell; however, there were studies about other MFS efflux pumps like MdfA (Nagarathinam et al., 2018) and LmrP (Mazurkiewicz, 2004) which showed that under the absence of the proton motive force and disruption of pH gradient, these pumps could influx the substrates through them. Therefore, by the hypothesis of metformin disrupting the PMF, it could do the same effect on TetC pump and use it as transporter inside the cell.

In contrast, the knockouts of *mrpA* genes were depleted at 0.5x MIC, indicating that *mrpA* was essential for survival under metformin stress. This finding is consistent with the transcriptomic data in *S. aureus,* which showed the upregulation of *mrp* genes in the presence of metformin, which supports the disruption of metformin on the PMF and the need for the antiporter to balance the H+ gradient.

It was observed that the knockouts of some glycolytic genes, such as *pgi* and *tpiA,* along with certain genes involved in the TCA cycle, including *aceE, aceF*, *gltA,* and *icd,* benefited the bacteria's survival at 1x MIC, despite being essential without drug stress. This observation supported the previously mentioned hypothesis that metformin caused an NADH/NAD + imbalance by inhibiting the electron transport chain, leading to NADH accumulation. Therefore, these knockouts blocked glycolysis and the TCA cycle, preventing excess NADH generation, which restored the balance and allowed the bacteria to grow better in the presence of metformin. Additionally, this finding aligned with the transcriptomic analysis of the corresponding glycolysis and TCA cycle genes in *S. aureus*, which were downregulated in the presence of metformin. Furthermore, there was selection for the knockouts of certain genes involved in the formation of ETC under metformin stress. Among these genes were *petABC*, which encode for the cytochrome bc1 (Soh et al., 2021), *ccmABCEF*, responsible for the maturation of cytochrome c (Verissimo & Daldal, 2014), along with *nuoB,* which encodes the NDH 1 subunit of NADH dehydrogenase (complex I) of the ETC (Ward et al., 2023). The selection of these knockouts under metformin stress could support the hypothesis that the bacteria attempt to tolerate metformin's effects by shutting down their energy processes and slowing their metabolic rate. It was reported that the knockouts of *nuo* genes in *E. coli* lead to increased cefiderocol resistance, a broad-spectrum cephalosporin, by decreasing NADH levels and lowering oxidative stress (Du et al., 2022). There is insufficient data about the effect of metformin on the production of reactive oxygen species (ROS) in bacteria; however, it was reported that metformin could increase ROS in cancer cells (Warkad et al., 2021). As previously mentioned, metformin could inhibit mitochondrial complex I, resulting in partial inhibition, and it was reported that the partial inhibition of the mitochondrial ETC leads to ROS production (Pelicano et al., 2003). Therefore, this could explain why full inhibition of the bacterial ETC is more beneficial to the cell under metformin stress so as to avoid ROS production.

The disruption of *bioABCDEF* genes was found to be beneficial in resisting the effects of metformin. As mentioned previously, *bio* genes are important in biotin biosynthesis, and this study hypothesises that metformin could inhibit the biotin ligase enzyme, leading to the removal of regulation on the *bio* genes and excess production of biotin, which is energy costly in energy-deficient bacteria. Thus, by knocking out those genes, this effect would cease.

The knockouts in *mlaABCDEF* were selected due to the high concentration of metformin. The Mla system is crucial for maintaining the asymmetry of the outer membrane and preventing its damage. Normally, the outer membrane renders the bacteria highly resistant to various toxic compounds and antibiotics (Munguia et al., 2017). It has been reported in *Acinetobacter baumannii* that the loss of lipopolysaccharides could result in resistance to cationic antimicrobial agents like colistin, which is known to interact with LPS (Moffatt et al., 2010). Another study in *E. coli* demonstrated that the mutant in the *mlaA* gene was resistant to some antimicrobial agents like chlorhexidine (Nasu et al., 2022). Metformin is recognised as a cationic compound, supporting the hypothesis that it interacts with the negative charge of LPS, potentially affecting its permeability. This finding aligns with the transcriptomic analysis in *P. aeruginosa* samples, as the bacteria responded to metformin by overexpressing *arn* resistance genes to modify the LPS.

From the previous findings of both RNA-seq data and TraDIS ones, there were some main proposed mechanisms for metformin's action in the bacteria which are summarised in the following table according to the different pathways that get affected (Table 5-2).

Table 5-2: Combined interpretation of RNA-seq and TraDIS results identifying pathways involved in the response to metformin showing the pathways and genes affected

Pathway	Gene	RNA-Seq	TraDIS	Proposed Effect
RND Efflux pumps	*mexCD*	upregulation		Both data supported that the bacteria would need the efflux pump to get rid of metformin and decrease its efficacy.
	oprJ	upregulation		
	mexAB		Knockout depletion	
	oprM		Knockout depletion	
	mexR (efflux repressor)		Knockout selection	
Respiratory electron transport chain	*qoxABCD*	downregulation		Both data supported that the antibacterial effect of metformin could be due to the disruption of PMF by the redox imbalance as a result of the partial inhibition of the respiratory chain reaction
	atpB	downregulation		
	ndhB	downregulation		
	petABC		Knockout selection	
	nuoB		Knockout selection	
	ccmABCEF		Knockout selection	
Glycolysis and Krebs cycle	*pts*	downregulation		Following the hypothesis of the partial inhibition of the respiratory chain, both data supported that the bacteria may adapt to this effect by shutting down all the energy processes, and any metabolic step that could lead to an increase in NADH, which could lead to an increase in metabolic stress, which includes glycolysis.
	pgi	downregulation	Knockout selection	
	pfk	downregulation		
	fba	downregulation		
	tpiA	downregulation	Knockout selection	
	gapA	downregulation		
	pgk	downregulation		
	eno	downregulation		
	gpmI	downregulation		
	pyk	downregulation		
	pdhA	downregulation		
	pdhB	downregulation		
	aceEF		Knockout selection	
	gltA		Knockout selection	
	icd		Knockout selection	
Bacterial outer membrane	*arnABCDT*	upregulation		Both data supported that Metformin may enter the bacterial cell through interaction with the negative charge of the LPS on the outer membrane in Gram-negative bacteria and the bacteria adapt by changing it.
	mlaABCDEF		Knockout depletion	
Putrescine metabolism	*aguA* (synthesis)		Knockout selection	One proposed mechanism supported that metformin may inhibit enzyme responsible for production of
	puuAB (utilization)	upregulation		

	puuC (utilization)		Knockout selection	putrescine (polyamine compound). Also, it may recognize metformin as putrescine, so increase utilization of putrescine leading to its depletion.
Biotin synthesis	*birA* (biotin repressor)	upregulation		Both data supported the hypothesis of metformin could inhibit biotin ligase leading to increase the bacterial bioburden in biotin synthesis
	bioDKFW	upregulation		
	bioABCDEF		Knockout selection	

5.3.3. The effect of metformin on the metabolic activity of different bacterial species

Using measurements of the changes in the redox tetrazolium dye, the metabolic rate of metformin on different species was investigated in comparison to a drug-free medium. Additionally, as noted in Chapter 3, the MICs of metformin against various bacterial species were tested. It was revealed that the reduction of metabolic activity due to metformin was highest for *E. coli* NCTC 10418, with a percentage reduction of around 90%, despite the MIC of this strain being 40 µg/mL; similar to the other *E. coli* strain. However, the percentage reduction for the other strain was much lower, at around 14%. This was followed by its effect on *S. aureus* NCTC 6571, with approximately 46% reduction, even though its MIC was 10 µg/ml. The percentage reduction for *S. aureus* ATCC 25923 and *P. aeruginosa* NCTC 10662 was around 32%, with an MIC of 40 µg/ml. In contrast, there was about a 16% reduction for the *P. aeruginosa* strain, ATCC 27853, which shared the same MIC of 40 µg/ml. For the *K. pneumoniae* strains, they exhibited the least reduction in metabolic rate, around 12%, with an MIC of 80 ug/ml. This indicates that the effect of metformin is strain-specific, not merely species-specific, and its impact on metabolic rate can differ from its effect on growth. It has been reported that bacterial growth inhibition does not necessarily imply a decrease in cellular respiration alone; it could involve broader metabolism with various compensatory mechanisms from the bacteria (Lobritz et al., 2015).

The effect of combinations of metformin with different known mitochondrial inhibitors was tested, and the analysis revealed that combinations of alexidine with metformin were significantly different from metformin alone in all strains tested. For the *S. aureus* strains, one *P. aeruginosa* strain, and one *E. coli* strain, the combination showed a synergistic effect. Alexidine is a bisbiguanide antimicrobial compound that has shown mitochondrial inhibition in mammalian cells, and it has been reported to disrupt mitochondrial functions by inhibiting mitochondrial phosphatases. In bacterial cells, it is known to disrupt the cell membrane, cause ROS production, and disrupt PMF. It was tested in combination with colistin and rifampicin against *A. baumannii,* showing an additive effect (Doughty-Shenton et al., 2010;

Moffatt et al., 2010). This finding can be explained by the fact that both drugs share closely related structures, with the presence of the biguanide group suggesting they may exhibit similar mechanisms that contribute to their synergistic/additive effect.

Trifluoperazine combinations with metformin were significantly different from the effect of metformin alone in all strains except one, *P. aeruginosa*. For one strain of *S. aureus,* one of *P. aeruginosa,* and one of *K. pneumoniae*, it showed a synergistic effect, and it was additive in the rest, except in *E. coli* NCTC 10418, where it was antagonistic. Trifluoperazine is an antipsychotic drug known to inhibit the mitochondria by blocking calmodulin (Ca^{2+}/Na^{+} transporter), which leads to disruption of cellular respiration and a decrease in ATP synthesis. It has been reported that it could inhibit calmodulin-like peptides in *Mycobacterium,* resulting in decreased ATP production. Additionally, it has been shown to possess some antibacterial activity against *S. aureus, E. coli, A. baumannii,* and *K. pneumoniae* to different extents (Katoch et al., 1998; Nehme et al., 2018; Snelling & Nicholls, 1984). Therefore, this supports the synergistic/additive effect of the combination with trifluoperazine, as both drugs cause a decrease in ATP production by affecting cellular respiration.

The combination of nordihydroguaiaretic (NDGA) with metformin was significantly different in the reduction of the metabolic activity compared to metformin in one *S. aureus* and one *E. coli,* with a synergistic effect, and one *K. pneumoniae* strain with an antagonistic effect. NDGA is a herbal compound that was used before as food preservative; however, it has been revealed that it has some antitumor, antiviral and anti-inflammatory effects. It is reported that NDGA causes mitochondrial dysfunction by disrupting the cell membrane and by inhibition of complex I in the ETC, resulting in a reduction of ATP synthesis. It was studied for its antibacterial effects and tested with the combination of an aminoglycoside, which showed a synergistic effect, suggesting it could be because of the cell membrane damage. The same effect was found with the combination of colistin and caused the reversal of the colistin resistance phenotype (Lü et al., 2010; Pavani et al., 1994; Song et al., 2022). This could suggest that the effect of the combination was strain specific. For the synergistic effect, it may be due to the shared mechanism of NDGA and metformin in decreasing the ATP production. While the antagonistic effect, it may be due to the effect of NDGA in decreasing the ROS and working as antioxidants in some cells (Guzmán-Beltrán et al., 2013).

Celastrol combined with metformin showed an antagonistic effect in one *S. aureus* strain and an additive effect in another *S. aureus* strain, as well as in two *K. pneumoniae* strains. Celastrol is a natural product traditionally used in Chinese medicine as an herbal remedy. It is known for its anti-inflammatory, antioxidant, antitumor effects, and neuroprotective properties. It can function in two different ways: the

first is its antioxidant effect on the mitochondria, which protects the inner membrane, and the second is the increase in reactive oxygen species (ROS) production due to the inhibition of mitochondrial complex I. The mechanism of its action depends on the type of cell. Recently, it was discovered that celastrol has antibacterial properties as an antimetabolic drug, causing an increase in oxidative stress in bacteria (Chen et al., 2011; Diao et al., 2024; ni et al., 2014; Yuan et al., 2023). This could explain the additive effect of the combination, as both drugs inhibit the ETC, resulting in an increase in ROS.

The combination of diclofenac with metformin showed an additive effect in one *S. aureus* and one *K. pneumoniae* strain, while it was antagonistic in another *K. pneumoniae* strain, similar to celastrol. Diclofenac is a non-steroidal anti-inflammatory drug widely used for various inflammatory conditions, including arthritis, musculoskeletal pain, postoperative and post-traumatic pain, and migraine attacks. It has been reported that diclofenac can cause mitochondrial dysfunction by increasing the production of ROS through the accumulation of mitochondrial H_2O_2. Additionally, it has been discovered that diclofenac can inhibit the oxidative phosphorylation process, leading to a reduction in ATP production. In the bacterial community, it was found that diclofenac could inhibit different bacterial species and could resensitize MRSA to β-lactams. There are not enough studies on its effects on the bacterial ETC, but it was found that diclofenac can cause oxidative stress and stimulate the bacterial SOS response (Gan, 2010; S. R. Kim et al., 2024; Li et al., 2023; Zhang et al., 2021). The additive effect could be explained by the possibility that both drugs induce oxidative stress, leading to reduced metabolic activity of the bacterial cells, depending on the strains.

Polymyxin B and metformin combination was found to be antagonistic in the two *P. aeruginosa* and *E. coli* strains. While it exerted an additive effect in the *K. pneumoniae* combination. Polymyxin B, as mentioned previously, is a cationic antimicrobial agent that works mainly on Gram-negative bacteria by disrupting their outer membrane and disrupting the membrane potential. It was discovered that it has some inhibitory effect on the NADH dehydrogenase and reduction of ATP synthesis. In mammalian cells, it was found that polymyxin B can cause a reduction in the mitochondrial membrane potential, induction of ROS production and a decrease in ATP production, which causes cell apoptosis, as tested in nephrotic cells (Azad et al., 2015; Constable et al., 2017; Yu et al., 2019). The antagonistic effect could be explained by the fact that the effect of polymyxin B is much more potent against bacterial cell as a bactericidal agent compared to metformin, so it may kill the cell before causes its function.

The combination of phenformin with metformin showed an antagonistic effect with one *P. aeruginosa* and one *K. pneumoniae*. Phenformin is an old antidiabetic biguanide compound that has antitumor effect as well. It is known to inhibit the mitochondrial complex I, as well as being able to inhibit complex II and IV. In mammalian cells, due to its hydrophobicity, it is more potent than metformin producing ROS

as well (Skemiene et al., 2020). Its effect on the bacterial ETC is not well-studied; however, there is a study showing its antibacterial activity against different bacterial species in comparison to other hypoglycemic drugs including metformin, which showed the similar effect (Dash et al., 2011). Due to the similarities between the two compounds, they may compete to the same inhibitory targets, decreasing their function.

The combination of papaverine and metformin was significantly antagonistic in one *S. aureus* and one *P. aeruginosa* strain, while it exhibited synergy in one *E. coli* strain. Papaverine is an alkaloid extracted from the opium plant, known for its skeletal muscle relaxant effects. It is identified as a potent inhibitor of mitochondrial complex I and increases ROS production, which can be utilised to resensitize tumors to radiotherapy. Additionally, it has some antiviral and antifungal properties, alongside its anti-inflammatory, antitumor, and neuroprotective effects. Although the detailed mechanism of action of papaverine is well understood, it has been reported that the extract of *Papaver spp.* possesses some antibacterial effects (Ashrafi et al., 2023; Benej et al., 2018). As with other combinations, this one is strain-specific as well. It was observed that the effect of papaverine alone is much less in *S. aureus* and *P. aeruginosa* compared to metformin, relative to what occurs in *E. coli*. This may indicate that metformin is more potent against *S. aureus* and *P. aeruginosa*; if they share similar targets, papaverine may compete with metformin or cause cells to sense them faster, increasing the adaptation rate.

The combination of amitriptyline with metformin has a significantly additive effect with one *P. aeruginosa* strain, a synergistic effect with one *E. coli* strain and an antagonistic effect with one *K. pneumoniae* strain. Amitriptyline is an antidepressant drug that shows oxidative stress effects in mammalian cells. It was investigated because of its antitumor effect was found to be as effective as some chemotherapeutics because of the resultant cytotoxicity. Also, it was reported that it causes a deficiency of Coenzyme Q10 (CoQ10), which is an important part of the mitochondrial respiratory chain. This can lead to an increase in the production of ROS and disruption of membrane potential. Despite its effect on the bacterial respiratory chain not being well studied, it was reported that amitriptyline inhibits various species of bacteria (Mandal et al., 2010; Moreno-Fernández et al., 2012; Villanueva et al., 2016).

$CaCl_2$ was tested in combination with metformin, and it was found to have an additive effect for one *P. aeruginosa* and one *K. pneumoniae* strain, while it showed an antagonistic effect for one *E. coli* and the other *K. pneumoniae* strain. The studies showed that $CaCl_2$ can cause indirect mitochondrial inhibition by causing an overload of Ca^{2+} on the mitochondria, which disrupts the ion homeostasis needed for the respiratory process (Duchen, 2000). In the microbiology field, $CaCl_2$ is used in bacterial transformation due to its positive charge, so it can neutralise the charge on the bacterial cell and increase the uptake of DNA (Asif et al., 2017). In the literature there is controversy regarding the action of $CaCl_2$, as some

studies demonstrate its antibacterial effect on certain species, like in the study of Rajamma et al. (2021), while other studies indicate that it could increase the growth of some bacteria, such as *E. coli*, in the study of Dupree et al. (2019). This discrepancy could explain the antagonistic effect between $CaCl_2$ and metformin in the *E. coli* strain, as $CaCl_2$ alone showed increased growth compared to the control.

In conclusion, metformin showed a strain-dependent reduction in bacterial metabolic activity that did not consistently correlate with MIC values, indicating that inhibition of cellular respiration is not the only factor in growth suppression. This supports the idea that bacterial viability can be occurred due to compensatory pathways despite impaired ETC function. The combination studies between metformin and the other mitochondrial inhibitors revealed that the synergy was most evident when compounds depend on ATP depletion or ETC disruption, whereas antagonism likely arose from target competition, opposing effects on reactive oxygen species (ROS), or differences in bactericidal kinetics.

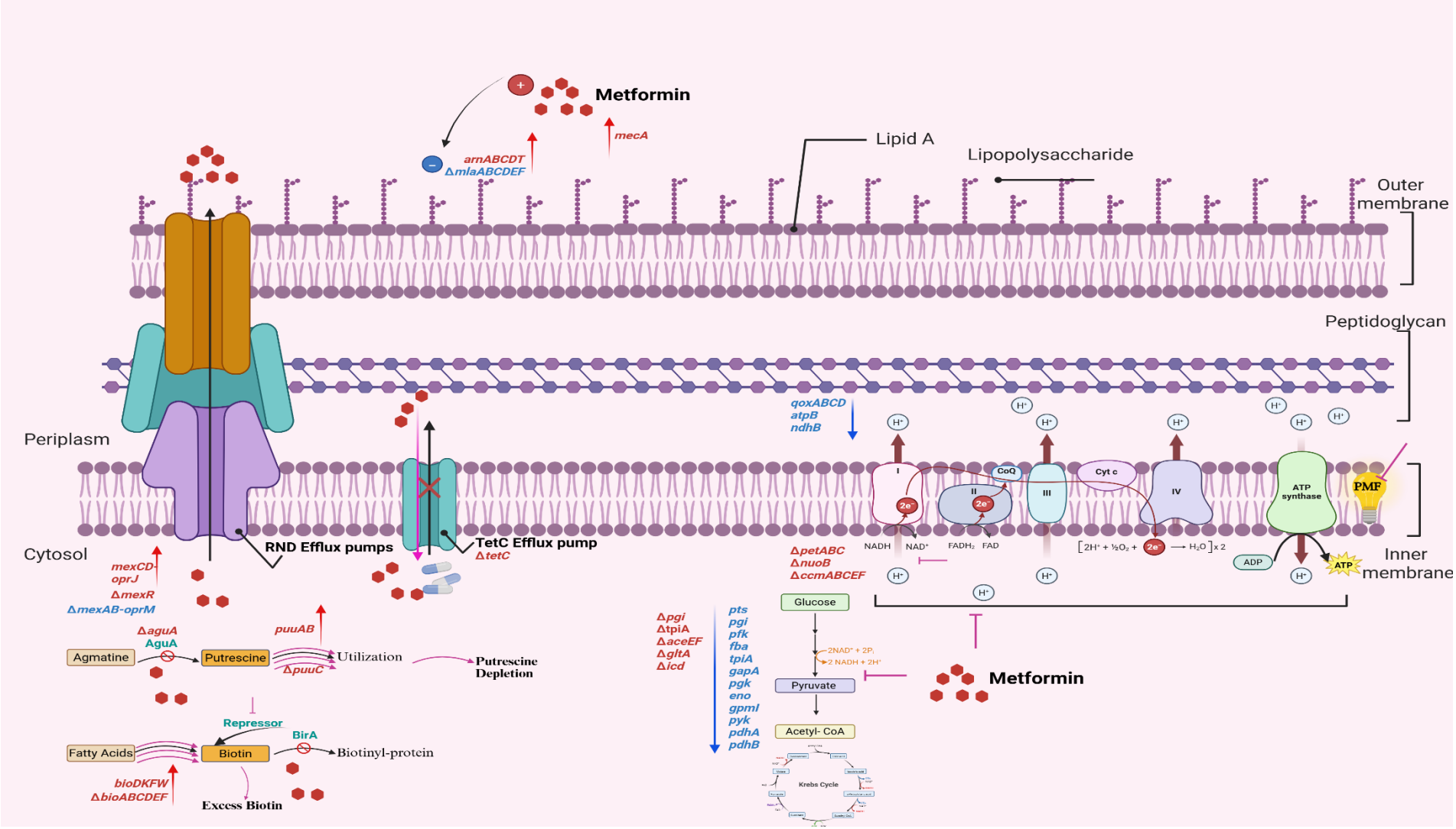

Figure 5-30 Illustration summarizing the main proposed mechanisms of metformin's action on the bacteria and how the bacteria could respond.
The red arrows (↑) with genes besides indicate upregulation of these genes; the blue arrows (↓) with genes besides indicate downregulation of these genes; the red delta Δ with genes besides indicates that the knockout of this gene is selected in metformin; the blue delta Δ with genes besides indicates that the knockout of this gene is depleted in metformin; ⊥ indicates inhibitory effect. Created in https://BioRender.com

CHAPTER 6- General Discussion

6. General Discussion

Metformin, the antidiabetic drug, has been investigated in recent years for its antibacterial effects. However, it remains unclear how it works specifically and whether it acts on bacterial cells similarly to its effects on mammalian mitochondria as part of its antidiabetic action. Additionally, inconsistencies have emerged regarding its effects, particularly whether it possesses antivirulence activity or increases virulence gene expression, and whether it serves as a general efflux pump inhibitor or enhances the expression of efflux genes. Furthermore, it is important to explore its potential as an adjuvant drug and whether it is beneficial across various species. Moreover, as a long-term medication, it is crucial to examine whether continuous exposure to metformin can lead to a reduced susceptibility in bacteria, especially when combined with other antibiotics. Therefore, this thesis aimed to address some of these gaps and study more comprehensively the mechanism of action of metformin and how bacteria adapt to it.

Metformin as an antibacterial, antivirulence agent and antimetabolic agent

In this thesis, the effect of metformin on bacterial phenotype was investigated and it was revealed that it had an inhibitory effect on the growth of different bacterial species, both Gram-positive and Gram-negative, but in a species-strain-specific manner, which could be due to the different genetic backgrounds that reduced its inhibitory effects with some strains. This was consistent with the reported studies in the literature (Abbas et al., 2017; Meherunisa et al., 2018; X. Xiao et al., 2022); however, one focus of this project was to investigate the effect of metformin at therapeutic levels, not just very high concentrations. Mainly, metformin showed inhibitory effect on growth at sub-inhibitory concentrations, but in supra-therapeutic levels, except in one *S. aureus* strain.

Metformin showed antivirulence activity against protease and biofilm formation at some concentrations that did not significantly inhibit growth, which was reported on some strains in the literature indicating that its antivirulence activity was not due to a decrease in cell number but rather to its action on the cell itself, which could be explained by the reported idea that metformin can act as quorum sensing inhibitor (Abbas et al., 2017; Jatin Chadha et al., 2023).

Metformin exposure resulted in a decrease in the metabolic rates of the different bacterial species to different extents despite their MICs, which supports the idea that metformin has a strain-specific activity with a different mechanism of action. To the best of our knowledge, this observation has not been previously reported.

Disruption of bacterial respiration and proton motive force as a unifying mechanism

One of the hypotheses studied in this thesis was that the antibacterial effect of metformin could be due to the disruption of PMF by the redox imbalance as a result of inhibition of the respiratory chain reaction. This was slightly tested in the literature with some experiments for measuring the membrane potential in the presence and absence of high concentrations of metformin in combination with other antibiotics (Liu et al., 2020b; Y. Xiao et al., 2022). However, in this thesis, this observation was molecularly supported by the down-regulation of several components of the electron transport chain. As a result, the bacteria adapt to that by shutting down all the energy processes, and any metabolic step that could lead to an increase in NADH, which could lead to an increase in metabolic stress. Therefore, it was noticed that there was down-regulation of all genes responsible for glycolysis, and the knockouts of the glycolytic genes were beneficial for the bacterial cell to survive under the metformin stress. In addition, the knockouts of some of the electron transport chain components were selected in the presence of metformin, which supports the hypothesis that metformin partially inhibits the bacterial electron transport chain, and therefore completely blocking it by knocking out it's function, reduces the oxidative stress. Furthermore, the combination of metformin with some of the mitochondrial inhibitors that shared the same supposed mechanism showed additive/synergistic effect on the bacterial metabolic activity, like with alexidine, trifluoperazine, NDGA, celastrol, diclofenac and amitriptyline. This collectively supports the effect of metformin in inhibition of bacterial respiration, which could result in oxidative stress, ROS production and energy depletion, which aligns with the reported hypothesis about metformin's mechanism of action; however, there is no published data yet on the explanatory function of metformin on the molecular level.

The disruption of PMF has been studied generally in the literature and has been shown to affect the bacterial physiology. One of these changes is its effect on the growth of the bacteria, slowing down their dynamics and potentially increasing bacterial tolerance to antibiotics (Wan et al., 2024). This phenomenon was observed in this study through prolonged lag and slowing exponential phases, a general pattern across most tested bacterial strains following exposure to metformin.

The variable effect of metformin on bacterial efflux pumps and concentration-dependent responses

One of the contradictions in the literature was whether metformin could act as an efflux pump inhibitor or not. Some studies have shown that metformin is an efflux pump inhibitor, and others have shown that exposure to metformin causes overexpression of efflux genes (Abbas et al., 2021b; Wei et al., 2022). Therefore, this thesis presented a novel explanatory side of this contradictory aspect.

Metformin showed no efflux inhibitory effect at sub-inhibitory concentrations phenotypically. This aligns with the up-regulation of various efflux pumps such as *mexCD-oprJ, smvA,* and *emrE* when *P. aeruginosa* was exposed to a sub-inhibitory concentration of metformin, indicating that these efflux pumps are crucial for eliminating metformin and for bacterial survival. Consequently, the knockouts of *mexAB-oprM* genes could not survive in sub-inhibitory concentrations of metformin. In contrast, the higher concentrations of metformin could indirectly inhibit bacterial efflux as shown in the efflux activity in *S. aureus* only at the MIC concentration, which could be explained by the fact that efflux pumps need PMF to work efficiently (Kabra et al., 2019). In line with the proposed mechanism of metformin discussed earlier, the high concentrations of it may lead to high level of disruptions of PMF which result in inhibiting the effect of the efflux pump, which could reveal now the contradictories in the literature.

Another newly discussed hypothesis in this thesis was that metformin could utilise the TetC efflux pump as an importer to enter the cell as a result of the disruption in PMF, which TetC relies on for its activity. This was supported by the knockouts of the *tetC* gene, which grew better at high concentrations of metformin. This could explain the synergistic effect of metformin with doxycycline against *P. aeruginosa* and *K. pneumoniae*, which are doxycycline-resistant strains that may have the TetC, tetracycline efflux pump, which align with some reported studies for the synergism between metformin and tetracyclines (Guo et al., 2022; Liu et al., 2020b) but with new explanation in this study.

Conversely, the disruption of PMF due to metformin could be the reason for the antagonistic effect with gentamicin against *K. pneumoniae* which aligned with the literature (Y. Xiao et al., 2022), but here we could explain it as the bacteria needs the PMF for the cellular uptake of gentamicin.

Novel insights into metformin's interaction with the bacterial cell

Metformin, a cationic compound, may enter the bacterial cell through interaction with the negative charge of the LPS in Gram-negative bacteria. Therefore, the bacteria may adapt to the presence of metformin by alteration of the lipid A part of LPS. This was supported by the overexpression of *arn* genes. In addition, the loss of LPS integrity by the knockouts of *mla* genes resulted in more survival in the presence of metformin. Metformin could cause the same effect in Gram-positive bacteria, causing cell wall stress, and this was supported by the up-regulation of *the mecA* resistant gene. Together, these findings represent a previously unexplored dimension of metformin's interaction with bacterial cell envelope structures.

Two additional hypotheses regarding metformin's mechanism of action in the bacterial cell were also explored. One suggests that metformin may inhibit the agmatine deaminase enzyme, which is important in the production of putrescine, a polyamine compound, leading to the formation of some toxic

metabolites (Martinez-Vaz et al., 2022). Additionally, the bacteria recognise metformin as a polyamine compound and, therefore, up-regulate the *puu* genes for its utilisation. These combined actions could lead to the depletion of putrescine, a critical compound for many cellular processes. This is supported by the knockdown of the agmatine deaminase-encoding gene (*aguA),* which was selective in the presence of metformin. One recent paper supported this idea by discussing metformin as a competitive inhibitor to agmatinase (a microbial enzyme similar to agmatine deaminase) (Tassoulas & Wackett, 2024) but without knowing the resulting effect of that on the expression of the genes.

The other hypothesis indicates that metformin could inhibit the biotin ligase enzyme (BirA). This is supported by the up-regulation of biotin biosynthesis genes (*bio)* due to the absence of their repressor, as well as the upregulation of *birA* itself as a feedback response, resulting in the dysregulation of biotin synthesis, which creates metabolic burden on the bacterial cell (Satiaputra et al., 2018). This is further supported by the knockouts of *bio* genes that were selected in high concentrations of metformin, which is a newly discussed hypothesis about the effect of metformin on the bacterial cell. Collectively, both hypotheses suggest that the bacteria may mistakenly recognise metformin, which contains one amino group and a biguanide group, as a natural polyamine compound, resulting in these inhibitory effects. Although there is little data in the literature on this idea and its inhibitory effect, some articles suggest that bacteria can recognise metformin as a polyamine compound that can serve as a nitrogen source for their metabolism (Hillmann & Niehaus, 2022; Tassoulas et al., 2024).

Adaptation to chronic metformin exposure: tolerance and persistence

Another dimension of this thesis was to investigate how bacteria could adapt to continuous exposure to low physiological concentrations of metformin, a topic that is rarely discussed in the literature. There are a few papers that have discussed the long-term exposure of bacteria to metformin, but either at very low concentrations (Wei et al., 2022), which may not reveal all possible effects, or on the gut microbiome (Kim et al., 2024), not a highly resistant pathogen, without investigations into the bacterial kinetics, phenotypic and genotypic properties and the cross-resistance of other antibiotics. In these studies, the primary reported outcome of prolonged metformin exposure has been efflux pump up-regulation, which represents only one of the adaptive strategies observed in this thesis.

The evolutionary experiment showed that the bacteria could adapt in different ways to metformin, even if there was no change in the MIC. The tolerance in some drug-evolved populations appeared as an increase in bacterial growth, especially in high concentrations of metformin, alongside a reduction in metformin's effect on proteolytic activity, which may suggest that the bacteria could adapt to the presence of metformin by enhancing their growth and protease production as a form of protection. The same evolved lines in *P. aeruginosa* exhibited decreased susceptibility to other antibiotics at sub-inhibitory concentrations, such as gentamicin, colistin, and ciprofloxacin, as well as to erythromycin,

doxycycline, linezolid, and vancomycin in the *S. aureus* evolved population. These evolved lines contained mutations that indicate these changes in the phenotypic properties as a result of metformin stress could be related to biofilm formation (*fbnA),* cell wall metabolism, and energy production through the formation of metabolic intermediates in glycolysis (*gatD)* in *S. aureus* or acetoin catabolism (*acoR)* and redox balance (*pntB* and *dsbD) in P. aeruginosa,* suggesting that the bacteria could adapt to metformin by lowering their energy production and employing alternative pathways for cellular processes.

In other evolved populations, adaptation occurred by slowing the growth of the bacteria as a fitness cost of the mutation that could have happened, preparing itself to be biofilm-like or persistent-like cells. Those evolved lines showed a decrease in their protease activity and an increase in biofilm formation, which could also explain the reduction in the area under the curves of the different antibiotics tested in those strains. This could be supported by the mutation in the intergenic areas of *t-RNA* in some of those evolved lines and in *argJ* in others, known to play a role in the formation of persisters in different bacterial species. This could suggest that the bacteria could adapt to metformin by down-regulating their cellular processes to enter the dormant stage, which is supported by the up-regulation of *deo* and downregulation of *wbpI* genes in *S. aureus* evolved line compared to the wild type without exposure to the drug, directing the cell to import new nucleotides required for DNA repair under stress rather than for synthesis. Also, in the same evolved population, the exposure of metformin led to down-regulation of the quorum-sensing regulator *agrA* which impacts on the other virulence factors. Supporting the same idea of the persisters, the evolved line adapted to metformin by down-regulating *walKR* genes that result in thickening of the cell wall. All these findings could suggest that the exposure to metformin can result in formation of persisters with slower growth and could explain the reduction of the area under the curve of this evolved line in the different antibiotics tested.

It was found that one way of adaptation to metformin involved efflux pumps which is the only published way, either by up-regulating more efficient ones like SmvA and EmrE, or through mutations in one of them that could enable the pump to operate more efficiently than the wildtype, such as MexD, which could explain the decrease in susceptibility to various antibiotics.

Conclusion

In conclusion, metformin exhibits strain-species specific antibacterial effects at various concentrations, including certain physiological concentrations. Generally, its impact may be attributed to its effect on different metabolic processes within bacterial cells that lead to redox stress, energy depletion, and disruption of the PMF, which may also serve as one mechanism for entering the bacterial cell. One proposed mechanism is that bacteria mistakenly recognise metformin as a natural polyamine compound,

which interferes with enzymatic actions. Due to metformin's mode of action, it may have a synergistic effect with some antibiotics while being antagonistic to others, so its use as adjunct therapy should be approached with caution, depending on the bacterial strain and the antibiotic. Additionally, it has been observed that bacteria can adapt to the presence of metformin by utilising efflux pumps, up-regulating certain resistance genes, and developing persistent-like cells by reducing energy processes within the cell. Despite prolonged exposure to metformin not resulting in the generation of resistant strains, which is clinically good for the diabetic patients taking metformin, the formation of persisters could contribute to longer-lasting infections, making it crucial to conduct further investigations to better understand its effects in conjunction with various antibiotics, particularly in diabetic patients who are vulnerable to bacterial infections.

Future Work

The findings of this thesis have revealed several important questions that need further investigation. Addressing these areas will be essential for validating the proposed mechanisms and assessing the clinical relevance of metformin–bacteria interactions:

1. Future studies should directly quantify changes in proton motive force, membrane potential, and intracellular redox balance in metformin-treated bacterial cells. Measurement of reactive oxygen species production would further clarify whether oxidative stress contributes to metformin-mediated metabolic inhibition.

2. Further investigation is needed to clarify the importance of the TetC pump in the action of metformin and its effect on the synergistic interaction with doxycycline in resistant strains. And whether this is the only explanation of this interaction or there are other ones.

3. More validation should be employed to test if the proposed mechanism of metformin's inhibition is truly happening in the candidate targets identified in this thesis, including agmatine deaminase (AguA) and biotin ligase (BirA), which could be tested by measuring the enzyme activity assays in the presence and absence of metformin

4. The changes in the susceptibilities of different antibiotics due to long-term exposure to metformin need to be repeated with more replicates to yield statistically meaningful results, especially given the interesting patterns observed in the drug-evolution populations.

5. In vivo infection models, particularly in diabetic hosts receiving long-term metformin therapy, would help assess whether bacterial adaptations influence infection duration or treatment outcomes. Also, testing the effect of metformin on clinical strains, especially multidrug-resistant ones, would be important for providing a clearer picture of its impact in the antibiotic resistance environment.

REFERENCES

References

Abbas, H., Shaker, G., Khattab, R., & Askoura, M. (2021a). A NEW ROLE OF METFORMIN AS AN EFFLUX PUMP INHIBITOR IN KLEBSIELLA PNEUMONIA. *Journal of microbiology, biotechnology and food sciences*, *11*. https://doi.org/10.15414/jmbfs.4232

Abbas, H., Shaker, G., Khattab, R., & Askoura, M. (2021b). A NEW ROLE OF METFORMIN AS AN EFFLUX PUMP INHIBITOR IN KLEBSIELLA PNEUMONIA. *Journal of microbiology, biotechnology and food sciences*, *11*(1), e4232. https://doi.org/10.15414/jmbfs.4232

Abbas, H. A., Elsherbini, A. M., & Shaldam, M. A. (2017). Repurposing metformin as a quorum sensing inhibitor in Pseudomonas aeruginosa. *African health sciences*, *17*(3), 808–819. https://doi.org/10.4314/ahs.v17i3.24

Abbas, H. A., Shaker, G. H., Mosallam, F. M., & Gomaa, S. E. (2022). Novel silver metformin nano-structure to impede virulence of Staphylococcus aureus. *AMB Express*, *12*(1), 84. https://doi.org/10.1186/s13568-022-01426-6

Agius, L., Ford, B. E., & Chachra, S. S. (2020). The Metformin Mechanism on Gluconeogenesis and AMPK Activation: The Metabolite Perspective. *International journal of molecular sciences*, *21*(9). https://doi.org/10.3390/ijms21093240

Ahmad, M., Wolberg, A., & Kahwaji, C. I. (2025). Biochemistry, Electron Transport Chain. In *StatPearls* (Updated 2023 Sep 4 ed.). StatPearls Publishing.

Ahmed, M. N., Abdelsamad, A., Wassermann, T., Porse, A., Becker, J., Sommer, M. O. A., Høiby, N., & Ciofu, O. (2020). The evolutionary trajectories of P. aeruginosa in biofilm and planktonic growth modes exposed to ciprofloxacin: beyond selection of antibiotic resistance. *npj Biofilms and Microbiomes*, *6*(1), 28. https://doi.org/10.1038/s41522-020-00138-8

Alberts, B., Johnson, A., Lewis, J., & et al. (2002). The Evolution of Electron-Transport Chains. In *Molecular Biology of the Cell* (4th edition ed.). Garland Science.

Aljofan, M., & Riethmacher, D. (2019). Anticancer activity of metformin: a systematic review of the literature. *Future Sci OA*, *5*(8), Fso410. https://doi.org/10.2144/fsoa-2019-0053

Altman, D. G., & Bland, J. M. (2005). Standard deviations and standard errors. *Bmj*, *331*(7521), 903. https://doi.org/10.1136/bmj.331.7521.903

Alzahrani, A. K., & Alzahrani, H. A. (2025). Ibuprofen inhibits quorum sensing and biofilm formation in Pseudomonas aeruginosa. *Frontiers in pharmacology*, *10*(1557333).

Andersson, S. G., Zomorodipour, A., Andersson, J. O., Sicheritz-Pontén, T., Alsmark, U. C., Podowski, R. M., Näslund, A. K., Eriksson, A. S., Winkler, H. H., & Kurland, C. G. (1998). The genome sequence of Rickettsia prowazekii and the origin of mitochondria. *Nature*, *396*(6707), 133–140. https://doi.org/10.1038/24094

Andrews, S. (2010). FastQC: A quality control analysis tool for high throughput sequencing data. In.

Angaroni, F., Peruzzi, A., Alvarenga, E. Z., & Pinheiro, F. (2025). Translating microbial kinetics into quantitative responses and testable hypotheses using Kinbiont. *Nat Commun*, *16*(1), 6440. https://doi.org/10.1038/s41467-025-61592-6

Aroca Molina, K. J., Gutiérrez, S. J., Benítez-Campo, N., & Correa, A. (2024). Genomic Differences Associated with Resistance and Virulence in Pseudomonas aeruginosa Isolates from Clinical and Environmental Sites. *Microorganisms*, *12*(6), 1116.

Balaban, N. Q., Helaine, S., Lewis, K., Ackermann, M., Aldridge, B., Andersson, D. I., Brynildsen, M. P., Bumann, D., Camilli, A., Collins, J. J., Dehio, C., Fortune, S., Ghigo, J. M., Hardt, W. D., Harms, A., Heinemann, M., Hung, D. T., Jenal, U., Levin, B. R.,...Zinkernagel, A. (2019).

Definitions and guidelines for research on antibiotic persistence. *Nat Rev Microbiol*, *17*(7), 441–448. https://doi.org/10.1038/s41579-019-0196-3

Barbarossa, A., Bragagni, M., & Dini, I. (2022). Repurposing non-antibiotic drugs as antibacterial agents: focus on NSAIDs and statins. *Pharmaceuticals*, *15*(11), 1301. https://doi.org/10.3390/ph15111301

Barbarossa, A., Rosato, A., Corbo, F., Clodoveo, M. L., Fracchiolla, G., Carrieri, A., & Carocci, A. (2022). Non-Antibiotic Drug Repositioning as an Alternative Antimicrobial Approach. *Antibiotics*, *11*(6), 816.

Barquist, L., Mayho, M., Cummins, C., Cain, A. K., Boinett, C. J., Page, A. J., Langridge, G. C., Quail, M. A., Keane, J. A., & Parkhill, J. (2016). The TraDIS toolkit: sequencing and analysis for dense transposon mutant libraries. *Bioinformatics*, *32*(7), 1109–1111. https://doi.org/10.1093/bioinformatics/btw022

Barrick, J. E., & Lenski, R. E. (2013). Genome dynamics during experimental evolution. *Nat Rev Genet*, *14*(12), 827–839. https://doi.org/10.1038/nrg3564

Baseri, N., Najar-Peerayeh, S., & Bakhshi, B. (2021). The effect of subinhibitory concentration of chlorhexidine on the evolution of vancomycin-intermediate Staphylococcus aureus and the induction of mutations in walKR and vraTSR systems. *Infection, Genetics and Evolution*, *87*, 104628. https://doi.org/https://doi.org/10.1016/j.meegid.2020.104628

Beetham, C. M., Schuster, C. F., Santiago, M., Walker, S., & Gründling, A. (2023). Histidine and its uptake are essential for the growth of Staphylococcus aureus at low pH. *bioRxiv*, 2023.2007.2025.550546. https://doi.org/10.1101/2023.07.25.550546

Begeç, Z., Gulhas, N., Toprak, H., Yetkin, G., Kuzucu, C., & Ersoy, O. (2007). Comparison of the Antibacterial Activity of Lidocaine 1% Versus Alkalinized Lidocaine In Vitro. *Current therapeutic research, clinical and experimental*, *68*, 242–248. https://doi.org/10.1016/j.curtheres.2007.08.007

Berbers, B., Vanneste, K., Roosens, N., Marchal, K., Ceyssens, P. J., & De Keersmaecker, S. C. J. (2023). Using a combination of short- and long-read sequencing to investigate the diversity in plasmid- and chromosomally encoded extended-spectrum beta-lactamases (ESBLs) in clinical Shigella and Salmonella isolates in Belgium. *Microb Genom*, *9*(1). https://doi.org/10.1099/mgen.0.000925

Bertrand, R. L. (2019). Lag Phase Is a Dynamic, Organized, Adaptive, and Evolvable Period That Prepares Bacteria for Cell Division. *J Bacteriol*, *201*(7). https://doi.org/10.1128/jb.00697-18

Bohnert, J. A., Szymaniak-Vits, M., Schuster, S., & Kern, W. V. (2011). Efflux inhibition by selective serotonin reuptake inhibitors in Escherichia coli. *J Antimicrob Chemother*, *66*(9), 2057–2060. https://doi.org/10.1093/jac/dkr258

Bolger, A. M., Lohse, M., & Usadel, B. (2014). Trimmomatic: a flexible trimmer for Illumina sequence data. *Bioinformatics*, *30*(15), 2114–2120. https://doi.org/10.1093/bioinformatics/btu170

Bouras, G., Houtak, G., Wick, R. R., Mallawaarachchi, V., Roach, M. J., Papudeshi, B., Judd, L. M., Sheppard, A. E., Edwards, R. A., & Vreugde, S. (2024). Hybracter: enabling scalable, automated, complete and accurate bacterial genome assemblies. *Microb Genom*, *10*(5). https://doi.org/10.1099/mgen.0.001244

Brämer, C., Silva, L., Gomez, G., Priefert, H., & Steinbüchel, A. (2002). Identification of the 2-Methylcitrate Pathway Involved in the Catabolism of Propionate in the Polyhydroxyalkanoate-Producing Strain Burkholderia sacchari IPT101T and Analysis of a Mutant Accumulating a Copolyester with Higher 3-Hydroxyvalerate Content. *Applied and environmental microbiology*, *68*, 271–279. https://doi.org/10.1128/AEM.68.1.271-279.2002

British Society for Antimicrobial, C. (2013). *BSAC standardized disc susceptibility testing method*. https://bsac.org.uk/wp-content/uploads/2012/02/Version-12-Apr-2013_final.pdf

Butcher, B. G., Chakravarthy, S., D'Amico, K., Stoos, K. B., & Filiatrault, M. J. (2016). Disruption of the carA gene in Pseudomonas syringae results in reduced fitness and alters motility. *BMC Microbiology*, *16*(1), 194. https://doi.org/10.1186/s12866-016-0819-z

Cabral, D. J., Wurster, J. I., & Belenky, P. (2018). Antibiotic Persistence as a Metabolic Adaptation: Stress, Metabolism, the Host, and New Directions. *Pharmaceuticals*, *11*(1), 14.

Cabreiro, F., Au, C., Leung, K.-Y., Vergara-Irigaray, N., Cochemé, H. M., Noori, T., Weinkove, D., Schuster, E., Greene, N. D. E., & Gems, D. (2013). Metformin retards aging in C. elegans by altering microbial folate and methionine metabolism. *Cell*, *153*(1), 228–239. https://doi.org/10.1016/j.cell.2013.02.035

Calvert, J. W., Gundewar, S., Jha, S., Greer, J. J., Bestermann, W. H., Tian, R., & Lefer, D. J. (2008). Acute metformin therapy confers cardioprotection against myocardial infarction via AMPK-eNOS-mediated signaling. *Diabetes*, *57*(3), 696–705. https://doi.org/10.2337/db07-1098

Calvio, C., Celandroni, F., Ghelardi, E., Amati, G., Salvetti, S., Ceciliani, F., Galizzi, A., & Senesi, S. (2005). Swarming differentiation and swimming motility in Bacillus subtilis are controlled by swrA, a newly identified dicistronic operon. *J Bacteriol*, *187*(15), 5356–5366. https://doi.org/10.1128/jb.187.15.5356-5366.2005

Cameron, D. R., Jiang, J.-H., Kostoulias, X., Foxwell, D. J., & Peleg, A. Y. (2016). Vancomycin susceptibility in methicillin-resistant Staphylococcus aureus is mediated by YycHI activation of the WalRK essential two-component regulatory system. *Scientific Reports*, *6*(1), 30823. https://doi.org/10.1038/srep30823

Carvajal-Garcia, J., Samadpour, A. N., Hernandez Viera, A. J., & Merrikh, H. (2023). Oxidative stress drives mutagenesis through transcription-coupled repair in bacteria. *Proceedings of the National Academy of Sciences*, *120*(27), e2300761120. https://doi.org/doi:10.1073/pnas.2300761120

Carver, T., Harris, S. R., Berriman, M., Parkhill, J., & McQuillan, J. A. (2012). Artemis: an integrated platform for visualization and analysis of high-throughput sequence-based experimental data. *Bioinformatics*, *28*(4), 464–469. https://doi.org/10.1093/bioinformatics/btr703

Casqueiro, J., Casqueiro, J., & Alves, C. (2012). Infections in patients with diabetes mellitus: A review of pathogenesis. *Indian journal of endocrinology and metabolism*, *16 Suppl 1*(Suppl1), S27–S36. https://doi.org/10.4103/2230-8210.94253

Chadha, J., Khullar, L., Gulati, P., Chhibber, S., & Harjai, K. (2023). Anti-virulence prospects of Metformin against Pseudomonas aeruginosa: A new dimension to a multifaceted drug. *Microbial Pathogenesis*, *183*, 106281. https://doi.org/https://doi.org/10.1016/j.micpath.2023.106281

Chadha, J., Khullar, L., Gulati, P., Chhibber, S., & Harjai, K. (2023). Anti-virulence prospects of Metformin against Pseudomonas aeruginosa: A new dimension to a multifaceted drug. *Microb Pathog*, *183*, 106281. https://doi.org/10.1016/j.micpath.2023.106281

Chaffin, D. O., Taylor, D., Skerrett, S. J., & Rubens, C. E. (2012). Changes in the Staphylococcus aureus Transcriptome during Early Adaptation to the Lung. *PloS one*, *7*(8), e41329. https://doi.org/10.1371/journal.pone.0041329

Chandra, S., Prithvi, P. P. R., Srija, K., Jauhari, S., & Grover, A. (2020). Antimicrobial resistance: Call for rational antibiotics practice in India. *Journal of family medicine and primary care*, *9*(5), 2192–2199. https://doi.org/10.4103/jfmpc.jfmpc_1077_19

Chen, Q., Yu, Y., Xu, Y., Quan, H., Liu, D., Li, C., Liu, M., & Gong, X. (2024). Salmonella Typhimurium alters galactitol metabolism under ciprofloxacin treatment to balance resistance and virulence. *J Bacteriol*, *206*(8), e00178–00124. https://doi.org/doi:10.1128/jb.00178-24

Cheng, F. F., Liu, Y. L., Du, J., & Lin, J. T. (2022). Metformin's Mechanisms in Attenuating Hallmarks of Aging and Age-Related Disease. *Aging Dis*, *13*(4), 970–986. https://doi.org/10.14336/ad.2021.1213

Chopra, I., & Roberts, M. (2001). Tetracycline antibiotics: Mode of action, applications, molecular biology, and epidemiology of bacterial resistance. *Microbiology and Molecular Biology Reviews*, *65*(2), 232–260.

Chou, H. T., Kwon, D. H., Hegazy, M., & Lu, C. D. (2008). Transcriptome analysis of agmatine and putrescine catabolism in Pseudomonas aeruginosa PAO1. *J Bacteriol*, *190*(6), 1966–1975. https://doi.org/10.1128/jb.01804-07

Chowdhury, S., Yung, E., Pintilie, M., Muaddi, H., Chaib, S., Yeung, M., Fusciello, M., Sykes, J., Pitcher, B., Hagenkort, A., McKee, T., Vellanki, R., Chen, E., Bristow, R. G., Wouters, B. G., & Koritzinsky, M. (2016). MATE2 Expression Is Associated with Cancer Cell Response to Metformin. *PLoS One*, *11*(12), e0165214. https://doi.org/10.1371/journal.pone.0165214

Chuanchuen, R., Beinlich, K., Hoang, T. T., Becher, A., Karkhoff-Schweizer, R. R., & Schweizer, H. P. (2001). Cross-resistance between triclosan and antibiotics in Pseudomonas aeruginosa is mediated by multidrug efflux pumps: exposure of a susceptible mutant strain to triclosan selects nfxB mutants overexpressing MexCD-OprJ. *Antimicrob Agents Chemother*, *45*(2), 428–432. https://doi.org/10.1128/aac.45.2.428-432.2001

CLSI. (2015). *Methods for Dilution Antimicrobial Susceptibility Tests for Bacteria That Grow Aerobically; Approved Standard—Tenth Edition*. (CLSI).

Clyne, M. (2014). Metformin—the new wonder drug? *Nature Reviews Urology*, *11*(7), 366–366. https://doi.org/10.1038/nrurol.2014.136

Croucher, N. J., & Thomson, N. R. (2010). Studying bacterial transcriptomes using RNA-seq. *Current Opinion in Microbiology*, *13*(5), 619–624. https://doi.org/https://doi.org/10.1016/j.mib.2010.09.009

Cutrona, N., Gillard, K., Ulrich, R., Seemann, M., Miller, H. B., & Blackledge, M. S. (2019). From Antihistamine to Anti-infective: Loratadine Inhibition of Regulatory PASTA Kinases in Staphylococci Reduces Biofilm Formation and Potentiates β-Lactam Antibiotics and Vancomycin in Resistant Strains of Staphylococcus aureus. *ACS Infect Dis*, *5*(8), 1397–1410. https://doi.org/10.1021/acsinfecdis.9b00096

Darby, E. M., Trampari, E., Siasat, P., Gaya, M. S., Alav, I., Webber, M. A., & Blair, J. M. A. (2023). Molecular mechanisms of antibiotic resistance revisited. *Nature Reviews Microbiology*, *21*(5), 280–295. https://doi.org/10.1038/s41579-022-00820-y

Dastidar, S. G., Ganguly, K., Chaudhuri, K., & Chakrabarty, A. N. (2011). The antibacterial action of diclofenac. *Annals of Clinical Microbiology and Antimicrobials*, *10*(30).

Davies, J., & Davies, D. (2010). Origins and evolution of antibiotic resistance. *Microbiology and Molecular Biology Reviews*, *74*(3), 417–433.

De Coster, W., & Van Broeckhoven, C. (2019). Newest Methods for Detecting Structural Variations. *Trends in Biotechnology*, *37*(9), 973–982. https://doi.org/https://doi.org/10.1016/j.tibtech.2019.02.003

de la Cuesta-Zuluaga, J., Mueller, N. T., Corrales-Agudelo, V., Velásquez-Mejía, E. P., Carmona, J. A., Abad, J. M., & Escobar, J. S. (2017). Metformin Is Associated With Higher Relative Abundance of Mucin-Degrading Akkermansia muciniphila and Several Short-Chain Fatty Acid-Producing Microbiota in the Gut. *40*(1), 54–62. https://doi.org/10.2337/dc16-1324

de Winter, J. (2013). Using the Student's t-test with extremely small sample sizes. *Practical Assessment, Research & Evaluation*, *18*.

Deatherage, D. E., & Barrick, J. E. (2014). Identification of mutations in laboratory-evolved microbes from next-generation sequencing data using breseq. *Methods Mol Biol*, *1151*, 165–188. https://doi.org/10.1007/978-1-4939-0554-6_12

Decensi, A., Puntoni, M., Goodwin, P., Cazzaniga, M., Gennari, A., Bonanni, B., & Gandini, S. (2010). Metformin and cancer risk in diabetic patients: a systematic review and meta-analysis. *Cancer Prev Res (Phila)*, *3*(11), 1451–1461. https://doi.org/10.1158/1940-6207.Capr-10-0157

Dettman, J. R., Sztepanacz, J. L., & Kassen, R. (2016). The properties of spontaneous mutations in the opportunistic pathogen Pseudomonas aeruginosa. *BMC Genomics*, *17*(1), 27. https://doi.org/10.1186/s12864-015-2244-3

Didelot, X., Bowden, R., Wilson, D. J., Peto, T. E. A., & Crook, D. W. (2012). Transforming clinical microbiology with bacterial genome sequencing. *Nat Rev Genet*, *13*(9), 601–612. https://doi.org/10.1038/nrg3226

Doughty-Shenton, D., Joseph, J. D., Zhang, J., Pagliarini, D. J., Kim, Y., Lu, D., Dixon, J. E., & Casey, P. J. (2010). Pharmacological targeting of the mitochondrial phosphatase PTPMT1. *J Pharmacol Exp Ther*, *333*(2), 584–592. https://doi.org/10.1124/jpet.109.163329

Du, G.-F., Dong, Y., Fan, X., Yin, A., Le, Y.-J., & Yang, X.-Y. (2022). Proteomic Investigation of the Antibacterial Mechanism of Cefiderocol against Escherichia coli. *Microbiology Spectrum*, *10*(5), e01093–01022. https://doi.org/10.1128/spectrum.01093-22

Duckworth, B. P., Geders, T. W., Tiwari, D., Boshoff, H. I., Sibbald, P. A., Barry, C. E., 3rd, Schnappinger, D., Finzel, B. C., & Aldrich, C. C. (2011). Bisubstrate adenylation inhibitors of biotin protein ligase from Mycobacterium tuberculosis. *Chem Biol*, *18*(11), 1432–1441. https://doi.org/10.1016/j.chembiol.2011.08.013

Elbere, I., Kalnina, I., Silamikelis, I., Konrade, I., Zaharenko, L., Sekace, K., Radovica-Spalvina, I., Fridmanis, D., Gudra, D., Pirags, V., & Klovins, J. (2018). Association of metformin administration with gut microbiome dysbiosis in healthy volunteers. *PLoS One*, *13*(9), e0204317–e0204317. https://doi.org/10.1371/journal.pone.0204317

Elkins, C. A., & Nikaido, H. (2002). Substrate specificity of the RND-type multidrug efflux pumps AcrB and AcrD of Escherichia coli is determined predominantly by two large periplasmic loops. *J Bacteriol*, *184*(23), 6490–6498. https://doi.org/10.1128/jb.184.23.6490-6499.2002

Ezzamouri, B., Rosario, D., Bidkhori, G., Lee, S., Uhlen, M., & Shoaie, S. (2023). Metabolic modelling of the human gut microbiome in type 2 diabetes patients in response to metformin treatment. *npj Systems Biology and Applications*, *9*(1), 2. https://doi.org/10.1038/s41540-022-00261-6

Fang, H., Zeng, G., Gu, W., Wang, Y., Zhao, J., Zheng, T., Xu, L., Liu, Y., Zhang, J., Sun, X., & Zhang, G. (2022). Genome Recombination-Mediated tRNA Up-Regulation Conducts General Antibiotic Resistance of Bacteria at Early Stage. *Frontiers in Microbiology*, *12*. https://doi.org/10.3389/fmicb.2021.793923

Fang, X., Fang, Z., Zhao, J., Zou, Y., Li, T., Wang, J., Guo, Y., Chang, D., Su, L., Ni, P., & Liu, C. (2012). Draft genome sequence of Pseudomonas aeruginosa strain ATCC 27853. *J Bacteriol*, *194*(14), 3755. https://doi.org/10.1128/jb.00690-12

Fontaine, E. (2018). Metformin-Induced Mitochondrial Complex I Inhibition: Facts, Uncertainties, and Consequences. *Frontiers in endocrinology*, *9*, 753. https://doi.org/10.3389/fendo.2018.00753

Foreman, S., Ferrara, K., Hreha, T. N., Duran-Pinedo, A. E., Frias-Lopez, J., & Barquera, B. (2021). Genetic and Biochemical Characterization of the Na(+)/H(+) Antiporters of Pseudomonas aeruginosa. *J Bacteriol*, *203*(18), e0028421. https://doi.org/10.1128/jb.00284-21

Foretz, M., Guigas, B., Bertrand, L., Pollak, M., & Viollet, B. (2014). Metformin: From Mechanisms of Action to Therapies. *Cell Metabolism*, *20*(6), 953–966. https://doi.org/https://doi.org/10.1016/j.cmet.2014.09.018

Foretz, M., Guigas, B., & Viollet, B. (2023). Metformin: update on mechanisms of action and repurposing potential. *Nat Rev Endocrinol*, *19*(8), 460–476. https://doi.org/10.1038/s41574-023-00833-4

Forslund, K., Hildebrand, F., Nielsen, T., Falony, G., Le Chatelier, E., Sunagawa, S., Prifti, E., Vieira-Silva, S., Gudmundsdottir, V., Krogh Pedersen, H., Arumugam, M., Kristiansen, K., Yvonne Voigt, A., Vestergaard, H., Hercog, R., Igor Costea, P., Roat Kultima, J., Li, J., Jørgensen, T.,…Meta, H. I. T. c. (2015). Disentangling type 2 diabetes and metformin treatment signatures in the human gut microbiota. *Nature*, *528*(7581), 262–266. https://doi.org/10.1038/nature15766

Founou, R. C., Founou, L. L., & Essack, S. Y. (2017). Clinical and economic impact of antibiotic resistance in developing countries: A systematic review and meta-analysis. *PLoS One*, *12*(12), e0189621–e0189621. https://doi.org/10.1371/journal.pone.0189621

Gao, J., & Gussin, G. N. (1991). Mutations in TrpI binding site II that differentially affect activation of the trpBA promoter of Pseudomonas aeruginosa. *Embo j*, *10*(13), 4137–4144. https://doi.org/10.1002/j.1460-2075.1991.tb04991.x

Garay, L. A., Boundy-Mills, K. L., & German, J. B. (2014). Accumulation of high-value lipids in single-cell microorganisms: a mechanistic approach and future perspectives. *J Agric Food Chem*, *62*(13), 2709–2727. https://doi.org/10.1021/jf4042134

Garnett, J. P., Baker, E. H., Naik, S., Lindsay, J. A., Knight, G. M., Gill, S., Tregoning, J. S., & Baines, D. L. (2013). Metformin reduces airway glucose permeability and hyperglycaemia-induced Staphylococcus aureus load independently of effects on blood glucose. *Thorax*, *68*(9), 835–845. https://doi.org/10.1136/thoraxjnl-2012-203178

Gaynes, R. (2017). The discovery of penicillin—New insights after more than 75 years of clinical use. *Emerging Infectious Diseases*, *23*(5), 849–853.

Ge, S. X., Jung, D., & Yao, R. (2019). ShinyGO: a graphical gene-set enrichment tool for animals and plants. *Bioinformatics*, *36*(8), 2628–2629. https://doi.org/10.1093/bioinformatics/btz931

Goel, M., & Schneeberger, K. (2022). plotsr: visualizing structural similarities and rearrangements between multiple genomes. *Bioinformatics*, *38*(10), 2922–2926. https://doi.org/10.1093/bioinformatics/btac196

Goel, M., Sun, H., Jiao, W.-B., & Schneeberger, K. (2019). SyRI: finding genomic rearrangements and local sequence differences from whole-genome assemblies. *Genome Biology*, *20*(1), 277. https://doi.org/10.1186/s13059-019-1911-0

Gomaa, S. E., Shaker, G. H., Mosallam, F. M., & Abbas, H. A. (2022). Knocking down Pseudomonas aeruginosa virulence by oral hypoglycemic metformin nano emulsion. *World Journal of Microbiology and Biotechnology*, *38*(7), 119. https://doi.org/10.1007/s11274-022-03302-8

Gong, L., Goswami, S., Giacomini, K. M., Altman, R. B., & Klein, T. E. (2012). Metformin pathways: pharmacokinetics and pharmacodynamics. *Pharmacogenetics and genomics*, *22*(11), 820–827. https://doi.org/10.1097/FPC.0b013e3283559b22

Graziano, T. S., Cuzzullin, M. C., Franco, G. C., Schwartz-Filho, H. O., de Andrade, E. D., Groppo, F. C., & Cogo-Müller, K. (2015). Statins and Antimicrobial Effects: Simvastatin as a

Potential Drug against Staphylococcus aureus Biofilm. *PLoS One*, *10*(5), e0128098. https://doi.org/10.1371/journal.pone.0128098

Grimsey, E. M., & Piddock, L. J. V. (2019). Do phenothiazines possess antimicrobial and efflux inhibitory properties? *FEMS Microbiology Reviews*, *43*(6), 577–590. https://doi.org/10.1093/femsre/fuz017

Guo, T., Sun, X., Yang, J., Yang, L., Li, M., Wang, Y., Jiao, H., & Li, G. (2022). Metformin reverse minocycline to inhibit minocycline-resistant Acinetobacter baumannii by destroy the outer membrane and enhance membrane potential in vitro. *BMC Microbiology*, *22*(1), 215. https://doi.org/10.1186/s12866-022-02629-4

Hall-Stoodley, L., Costerton, J. W., & Stoodley, P. (2004). Bacterial biofilms: from the natural environment to infectious diseases. *Nat Rev Microbiol*, *2*(2), 95–108. https://doi.org/10.1038/nrmicro821

Hankins, J. V., Madsen, J. A., Needham, B. D., Brodbelt, J. S., & Trent, M. S. (2013). The outer membrane of Gram-negative bacteria: lipid A isolation and characterization. *Methods Mol Biol*, *966*, 239–258. https://doi.org/10.1007/978-1-62703-245-2_15

Heller, D., & Vingron, M. (2020). SVIM-asm: structural variant detection from haploid and diploid genome assemblies. *Bioinformatics*, *36*(22-23), 5519–5521. https://doi.org/10.1093/bioinformatics/btaa1034

Herman-Bausier, P., El-Kirat-Chatel, S., Foster, T. J., Geoghegan, J. A., & Dufrêne, Y. F. (2015). Staphylococcus aureus Fibronectin-Binding Protein A Mediates Cell-Cell Adhesion through Low-Affinity Homophilic Bonds. *mBio*, *6*(3), e00413–00415. https://doi.org/10.1128/mBio.00413-15

Hillmann, K. B., & Niehaus, T. D. (2022). Genome Sequences of Two Pseudomonas Isolates That Can Use Metformin as the Sole Nitrogen Source. *Microbiol Resour Announc*, *11*(9), e0063922. https://doi.org/10.1128/mra.00639-22

Hinz, A., Lee, S., Jacoby, K., & Manoil, C. (2011). Membrane proteases and aminoglycoside antibiotic resistance. *J Bacteriol*, *193*(18), 4790–4797. https://doi.org/10.1128/jb.05133-11

Hooper, D. C. (2001). Emerging mechanisms of fluoroquinolone resistance. *Emerging Infectious Diseases*, *7*(2), 337–341.

Horakova, O., Kroupova, P., Bardova, K., Buresova, J., Janovska, P., Kopecky, J., & Rossmeisl, M. (2019). Metformin acutely lowers blood glucose levels by inhibition of intestinal glucose transport. *Scientific Reports*, *9*(1), 6156. https://doi.org/10.1038/s41598-019-42531-0

Huang, L., Wu, C., Gao, H., Xu, C., Dai, M., Huang, L., Hao, H., Wang, X., & Cheng, G. (2022). Bacterial Multidrug Efflux Pumps at the Frontline of Antimicrobial Resistance: An Overview. *Antibiotics (Basel)*, *11*(4). https://doi.org/10.3390/antibiotics11040520

Huang, Y., Wang, X., Yan, C., Li, C., Zhang, L., Zhang, L., Liang, E., Liu, T., & Mao, J. (2022). Effect of metformin on nonalcoholic fatty liver based on meta-analysis and network pharmacology. *Medicine (Baltimore)*, *101*(43), e31437. https://doi.org/10.1097/md.0000000000031437

Huemer, M., Shambat, S., Bergada-Pijuan, J., Söderholm, S., Boumasmoud-Puginier, M., Vulin, c., Gomez Mejia, A., Antelo, M., Tripathi, V., Götschi, S., Maggio, E., Hasse, B., Brugger, S., Bumann, D., Schuepbach, R., & Zinkernagel, A. (2021). Molecular reprogramming and phenotype switching in Staphylococcus aureus lead to high antibiotic persistence and affect therapy success. *Proceedings of the National Academy of Sciences*, *118*, e2014920118. https://doi.org/10.1073/pnas.2014920118

Janet-Maitre, M., Job, V., Bour, M., Robert-Genthon, M., Brugière, S., Triponney, P., Cobessi, D., Couté, Y., Jeannot, K., & Attrée, I. (2024). Pseudomonas aeruginosa MipA-MipB envelope

proteins act as new sensors of polymyxins. *mBio*, *15*(3), e0221123. https://doi.org/10.1128/mbio.02211-23
Jiang, Y., Chen, H., Wang, J., & Liu, X. (2023). Metformin Promotes Bacterial Surface Aggregation by Inhibiting Swimming Motility of Flagellated Escherichia coli. *Microbiology Spectrum*, *11*(3), e04768–04722. https://doi.org/10.1128/spectrum.04768-22
Jones, C. H., Bolken, T. C., Jones, K. F., Zeller, G. O., & Hruby, D. E. (2001). Conserved DegP protease in gram-positive bacteria is essential for thermal and oxidative tolerance and full virulence in Streptococcus pyogenes. *Infect Immun*, *69*(9), 5538–5545. https://doi.org/10.1128/iai.69.9.5538-5545.2001
Kabra, R., Chauhan, N., Kumar, A., Ingale, P., & Singh, S. (2019). Efflux pumps and antimicrobial resistance: Paradoxical components in systems genomics. *Prog Biophys Mol Biol*, *141*, 15–24. https://doi.org/10.1016/j.pbiomolbio.2018.07.008
Kanehisa, M., & Sato, Y. (2020). KEGG Mapper for inferring cellular functions from protein sequences. *Protein Sci*, *29*(1), 28–35. https://doi.org/10.1002/pro.3711
Kanehisa, M., Sato, Y., & Morishima, K. (2016). BlastKOALA and GhostKOALA: KEGG Tools for Functional Characterization of Genome and Metagenome Sequences. *J Mol Biol*, *428*(4), 726–731. https://doi.org/10.1016/j.jmb.2015.11.006
Katoch, V. M., Saxena, N., Shivannavar, C. T., Sharma, V. D., Katoch, K., Sharma, R. K., & Murthy, P. S. (1998). Effect of trifluoperazine on in vitro ATP synthesis by Mycobacterium leprae. *FEMS Immunology & Medical Microbiology*, *20*(2), 99–102. https://doi.org/10.1111/j.1574-695X.1998.tb01115.x
Kearns, D. B. (2010). A field guide to bacterial swarming motility. *Nat Rev Microbiol*, *8*(9), 634–644. https://doi.org/10.1038/nrmicro2405
Khayat, M. T., Abbas, H. A., Ibrahim, T. S., Elbaramawi, S. S., Khayyat, A. N., Alharbi, M., Hegazy, W. A. H., & Yehia, F. A.-z. A. (2023). Synergistic Benefits: Exploring the Anti-Virulence Effects of Metformin/Vildagliptin Antidiabetic Combination against Pseudomonas aeruginosa via Controlling Quorum Sensing Systems. *Biomedicines*, *11*(5), 1442.
Khil, P. P., & Camerini-Otero, R. D. (2002). Over 1000 genes are involved in the DNA damage response of Escherichia coli. *Molecular Microbiology*, *44*(1), 89–105. https://doi.org/https://doi.org/10.1046/j.1365-2958.2002.02878.x
Kim, H. B., Cho, Y. J., & Choi, S. S. (2024). Metformin increases gut multidrug resistance genes in type 2 diabetes, potentially linked to Escherichia coli. *Sci Rep*, *14*(1), 21480. https://doi.org/10.1038/s41598-024-72467-z
Kim, S., Patel, D. S., Park, S., Slusky, J., Klauda, J. B., Widmalm, G., & Im, W. (2016). Bilayer Properties of Lipid A from Various Gram-Negative Bacteria. *Biophys J*, *111*(8), 1750–1760. https://doi.org/10.1016/j.bpj.2016.09.001
Ko, H. H. T., Lareu, R. R., Dix, B. R., & Hughes, J. D. (2017). Statins: antimicrobial resistance breakers or makers? *PeerJ*, *5*, e3952. https://doi.org/10.7717/peerj.3952
Koh, C. S., & Sarin, L. P. (2018). Transfer RNA modification and infection – Implications for pathogenicity and host responses. *Biochimica et Biophysica Acta (BBA) - Gene Regulatory Mechanisms*, *1861*(4), 419–432. https://doi.org/https://doi.org/10.1016/j.bbagrm.2018.01.015
Kohanski, M. A., DePristo, M. A., & Collins, J. J. (2010). Sublethal antibiotic treatment leads to multidrug resistance via radical-induced mutagenesis. *Mol Cell*, *37*(3), 311–320. https://doi.org/10.1016/j.molcel.2010.01.003
Koren, S., Walenz, B. P., Berlin, K., Miller, J. R., Bergman, N. H., & Phillippy, A. M. (2017). Canu: scalable and accurate long-read assembly via adaptive k-mer weighting and repeat separation. *Genome Res*, *27*(5), 722–736. https://doi.org/10.1101/gr.215087.116

Kracke, F., Vassilev, I., & Krömer, J. O. (2015). Microbial electron transport and energy conservation – the foundation for optimizing bioelectrochemical systems [Review]. *Frontiers in Microbiology*, *Volume 6 - 2015*. https://doi.org/10.3389/fmicb.2015.00575

Krzyżek, P., Migdał, P., Tusiewicz, K., Zawadzki, M., & Szpot, P. (2024). Subinhibitory concentrations of antibiotics affect development and parameters of Helicobacter pylori biofilm. *Front Pharmacol*, *15*, 1477317. https://doi.org/10.3389/fphar.2024.1477317

Lagadinou, M., Kofteridis, D. P., & Samonis, G. (2020). Drug repurposing for antibacterial therapy: an update. *International Journal of Antimicrobial Agents*, *56*(6). https://doi.org/10.1016/j.ijantimicag.2020.106210

Lalau, J.-D., Lemaire-Hurtel, A.-S., & Lacroix, C. (2011). Establishment of a Database of Metformin Plasma Concentrations and Erythrocyte Levels in Normal and Emergency Situations. *Clinical drug investigation*, *31*(6), 435–438. https://doi.org/10.2165/11588310-000000000-00000

Lalau, J. D., Lemaire-Hurtel, A. S., & Lacroix, C. (2011). Establishment of a database of metformin plasma concentrations and erythrocyte levels in normal and emergency situations. *Clin Drug Investig*, *31*(6), 435–438. https://doi.org/10.2165/11588310-000000000-00000

Lamichhane-Khadka, R., Dulal, S., Cuaron, J. A., Pfeltz, R., Gupta, S. K., Wilkinson, B. J., & Gustafson, J. E. (2021). Apt (Adenine Phosphoribosyltransferase) Mutation in Laboratory-Selected Vancomycin-Intermediate Staphylococcus aureus. *Antibiotics*, *10*(5), 583.

Łasica, A. M., & Jagusztyn-Krynicka, E. K. (2007). The role of Dsb proteins of Gram-negative bacteria in the process of pathogenesis. *FEMS Microbiology Reviews*, *31*(5), 626–636. https://doi.org/10.1111/j.1574-6976.2007.00081.x

Lázár, V., Pal Singh, G., Spohn, R., Nagy, I., Horváth, B., Hrtyan, M., Busa-Fekete, R., Bogos, B., Méhi, O., Csörgő, B., Pósfai, G., Fekete, G., Szappanos, B., Kégl, B., Papp, B., & Pál, C. (2013). Bacterial evolution of antibiotic hypersensitivity. *Mol Syst Biol*, *9*, 700. https://doi.org/10.1038/msb.2013.57

Leclercq, R., & Courvalin, P. (1997). Resistance to glycopeptides in enterococci. *Clinical Infectious Diseases*, *24*(4), 545–556.

Lee, H.-J., & Cha, J.-Y. (2018). Recent insights into the role of ChREBP in intestinal fructose absorption and metabolism. *BMB reports*, *51*. https://doi.org/10.5483/BMBRep.2018.51.9.197

Lee, H., & Ko, G. (2014). Effect of metformin on metabolic improvement and gut microbiota. *Applied and environmental microbiology*, *80*(19), 5935–5943. https://doi.org/10.1128/AEM.01357-14

Lee, Y., Kim, A. H., Kim, E., Lee, S., Yu, K.-S., Jang, I.-J., Chung, J.-Y., & Cho, J.-Y. (2021). Changes in the gut microbiome influence the hypoglycemic effect of metformin through the altered metabolism of branched-chain and nonessential amino acids. *Diabetes Research and Clinical Practice*, *178*. https://doi.org/10.1016/j.diabres.2021.108985

Lexis, C. P., van der Horst, I. C., Lipsic, E., van der Harst, P., van der Horst-Schrivers, A. N., Wolffenbuttel, B. H., de Boer, R. A., van Rossum, A. C., van Veldhuisen, D. J., & de Smet, B. J. (2012). Metformin in non-diabetic patients presenting with ST elevation myocardial infarction: rationale and design of the glycometabolic intervention as adjunct to primary percutaneous intervention in ST elevation myocardial infarction (GIPS)-III trial. *Cardiovasc Drugs Ther*, *26*(5), 417–426. https://doi.org/10.1007/s10557-012-6413-1

Li, B., Qiu, Y., Shi, H., & Yin, H. (2016). The importance of lag time extension in determining bacterial resistance to antibiotics. *Analyst*, *141*(10), 3059–3067. https://doi.org/10.1039/c5an02649k

Li, B., Qiu, Y., Shi, H., & Yin, H. (2016). The importance of lag time extension in determining bacterial resistance to antibiotics. *The Analyst*, *141*. https://doi.org/10.1039/C5AN02649K

Li, H. (2018). Minimap2: pairwise alignment for nucleotide sequences. *Bioinformatics*, *34*(18), 3094–3100. https://doi.org/10.1093/bioinformatics/bty191

Li, H., Handsaker, B., Wysoker, A., Fennell, T., Ruan, J., Homer, N., Marth, G., Abecasis, G., Durbin, R., & Subgroup, G. P. D. P. (2009). The Sequence Alignment/Map format and SAMtools. *Bioinformatics*, *25*(16), 2078–2079. https://doi.org/10.1093/bioinformatics/btp352

Li, X. Z., Poole, K., & Nikaido, H. (2003). Contributions of MexAB-OprM and an EmrE homolog to intrinsic resistance of Pseudomonas aeruginosa to aminoglycosides and dyes. *Antimicrob Agents Chemother*, *47*(1), 27–33. https://doi.org/10.1128/aac.47.1.27-33.2003

Lindsay, S., Oates, A., & Bourdillon, K. (2017). The detrimental impact of extracellular bacterial proteases on wound healing. *Int Wound J*, *14*(6), 1237–1247. https://doi.org/10.1111/iwj.12790

Liu, Q., Liu, Y., Kang, Z., Xiao, D., Gao, C., Xu, P., & Ma, C. (2018). 2,3-Butanediol catabolism in Pseudomonas aeruginosa PAO1. *Environmental Microbiology*, *20*(11), 3927–3940. https://doi.org/https://doi.org/10.1111/1462-2920.14332

Liu, Y., Jia, Y., Yang, K., Li, R., Xiao, X., Zhu, K., & Wang, Z. (2020a). Metformin Restores Tetracyclines Susceptibility against Multidrug Resistant Bacteria. *Advanced Science*, *7*, 1902227. https://doi.org/10.1002/advs.201902227

Liu, Y., Jia, Y., Yang, K., Li, R., Xiao, X., Zhu, K., & Wang, Z. (2020b). Metformin Restores Tetracyclines Susceptibility against Multidrug Resistant Bacteria [https://doi.org/10.1002/advs.201902227]. *Advanced Science*, *7*(12), 1902227. https://doi.org/https://doi.org/10.1002/advs.201902227

Lo Sciuto, A., Cervoni, M., Stefanelli, R., Mancone, C., & Imperi, F. (2020). Effect of lipid A aminoarabinosylation on Pseudomonas aeruginosa colistin resistance and fitness. *International Journal of Antimicrobial Agents*, *55*(5), 105957. https://doi.org/https://doi.org/10.1016/j.ijantimicag.2020.105957

Lobritz, M. A., Belenky, P., Porter, C. B. M., Gutierrez, A., Yang, J. H., Schwarz, E. G., Dwyer, D. J., Khalil, A. S., & Collins, J. J. (2015). Antibiotic efficacy is linked to bacterial cellular respiration. *Proceedings of the National Academy of Sciences*, *112*(27), 8173–8180. https://doi.org/doi:10.1073/pnas.1509743112

Lorusso, A. B., Carrara, J. A., Barroso, C. D. N., Tuon, F. F., & Faoro, H. (2022). Role of Efflux Pumps on Antimicrobial Resistance in Pseudomonas aeruginosa. *International journal of molecular sciences*, *23*(24). https://doi.org/10.3390/ijms232415779

Lü, J. M., Nurko, J., Weakley, S. M., Jiang, J., Kougias, P., Lin, P. H., Yao, Q., & Chen, C. (2010). Molecular mechanisms and clinical applications of nordihydroguaiaretic acid (NDGA) and its derivatives: an update. *Med Sci Monit*, *16*(5), Ra93–100.

Luengo, A., Sullivan, L. B., & Heiden, M. G. V. (2014). Understanding the complex-I-ty of metformin action: limiting mitochondrial respiration to improve cancer therapy. *BMC Biology*, *12*(1), 82. https://doi.org/10.1186/s12915-014-0082-4

M. Shafik, S., Abbas, H. A., Yousef, N., & Saleh, M. M. (2023). Crippling of Klebsiella pneumoniae virulence by metformin, N-acetylcysteine and secnidazole. *BMC Microbiology*, *23*(1), 229. https://doi.org/10.1186/s12866-023-02969-9

Maarouf, L., Amin, M., Evans, B. A., & Abouelfetouh, A. (2023). Knowledge, attitudes and behaviour of Egyptians towards antibiotic use in the community: can we do better?

Antimicrobial Resistance & Infection Control, *12*(1), 50. https://doi.org/10.1186/s13756-023-01249-5

Madiraju, A. K., Erion, D. M., Rahimi, Y., Zhang, X. M., Braddock, D. T., Albright, R. A., Prigaro, B. J., Wood, J. L., Bhanot, S., MacDonald, M. J., Jurczak, M. J., Camporez, J. P., Lee, H. Y., Cline, G. W., Samuel, V. T., Kibbey, R. G., & Shulman, G. I. (2014). Metformin suppresses gluconeogenesis by inhibiting mitochondrial glycerophosphate dehydrogenase. *Nature*, *510*(7506), 542–546. https://doi.org/10.1038/nature13270

Magiorakos, A. P., Srinivasan, A., Carey, R. B., Carmeli, Y., Falagas, M. E., Giske, C. G., Harbarth, S., Hindler, J. F., Kahlmeter, G., Olsson-Liljequist, B., Paterson, D. L., Rice, L. B., Stelling, J., Struelens, M. J., Vatopoulos, A., Weber, J. T., & Monnet, D. L. (2012). Multidrug-resistant, extensively drug-resistant and pandrug-resistant bacteria: an international expert proposal for interim standard definitions for acquired resistance. *Clinical Microbiology and Infection*, *18*(3), 268–281. https://doi.org/10.1111/j.1469-0691.2011.03570.x

Maier, L., Pruteanu, M., Kuhn, M., Zeller, G., Telzerow, A., Anderson, E. E., Brochado, A. R., Fernandez, K. C., Dose, H., Mori, H., Patil, K. R., Bork, P., & Typas, A. (2018). Extensive impact of non-antibiotic drugs on human gut bacteria. *Nature*, *555*(7698), 623–628. https://doi.org/10.1038/nature25979

Maity, S., Leton, N., Nayak, N., Jha, A., Anand, N., Thompson, K., Boothe, D., Cromer, A., Garcia, Y., Al-Islam, A., & Nauhria, S. (2024). A systematic review of diabetic foot infections: pathogenesis, diagnosis, and management strategies. *Front Clin Diabetes Healthc*, *5*, 1393309. https://doi.org/10.3389/fcdhc.2024.1393309

Maji, H. S., Maji, S., & Bhattacharya, M. (2017). An Exploratory Study on the Antimicrobial Activity of Cetirizine Dihydrochloride. *Indian Journal of Pharmaceutical Sciences*, *79*(5), 751–757.

Martinez-Vaz, B. M., Dodge, A. G., Lucero, R. M., Stockbridge, R. B., Robinson, A. A., Tassoulas, L. J., & Wackett, L. P. (2022). Wastewater bacteria remediating the pharmaceutical metformin: Genomes, plasmids and products [Original Research]. *Frontiers in Bioengineering and Biotechnology*, *Volume 10 - 2022*. https://doi.org/10.3389/fbioe.2022.1086261

Masadeh, M., Mhaidat, N., Alzoubi, K., Al-Azzam, S., & Alnasser, Z. (2012). Antibacterial activity of statins: a comparative study of atorvastatin, simvastatin, and rosuvastatin. *Ann Clin Microbiol Antimicrob*, *11*, 13. https://doi.org/10.1186/1476-0711-11-13

Masadeh, M. M., Alzoubi, K. H., Masadeh, M. M., & Aburashed, Z. O. (2021). Metformin as a Potential Adjuvant Antimicrobial Agent Against Multidrug Resistant Bacteria. *Clin Pharmacol*, *13*, 83–90. https://doi.org/10.2147/cpaa.S297903

Masuda, N., Sakagawa, E., Ohya, S., Gotoh, N., Tsujimoto, H., & Nishino, T. (2000). Substrate specificities of MexAB-OprM, MexCD-OprJ, and MexXY-oprM efflux pumps in Pseudomonas aeruginosa. *Antimicrob Agents Chemother*, *44*(12), 3322–3327. https://doi.org/10.1128/aac.44.12.3322-3327.2000

Mateus, A., Shah, M., Hevler, J., Kurzawa, N., Bobonis, J., Typas, A., & Savitski Mikhail, M. (2021). Transcriptional and Post-Transcriptional Polar Effects in Bacterial Gene Deletion Libraries. *mSystems*, *6*(5), 10.1128/msystems.00813–00821. https://doi.org/10.1128/msystems.00813-21

Mazumdar, K., Dastidar, S. G., & Park, J. H. (2021). Mechanism of action of diclofenac on bacterial cells: transcriptomic insights. *International journal of clinical and experimental medicine*, *14*(3).

Mazurkiewicz, P. S. (2004). *Drug efflux mechanism by a secondary transporter LmrP of Lactococcus lactis* [Thesis fully internal (DIV)]. s.n.

Meherunisa, Sapna, J., & Vikas, S. (2018). Study of Metformin Effect on Antimicrobial Property. *International Archives of BioMedical and Clinical Research*, *4*(3). https://doi.org/10.21276/iabcr.2018.4.3.24

Menendez, J. A., Oliveras-Ferraros, C., Cufí, S., Corominas-Faja, B., Joven, J., Martin-Castillo, B., & Vazquez-Martin, A. (2012). Metformin is synthetically lethal with glucose withdrawal in cancer cells. *Cell Cycle*, *11*(15), 2782–2792. https://doi.org/10.4161/cc.20948

Moffatt, J. H., Harper, M., Harrison, P., Hale, J. D., Vinogradov, E., Seemann, T., Henry, R., Crane, B., St Michael, F., Cox, A. D., Adler, B., Nation, R. L., Li, J., & Boyce, J. D. (2010). Colistin resistance in Acinetobacter baumannii is mediated by complete loss of lipopolysaccharide production. *Antimicrob Agents Chemother*, *54*(12), 4971–4977. https://doi.org/10.1128/aac.00834-10

Mohiuddin, S. G., Nguyen, T. V., & Orman, M. A. (2022). Pleiotropic actions of phenothiazine drugs are detrimental to Gram-negative bacterial persister cells. *Communications Biology*, *5*(1), 217. https://doi.org/10.1038/s42003-022-03172-8

Monti, M. R., Morero, N. R., Miguel, V., & Argaraña, C. E. (2013). nfxB as a Novel Target for Analysis of Mutation Spectra in Pseudomonas aeruginosa. *PLoS One*, *8*(6), e66236. https://doi.org/10.1371/journal.pone.0066236

Munguia, J., LaRock, D. L., Tsunemoto, H., Olson, J., Cornax, I., Pogliano, J., & Nizet, V. (2017). The Mla pathway is critical for Pseudomonas aeruginosa resistance to outer membrane permeabilization and host innate immune clearance. *Journal of Molecular Medicine*, *95*(10), 1127–1136. https://doi.org/10.1007/s00109-017-1579-4

Murray, C. J. L., Ikuta, K. S., Sharara, F., Swetschinski, L., Robles Aguilar, G., Gray, A., Han, C., Bisignano, C., Rao, P., Wool, E., Johnson, S. C., Browne, A. J., Chipeta, M. G., Fell, F., Hackett, S., Haines-Woodhouse, G., Kashef Hamadani, B. H., Kumaran, E. A. P., McManigal, B.,...Naghavi, M. (2022). Global burden of bacterial antimicrobial resistance in 2019: a systematic analysis. *The Lancet*, *399*(10325), 629–655. https://doi.org/10.1016/S0140-6736(21)02724-0

Mutlu, E. (2018). In Vitro Investigation of the Antibacterial Effects of Lidocaine and Bupivacaine Alone and in Combinations with Fentanyl. *Turkiye Klinikleri Journal of Medical Sciences*, *38*, 334–339. https://doi.org/10.5336/medsci.2018-61628

My, L., Rekoske, B., Lemke, J. J., Viala, J. P., Gourse, R. L., & Bouveret, E. (2013). Transcription of the Escherichia coli fatty acid synthesis operon fabHDG is directly activated by FadR and inhibited by ppGpp. *J Bacteriol*, *195*(16), 3784–3795. https://doi.org/10.1128/jb.00384-13

Nagarathinam, K., Nakada-Nakura, Y., Parthier, C., Terada, T., Juge, N., Jaenecke, F., Liu, K., Hotta, Y., Miyaji, T., Omote, H., Iwata, S., Nomura, N., Stubbs, M., & Tanabe, M. (2018). Outward open conformation of a Major Facilitator Superfamily multidrug/H + antiporter provides insights into switching mechanism. *Nature Communications*, *9*, 1–9. https://doi.org/10.1038/s41467-018-06306-x

Nasri, H., & Rafieian-Kopaei, M. (2014). Metformin: Current knowledge. *Journal of research in medical sciences : the official journal of Isfahan University of Medical Sciences*, *19*(7), 658–664.

Nasu, H., Shirakawa, R., Furuta, K., & Kaito, C. (2022). Knockout of mlaA increases Escherichia coli virulence in a silkworm infection model. *PloS one*, *17*(7), e0270166. https://doi.org/10.1371/journal.pone.0270166

Nehme, H., Saulnier, P., Ramadan, A. A., Cassisa, V., Guillet, C., Eveillard, M., & Umerska, A. (2018). Antibacterial activity of antipsychotic agents, their association with lipid nanocapsules and its impact on the properties of the nanocarriers and on antibacterial activity. *PloS one*, *13*(1), e0189950. https://doi.org/10.1371/journal.pone.0189950

Neidig, A., Yeung, A. T., Rosay, T., Tettmann, B., Strempel, N., Rueger, M., Lesouhaitier, O., & Overhage, J. (2013). TypA is involved in virulence, antimicrobial resistance and biofilm formation in Pseudomonas aeruginosa. *BMC Microbiol*, *13*, 77. https://doi.org/10.1186/1471-2180-13-77

Nielsen, R., Paul, J. S., Albrechtsen, A., & Song, Y. S. (2011). Genotype and SNP calling from next-generation sequencing data. *Nat Rev Genet*, *12*(6), 443–451. https://doi.org/10.1038/nrg2986

Nikel, P. I., Pérez-Pantoja, D., & de Lorenzo, V. (2016). Pyridine nucleotide transhydrogenases enable redox balance of Pseudomonas putida during biodegradation of aromatic compounds. *Environmental Microbiology*, *18*(10), 3565–3582. https://doi.org/https://doi.org/10.1111/1462-2920.13434

Njenga, R., Boele, J., Öztürk, Y., & Koch, H. G. (2023). Coping with stress: How bacteria fine-tune protein synthesis and protein transport. *The Journal of biological chemistry*, *299*(9), 105163. https://doi.org/10.1016/j.jbc.2023.105163

Nolle, N., Felsl, A., Heermann, R., & Fuchs, T. M. (2017). Genetic Characterization of the Galactitol Utilization Pathway of Salmonella enterica Serovar Typhimurium. *J Bacteriol*, *199*(4). https://doi.org/10.1128/jb.00595-16

Nordmann, P., Naas, T., & Poirel, L. (2011). Global spread of carbapenemase-producing Enterobacteriaceae. *Emerging Infectious Diseases*, *17*(10), 1791–1798.

Nyhan, W. L. (2014). Nucleotide Synthesis via Salvage Pathway. In *eLS*. https://doi.org/https://doi.org/10.1002/9780470015902.a0001399.pub3

O'Neill, E., Pozzi, C., Houston, P., Humphreys, H., Robinson, D. A., Loughman, A., Foster Timothy, J., & O'Gara James, P. (2008). A Novel Staphylococcus aureus Biofilm Phenotype Mediated by the Fibronectin-Binding Proteins, FnBPA and FnBPB. *J Bacteriol*, *190*(11), 3835–3850. https://doi.org/10.1128/jb.00167-08

O'Neill, J. (2016). Tackling drug-resistant infections globally: final report and recommendations.

Page, A. J., Ainsworth, E. V., & Langridge, G. C. (2020). socru: typing of genome-level order and orientation around ribosomal operons in bacteria. *Microb Genom*, *6*(7). https://doi.org/10.1099/mgen.0.000396

Page, A. J., Bastkowski, S., Yasir, M., Turner, A. K., Le Viet, T., Savva, G. M., Webber, M. A., & Charles, I. G. (2020). AlbaTraDIS: Comparative analysis of large datasets from parallel transposon mutagenesis experiments. *PLOS Computational Biology*, *16*(7), e1007980. https://doi.org/10.1371/journal.pcbi.1007980

Painter, K. L., Krishna, A., Wigneshweraraj, S., & Edwards, A. M. (2014). What role does the quorum-sensing accessory gene regulator system play during Staphylococcus aureus bacteremia? *Trends in Microbiology*, *22*(12), 676–685. https://doi.org/https://doi.org/10.1016/j.tim.2014.09.002

Pal, A., & Andersson, D. I. (2024). Bacteria can compensate the fitness costs of amplified resistance genes via a bypass mechanism. *Nature Communications*, *15*(1), 2333. https://doi.org/10.1038/s41467-024-46571-7

Palmer, G., & Buckley, G. (2021). The Health and Economic Burden of Resistance. In G. H. Palmer & G. J. Buckley (Eds.), *Combating Antimicrobial Resistance and Protecting the Miracle of Modern Medicine* (Health and Medicine Division; Board on Population Health and Public Health Practice; Committee on the Long-Term Health and Economic Effects of Antimicrobial Resistance in the United States ed., pp. Chapter 3). National Academies Press (US).

Park, H.-E., Shin, J.-I., Kim, K.-M., Choi, J.-G., Anh, W. J., Trinh, M. P., Kang, K.-M., Byun, J.-H., Yoo, J.-W., Kang, H.-L., Baik, S.-C., Lee, W.-K., Jung, M., & Shin, M.-K. (2025). Genetic variations underlying aminoglycoside resistance in antibiotic-induced Mycobacterium

intracellulare mutants. *Infection, Genetics and Evolution*, *128*, 105716. https://doi.org/https://doi.org/10.1016/j.meegid.2025.105716
Paterson, D. L., & Bonomo, R. A. (2005). Extended-spectrum β-lactamases: A clinical update. *Clinical Microbiology Reviews*, *18*(4), 657–686.
Patro, R., Duggal, G., Love, M. I., Irizarry, R. A., & Kingsford, C. (2017). Salmon provides fast and bias-aware quantification of transcript expression. *Nature Methods*, *14*(4), 417–419. https://doi.org/10.1038/nmeth.4197
Pavani, M., Fones, E., Oksenberg, D., Garcia, M., Hernandez, C., Cordano, G., Muñoz, S., Mancilla, J., Guerrero, A., & Ferreira, J. (1994). Inhibition of tumoral cell respiration and growth by nordihydroguaiaretic acid. *Biochemical Pharmacology*, *48*(10), 1935–1942. https://doi.org/https://doi.org/10.1016/0006-2952(94)90592-4
Pelicano, H., Feng, L., Zhou, Y., Carew, J. S., Hileman, E. O., Plunkett, W., Keating, M. J., & Huang, P. (2003). Inhibition of Mitochondrial Respiration: A NOVEL STRATEGY TO ENHANCE DRUG-INDUCED APOPTOSIS IN HUMAN LEUKEMIA CELLS BY A REACTIVE OXYGEN SPECIES-MEDIATED MECHANISM*. *Journal of Biological Chemistry*, *278*(39), 37832–37839. https://doi.org/https://doi.org/10.1074/jbc.M301546200
Penesyan, A., Nagy, S. S., Kjelleberg, S., Gillings, M. R., & Paulsen, I. T. (2019). Rapid microevolution of biofilm cells in response to antibiotics. *npj Biofilms and Microbiomes*, *5*(1), 34. https://doi.org/10.1038/s41522-019-0108-3
Peng, K., Li, C., Wang, Q., Xin, X., Wang, Z., & Li, R. (2025). The applications and advantages of nanopore sequencing in bacterial antimicrobial resistance surveillance and research. *npj Antimicrobials and Resistance*, *3*(1), 87. https://doi.org/10.1038/s44259-025-00157-5
Pietiäinen, M., François, P., Hyyryläinen, H. L., Tangomo, M., Sass, V., Sahl, H. G., Schrenzel, J., & Kontinen, V. P. (2009). Transcriptome analysis of the responses of Staphylococcus aureus to antimicrobial peptides and characterization of the roles of vraDE and vraSR in antimicrobial resistance. *BMC Genomics*, *10*, 429. https://doi.org/10.1186/1471-2164-10-429
Poirel, L., Jayol, A., & Nordmann, P. (2017). Polymyxins: Antibacterial activity, susceptibility testing, and resistance mechanisms. *Clinical Microbiology Reviews*, *30*(2), 557–596.
Poole, K., Tetro, K., Zhao, Q., Neshat, S., Heinrichs, D. E., & Bianco, N. (1996). Expression of the multidrug resistance operon mexA-mexB-oprM in Pseudomonas aeruginosa: mexR encodes a regulator of operon expression. *Antimicrob Agents Chemother*, *40*(9), 2021–2028. https://doi.org/10.1128/aac.40.9.2021
Pope, C. F., O'Sullivan, D. M., McHugh, T. D., & Gillespie, S. H. (2008). A practical guide to measuring mutation rates in antibiotic resistance. *Antimicrob Agents Chemother*, *52*(4), 1209–1214. https://doi.org/10.1128/aac.01152-07
Powell, D. R. (2019). *Degust: interactive RNA-seq analysis*. In https://doi.org/10.5281/zenodo.3258932
Pray, L. (2008). Antibiotic resistance, mutation rates and MRSA. *Nature Education*, *1*(1), 30.
Prjibelski, A., Antipov, D., Meleshko, D., Lapidus, A., & Korobeynikov, A. (2020). Using SPAdes De Novo Assembler. *Current Protocols in Bioinformatics*, *70*(1), e102. https://doi.org/https://doi.org/10.1002/cpbi.102
Ram, Y., Dellus-Gur, E., Bibi, M., Karkare, K., Obolski, U., Feldman, M. W., Cooper, T. F., Berman, J., & Hadany, L. (2019). Predicting microbial growth in a mixed culture from growth curve data. *Proceedings of the National Academy of Sciences*, *116*(29), 14698–14707. https://doi.org/doi:10.1073/pnas.1902217116
Rasko, D. A., & Sperandio, V. (2010). Anti-virulence strategies to combat bacteria-mediated disease. *Nature Reviews Drug Discovery*, *9*(2), 117–128. https://doi.org/10.1038/nrd3013

Ren, Z., Yu, J., Du, J., Zhang, Y., Hamushan, M., Jiang, F., Zhang, F., Wang, B., Tang, J., Shen, H., & Han, P. (2022). A General Map of Transcriptional Expression of Virulence, Metabolism, and Biofilm Formation Adaptive Changes of Staphylococcus aureus When Exposed to Different Antimicrobials [Original Research]. *Frontiers in Microbiology*, *Volume 13 - 2022*. https://doi.org/10.3389/fmicb.2022.825041

Rena, G., Hardie, D. G., & Pearson, E. R. (2017). The mechanisms of action of metformin. *Diabetologia*, *60*(9), 1577–1585. https://doi.org/10.1007/s00125-017-4342-z

Reygaert, W. C. (2018). An overview of the antimicrobial resistance mechanisms of bacteria. *AIMS microbiology*, *4*(3), 482–501. https://doi.org/10.3934/microbiol.2018.3.482

Roager, H. M., & Licht, T. R. (2018). Microbial tryptophan catabolites in health and disease. *Nat Commun*, *9*(1), 3294. https://doi.org/10.1038/s41467-018-05470-4

Rogall, E. T., Jacob, S., Triebskorn, R., & Schwartz, T. (2020). The impact of the anti-diabetic drug metformin on the intestinal microbiome of larval brown trout (Salmo trutta f. fario). *Environmental Sciences Europe*, *32*(1), 65. https://doi.org/10.1186/s12302-020-00341-6

Ruiz, C., & Levy, S. B. (2013). Regulation of acrAB expression by cellular metabolites in Escherichia coli. *Journal of Antimicrobial Chemotherapy*, *69*(2), 390–399. https://doi.org/10.1093/jac/dkt352

Sakata, N. (2024). The anti-inflammatory effect of metformin: The molecular targets. *Genes Cells*, *29*(3), 183–191. https://doi.org/10.1111/gtc.13098

Salam, M. A., Al-Amin, M. Y., Salam, M. T., Pawar, J. S., Akhter, N., Rabaan, A. A., & Alqumber, M. A. A. (2023). Antimicrobial Resistance: A Growing Serious Threat for Global Public Health. *Healthcare*, *11*(13), 1946.

Salazar, M. J., Machado, H., Dillon, N. A., Tsunemoto, H., Szubin, R., Dahesh, S., Pogliano, J., Sakoulas, G., Palsson, B. O., Nizet, V., & Feist, A. M. (2020). Genetic Determinants Enabling Medium-Dependent Adaptation to Nafcillin in Methicillin-Resistant Staphylococcus aureus. *mSystems*, *5*(2). https://doi.org/10.1128/mSystems.00828-19

Sarah, E. H., El Omri, N., Ibrahimi, A., & El Jaoudi, R. (2020). Metabolic and genetic studies of glimepiride and metformin and their association with type 2 diabetes. *Gene Reports*, *21*, 100787. https://doi.org/https://doi.org/10.1016/j.genrep.2020.100787

Satiaputra, J., Eijkelkamp, B. A., McDevitt, C. A., Shearwin, K. E., Booker, G. W., & Polyak, S. W. (2018). Biotin-mediated growth and gene expression in Staphylococcus aureus is highly responsive to environmental biotin. *Applied Microbiology and Biotechnology*, *102*(8), 3793–3803. https://doi.org/10.1007/s00253-018-8866-z

Seemann, T. (2014). Prokka: rapid prokaryotic genome annotation. *Bioinformatics*, *30*(14), 2068–2069. https://doi.org/10.1093/bioinformatics/btu153

Seemann, T. (2015). Snippy: fast bacterial variant calling from NGS reads. In.

Sharma, A. (2011). Antimicrobial resistance: no action today, no cure tomorrow. *Indian J Med Microbiol*, *29*(2), 91–92. https://doi.org/10.4103/0255-0857.81774

Simonsen, J. R., Harjutsalo, V., Järvinen, A., Kirveskari, J., Forsblom, C., Groop, P.-H., & Lehto, M. (2015). Bacterial infections in patients with type 1 diabetes: a 14-year follow-up study. *BMJ Open Diabetes Research & Care*, *3*(1), e000067. https://doi.org/10.1136/bmjdrc-2014-000067

Singh, R. P., Shelke, G. M., Kumar, A., & Jha, P. N. (2015). Biochemistry and genetics of ACC deaminase: a weapon to “stress ethylene” produced in plants [Review]. *Frontiers in Microbiology*, *Volume 6 - 2015*. https://doi.org/10.3389/fmicb.2015.00937

Singhal, A., Jie, L., Kumar, P., Hong, G. S., Leow, M. K.-S., Paleja, B., Tsenova, L., Kurepina, N., Chen, J., Zolezzi, F., Kreiswirth, B., Poidinger, M., Chee, C., Kaplan, G., Wang, Y. T., & De Libero, G. (2014). Metformin as adjunct antituberculosis therapy. *Science Translational Medicine*, *6*(263), 263ra159. https://doi.org/10.1126/scitranslmed.3009885

Snelling, R., & Nicholls, D. (1984). The calmodulin antagonists, trifluoperazine and R24571, depolarize the mitochondria within guinea pig cerebral cortical synaptosomes. *J Neurochem*, *42*(6), 1552–1557. https://doi.org/10.1111/j.1471-4159.1984.tb12741.x

Soares da Costa, T. P., Tieu, W., Yap, M. Y., Pendini, N. R., Polyak, S. W., Sejer Pedersen, D., Morona, R., Turnidge, J. D., Wallace, J. C., Wilce, M. C. J., Booker, G. W., & Abell, A. D. (2012). Selective inhibition of Biotin Protein Ligase from Staphylococcus aureus*. *Journal of Biological Chemistry*, *287*(21), 17823–17832. https://doi.org/10.1074/jbc.M112.356576

Soh, E. Y.-C., Smith, F., Gimenez, M. R., Yang, L., Vejborg, R. M., Fletcher, M., Halliday, N., Bleves, S., Heeb, S., Cámara, M., Givskov, M., Hardie, K. R., Tolker-Nielsen, T., Ize, B., & Williams, P. (2021). Disruption of the Pseudomonas aeruginosa Tat system perturbs PQS-dependent quorum sensing and biofilm maturation through lack of the Rieske cytochrome bc1 sub-unit. *PLOS Pathogens*, *17*(8), e1009425. https://doi.org/10.1371/journal.ppat.1009425

Song, G., Zhou, Y., Niu, S., Deng, X., Qiu, J., Li, L., & Wang, J. (2022). Nordihydroguaiaretic acid reverses the antibacterial activity of colistin against MCR-1-positive bacteria in vivo/in vitro by inhibiting MCR-1 activity and injuring the bacterial cell membrane. *Phytomedicine*, *98*, 153946. https://doi.org/10.1016/j.phymed.2022.153946

Soukas, A. A., Hao, H., & Wu, L. (2019). Metformin as Anti-Aging Therapy: Is It for Everyone? *Trends Endocrinol Metab*, *30*(10), 745–755. https://doi.org/10.1016/j.tem.2019.07.015

Sprouffske, K., & Wagner, A. (2016). Growthcurver: an R package for obtaining interpretable metrics from microbial growth curves. *BMC Bioinformatics*, *17*, 172. https://doi.org/10.1186/s12859-016-1016-7

Stepanović, S., Vuković, D., Hola, V., Di Bonaventura, G., Djukić, S., Cirković, I., & Ruzicka, F. (2007). Quantification of biofilm in microtiter plates: overview of testing conditions and practical recommendations for assessment of biofilm production by staphylococci. *Apmis*, *115*(8), 891–899. https://doi.org/10.1111/j.1600-0463.2007.apm_630.x

Sulaiman, J. E., & Lam, H. (2021). Evolution of Bacterial Tolerance Under Antibiotic Treatment and Its Implications on the Development of Resistance [Mini Review]. *Frontiers in Microbiology*, *Volume 12 - 2021*. https://doi.org/10.3389/fmicb.2021.617412

Tan, S., Cho, K., & Nodwell, J. R. (2022). A defect in cell wall recycling confers antibiotic resistance and sensitivity in Staphylococcus aureus. *The Journal of biological chemistry*, *298*(10), 102473. https://doi.org/10.1016/j.jbc.2022.102473

Tassoulas, L. J., Rankin, J. A., Elias, M. H., & Wackett, L. P. (2024). Dinickel enzyme evolved to metabolize the pharmaceutical metformin and its implications for wastewater and human microbiomes. *Proceedings of the National Academy of Sciences*, *121*(10), e2312652121. https://doi.org/doi:10.1073/pnas.2312652121

Tassoulas, L. J., & Wackett, L. P. (2024). Insights into the action of the pharmaceutical metformin: Targeted inhibition of the gut microbial enzyme agmatinase. *iScience*, *27*(2), 108900. https://doi.org/https://doi.org/10.1016/j.isci.2024.108900

Theophel, K., Schacht, V. J., Schlüter, M., Schnell, S., Stingu, C. S., Schaumann, R., & Bunge, M. (2014). The importance of growth kinetic analysis in determining bacterial susceptibility against antibiotics and silver nanoparticles. *Front Microbiol*, *5*, 544. https://doi.org/10.3389/fmicb.2014.00544

Toniolo, A., Cassani, G., Puggioni, A., Rossi, A., Colombo, A., Onodera, T., & Ferrannini, E. (2019). The diabetes pandemic and associated infections: suggestions for clinical microbiology. *Reviews in medical microbiology : a journal of the Pathological Society of Great Britain and Ireland*, *30*(1), 1–17. https://doi.org/10.1097/MRM.0000000000000155

Traber, K. E., Lee, E., Benson, S., Corrigan, R., Cantera, M., Shopsin, B., & Novick, R. P. (2008). agr function in clinical Staphylococcus aureus isolates. *Microbiology (Reading)*, *154*(Pt 8), 2265–2274. https://doi.org/10.1099/mic.0.2007/011874-0

Tsalidou, M., Stergiopoulou, T., Bostanitis, I., Nikaki, C., Skoumpa, K., Koutsoukou, T., & Papaioannidou, P. (2023). Surveillance of Antimicrobial Resistance and Multidrug Resistance Prevalence of Clinical Isolates in a Regional Hospital in Northern Greece. *Antibiotics (Basel)*, *12*(11). https://doi.org/10.3390/antibiotics12111595

Valadbeigi, H., Khoshnood, S., Negahdari, B., Abdullah, M. A., & Haddadi, M. H. (2023). Antibacterial and Immunoregulatory Effects of Metformin against Helicobacter pylori Infection in Rat Model. *BioMed Research International*, *2023*(1), 5583286. https://doi.org/https://doi.org/10.1155/2023/5583286

Vashisht, R., & Brahmachari, S. K. (2015). Metformin as a potential combination therapy with existing front-line antibiotics for Tuberculosis. *Journal of translational medicine*, *13*, 83–83. https://doi.org/10.1186/s12967-015-0443-y

Vasilchenko, A. S., & Rogozhin, E. A. (2019). Sub-inhibitory Effects of Antimicrobial Peptides. *Front Microbiol*, *10*, 1160. https://doi.org/10.3389/fmicb.2019.01160

Verissimo, A. F., & Daldal, F. (2014). Cytochrome c biogenesis System I: an intricate process catalyzed by a maturase supercomplex? *Biochim Biophys Acta*, *1837*(7), 989–998. https://doi.org/10.1016/j.bbabio.2014.03.003

Walker, B. J., Abeel, T., Shea, T., Priest, M., Abouelliel, A., Sakthikumar, S., Cuomo, C. A., Zeng, Q., Wortman, J., Young, S. K., & Earl, A. M. (2014). Pilon: An Integrated Tool for Comprehensive Microbial Variant Detection and Genome Assembly Improvement. *PloS one*, *9*(11), e112963. https://doi.org/10.1371/journal.pone.0112963

Wan, Y., Zheng, J., Chan, E. W., & Chen, S. (2024). Proton motive force and antibiotic tolerance in bacteria. *Microb Biotechnol*, *17*(11), e70042. https://doi.org/10.1111/1751-7915.70042

Wang, D., Kompaniiets, D., Hu, Y., & Liu, B. (2023). Editorial: Transcription and its regulation in bacteria [Editorial]. *Frontiers in Microbiology*, *Volume 14 - 2023*. https://doi.org/10.3389/fmicb.2023.1200443

Wang, Y.-W., He, S.-J., Feng, X., Cheng, J., Luo, Y.-T., Tian, L., & Huang, Q. (2017). Metformin: a review of its potential indications. *Drug design, development and therapy*, *11*, 2421–2429. https://doi.org/10.2147/DDDT.S141675

Wang, Y., Lu, J., Engelstädter, J., Zhang, S., Ding, P., Mao, L., Yuan, Z., Bond, P. L., & Guo, J. (2020). Non-antibiotic pharmaceuticals enhance the transmission of exogenous antibiotic resistance genes through bacterial transformation. *Isme j*, *14*(8), 2179–2196. https://doi.org/10.1038/s41396-020-0679-2

Wang, Y., Wang, L., Zhang, J., Duan, X., Feng, Y., Wang, S., & Shen, L. (2020). PA0335, a Gene Encoding Histidinol Phosphate Phosphatase, Mediates Histidine Auxotrophy in Pseudomonas aeruginosa. *Applied and environmental microbiology*, *86*(5). https://doi.org/10.1128/aem.02593-19

Ward, R. D., Tran, J. S., Banta, A. B., Bacon, E. E., Rose, W. E., & Peters, J. M. (2023). Essential Gene Knockdowns Reveal Genetic Vulnerabilities and Antibiotic Sensitivities in Acinetobacter baumannii. *bioRxiv*. https://doi.org/10.1101/2023.08.02.551708

Warkad, M. S., Kim, C.-H., Kang, B.-G., Park, S.-H., Jung, J.-S., Feng, J.-H., Inci, G., Kim, S.-C., Suh, H.-W., Lim, S. S., & Lee, J.-Y. (2021). Metformin-induced ROS upregulation as amplified by apigenin causes profound anticancer activity while sparing normal cells. *Scientific Reports*, *11*(1), 14002. https://doi.org/10.1038/s41598-021-93270-0

Webster, C. M., & Shepherd, M. (2022). A mini-review: environmental and metabolic factors affecting aminoglycoside efficacy. *World Journal of Microbiology and Biotechnology*, *39*(1), 7. https://doi.org/10.1007/s11274-022-03445-8

Wei, Z., Wei, Y., Li, H., Shi, D., Yang, D., Yin, J., Zhou, S., Chen, T., Li, J., & Jin, M. (2022). Emerging pollutant metformin in water promotes the development of multiple-antibiotic resistance in Escherichia coli via chromosome mutagenesis. *Journal of Hazardous Materials*, *430*, 128474. https://doi.org/https://doi.org/10.1016/j.jhazmat.2022.128474

WHO. (2024). *WHO Bacterial Priority Pathogens List, 2024*. https://www.who.int/publications/i/item/9789240093461

Wick, R. R., & Holt, K. E. (2022). Polypolish: Short-read polishing of long-read bacterial genome assemblies. *PLOS Computational Biology*, *18*(1), e1009802. https://doi.org/10.1371/journal.pcbi.1009802

Wick, R. R., Judd, L. M., Gorrie, C. L., & Holt, K. E. (2017). Unicycler: Resolving bacterial genome assemblies from short and long sequencing reads. *PLOS Computational Biology*, *13*(6), e1005595. https://doi.org/10.1371/journal.pcbi.1005595

Wielders, C. L., Fluit, A. C., Brisse, S., Verhoef, J., & Schmitz, F. J. (2002). mecA gene is widely disseminated in Staphylococcus aureus population. *J Clin Microbiol*, *40*(11), 3970–3975. https://doi.org/10.1128/jcm.40.11.3970-3975.2002

World Health, O. (2024). *Antimicrobial resistance: Global report on surveillance 2024*.

Wu, H., Esteve, E., Tremaroli, V., Khan, M. T., Caesar, R., Mannerås-Holm, L., Ståhlman, M., Olsson, L. M., Serino, M., Planas-Fèlix, M., Xifra, G., Mercader, J. M., Torrents, D., Burcelin, R., Ricart, W., Perkins, R., Fernàndez-Real, J. M., & Bäckhed, F. (2017). Metformin alters the gut microbiome of individuals with treatment-naive type 2 diabetes, contributing to the therapeutic effects of the drug. *Nat Med*, *23*(7), 850–858. https://doi.org/10.1038/nm.4345

Xiao, X., Huan, Q., Huang, Y., Liu, Y., Li, R., Xu, X., & Wang, Z. (2022). Metformin Reverses tmexCD1-toprJ1- and tet(A)-Mediated High-Level Tigecycline Resistance in K. pneumoniae. *Antibiotics (Basel)*, *11*(2). https://doi.org/10.3390/antibiotics11020162

Xiao, Y., Liu, Y., Chen, X., Wang, J., & Zhang, T. (2022). Metformin Reverses tmexCD1-toprJ1- and tet(A)-Mediated Tigecycline Resistance by Disrupting the Proton Motive Force. *Antibiotics*, *11*(2), 162. https://doi.org/10.3390/antibiotics11020162

Xu, B., & Wozniak, D. J. (2015). Development of a Novel Method for Analyzing Pseudomonas aeruginosa Twitching Motility and Its Application to Define the AmrZ Regulon. *PLoS One*, *10*(8), e0136426. https://doi.org/10.1371/journal.pone.0136426

Yamaguchi, A., Nakashima, R., & Sakurai, K. (2015). Structural basis of RND-type multidrug exporters. *Front Microbiol*, *6*, 327. https://doi.org/10.3389/fmicb.2015.00327

Yamamoto, S., Gunji, W., Suzuki, H., Toda, H., Suda, M., Jojima, T., Inui, M., & Yukawa, H. (2012). Overexpression of genes encoding glycolytic enzymes in Corynebacterium glutamicum enhances glucose metabolism and alanine production under oxygen deprivation conditions. *Applied and environmental microbiology*, *78*(12), 4447–4457. https://doi.org/10.1128/aem.07998-11

Yang, Y., Chen, Y., Zhang, G., Sun, J., Guo, L., Jiang, M., Ou, B., Zhang, W., & Si, H. (2020). Transcriptomic Analysis of Staphylococcus aureus Under the Stress Condition Caused by Litsea cubeba L. Essential Oil via RNA Sequencing. *Front Microbiol*, *11*, 1693. https://doi.org/10.3389/fmicb.2020.01693

Yao, L., Wang, Y., Qin, S., Zhu, S., & Wu, L. (2023). The antidiabetic drug metformin aids bacteria in hijacking vitamin B12 from the environment through RcdA. *Communications Biology*, *6*(1), 96. https://doi.org/10.1038/s42003-023-04475-0

Yao, X., He, W., & Lu, C. D. (2011). Functional characterization of seven γ-Glutamylpolyamine synthetase genes and the bauRABCD locus for polyamine and β-Alanine utilization in Pseudomonas aeruginosa PAO1. *J Bacteriol*, *193*(15), 3923–3930. https://doi.org/10.1128/jb.05105-11

Yasir, M., Turner, A. K., Bastkowski, S., Baker, D., Page, A. J., Telatin, A., Phan, M. D., Monahan, L., Savva, G. M., Darling, A., Webber, M. A., & Charles, I. G. (2020). TraDIS-Xpress: a high-resolution whole-genome assay identifies novel mechanisms of triclosan action and resistance. *Genome Res*, *30*(2), 239–249. https://doi.org/10.1101/gr.254391.119

Ye, J., Wang, J., Li, X., Chen, Y., & Zhang, T. (2021). Metformin Alters Chemotaxis and Flagellar Motility of Escherichia coli. *Frontiers in Microbiology*, *12*, 792406. https://doi.org/10.3389/fmicb.2021.792406

Ye, Y., Jiang, P., Huang, C., Li, J., Chen, J., Wang, L., Lin, Y., Wang, F., & Liu, J. (2022). Metformin Alters the Chemotaxis and Flagellar Motility of Escherichia coli [Original Research]. *Frontiers in Microbiology*, *Volume 12 - 2021*. https://doi.org/10.3389/fmicb.2021.792406

Yee, R., Cui, P., Shi, W., Feng, J., Wang, J., & Zhang, Y. (2020). Identification of a novel gene argJ involved in arginine biosynthesis critical for persister formation in Staphylococcus aureus. *Discov Med*, *29*(156), 65–77.

Yokoyama, R., Itoh, S., Kamoshida, G., Takii, T., Fujii, S., Tsuji, T., & Onozaki, K. (2012). Staphylococcal Superantigen-Like Protein 3 Binds to the Toll-Like Receptor 2 Extracellular Domain and Inhibits Cytokine Production Induced by Staphylococcus aureus, Cell Wall Component, or Lipopeptides in Murine Macrophages. *Infection and Immunity*, *80*(8), 2816–2825. https://doi.org/doi:10.1128/iai.00399-12

Yu, W.-B., Pan, Q., & Ye, B.-C. (2019). Glucose-Induced Cyclic Lipopeptides Resistance in Bacteria via ATP Maintenance through Enhanced Glycolysis. *iScience*, *21*, 135–144. https://doi.org/https://doi.org/10.1016/j.isci.2019.10.009

Zhang, Yanjia J., Reddy, Manchi C., Ioerger, Thomas R., Rothchild, Alissa C., Dartois, V., Schuster, Brian M., Trauner, A., Wallis, D., Galaviz, S., Huttenhower, C., Sacchettini, James C., Behar, Samuel M., & Rubin, Eric J. (2013). Tryptophan Biosynthesis Protects Mycobacteria from CD4 T-Cell-Mediated Killing. *Cell*, *155*(6), 1296–1308. https://doi.org/10.1016/j.cell.2013.10.045

Zhao, W., Sachsenmeier, K., Zhang, L., Sult, E., Hollingsworth, R. E., & Yang, H. (2014). A New Bliss Independence Model to Analyze Drug Combination Data. *SLAS Discovery*, *19*(5), 817–821. https://doi.org/https://doi.org/10.1177/1087057114521867

Zhu, L., Yang, K., Ren, Z., Yin, D., & Zhou, Y. (2024). Metformin as anticancer agent and adjuvant in cancer combination therapy: Current progress and future prospect. *Transl Oncol*, *44*, 101945. https://doi.org/10.1016/j.tranon.2024.101945

Zimin, A. V., & Salzberg, S. L. (2020). The genome polishing tool POLCA makes fast and accurate corrections in genome assemblies. *PLOS Computational Biology*, *16*(6), e1007981. https://doi.org/10.1371/journal.pcbi.1007981

Ziqubu, K., Mazibuko-Mbeje, S. E., Mthembu, S. X. H., Mabhida, S. E., Jack, B. U., Nyambuya, T. M., Nkambule, B. B., Basson, A. K., Tiano, L., & Dludla, P. V. (2023). Anti-Obesity Effects of Metformin: A Scoping Review Evaluating the Feasibility of Brown Adipose Tissue as a Therapeutic Target. *International journal of molecular sciences*, *24*(3), 2227.

Zuo, J., Shen, Y., Wang, H., Gao, S., Yuan, S., Song, D., Wang, Y., & Wang, Y. (2023). Effects of metformin on Streptococcus suis LuxS/AI-2 quorum sensing system and biofilm formation. *Microbial Pathogenesis*, *181*, 106183. https://doi.org/https://doi.org/10.1016/j.micpath.2023.106183

Zuo, J., Shen, Y., Wang, H., Gao, S., Yuan, S., Song, D., Wang, Y., & Wang, Y. (2023). Effects of metformin on Streptococcus suis LuxS/AI-2 quorum sensing system and biofilm formation. *Microb Pathog*, *181*, 106183. https://doi.org/10.1016/j.micpath.2023.106183

Zwietering, M. H., Jongenburger, I., Rombouts, F. M., & van 't Riet, K. (1990). Modeling of the bacterial growth curve. *Applied and environmental microbiology*, *56*(6), 1875–1881. https://doi.org/10.1128/aem.56.6.1875-1881.1990

APPENDIX

7. APPENDIX

A1 No inhibitor No Glucose	A2 No inhibitor No Glucose	A3 No inhibitor No Glucose	A4 No inhibitor No Glucose	A5 No inhibitor With Glucose	A6 No inhibitor With Glucose	A7 No inhibitor With Glucose	A8 No inhibitor With Glucose	A9 Meclizine 1	A10 2	A11 3	A12 4
B1 Complex I Inhibitor Rotenone 1	B2 2	B3 3	B4 4	B5 Complex I Inhibitor Pyridaben 1	B6 2	B7 3	B8 4	B9 Berberine 1	B10 2	B11 3	B12 4
C1 Complex II Inhibitor Malonate 1	C2 2	C3 3	C4 4	C5 Complex II Inhibitor Carboxin 1	C6 2	C7 3	C8 4	C9 Alexidine 1	C10 2	C11 3	C12 4
D1 Complex III Inhibitor Antimycin A 1	D2 2	D3 3	D4 4	D5 Complex III Inhibitor Myxothiazol 1	D6 2	D7 3	D8 4	D9 Phenformin 1	D10 2	D11 3	D12 4
E1 Uncoupler FCCP 1	E2 2	E3 3	E4 4	E5 Uncoupler 2,4-Dinitrophenol 1	E6 2	E7 3	E8 4	E9 Diclofenac 1	E10 2	E11 3	E12 4
F1 Ionophore, K Valinomycin 1	F2 2	F3 3	F4 4	F5 Calcium CaCl2 1	F6 2	F7 3	F8 4	F9 Celastrol 1	F10 2	F11 3	F12 4
G1 Gossypol 1	G2 2	G3 3	G4 4	G5 Nordihydro-guaiaretic acid 1	G6 2	G7 3	G8 4	G9 Trifluoperazine 1	G10 2	G11 3	G12 4
H1 Polymyxin B 1	H2 2	H3 3	H4 4	H5 Amitriptyline 1	H6 2	H7 3	H8 4	H9 Papaverine 1	H10 2	H11 3	H12 4

Figure 7-1: Mitoplate I-1 layout.
The wells A1-A4 were for testing without the glucose as substrate and without embedded inhibitor. Wells A5-A8 were for testing in presence of glucose but without embedded inhibitor. The rest of plate contained the inhibitors shown in the figure as four wells for each inhibitor.

Table 7-1: All the mutations that found in mutant and control of *S. aureus* as a result of the whole genome sequencing analysis for the short and long reads samples using Breseq and Snippy

Strain	Gene	Mutation	Annotation	Type	Effect	Product
Met-R1	*sdrD* →	+TGTT	coding (2723/2757 nt)	INS	Frameshift	Serine aspartate repeat containing protein D
	*P_01585 ←	GAACTGTGTC→TGAGTCGCTGTCT	T798_F800del&insD,S,D,S	Complex	Missense & disruptive inframe insertion	hypothetical protein
Met-R2	*sdrD* →	+TGTT	coding (2723/2757 nt)	INS	Frameshift	Serine aspartate repeat containing protein D
	dinG →	A→T	G607G (GGA→GGT)	SUB	synonymous	3' 5' exonuclease DinG
	*P_01585 ←	GAACTGTGTC→TGAGTCGCTGTCT	T798_F800del&insD,S,D,S	Complex	Missense & disruptive inframe insertion	hypothetical protein
	*P_01585 ←	A→G	Asp768Asp	SUB	synonymous	hypothetical protein
Met-R3	*sdrD* →	+TGTT	coding (2723/2757 nt)	INS	Frameshift	Serine aspartate repeat containing protein D
	dinG →	A→T	G607G (GGA→GGT)	SUB	synonymous	3' 5' exonuclease DinG
	*P_01585 ←	GAACTGTGTC→TGAGTCGCTGTCT	T798_F800del&insD,S,D,S	Complex	Missense & disruptive inframe insertion	hypothetical protein
	*P_01585 ←	GAACTGTGTC→TGAGTCGCTGTCT	T798_F800del&insD,S,D,S	Complex	Missense & disruptive inframe insertion	hypothetical protein
	sdrD →	+TGTT	coding (2723/2757 nt)	INS	Frameshift	Serine aspartate repeat containing protein D

	groL → / → P_02135	T→G	intergenic (+177/-365)	SUB	Intergenic	60 kDa chaperonin/hypothetical protein
	arcB →	Δ1 bp	coding (995/1011 nt)	DEL	Frameshift	Ornithine carbamoyltransferase, catabolic
Met-R5	P_02504 →	C→A	T267N (ACT→AAT)	SUB	Missense	Hypothetical protein
	sdrD →	+TGTT	coding (2723/2757 nt)	INS	Frameshift	Serine aspartate repeat containing protein D
	ypcP → / → ald1	+AA	intergenic (+357/-118)	INS	Intergenic	5'-3' exonuclease/Alanine dehydrogenase 1
	*P_01585 ←	GAACTGTGTC→TGAGTCGCTGTCT	T798_F800del&insD,S,D,S	Complex	Missense & disruptive inframe insertion	hypothetical protein
	*P_01585 ←	A→G	Asp768Asp	SUB	synonymous	hypothetical protein
Met-R6	*sdrD* →	+TGTT	coding (2723/2757 nt)	INS	Frameshift	Serine aspartate repeat containing protein D

Table 7-2: All the mutations that found the control only of *S. aureus* as a result of the whole genome sequencing analysis for the short and long reads samples using Breseq and Snippy

Strain	Gene	Mutation	Annotation	Type	Effect	Product
Ctrl-R1	*fnbA →	A→G	Pro883Pro	SUB	synonymous	Fibronectin-binding protein A
	*fnbA →	A→G	Pro886Pro	SUB	synonymous	Fibronectin-binding protein A
Ctrl-R2	*apt→	T→A	Phe60Ile	SUB	Missense	Adenine phosphoribosyltransferase
Ctrl-R4	*P_01585 ←	A→G	Asp768Asp	SUB	synonymous	hypothetical protein
Ctrl-R5	– / → fnbA_2	G→A	intergenic (–/-214)	SUB	Intergenic	–/Fibronectin-binding protein A
	– / → fnbA_2	A→G	intergenic (–/-208)	SUB	Intergenic	–/Fibronectin-binding protein A
	apt →	Δ12 bp	coding (401-412/519 nt)	DEL	Disruptive inframe deletion	Adenine phosphoribosyltransferase
	*P_01728←	ACTCT → GCTCA		Complex	synonymous	hypothetical protein
	*P_01728←	G→A	Leu22Leu	SUB	synonymous	hypothetical protein
	*P_01728←	TCTG → CCTA		Complex	synonymous	hypothetical protein
	*P_01728←	C →T	Val12Ile	SUB	Missense	hypothetical protein
Ctrl-R6	apt →	A→C	T37P (ACA→CCA)	SUB	Missense	Adenine phosphoribosyltransferase

Table 7-3: Mutations that found mutants only of *P. aeruginosa* and not present in their corresponding controls as a result of the whole genome sequencing analysis for the short and long reads samples using Breseq and Snippy

Strain	Gene	Mutation	Annotation	Type	Effect	Product
Met-R1	*P_04101 → / ← plcN_2*	A→C	intergenic (+18/+40)	SUB	Intergenic	hypothetical protein/Non-hemolytic phospholipase C
	typA → / –	G→T	intergenic (+61/–)	SUB	Intergenic	GTP-binding protein TypA/BipA/–
	– / → mip	+75 bp	intergenic (–/-600)	INS	Intergenic	–/Peptidyl-prolyl cis-trans isomerase Mip
	P_05131 → / –	G→T	intergenic (+232/–)	SUB	Intergenic	hypothetical protein/–
	– / → P_05850	C→A	intergenic (–/-118)	SUB	Intergenic	–/hypothetical protein
	dltA ←	C→A	G437W (GGG→TGG)	SUB	Missense	D-alanine--D-alanyl carrier protein ligase
	P_01801 ← / ← lon_1	C→A	intergenic (-98/+13)	SUB	Intergenic	hypothetical protein/Lon protease
	mhbT →	G→T	R11L (CGG→CTG)	SUB	Missense	3-hydroxybenzoate transporter MhbT
	P_06174 ← / –	G→T	intergenic (-42/–)	SUB	Intergenic	hypothetical protein/–
	– / ← P_06214	G→T	intergenic (–/+943)	SUB	Intergenic	–/hypothetical protein
	P_02408 → / –	Δ1 bp	intergenic (+41/–)	DEL	Intergenic	Isocitrate lyase/–
	lgrE_4 → / –	C→G	intergenic (+21/–)	SUB	Intergenic	Linear gramicidin dehydrogenase LgrE/–
	– / ← P_02531	C→A	intergenic (–/+62)	SUB	Intergenic	–/hypothetical protein
	P_02645 →	G→C	G26G (GGG→GGC)	SUB	Synonymous	hypothetical protein
	hemH → / → exuT_1	C→T	intergenic (+130/-150)	SUB	Intergenic	Ferrochelatase/Hexuronate transporter
	aphB → / –	C→G	intergenic (+42/–)	SUB	Intergenic	Acetylpolyamine amidohydrolase 2/–

	**P_05599 ←*	T→G	G53P	SUB	Missense	hypothetical protein
Met-2	*– / ← P_04807*	C→A	intergenic (–/+246)	SUB	Intergenic	–/hypothetical protein
	rodZ ←	G→T	L176I (CTC→ATC)	SUB	Missense	Cytoskeleton protein RodZ
	aroH_2 →	A→T	Q15L (CAG→CTG)	SUB	Missense	Phospho-2-dehydro-3-deoxyheptonate aldolase
	aroH_2 →	G→T	S9I (AGC→ATC)	SUB	Missense	Phospho-2-dehydro-3-deoxyheptonate aldolase
	aroH_2 →	G→T	W14L (TGG→TTG)	SUB	Missense	Phospho-2-dehydro-3-deoxyheptonate aldolase
	P_05904 → / –	G→T	intergenic (+82/–)	SUB	Intergenic	hypothetical protein/–
	lrp_5 ← / –	C→A	intergenic (-1045/–)	SUB	Intergenic	Leucine-responsive regulatory protein/–
	– / ← P_06214	G→T	intergenic (–/+943)	SUB	Intergenic	–/hypothetical protein
	cobI ←	G→T	A57D (GCC→GAC)	SUB	Missense	Precorrin-2 C(20)-methyltransferase
	aaeA_2 →	C→T	A42V (GCC→GTC)	SUB	Missense	p-hydroxybenzoic acid efflux pump subunit AaeA
	P_02461 ← / ← fabG_7	Δ9 bp	intergenic (-40/+15)		Intergenic	hypothetical protein/3-oxoacyl-[acyl-carrier-protein] reductase FabG
	fadJ → / ← pgrR_1	G→A	intergenic (+184/+70)	SUB	Intergenic	Fatty acid oxidation complex subunit alpha/HTH-type transcriptional regulator PgrR
	P_02645 →	G→C	G26G (GGG→GGC)	SUB	Synonymous	hypothetical protein
	acdS ←	C→A	G204V (GGC→GTC)	SUB	Missense	1-aminocyclopropane-1-carboxylate deaminase
	acnM ← / ← prpC_2	C→G	intergenic (-120/+11)	SUB	Intergenic	Aconitate hydratase A/2-methylcitrate synthase
	**argJ←*	G→T	A86E	SUB	Missense	Arginine biosynthesis bifunctional protein ArgJ

	*P_04871→	A→C	E32D	SUB	Missense	hypothetical protein
	*P_04871→	T→G	L34R	SUB	Missense	hypothetical protein
Met-R3	– / → *mip*	C→A	intergenic (–/-614)	SUB	Intergenic	–/Peptidyl-prolyl cis-trans isomerase Mip
	– / → *mip*	T→C	intergenic (–/-602)	SUB	Intergenic	–/Peptidyl-prolyl cis-trans isomerase Mip
	– / → *mip*	T→C	intergenic (–/-612)	SUB	Intergenic	–/Peptidyl-prolyl cis-trans isomerase Mip
	nemA_3 ← / –	C→A	intergenic (-201/–)	SUB	Intergenic	N-ethylmaleimide reductase/–
	P_02104 ←	T→G	R41R (AGG→CGG)	SUB	Synonymous	IS3 family transposase IS222
	cobH ← / –	G→A	intergenic (-32/–)	SUB	Intergenic	Precorrin-8X methylmutase/–
	acnM ← / ← *prpC_2*	C→G	intergenic (-120/+11)	SUB	Intergenic	Aconitate hydratase A/2-methylcitrate synthase
	**pntB* →	T→G	F288V	SUB	Missense	NAD(P) transhydrogenase subunit beta
	**hcnB_2* →	C→T	A196A	SUB	Synonymous	Hydrogen cyanide synthase subunit HcnB
Met-R4	*P_00002* ←	C→A	D203Y (GAC→TAC)	SUB	Missense	putative HTH-type transcriptional regulator
	cmk ←	C→A	A125A (GCG→GCT)	SUB	Synonymous	Cytidylate kinase
	P_04101 → / ← *plcN_2*	A→C	intergenic (+18/+40)	SUB	Intergenic	hypothetical protein/Non-hemolytic phospholipase C
	ttr →	G→T	R118L (CGC→CTC)	SUB	Missense	Acetyltransferase
	P_04610 → / ← *pcaK_1*	+CC	intergenic (+30/+107)		Intergenic	hypothetical protein/4-hydroxybenzoate transporter PcaK
	algD ← / ← *yaaA*	C→G	intergenic (-879/+23)	SUB	Intergenic	GDP-mannose 6-dehydrogenase/Peroxide stress resistance protein YaaA

	P_02408 → / –	Δ1 bp	intergenic (+41/–)		Intergenic	Isocitrate lyase/–
	P_02862 ←	C→G	W312S (TGG→TCG)	SUB	Missense	hypothetical protein
	P_03007 →	A→G	T123A (ACT→GCT)	SUB	Missense	hypothetical protein
	**acoR* →	T→G	L504R	SUB	Missense	Acetoin catabolism regulatory protein
	**trpI_1* →	T→G	L256R	SUB	Missense	HTH-type transcriptional regulator TrpI
Met-R5	*cmk* ←	C→A	A125A (GCG→GCT)	SUB	Synonymous	Cytidylate kinase
	P_01040 → / → *P 01041*	C→G	intergenic (+36/-127)	SUB	Intergenic	hypothetical protein/hypothetical protein
	P_04968 ← / –	C→G	intergenic (-381/–)	SUB	Intergenic	hypothetical protein/–
	rcsC_2 →	G→A	G1036D (GGC→GAC)	SUB	Missense	Sensor histidine kinase RcsC
	rcsC_2 →	G→C	G1035A (GGC→GCC)	SUB	Missense	Sensor histidine kinase RcsC
	rocC → / –	C→G	intergenic (+27/–)	SUB	Intergenic	Amino-acid permease RocC/–
	– / → *P_06166*	G→T	intergenic (–/-862)	SUB	Intergenic	–/hypothetical protein
	P_06174 ← / –	G→T	intergenic (-42/–)	SUB	Intergenic	hypothetical protein/–
	– / ← *cobC*	G→A	intergenic (–/+388)	SUB	Intergenic	–/Adenosylcobalamin/alpha-ribazole phosphatase
	P_02408 → / –	Δ1 bp	intergenic (+41/–)	DEL	Intergenic	Isocitrate lyase/–
	P_02862 ←	C→G	W312S (TGG→TCG)	SUB	Missense	hypothetical protein
	ligD ←	A→T	F10I (TTC→ATC)	SUB	Missense	Multifunctional non-homologous end joining protein LigD
	**acrB_1* →	A→T	E119A	SUB	Missense	Multidrug efflux pump subunit AcrB
Met-R6	– / → *mip*	C→A	intergenic (–/-614)	SUB	Intergenic	–/Peptidyl-prolyl cis-trans isomerase Mip

	– / → mip	G→A	intergenic (–/-647)	SUB	Intergenic	–/Peptidyl-prolyl cis-trans isomerase Mip
	– / → mip	T→C	intergenic (–/-602)	SUB	Intergenic	–/Peptidyl-prolyl cis-trans isomerase Mip
	– / → mip	T→C	intergenic (–/-612)	SUB	Intergenic	–/Peptidyl-prolyl cis-trans isomerase Mip
	glyA_2 →	C→T	H29H (CAC→CAT)	SUB	Synonymous	Serine hydroxymethyltransferase
	glyA_2 →	G→C	R25R (CGG→CGC)	SUB	Synonymous	Serine hydroxymethyltransferase
	rcsC_2 →	G→A	G1036D (GGC→GAC)	SUB	Missense	Sensor histidine kinase RcsC
	rcsC_2 →	G→C	G1035A (GGC→GCC)	SUB	Missense	Sensor histidine kinase RcsC
	– / → P_05850	C→T	intergenic (–/-130)	SUB	Intergenic	–/hypothetical protein
	dltA ←	C→A	G437W (GGG→TGG)	SUB	Missense	D-alanine--D-alanyl carrier protein ligase
	P_02104 ←	T→G	R41R (AGG→CGG)	SUB	Synonymous	IS3 family transposase IS222
	– / ← garP	C→A	intergenic (–/+262)	SUB	Intergenic	–/putative galactarate transporter
	lgrE_4 → / –	C→G	intergenic (+21/–)	SUB	Intergenic	Linear gramicidin dehydrogenase LgrE/–
	P_02645 →	G→C	G26G (GGG→GGC)	SUB	Synonymous	hypothetical protein
	ligD ←	A→T	F10I (TTC→ATC)	SUB	Missense	Multifunctional non-homologous end joining protein LigD
	P_03701 →	C→T	L6F (CTC→TTC)	SUB	Missense	hypothetical protein
	**dsbD_2 →*	A→C	T31P	SUB	Missense	Thiol:disulfide interchange protein DsbD

Table 7-4: Mutations found in both mutant and control of *P. aeruginosa* as a result of the whole genome sequencing analysis for the short and long reads samples using Breseq and Snippy

Strain	Gene	Mutation	Annotation	Type	Effect	Product

Met-R1 & Ctrl-R1	– / → *P_03980*	C→A	intergenic (–/-66)	SUB	Intergenic	–/hypothetical protein
	cmk ←	C→A	A125A (GCG→GCT)	SUB	Synonymous	Cytidylate kinase
	P_00895 →	A→G	D60G (GAT→GGT)	SUB	Missense	hypothetical protein
	P_04341 →	T→G	C71G (TGC→GGC)	SUB	Missense	hypothetical protein
	– / → *P_04361*	C→A	intergenic (–/-20)	SUB	Intergenic	–/hypothetical protein
	puuC_2 →	C→G	L57V (CTC→GTC)	SUB	Missense	NADP/NAD-dependent aldehyde dehydrogenase PuuC
	yddE_2 → / ← *P_04725*	G→C	intergenic (+153/+635)	SUB	Intergenic	putative isomerase YddE/hypothetical protein
	– / ← *P_04807*	C→A	intergenic (–/+246)	SUB	Intergenic	–/hypothetical protein
	rodZ ←	G→T	L176I (CTC→ATC)	SUB	Missense	Cytoskeleton protein RodZ
	rcsC_2 →	G→A	G1036D (GGC→GAC)	SUB	Missense	Sensor histidine kinase RcsC
	rcsC_2 →	G→C	G1035A (GGC→GCC)	SUB	Missense	Sensor histidine kinase RcsC
	xanP_2 ← / ← *P_05164*	T→C	intergenic (-172/+70)	SUB	Intergenic	Xanthine permease XanP/hypothetical protein
	P_05167 →	C→G	P236A (CCG→GCG)	SUB	Missense	putative FAD-linked oxidoreductase
	P_01362 →	A→G	T219A (ACT→GCT)	SUB	Missense	hypothetical protein
	P_05522 ←	T→C	*130* (TAA→TAG)	SUB	Stop retained variant	hypothetical protein
	– / ← *P_05595*	+CG	intergenic (–/+440)	INS	Intergenic	–/hypothetical protein
	oprB_2 →	T→C	A102A (GCT→GCC)	SUB	Synonymous	Porin B
	ydhC →	C→T	A169V (GCG→GTG)	SUB	Missense	Inner membrane transport protein YdhC
	tamB ← / –	C→A	intergenic (-38/–)	SUB	Intergenic	Translocation and assembly module subunit TamB/–
	tamB ← / –	C→A	intergenic (-41/–)	SUB	Intergenic	Translocation and assembly module subunit TamB/–

	tamB ← / –	C→A	intergenic (-46/–)	SUB	Intergenic	Translocation and assembly module subunit TamB/–
	– / → *P_05850*	C→T	intergenic (–/-130)	SUB	Intergenic	–/hypothetical protein
	jefA → / → *rhaS_13*	A→G	intergenic (+26/-16)	SUB	Intergenic	Drug efflux pump JefA/HTH-type transcriptional activator RhaS
	P_05904 → / –	G→T	intergenic (+82/–)	SUB	Intergenic	hypothetical protein/–
	P_05911 ← / –	C→A	intergenic (-161/–)	SUB	Intergenic	hypothetical protein/–
	– / ← *rcsC_12*	C→A	intergenic (–/+76)	SUB	Intergenic	–/Sensor histidine kinase RcsC
	P_05936 ←	A→C	R51R (CGT→CGG)	SUB	Synonymous	Delta(1)-pyrroline-2-carboxylate reductase
	nemA_3 ← / –	C→A	intergenic (-201/–)	SUB	Intergenic	N-ethylmaleimide reductase/–
	– / → *mhbT*	A→G	intergenic (–/-10)	SUB	Intergenic	–/3-hydroxybenzoate transporter MhbT
	napF ← / –	T→G	intergenic (-22/–)	SUB	Intergenic	Ferredoxin-type protein NapF/–
	P_06189 →	C→G	P149A (CCC→GCC)	SUB	Missense	hypothetical protein
	P_06223 → / –	G→A	intergenic (+53/–)	SUB	Intergenic	hypothetical protein/–
	P_06223 →	T→G	*109E (TAG→GAG)	SUB	Readthrough mutation	hypothetical protein
	cobI ←	G→C	P62R (CCC→CGC)	SUB	Missense	Precorrin-2 C(20)-methyltransferase
	cobI ←	G→C	V61V (GTC→GTG)	SUB	Synonymous	Precorrin-2 C(20)-methyltransferase
	– / –	G→T	intergenic (–/–)	SUB	Intergenic	–/–
	– / –	T→C	intergenic (–/–)	SUB	Intergenic	–/–
	– / ← *cobC*	G→A	intergenic (–/+388)	SUB	Intergenic	–/Adenosylcobalamin/alpha-ribazole phosphatase
	– / ← *garP*	C→A	intergenic (–/+262)	SUB	Intergenic	–/putative galactarate transporter
	– / –	A→C	intergenic (–/–)	SUB	Intergenic	–/–
	– / –	G→T	intergenic (–/–)	SUB	Intergenic	–/–

	aaeA_2 →	C→T	A42V (GCC→GTC)	SUB	Missense	p-hydroxybenzoic acid efflux pump subunit AaeA
	P_06296 ←	C→T	A86T (GCG→ACG)	SUB	Missense	hypothetical protein
	P_02461 ← / ← *fabG_7*	Δ9 bp	intergenic (-40/+15)	DEL	Intergenic	hypothetical protein/3-oxoacyl-[acyl-carrier-protein] reductase FabG
	– / –	A→C	intergenic (–/–)	SUB	Intergenic	–/–
	– / –	C→A	intergenic (–/–)	SUB	Intergenic	–/–
	P_02684 →	A→G	S91G (AGC→GGC)	SUB	Missense	hypothetical protein
	P_02756 →	C→A	A5D (GCT→GAT)	SUB	Missense	hypothetical protein
	P_02826 →	C→G	A273G (GCT→GGT)	SUB	Missense	NADH:quinone reductase
	P_02862 ←	C→G	W312S (TGG→TCG)	SUB	Missense	hypothetical protein
	P_03007 →	A→G	T123A (ACT→GCT)	SUB	Missense	hypothetical protein
	P_03382 ← / –	G→T	intergenic (-17/–)	SUB	Intergenic	hypothetical protein/–
	ureG → / –	A→G	intergenic (+389/–)	SUB	Intergenic	Urease accessory protein UreG/–
	P_03701 →	C→T	L6F (CTC→TTC)	SUB	Missense	hypothetical protein
	*fecR_2 →	A→C	T194P	SUB	Missense	Protein FecR
	*argJ←	G→T	A86E	SUB	Missense	Arginine biosynthesis bifunctional protein ArgJ

Strain	Gene	Mutation	Annotation	Type	Effect	Product
Met-R2& Ctrl-R2	– / → *P_03980*	C→A	intergenic (–/-66)	SUB	Intergenic	–/hypothetical protein
	hcp1_2 ← / ← *P_04084*	G→C	intergenic (-63/+11)	SUB	Intergenic	Protein hcp1/hypothetical protein

	P_00895 →	A→G	D60G (GAT→GGT)	SUB	Missense	hypothetical protein
	puuC_2 →	C→A	A56D (GCC→GAC)	SUB	Missense	NADP/NAD-dependent aldehyde dehydrogenase PuuC
	– / → P_04361	C→A	intergenic (–/-20)	SUB	Intergenic	–/hypothetical protein
	puuC_2 →	C→G	L57V (CTC→GTC)	SUB	Missense	NADP/NAD-dependent aldehyde dehydrogenase PuuC
	yddE_2 → / ← P_04725	G→C	intergenic (+153/+635)	SUB	Intergenic	putative isomerase YddE/hypothetical protein
	xanP_2 ← / ← P_05164	T→C	intergenic (-172/+70)	SUB	Intergenic	Xanthine permease XanP/hypothetical protein
	P_05167 →	C→G	P236A (CCG→GCG)	SUB	Missense	putative FAD-linked oxidoreductase
	– / ← sucA	G→C	intergenic (–/+239)	SUB	Intergenic	–/2-oxoglutarate dehydrogenase E1 component
	deaD → / ← ygiD	C→G	intergenic (+264/+103)	SUB	Intergenic	ATP-dependent RNA helicase DeaD/4,5-DOPA dioxygenase extradiol
	P_01362 →	A→G	T219A (ACT→GCT)	SUB	Missense	hypothetical protein
	P_05522 ←	T→C	*130* (TAA→TAG)	SUB	Stop retained variant	hypothetical protein
	– / ← P_05595	+CG	intergenic (–/+440)		Intergenic	–/hypothetical protein
	oprB_2 →	T→C	A102A (GCT→GCC)	SUB		Porin B
	ydhC →	C→T	A169V (GCG→GTG)	SUB	Missense	Inner membrane transport protein YdhC
	tamB ← / –	C→A	intergenic (-38/–)	SUB	Intergenic	Translocation and assembly module subunit TamB/–
	tamB ← / –	C→A	intergenic (-41/–)	SUB	Intergenic	Translocation and assembly module subunit TamB/–
	tamB ← / –	C→A	intergenic (-46/–)	SUB	Intergenic	Translocation and assembly module subunit TamB/–
	– / → P_05850	C→A	intergenic (–/-118)	SUB	Intergenic	–/hypothetical protein

	jefA → / → *rhaS_13*	A→G	intergenic (+26/-16)	SUB	Intergenic	Drug efflux pump JefA/HTH-type transcriptional activator RhaS
	P_05911 ← / –	C→A	intergenic (-161/–)	SUB	Intergenic	hypothetical protein/–
	– / ← *rcsC_12*	C→A	intergenic (–/+76)	SUB	Intergenic	–/Sensor histidine kinase RcsC
	P_05936 ←	A→C	R51R (CGT→CGG)	SUB	Synonymous	Delta(1)-pyrroline-2-carboxylate reductase
	dltA ←	C→A	G437W (GGG→TGG)	SUB	Missense	D-alanine--D-alanyl carrier protein ligase
	P_01801 ← / ← *lon_1*	C→A	intergenic (-98/+13)	SUB	Intergenic	hypothetical protein/Lon protease
	– / → *mhbT*	A→G	intergenic (–/-10)	SUB	Intergenic	–/3-hydroxybenzoate transporter MhbT
	mhbT →	G→T	R11L (CGG→CTG)	SUB	Missense	3-hydroxybenzoate transporter MhbT
	napF ← / –	T→G	intergenic (-22/–)	SUB	Intergenic	Ferredoxin-type protein NapF/–
	rocC → / –	C→G	intergenic (+27/–)	SUB	Intergenic	Amino-acid permease RocC/–
	P_06174 ← / –	G→T	intergenic (-42/–)	SUB	Intergenic	hypothetical protein/–
	P_06189 →	C→G	P149A (CCC→GCC)	SUB	Missense	hypothetical protein
	P_06223 → / –	G→A	intergenic (+53/–)	SUB	Intergenic	hypothetical protein/–
	P_06223 →	T→G	*109E (TAG→GAG)	SUB	Readthrough mutation	hypothetical protein
	cobI ←	G→C	P62R (CCC→CGC)	SUB	Missense	Precorrin-2 C(20)-methyltransferase
	cobI ←	G→C	V61V (GTC→GTG)	SUB	Synonymous	Precorrin-2 C(20)-methyltransferase
	– / –	G→T	intergenic (–/–)	SUB	Intergenic	–/–
	– / –	T→C	intergenic (–/–)	SUB	Intergenic	–/–
	– / ← *cobC*	G→A	intergenic (–/+388)	SUB	Intergenic	–/Adenosylcobalamin/alpha-ribazole phosphatase
	– / ← *garP*	C→A	intergenic (–/+262)	SUB	Intergenic	–/putative galactarate transporter
	– / –	A→C	intergenic (–/–)	SUB	Intergenic	–/–

	lgrE_4 → / –	C→G	intergenic (+21/–)	SUB	Intergenic	Linear gramicidin dehydrogenase LgrE/–
	– / –	G→T	intergenic (–/–)	SUB	Intergenic	–/–
	P_06296 ←	C→T	A86T (GCG→ACG)	SUB	Missense	hypothetical protein
	– / –	A→C	intergenic (–/–)	SUB	Intergenic	–/–
	– / –	C→A	intergenic (–/–)	SUB	Intergenic	–/–
	– / –	Δ281 bp	intergenic (–/–)	DEL	Intergenic	–/–
	P_02684 →	A→G	S91G (AGC→GGC)	SUB	Missense	hypothetical protein
	P_02756 →	C→A	A5D (GCT→GAT)	SUB	Missense	hypothetical protein
	P_02826 →	C→G	A273G (GCT→GGT)	SUB	Missense	NADH:quinone reductase
	P_02862 ←	C→G	W312S (TGG→TCG)	SUB	Missense	hypothetical protein
	P_03007 →	A→G	T123A (ACT→GCT)	SUB	Missense	hypothetical protein
	P_03382 ← / –	G→T	intergenic (-17/–)	SUB	Intergenic	hypothetical protein/–
	anoI ← / ← *sdiA*	G→C	intergenic (-155/+25)	SUB	Intergenic	Acyl-homoserine-lactone synthase/Regulatory protein SdiA
	P_03701 →	C→T	L6F (CTC→TTC)	SUB	Missense	hypothetical protein
	*sucB ←	G→C	Thr66Ser	SUB	Missense	Dihydrolipoyllysine-residue succinyltransferase component of 2-oxoglutarate dehydrogenase complex

Strain	Gene	Mutation	Annotation	Type	Effect	Product
	cmk ←	C→A	A125A (GCG→GCT)	SUB	Synonymous	Cytidylate kinase
	P_04101 → / ← *plcN_2*	A→C	intergenic (+18/+40)	SUB	Intergenic	hypothetical protein/Non-hemolytic phospholipase C

	P_00895 →	A→G	D60G (GAT→GGT)	SUB	Missense	hypothetical protein
	P_04341 →	T→G	C71G (TGC→GGC)	SUB	Missense	hypothetical protein
	puuC_2 →	C→A	A56D (GCC→GAC)	SUB	Missense	NADP/NAD-dependent aldehyde dehydrogenase PuuC
	– / → P_04361	C→A	intergenic (–/-20)	SUB	Intergenic	–/hypothetical protein
	puuC_2 →	C→G	L57V (CTC→GTC)	SUB	Missense	NADP/NAD-dependent aldehyde dehydrogenase PuuC
	yddE_2 → / ← P_0472 5	G→C	intergenic (+153/+635)	SUB	Intergenic	putative isomerase YddE/hypothetical protein
	P_01113 →	C→T	P18L (CCG→CTG)	SUB	Missense	2-haloacrylate reductase
	rodZ ←	G→T	L176I (CTC→ATC)	SUB	Missense	Cytoskeleton protein RodZ
	rcsC_2 →	G→A	G1036D (GGC→GAC)	SUB	Missense	Sensor histidine kinase RcsC
	xanP_2 ← / ← P_0516 4	T→C	intergenic (-172/+70)	SUB	Intergenic	Xanthine permease XanP/hypothetical protein
	P_05167 →	C→G	P236A (CCG→GCG)	SUB	Missense	putative FAD-linked oxidoreductase
	deaD → / ← ygiD	C→G	intergenic (+264/+103)	SUB	Intergenic	ATP-dependent RNA helicase DeaD/4,5-DOPA dioxygenase extradiol
	P_05522 ←	T→C	*130* (TAA→TAG)	SUB	Stop retained variant	hypothetical protein
	oprB_2 →	T→C	A102A (GCT→GCC)	SUB	Synonymous	Porin B
	tamB ← / –	C→A	intergenic (-38/–)	SUB	Intergenic	Translocation and assembly module subunit TamB/–
	tamB ← / –	C→A	intergenic (-41/–)	SUB	Intergenic	Translocation and assembly module subunit TamB/–
	tamB ← / –	C→A	intergenic (-46/–)	SUB	Intergenic	Translocation and assembly module subunit TamB/–
	jefA → / → rhaS_13	A→G	intergenic (+26/-16)	SUB	Intergenic	Drug efflux pump JefA/HTH-type transcriptional activator RhaS

	– / ← *rcsC_12*	C→A	intergenic (–/+76)	SUB	Intergenic	–/Sensor histidine kinase RcsC
	dltA ←	C→A	G437W (GGG→TGG)	SUB	Missense	D-alanine--D-alanyl carrier protein ligase
	– / → *mhbT*	A→G	intergenic (–/-10)	SUB	Intergenic	–/3-hydroxybenzoate transporter MhbT
	mhbT →	G→T	R11L (CGG→CTG)	SUB	Missense	3-hydroxybenzoate transporter MhbT
	napF ← / –	T→G	intergenic (-22/–)	SUB	Intergenic	Ferredoxin-type protein NapF/–
	rocC → / –	C→G	intergenic (+27/–)	SUB	Intergenic	Amino-acid permease RocC/–
	P_06174 ← / –	G→T	intergenic (-42/–)	SUB	Intergenic	hypothetical protein/–
	P_06189 →	C→G	P149A (CCC→GCC)	SUB	Missense	hypothetical protein
	cobI ←	G→C	P62R (CCC→CGC)	SUB	Missense	Precorrin-2 C(20)-methyltransferase
	cobI ←	G→C	V61V (GTC→GTG)	SUB	Synonymous	Precorrin-2 C(20)-methyltransferase
	cobI ←	G→T	A57D (GCC→GAC)	SUB	Missense	Precorrin-2 C(20)-methyltransferase
	– / ← *garP*	C→A	intergenic (–/+262)	SUB	Intergenic	–/putative galactarate transporter
	– / –	A→C	intergenic (–/–)	SUB	Intergenic	–/–
	– / –	G→T	intergenic (–/–)	SUB	Intergenic	–/–
	P_06296 ←	C→T	A86T (GCG→ACG)	SUB	Missense	hypothetical protein
	– / –	C→A	intergenic (–/–)	SUB	Intergenic	–/–
	– / –	Δ281 bp	intergenic (–/–)		Intergenic	–/–
	– / ← *P_02531*	C→A	intergenic (–/+62)	SUB	Intergenic	–/hypothetical protein
	P_02756 →	C→A	A5D (GCT→GAT)	SUB	Missense	hypothetical protein
	P_02826 →	C→G	A273G (GCT→GGT)	SUB	Missense	NADH:quinone reductase
	P_03007 →	A→G	T123A (ACT→GCT)	SUB	Missense	hypothetical protein
	ligD ←	A→T	F10I (TTC→ATC)	SUB	Missense	Multifunctional non-homologous end joining protein LigD

	P_03701 →	C→T	L6F (CTC→TTC)	SUB	Missense	hypothetical protein
	*argJ ←	G→T	Ala86Glu	SUB	Missense	Arginine biosynthesis bifunctional protein ArgJ
	*acoR →	A→C	Glu506Ala	SUB	Missense	Acetoin catabolism regulatory protein

Strain	Gene	Mutation	Annotation	Type	Effect	Product
Met-R4 & Ctrl-R4	*P_00895* →	A→G	D60G (GAT→GGT)	SUB	Missense	hypothetical protein
	– / → P_04361	C→A	intergenic (–/-20)	SUB	Intergenic	–/hypothetical protein
	– / ← P_04807	C→A	intergenic (–/+246)	SUB	Intergenic	–/hypothetical protein
	xanP_2 ← / ← P_05164	T→C	intergenic (-172/+70)	SUB	Intergenic	Xanthine permease XanP/hypothetical protein
	P_05167 →	C→G	P236A (CCG→GCG)	SUB	Missense	putative FAD-linked oxidoreductase
	deaD → / ← ygiD	C→G	intergenic (+264/+103)	SUB	Intergenic	ATP-dependent RNA helicase DeaD/4,5-DOPA dioxygenase extradiol
	– / ← P_05595	+CG	intergenic (–/+440)		Intergenic	–/hypothetical protein
	ydhC →	C→T	A169V (GCG→GTG)	SUB	Missense	Inner membrane transport protein YdhC
	– / → P_05850	C→A	intergenic (–/-118)	SUB	Intergenic	–/hypothetical protein
	jefA → / → rhaS_13	A→G	intergenic (+26/-16)	SUB	Intergenic	Drug efflux pump JefA/HTH-type transcriptional activator RhaS
	– / ← rcsC_12	C→A	intergenic (–/+76)	SUB	Intergenic	–/Sensor histidine kinase RcsC
	P_05936 ←	A→C	R51R (CGT→CGG)	SUB	Synonymous	Delta(1)-pyrroline-2-carboxylate reductase
	dltA ←	C→A	G437W (GGG→TGG)	SUB	Missense	D-alanine--D-alanyl carrier protein ligase
	nemA_3 ← / –	C→A	intergenic (-201/–)	SUB	Intergenic	N-ethylmaleimide reductase/–
	mhbT →	G→T	R11L (CGG→CTG)	SUB	Missense	3-hydroxybenzoate transporter MhbT
	napF ← / –	T→G	intergenic (-22/–)	SUB	Intergenic	Ferredoxin-type protein NapF/–
	P_06189 →	C→G	P149A (CCC→GCC)	SUB	Missense	hypothetical protein

	P_02104 ←	T→G	R41R (AGG→CGG)	SUB	Synonymous	IS3 family transposase IS222
	P_06223 → / –	G→A	intergenic (+53/–)	SUB	Intergenic	hypothetical protein/–
	cobI ←	G→C	P62R (CCC→CGC)	SUB	Missense	Precorrin-2 C(20)-methyltransferase
	cobI ←	G→C	V61V (GTC→GTG)	SUB	Synonymous	Precorrin-2 C(20)-methyltransferase
	– / ← *garP*	C→A	intergenic (–/+262)	SUB	Intergenic	–/putative galactarate transporter
	– / –	A→C	intergenic (–/–)	SUB	Intergenic	–/–
	– / –	G→T	intergenic (–/–)	SUB	Intergenic	–/–
	P_06296 ←	C→T	A86T (GCG→ACG)	SUB	Missense	hypothetical protein
	– / –	A→C	intergenic (–/–)	SUB	Intergenic	–/–
	– / –	Δ281 bp	intergenic (–/–)		Intergenic	–/–
	– / ← *P_02531*	C→A	intergenic (–/+62)	SUB	Intergenic	–/hypothetical protein
	P_02684 →	A→G	S91G (AGC→GGC)	SUB	Missense	hypothetical protein
	P_02826 →	C→G	A273G (GCT→GGT)	SUB	Missense	NADH:quinone reductase
	P_03382 ← / –	G→T	intergenic (-17/–)	SUB	Intergenic	hypothetical protein/–
	anoI ← / ← *sdiA*	G→C	intergenic (-155/+25)	SUB	Intergenic	Acyl-homoserine-lactone synthase/Regulatory protein SdiA

Strain	Gene	Mutation	Annotation	Type	Effect	Product
Met-R5 & Ctrl-R5	*P_00895* →	A→G	D60G (GAT→GGT)	SUB	Missense	hypothetical protein
	ttr →	G→T	R118L (CGC→CTC)	SUB	Missense	Acetyltransferase
	puuC_2 →	C→A	A56D (GCC→GAC)	SUB	Missense	NADP/NAD-dependent aldehyde dehydrogenase PuuC

	– / → P_04361	C→A	intergenic (–/-20)	SUB	Intergenic	–/hypothetical protein
	puuC_2 →	C→G	L57V (CTC→GTC)	SUB	Missense	NADP/NAD-dependent aldehyde dehydrogenase PuuC
	yddE_2 → / ← P_04725	G→C	intergenic (+153/+635)	SUB	Intergenic	putative isomerase YddE/hypothetical protein
	P_04806 ←	C→A	G384V (GGC→GTC)	SUB	Missense	hypothetical protein
	– / ← P_04807	C→A	intergenic (–/+246)	SUB	Intergenic	–/hypothetical protein
	P_05167 →	C→G	P236A (CCG→GCG)	SUB	Missense	putative FAD-linked oxidoreductase
	P_01362 →	A→G	T219A (ACT→GCT)	SUB	Missense	hypothetical protein
	– / ← P_05595	+CG	intergenic (–/+440)		Intergenic	–/hypothetical protein
	ydhC →	C→T	A169V (GCG→GTG)	SUB	Missense	Inner membrane transport protein YdhC
	tamB ← / –	C→A	intergenic (-38/–)	SUB	Intergenic	Translocation and assembly module subunit TamB/–
	tamB ← / –	C→A	intergenic (-41/–)	SUB	Intergenic	Translocation and assembly module subunit TamB/–
	tamB ← / –	C→A	intergenic (-46/–)	SUB	Intergenic	Translocation and assembly module subunit TamB/–
	jefA → / → rhaS_13	A→G	intergenic (+26/-16)	SUB	Intergenic	Drug efflux pump JefA/HTH-type transcriptional activator RhaS
	– / ← rcsC_12	C→A	intergenic (–/+76)	SUB	Intergenic	–/Sensor histidine kinase RcsC
	nemA_3 ← / –	C→A	intergenic (-201/–)	SUB	Intergenic	N-ethylmaleimide reductase/–
	– / → mhbT	A→G	intergenic (–/-10)	SUB	Intergenic	–/3-hydroxybenzoate transporter MhbT
	P_06189 →	C→G	P149A (CCC→GCC)	SUB	Missense	hypothetical protein
	P_06223 → / –	G→A	intergenic (+53/–)	SUB	Intergenic	hypothetical protein/–
	cobH ← / –	G→A	intergenic (-32/–)	SUB	Intergenic	Precorrin-8X methylmutase/–
	cobI ←	G→C	P62R (CCC→CGC)	SUB	Missense	Precorrin-2 C(20)-methyltransferase

	cobI ←	G→C	V61V (GTC→GTG)	SUB	Synonymous	Precorrin-2 C(20)-methyltransferase
	– / ← *garP*	C→A	intergenic (–/+262)	SUB	Intergenic	–/putative galactarate transporter
	– / –	A→C	intergenic (–/–)	SUB	Intergenic	–/–
	lgrE_4 → / –	C→G	intergenic (+21/–)	SUB	Intergenic	Linear gramicidin dehydrogenase LgrE/–
	aaeA_2 →	C→T	A42V (GCC→GTC)	SUB	Missense	p-hydroxybenzoic acid efflux pump subunit AaeA
	P_06296 ←	C→T	A86T (GCG→ACG)	SUB	Missense	hypothetical protein
	– / –	A→C	intergenic (–/–)	SUB	Intergenic	–/–
	P_02756 →	C→A	A5D (GCT→GAT)	SUB	Missense	hypothetical protein
	P_03007 →	A→G	T123A (ACT→GCT)	SUB	Missense	hypothetical protein
	anoI ← / ← *sdiA*	G→C	intergenic (-155/+25)	SUB	Intergenic	Acyl-homoserine-lactone synthase/Regulatory protein SdiA
	*argJ ←	G→T	Ala86Glu	SUB	Missense	Arginine biosynthesis bifunctional protein ArgJ

Strain	Gene	Mutation	Annotation	Type	Effect	Product
Met-R6 & Ctrl-R6	– / → *P_03980*	C→A	intergenic (–/-66)	SUB	Intergenic	–/hypothetical protein
	cmk ←	C→A	A125A (GCG→GCT)	SUB	Synonymous	Cytidylate kinase
	P_00895 →	A→G	D60G (GAT→GGT)	SUB	Missense	hypothetical protein
	P_04341 →	T→G	C71G (TGC→GGC)	SUB	Missense	hypothetical protein
	P_04356 →	A→T	Q107L (CAG→CTG)	SUB	Missense	hypothetical protein
	puuC_2 →	C→A	A56D (GCC→GAC)	SUB	Missense	NADP/NAD-dependent aldehyde dehydrogenase PuuC
	– / → *P_04361*	C→A	intergenic (–/-20)	SUB	Intergenic	–/hypothetical protein
	puuC_2 →	C→G	L57V (CTC→GTC)	SUB	Missense	NADP/NAD-dependent aldehyde dehydrogenase PuuC

	spuC_3 → / → *P_04369*	G→C	intergenic (+26/-138)	SUB	Intergenic	Putrescine--pyruvate aminotransferase/hypothetical protein
	yddE_2 → / ← *P_04725*	G→C	intergenic (+153/+635)	SUB	Intergenic	putative isomerase YddE/hypothetical protein
	– / ← *P_04807*	C→A	intergenic (–/+246)	SUB	Intergenic	–/hypothetical protein
	xanP_2 ← / ← *P_05164*	T→C	intergenic (-172/+70)	SUB	Intergenic	Xanthine permease XanP/hypothetical protein
	P_05167 →	C→G	P236A (CCG→GCG)	SUB	Missense	putative FAD-linked oxidoreductase
	deaD → / ← *ygiD*	C→G	intergenic (+264/+103)	SUB	Intergenic	ATP-dependent RNA helicase DeaD/4,5-DOPA dioxygenase extradiol
	P_05522 ←	T→C	*130* (TAA→TAG)	SUB	Stop retained variant	hypothetical protein
	oprB_2 →	T→C	A102A (GCT→GCC)	SUB	Synonymous	Porin B
	tamB ← / –	C→A	intergenic (-38/–)	SUB	Intergenic	Translocation and assembly module subunit TamB/–
	tamB ← / –	C→A	intergenic (-41/–)	SUB	Intergenic	Translocation and assembly module subunit TamB/–
	tamB ← / –	C→A	intergenic (-46/–)	SUB	Intergenic	Translocation and assembly module subunit TamB/–
	– / → *P_05850*	C→A	intergenic (–/-118)	SUB	Intergenic	–/hypothetical protein
	jefA → / → *rhaS_13*	A→G	intergenic (+26/-16)	SUB	Intergenic	Drug efflux pump JefA/HTH-type transcriptional activator RhaS
	P_05904 → / –	G→T	intergenic (+82/–)	SUB	Intergenic	hypothetical protein/–
	P_05911 ← / –	C→A	intergenic (-161/–)	SUB	Intergenic	hypothetical protein/–
	– / ← *rcsC_12*	C→A	intergenic (–/+76)	SUB	Intergenic	–/Sensor histidine kinase RcsC
	P_05936 ←	A→C	R51R (CGT→CGG)	SUB	Synonymous	Delta(1)-pyrroline-2-carboxylate reductase
	nemA_3 ← / –	C→A	intergenic (-201/–)	SUB	Intergenic	N-ethylmaleimide reductase/–

	– / → *mhbT*	A→G	intergenic (–/-10)	SUB	Intergenic	–/3-hydroxybenzoate transporter MhbT
	mhbT →	G→T	R11L (CGG→CTG)	SUB	Missense	3-hydroxybenzoate transporter MhbT
	napF ← / –	T→G	intergenic (-22/–)	SUB	Intergenic	Ferredoxin-type protein NapF/–
	rocC → / –	C→G	intergenic (+27/–)	SUB	Intergenic	Amino-acid permease RocC/–
	P_06174 ← / –	G→T	intergenic (-42/–)	SUB	Intergenic	hypothetical protein/–
	P_06189 →	C→G	P149A (CCC→GCC)	SUB	Missense	hypothetical protein
	P_06223 → / –	G→A	intergenic (+53/–)	SUB	Intergenic	hypothetical protein/–
	P_06223 →	T→G	*109E (TAG→GAG)	SUB	Readthrough mutation	hypothetical protein
	cobI ←	G→C	P62R (CCC→CGC)	SUB	Missense	Precorrin-2 C(20)-methyltransferase
	cobI ←	G→C	V61V (GTC→GTG)	SUB	Synonymous	Precorrin-2 C(20)-methyltransferase
	cobI ←	G→T	A57D (GCC→GAC)	SUB	Missense	Precorrin-2 C(20)-methyltransferase
	– / –	T→C	intergenic (–/–)	SUB	Intergenic	–/–
	– / ← *cobC*	G→A	intergenic (–/+388)	SUB	Intergenic	–/Adenosylcobalamin/alpha-ribazole phosphatase
	– / –	A→C	intergenic (–/–)	SUB	Intergenic	–/–
	– / –	G→T	intergenic (–/–)	SUB	Intergenic	–/–
	aaeA_2 →	C→T	A42V (GCC→GTC)	SUB	Missense	p-hydroxybenzoic acid efflux pump subunit AaeA
	P_06296 ←	C→T	A86T (GCG→ACG)	SUB	Missense	hypothetical protein
	– / –	Δ312 bp	intergenic (–/–)		Intergenic	–/–
	– / –	C→A	intergenic (–/–)	SUB	Intergenic	–/–
	– / –	Δ281 bp	intergenic (–/–)		Intergenic	–/–

	fadJ → / ← *pgrR_1*	G→A	intergenic (+184/+70)	SUB	Intergenic	Fatty acid oxidation complex subunit alpha/HTH-type transcriptional regulator PgrR
	P_02756 →	C→A	A5D (GCT→GAT)	SUB	Missense	hypothetical protein
	P_02826 →	C→G	A273G (GCT→GGT)	SUB	Missense	NADH:quinone reductase
	P_03007 →	A→G	T123A (ACT→GCT)	SUB	Missense	hypothetical protein
	P_03382 ← / –	G→T	intergenic (-17/–)	SUB	Intergenic	hypothetical protein/–
	anoI ← / ← *sdiA*	G→C	intergenic (-155/+25)	SUB	Intergenic	Acyl-homoserine-lactone synthase/Regulatory protein SdiA
	*argJ ←	G→T	Ala86Glu	SUB	Missense	Arginine biosynthesis bifunctional protein ArgJ

Table 7-5: Mutations that found only in controls of *P. aeruginosa* as a result of the whole genome sequencing analysis for the short and long reads samples using Breseq and Snippy

Strain	Gene	Mutation	Annotation	Type	Effect	Product
Ctrl-R1	*puuC_2* →	C→A	A56D (GCC→GAC)	SUB	Missense	NADP/NAD-dependent aldehyde dehydrogenase PuuC
	spuC_3 → / → *P_04369*	G→C	intergenic (+26/-138)	SUB	Intergenic	Putrescine--pyruvate aminotransferase/hypothetical protein
	P_01040 → / → *P_01041*	C→G	intergenic (+36/-127)	SUB	Intergenic	hypothetical protein/hypothetical protein
	P_04806 ←	C→A	G384V (GGC→GTC)	SUB	Missense	hypothetical protein
	P_04999 ← / –	G→T	intergenic (-89/–)	SUB	Intergenic	hypothetical protein/–
	P_05773 ← / –	C→A	intergenic (-62/–)	SUB	Intergenic	hypothetical protein/–
	P_05794 ← / –	G→T	intergenic (-287/–)	SUB	Intergenic	hypothetical protein/–
	lrp_5 ← / –	C→A	intergenic (-1045/–)	SUB	Intergenic	Leucine-responsive regulatory protein/–

	rocC → / –	C→G	intergenic (+27/–)	SUB	Intergenic	Amino-acid permease RocC/–
	– / → *P_06166*	G→T	intergenic (–/-862)	SUB	Intergenic	–/hypothetical protein
	– / –	C→T	intergenic (–/–)	SUB	Intergenic	–/–
	– / –	C→G	intergenic (–/–)	SUB	Intergenic	–/–
	– / –	T→C	intergenic (–/–)	SUB	Intergenic	–/–
	P_02619 ← / –	G→T	intergenic (-264/–)	SUB	Intergenic	hypothetical protein/–
	ligD ←	A→T	F10I (TTC→ATC)	SUB	Missense	Multifunctional non-homologous end joining protein LigD
	anoI ← / ← *sdiA*	G→C	intergenic (-155/+25)	SUB	Intergenic	Acyl-homoserine-lactone synthase/Regulatory protein SdiA
	*ethA ←	T→G	G487P	SUB	Missense	FAD-containing monooxygenase EthA
Ctrl-R2	*cmk* ←	C→A	A125A (GCG→GCT)	SUB	Synonymous	Cytidylate kinase
	P_04101 → / ← *plcN_2*	A→C	intergenic (+18/+40)	SUB	Intergenic	hypothetical protein/Non-hemolytic phospholipase C
	ttr →	G→T	R118L (CGC→CTC)	SUB	Missense	Acetyltransferase
	P_04341 →	T→G	C71G (TGC→GGC)	SUB	Missense	hypothetical protein
	– / → *mip*	C→A	intergenic (–/-614)	SUB	Intergenic	–/Peptidyl-prolyl cis-trans isomerase Mip
	– / → *mip*	G→A	intergenic (–/-647)	SUB	Intergenic	–/Peptidyl-prolyl cis-trans isomerase Mip
	– / → *mip*	T→C	intergenic (–/-602)	SUB	Intergenic	–/Peptidyl-prolyl cis-trans isomerase Mip
	– / → *mip*	T→C	intergenic (–/-612)	SUB	Intergenic	–/Peptidyl-prolyl cis-trans isomerase Mip
	P_01040 → / → *P_01041*	C→G	intergenic (+36/-127)	SUB	Intergenic	hypothetical protein/hypothetical protein

	P_04610 → / ← pcaK_1	+CC	intergenic (+30/+107)	INS	Intergenic	hypothetical protein/4-hydroxybenzoate transporter PcaK
	P_04610 → / ← pcaK_1	12 bp→113 bp	intergenic (+93/+33)	Complex	Intergenic	hypothetical protein/4-hydroxybenzoate transporter PcaK
	P_04610 → / ← pcaK_1	C→T	intergenic (+117/+20)	SUB	Intergenic	hypothetical protein/4-hydroxybenzoate transporter PcaK
	P_04806 ←	C→A	G384V (GGC→GTC)	SUB	Missense	hypothetical protein
	rcsC_2 →	G→A	G1036D (GGC→GAC)	SUB	Missense	Sensor histidine kinase RcsC
	rcsC_2 →	G→C	G1035A (GGC→GCC)	SUB	Missense	Sensor histidine kinase RcsC
	P_05121 ←	G→A	T53T (ACC→ACT)	SUB	Synonymous	hypothetical protein
	P_05794 ← / –	G→T	intergenic (-287/–)	SUB	Intergenic	hypothetical protein/–
	– / → P_05850	C→T	intergenic (–/-130)	SUB	Intergenic	–/hypothetical protein
	– / → fecR_5	C→G	intergenic (–/-82)	SUB	Intergenic	–/Protein FecR
	– / –	Δ312 bp	intergenic (–/–)	DEL	Intergenic	–/–
	P_02619 ← / –	G→T	intergenic (-264/–)	SUB	Intergenic	hypothetical protein/–
	hemH → / → exuT_1	C→T	intergenic (+130/-150)	SUB	Intergenic	Ferrochelatase/Hexuronate transporter
	ureG → / –	A→G	intergenic (+389/–)	SUB	Intergenic	Urease accessory protein UreG/–
	**hcnB_2 →*	T→G	Trp118Gly	SUB	Missense	Hydrogen cyanide synthase subunit HcnB
Ctrl-R3	*– / → P_03980*	C→A	intergenic (–/-66)	SUB	Intergenic	–/hypothetical protein
	ttr →	G→T	R118L (CGC→CTC)	SUB	Missense	Acetyltransferase
	P_01040 → / → P_01041	C→G	intergenic (+36/-127)	SUB	Intergenic	hypothetical protein/hypothetical protein
	glyA_2 →	T→G	L139L (CTT→CTG)	SUB	Synonymous	Serine hydroxymethyltransferase

	P_04610 → / ← pcaK_1	+CC	intergenic (+30/+107)	INS	Intergenic	hypothetical protein/4-hydroxybenzoate transporter PcaK
	P_04680 → / → iorA_2	G→C	intergenic (+21/-244)	SUB	Intergenic	hypothetical protein/Isoquinoline 1-oxidoreductase subunit alpha
	P_04806 ←	C→A	G384V (GGC→GTC)	SUB	Missense	hypothetical protein
	– / ← P_04807	C→A	intergenic (–/+246)	SUB	Intergenic	–/hypothetical protein
	P_04968 ← / –	C→G	intergenic (-381/–)	SUB	Intergenic	hypothetical protein/–
	rcsC_2 →	G→C	G1035A (GGC→GCC)	SUB	Missense	Sensor histidine kinase RcsC
	P_05131 → / –	G→T	intergenic (+232/–)	SUB	Intergenic	hypothetical protein/–
	– / → P_05233	A→G	intergenic (–/-15)	SUB	Intergenic	–/hypothetical protein
	P_01362 →	A→G	T219A (ACT→GCT)	SUB	Missense	hypothetical protein
	– / ← P_05595	+CG	intergenic (–/+440)	INS	Intergenic	–/hypothetical protein
	ydhC →	C→T	A169V (GCG→GTG)	SUB	Missense	Inner membrane transport protein YdhC
	P_05794 ← / –	C→A	intergenic (-284/–)	SUB	Intergenic	hypothetical protein/–
	P_05794 ← / –	G→T	intergenic (-287/–)	SUB	Intergenic	hypothetical protein/–
	– / → P_05850	C→A	intergenic (–/-118)	SUB	Intergenic	–/hypothetical protein
	– / → P_05850	C→T	intergenic (–/-130)	SUB	Intergenic	–/hypothetical protein
	potE_2 ← / –	G→C	intergenic (-164/–)	SUB	Intergenic	Putrescine transporter PotE/–
	ahpC_3 → / → ahpF	C→T	intergenic (+58/-87)	SUB	Intergenic	Alkyl hydroperoxide reductase C/Alkyl hydroperoxide reductase subunit F
	P_05904 → / –	G→T	intergenic (+82/–)	SUB	Intergenic	hypothetical protein/–
	P_05911 ← / –	C→A	intergenic (-161/–)	SUB	Intergenic	hypothetical protein/–
	P_05936 ←	A→C	R51R (CGT→CGG)	SUB	Synonymous	Delta(1)-pyrroline-2-carboxylate reductase

	– / ← *P_06214*	G→T	intergenic (–/+943)	SUB	Intergenic	–/hypothetical protein
	P_06223 → / –	G→A	intergenic (+53/–)	SUB	Intergenic	hypothetical protein/–
	P_06223 →	T→G	*109E (TAG→GAG)	SUB	Readthrough Mutation	hypothetical protein
	gltC_1 → / ← *dmlR_7*	C→G	intergenic (+56/+78)	SUB	Intergenic	HTH-type transcriptional regulator GltC/HTH-type transcriptional regulator DmlR
	– / –	G→T	intergenic (–/–)	SUB	Intergenic	–/–
	– / –	T→C	intergenic (–/–)	SUB	Intergenic	–/–
	– / ← *cobC*	G→A	intergenic (–/+388)	SUB	Intergenic	–/Adenosylcobalamin/alpha-ribazole phosphatase
	P_02408 → / –	Δ1 bp	intergenic (+41/–)	DEL	Intergenic	Isocitrate lyase/–
	lgrE_4 → / –	C→G	intergenic (+21/–)	SUB	Intergenic	Linear gramicidin dehydrogenase LgrE/–
	P_02461 ← / ← *fabG_7*	Δ8 bp	intergenic (-43/+13)	DEL	Intergenic	hypothetical protein/3-oxoacyl-[acyl-carrier-protein] reductase FabG
	– / –	A→C	intergenic (–/–)	SUB	Intergenic	–/–
	– / –	Δ312 bp	intergenic (–/–)	DEL	Intergenic	–/–
	fadJ → / ← *pgrR_1*	G→A	intergenic (+184/+70)	SUB	Intergenic	Fatty acid oxidation complex subunit alpha/HTH-type transcriptional regulator PgrR
	pdxH → / –	G→C	intergenic (+706/–)	SUB	Intergenic	Pyridoxine/pyridoxamine 5'-phosphate oxidase/–
	P_02862 ←	C→G	W312S (TGG→TCG)	SUB	Missense	hypothetical protein
	hemH → / → *exuT_1*	C→T	intergenic (+130/-150)	SUB	Intergenic	Ferrochelatase/Hexuronate transporter
	P_03382 ← / –	G→T	intergenic (-17/–)	SUB	Intergenic	hypothetical protein/–

	aphB → / –	C→G	intergenic (+42/–)	SUB	Intergenic	Acetylpolyamine amidohydrolase 2/–
	anoI ← / ← *sdiA*	G→C	intergenic (-155/+25)	SUB	Intergenic	Acyl-homoserine-lactone synthase/Regulatory protein SdiA
Ctrl-R4	– / → *P_03980*	C→A	intergenic (–/-66)	SUB	Intergenic	–/hypothetical protein
	P_04341 →	T→G	C71G (TGC→GGC)	SUB	Missense	hypothetical protein
	puuC_2 →	C→A	A56D (GCC→GAC)	SUB	Missense	NADP/NAD-dependent aldehyde dehydrogenase PuuC
	puuC_2 →	C→G	L57V (CTC→GTC)	SUB	Missense	NADP/NAD-dependent aldehyde dehydrogenase PuuC
	– / → *mip*	C→A	intergenic (–/-614)	SUB	Intergenic	–/Peptidyl-prolyl cis-trans isomerase Mip
	– / → *mip*	T→C	intergenic (–/-602)	SUB	Intergenic	–/Peptidyl-prolyl cis-trans isomerase Mip
	– / → *mip*	T→C	intergenic (–/-612)	SUB	Intergenic	–/Peptidyl-prolyl cis-trans isomerase Mip
	aroE_1 ← / –	G→T	intergenic (-35/–)	SUB	Intergenic	Quinate/shikimate dehydrogenase (NAD(+))/–
	yddE_2 → / ← *P_04725*	G→C	intergenic (+153/+635)	SUB	Intergenic	putative isomerase YddE/hypothetical protein
	– / → *aroC*	G→T	intergenic (–/-205)	SUB	Intergenic	–/Chorismate synthase
	P_05522 ←	T→C	*130* (TAA→TAG)	SUB	Stop retained variant	hypothetical protein
	oprB_2 →	T→C	A102A (GCT→GCC)	SUB	Synonymous	Porin B
	tamB ← / –	C→A	intergenic (-38/–)	SUB	Intergenic	Translocation and assembly module subunit TamB/–
	tamB ← / –	C→A	intergenic (-41/–)	SUB	Intergenic	Translocation and assembly module subunit TamB/–
	tamB ← / –	C→A	intergenic (-46/–)	SUB	Intergenic	Translocation and assembly module subunit TamB/–

	potE_2 ← / –	G→C	intergenic (-164/–)	SUB	Intergenic	Putrescine transporter PotE/–
	P_05904 → / –	G→T	intergenic (+82/–)	SUB	Intergenic	hypothetical protein/–
	P_05911 ← / –	C→A	intergenic (-161/–)	SUB	Intergenic	hypothetical protein/–
	lrp_5 ← / –	C→A	intergenic (-1045/–)	SUB	Intergenic	Leucine-responsive regulatory protein/–
	– / → *mhbT*	A→G	intergenic (–/-10)	SUB	Intergenic	–/3-hydroxybenzoate transporter MhbT
	– / → *P_06166*	G→T	intergenic (–/-862)	SUB	Intergenic	–/hypothetical protein
	P_06174 ← / –	G→T	intergenic (-42/–)	SUB	Intergenic	hypothetical protein/–
	P_06223 →	T→G	*109E (TAG→GAG)	SUB	Read through mutation	hypothetical protein
	P_06239 ← / –	C→T	intergenic (-17/–)	SUB	Intergenic	hypothetical protein/–
	gltC_1 → / ← *dmlR_7*	2 bp→AG	intergenic (+59/+74)	Complex	Intergenic	HTH-type transcriptional regulator GltC/HTH-type transcriptional regulator DmlR
	gltC_1 → / ← *dmlR_7*	C→G	intergenic (+56/+78)	SUB	Intergenic	HTH-type transcriptional regulator GltC/HTH-type transcriptional regulator DmlR
	cobI ←	G→T	A57D (GCC→GAC)	SUB	Missense	Precorrin-2 C(20)-methyltransferase
	– / –	G→T	intergenic (–/–)	SUB	Intergenic	–/–
	– / –	T→C	intergenic (–/–)	SUB	Intergenic	–/–
	– / ← *cobC*	G→A	intergenic (–/+388)	SUB	Intergenic	–/Adenosylcobalamin/alpha-ribazole phosphatase
	lgrE_4 → / –	C→G	intergenic (+21/–)	SUB	Intergenic	Linear gramicidin dehydrogenase LgrE/–
	aaeA_2 →	C→T	A42V (GCC→GTC)	SUB	Missense	p-hydroxybenzoic acid efflux pump subunit AaeA
	– / –	C→A	intergenic (–/–)	SUB	Intergenic	–/–

	P_02756 →	C→A	A5D (GCT→GAT)	SUB	Missense	hypothetical protein
	P_03701 →	C→T	L6F (CTC→TTC)	SUB	Missense	hypothetical protein
	*ethA ←	T→G	G487P	SUB	Missense	FAD-containing monooxygenase EthA
	*dap →	C→G	Pro258Pro	SUB	Synonymous	D-aminopeptidase
Ctrl-R5	– / → *P_03980*	C→A	intergenic (–/-66)	SUB	Intergenic	–/hypothetical protein
	P_04101 → / ← *plcN_2*	A→C	intergenic (+18/+40)	SUB	Intergenic	hypothetical protein/Non-hemolytic phospholipase C
	– / → *mip*	C→A	intergenic (–/-614)	SUB	Intergenic	–/Peptidyl-prolyl cis-trans isomerase Mip
	– / → *mip*	T→C	intergenic (–/-602)	SUB	Intergenic	–/Peptidyl-prolyl cis-trans isomerase Mip
	– / → *mip*	T→C	intergenic (–/-612)	SUB	Intergenic	–/Peptidyl-prolyl cis-trans isomerase Mip
	P_04610 → / ← *pcaK_1*	+CC	intergenic (+30/+107)	INS	Intergenic	hypothetical protein/4-hydroxybenzoate transporter PcaK
	rodZ ←	G→T	L176I (CTC→ATC)	SUB	Missense	Cytoskeleton protein RodZ
	– / → *P_05233*	A→G	intergenic (–/-15)	SUB	Intergenic	–/hypothetical protein
	deaD → / ← *ygiD*	C→G	intergenic (+264/+103)	SUB	Intergenic	ATP-dependent RNA helicase DeaD/4,5-DOPA dioxygenase extradiol
	aroH_2 →	A→T	Q15L (CAG→CTG)	SUB	Missense	Phospho-2-dehydro-3-deoxyheptonate aldolase
	aroH_2 →	G→T	G5V (GGC→GTC)	SUB	Missense	Phospho-2-dehydro-3-deoxyheptonate aldolase
	aroH_2 →	G→T	S9I (AGC→ATC)	SUB	Missense	Phospho-2-dehydro-3-deoxyheptonate aldolase
	aroH_2 →	G→T	W14L (TGG→TTG)	SUB	Missense	Phospho-2-dehydro-3-deoxyheptonate aldolase

	P_05904 → / –	G→T	intergenic (+82/–)	SUB	Intergenic	hypothetical protein/–
	P_05911 ← / –	C→A	intergenic (-161/–)	SUB	Intergenic	hypothetical protein/–
	P_05936 ←	A→C	R51R (CGT→CGG)	SUB	Synonymous	Delta(1)-pyrroline-2-carboxylate reductase
	dltA ←	C→A	G437W (GGG→TGG)	SUB	Missense	D-alanine--D-alanyl carrier protein ligase
	lrp_5 ← / –	C→A	intergenic (-1045/–)	SUB	Intergenic	Leucine-responsive regulatory protein/–
	– / ← *P_06214*	G→T	intergenic (–/+943)	SUB	Intergenic	–/hypothetical protein
	algD ← / ← *yaaA*	C→G	intergenic (-879/+23)	SUB	Intergenic	GDP-mannose 6-dehydrogenase/Peroxide stress resistance protein YaaA
	– / –	G→C	intergenic (–/–)	SUB	Intergenic	–/–
	P_02826 →	C→G	A273G (GCT→GGT)	SUB	Missense	NADH:quinone reductase
	P_03382 ← / –	G→T	intergenic (-17/–)	SUB	Intergenic	hypothetical protein/–
	P_03701 →	C→T	L6F (CTC→TTC)	SUB	Missense	hypothetical protein
	*potA_3	A→C	Leu256Arg	SUB	Missense	Spermidine/putrescine import ATP-binding protein PotA
	*potA_3	T→G	Gln248Pro	SUB	Missense	Spermidine/putrescine import ATP-binding protein PotA
Ctrl-R6	*P_01040* → / → *P_01041*	C→G	intergenic (+36/-127)	SUB	Intergenic	hypothetical protein/hypothetical protein
	P_04610 → / ← *pcaK_1*	+CC	intergenic (+30/+107)	INS	Intergenic	hypothetical protein/4-hydroxybenzoate transporter PcaK
	P_01162 → / → *P_01163*	G→T	intergenic (+35/-49)	SUB	Intergenic	hypothetical protein/hypothetical protein
	– / → *P_05233*	A→G	intergenic (–/-15)	SUB	Intergenic	–/hypothetical protein

	P_01418 ←	T→G	D78A (GAC→GCC)	SUB	Missense	hypothetical protein
	– / ← *P_05595*	+CG	intergenic (–/+440)	INS	Intergenic	–/hypothetical protein
	P_00389 ← / –	12 bp→126 bp	intergenic (-101/–)	Comple x	Intergenic	hypothetical protein/–
	algD ← / ← *yaaA*	C→G	intergenic (-879/+23)	SUB	Intergenic	GDP-mannose 6-dehydrogenase/Peroxide stress resistance protein YaaA
	– / ← *P_02531*	C→A	intergenic (–/+62)	SUB	Intergenic	–/hypothetical protein
	P_02619 ← / –	G→T	intergenic (-264/–)	SUB	Intergenic	hypothetical protein/–

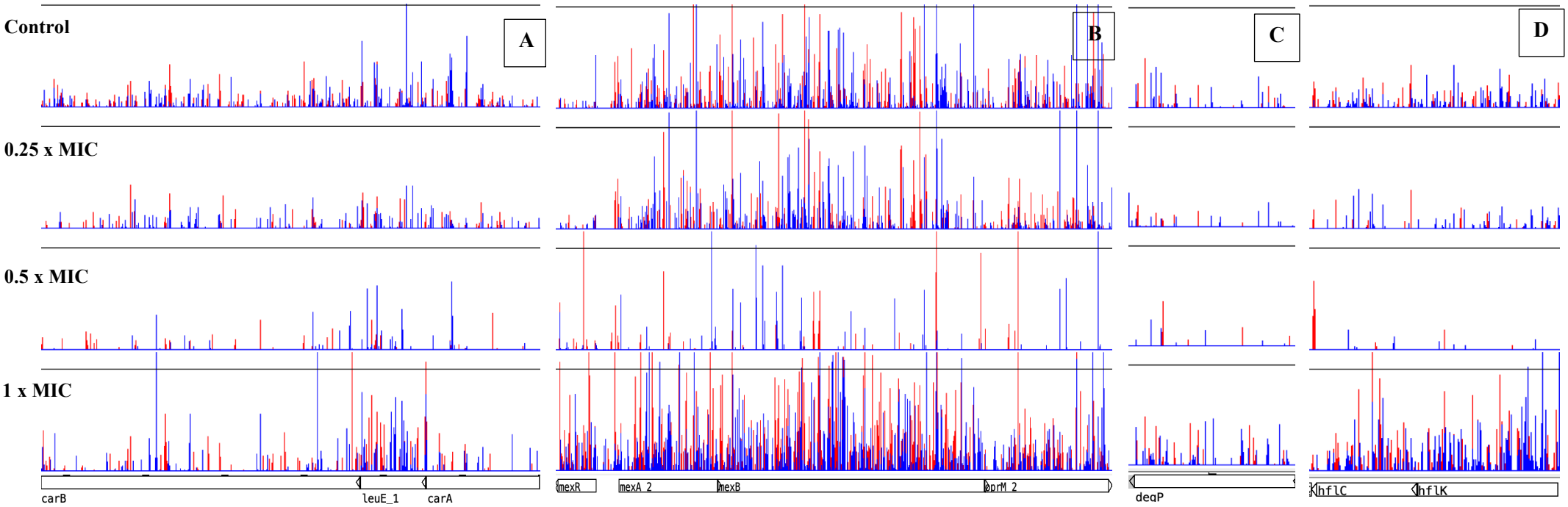

Figure 7-2: Transposon insertion pattern for A) *carAB* operon, B) *mexAB-OprM* operon and *mexR* gene, C) *degP* gene, D) *hflCK* operon.
Genetic map of the gene names is shown at the *bottom* of the panel. The top row in each plot shows untreated control cultures; the three rows below are for cultures grown in the presence of 0.25x, 0.5x, and 1x the MIC of metformin. Each row of vertical red or blue lines indicates the position of mapped reads, and the height of the bar represents the relative number of reads mapped. The red inserts indicate the transposon insertions from left to right (→), and the blue inserts indicate the transposon insertions from right to left (←). The A-D plots are showing a significant decrease in the insertions in the corresponding genes in 0.25x and 0.5x MIC compared to the control, except in mexR, which is showing an increase in the insertions in 1x MIC. The representing data has a significance cut-off of $q \leq 0.001$ for two independent experiments for each concentration (n=2). However, only one repeat of each concentration is displayed for clarity.

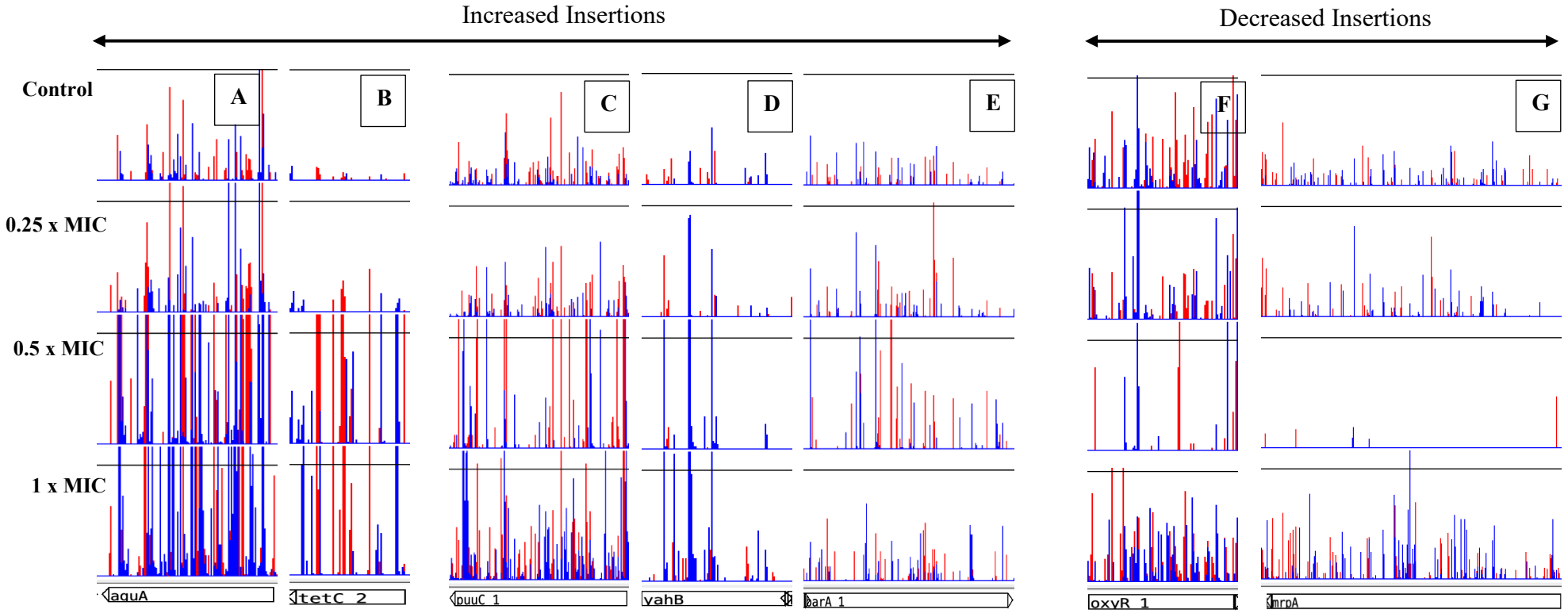

Figure 7-3: Transposon insertion pattern for A) *aguA* gene, B) *tetC* gene, C) *puuC* gene, D) *yahB gene,* E) *barA* gene, F) *oxyR* gene, and G) *mrpA* gene. Genetic map of the gene names is shown at the *bottom* of the panel. The top row in each plot shows untreated control cultures; the three rows below are for cultures grown in the presence of 0.25x, 0.5x, and 1x the MIC of metformin. Each row of vertical red or blue lines indicates the position of mapped reads, and the height of the bar represents the relative number of reads mapped. The red inserts indicate the transposon insertions from left to right (→), and the blue inserts indicate the transposon insertions from right to left (←). The plots A-F are showing a significant increase in insertions; in (A and B) are significant in 0.5x and 1xMIC compared to the control, and (C-E) are significant in 0.5x MIC compared to the control. (F and G) are showing a significant decrease in the corresponding genes in 0.5x MIC compared to the control. The representing data has a significance cut-off of $q \leq 0.001$ for two independent experiments for each concentration (n=2). However, only one repeat of each concentration is displayed for clarity.

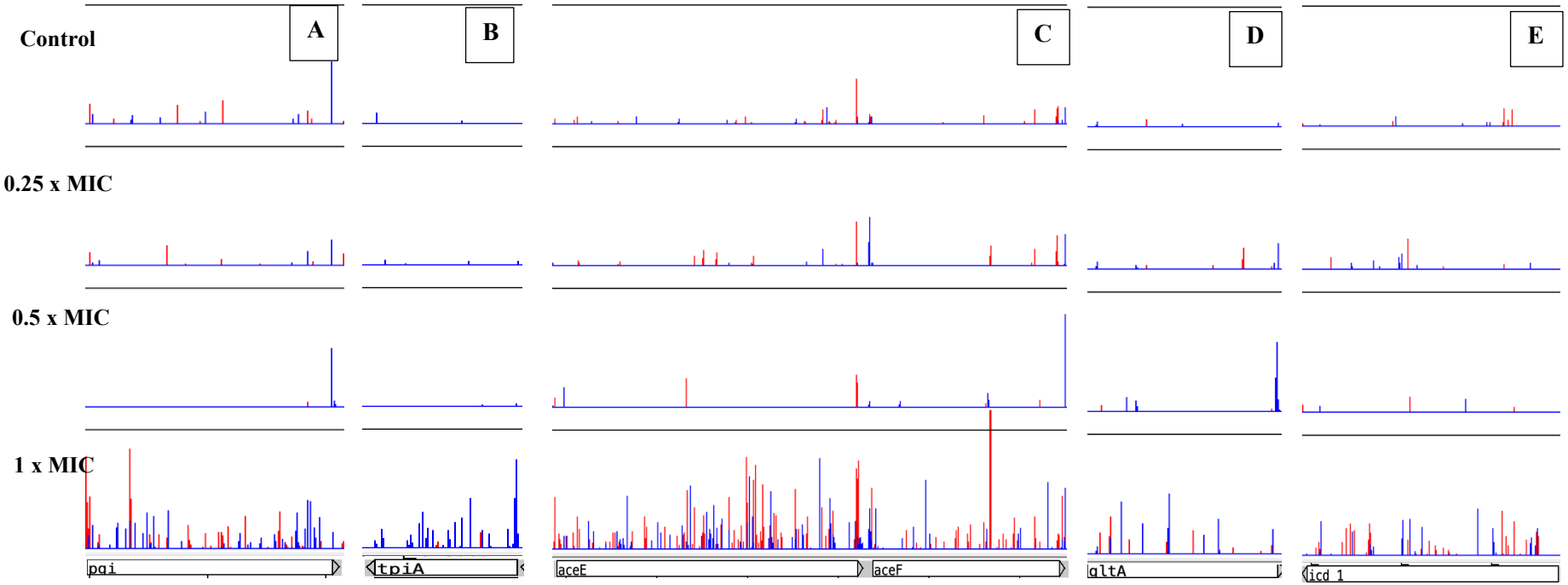

Figure 7-4: Transposon insertion pattern for A) *pgi* gene, B) *tpiA* gene, C) *aceE* and *aceF* genes, D) *gltA* gene, and E) *icd* gene.
Genetic map of the gene names is shown at the *bottom* of the panel. The top row in each plot shows untreated control cultures; the three rows below are for cultures grown in the presence of 0.25x, 0.5x, and 1x the MIC of metformin. Each row of vertical red or blue lines indicates the position of mapped reads, and the height of the bar represents the relative number of reads mapped. The red inserts indicate the transposon insertions from left to right (→), and the blue inserts indicate the transposon insertions from right to left (←). The plots A-E are showing a significant increase in insertions in 1x MIC compared to the control. The representing data has a significance cut-off of $q \leq 0.001$ for two independent experiments for each concentration (n=2). However, only one repeat of each concentration is displayed for clarity.

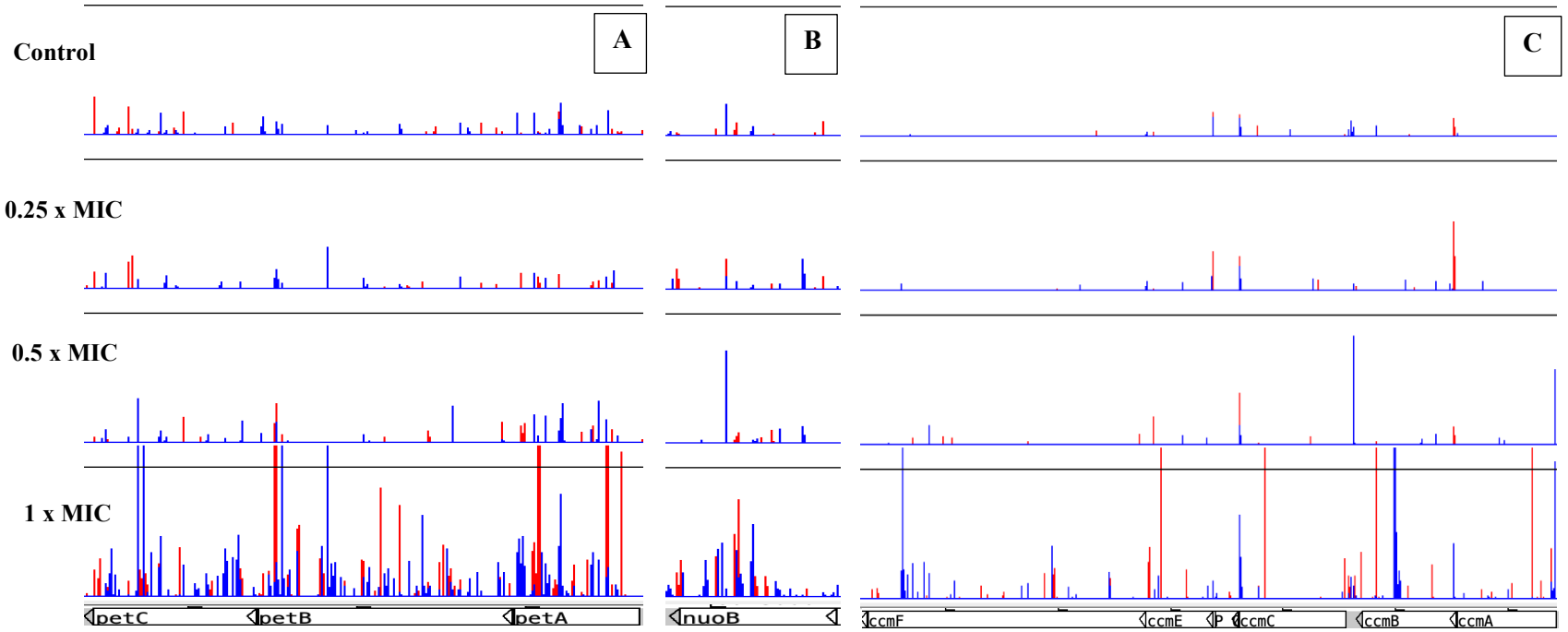

Figure 7-5: Transposon insertion pattern for A) *petABC* operon, B) *nuoB* gene, C) *ccmABCEF* operon.
Genetic map of the gene names is shown at the *bottom* of the panel. The top row in each plot shows untreated control cultures; the three rows below are for cultures grown in the presence of 0.25x, 0.5x, and 1x the MIC of metformin. Each row of vertical red or blue lines indicates the position of mapped reads, and the height of the bar represents the relative number of reads mapped. The red inserts indicate the transposon insertions from left to right (→), and the blue inserts indicate the transposon insertions from right to left (←). The plots A-C are showing a significant increase in insertions in 1x MIC compared to the control. The representing data has a significance cut-off of $q \leq 0.001$ for two independent experiments for each concentration (n=2). However, only one repeat of each concentration is displayed for clarity.

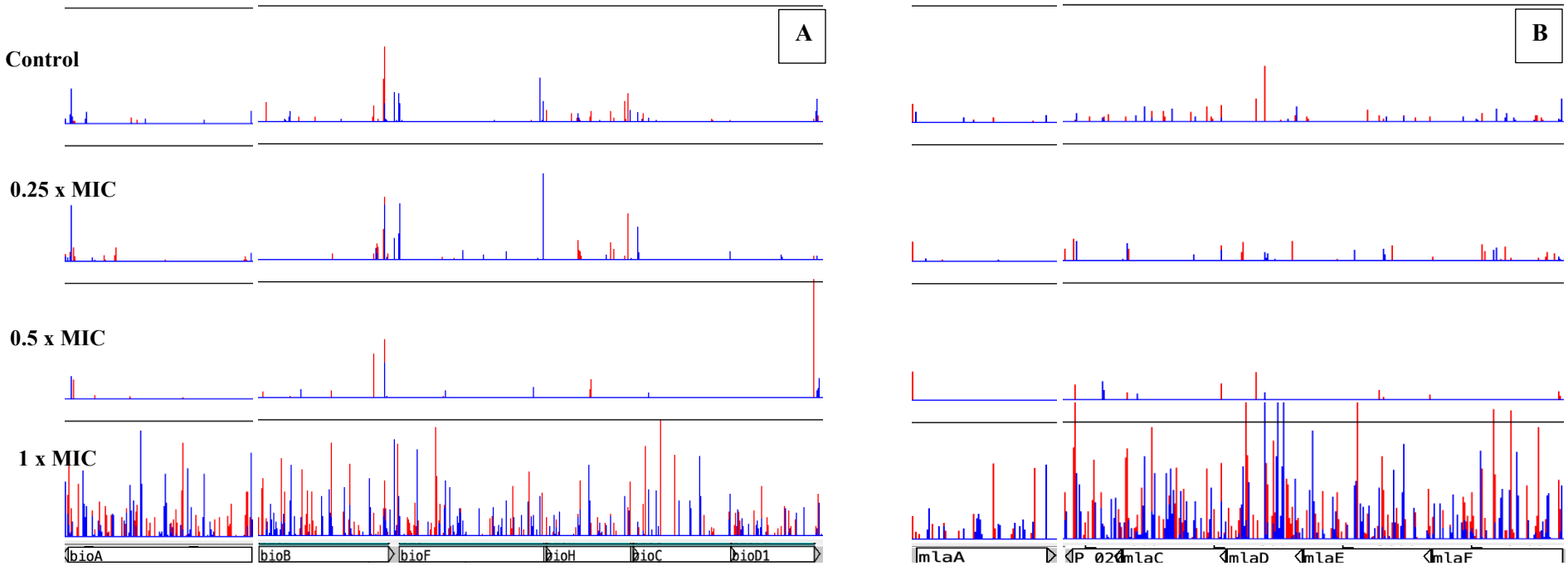

Figure 7-6: Transposon insertion pattern for A) *bioABCDEF* gene cluster, and B) *mlaABCDEF* gene cluster.
Genetic map of the gene names is shown at the *bottom* of the panel. The top row in each plot shows untreated control cultures; the three rows below are for cultures grown in the presence of 0.25x, 0.5x, and 1x the MIC of metformin. Each row of vertical red or blue lines indicates the position of mapped reads, and the height of the bar represents the relative number of reads mapped. The red inserts indicate the transposon insertions from left to right (→), and the blue inserts indicate the transposon insertions from right to left (←). The plots A and B are showing a significant increase in insertions in 1x MIC compared to the control. The representing data has a significance cut-off of $q \leq 0.001$ for two independent experiments for each concentration (n=2). However, only one repeat of each concentration is displayed for clarity.